

Ruthenium-Catalyzed Dehydrogenative and Dehydrative C-H Coupling Reactions of Arenes with Alcohols and Carbonyl Compounds

Hanbin Lee
Marquette University

Recommended Citation

Lee, Hanbin, "Ruthenium-Catalyzed Dehydrogenative and Dehydrative C-H Coupling Reactions of Arenes with Alcohols and Carbonyl Compounds" (2017). *Dissertations (2009 -)*. 698.
http://epublications.marquette.edu/dissertations_mu/698

**RUTHENIUM-CATALYZED DEHYDROGENATIVE AND DEHYDRATIVE
C-H COUPLING REACTIONS OF ARENES WITH ALCOHOLS
AND CARBONYL COMPOUNDS**

By

Hanbin Lee, B.Sc., M.Sc.

A Dissertation Submitted to the Faculty of the Graduate School,
Marquette University,
in Partial Fulfillment of the Requirements for
the Degree of Doctor of Philosophy

Milwaukee, Wisconsin

May 2017

ABSTRACT
RUTHENIUM-CATALYZED DEHYDROGENATIVE AND DEHYDRATIVE
C-H COUPLING REACTIONS OF ARENES WITH ALCOHOLS
AND CARBONYL COMPOUNDS

Hanbin Lee, B.Sc., M.Sc.

Marquette University, 2017

Despite their outstanding achievements, the requirement of preformed functional groups and wasteful byproduct formation are inherent disadvantages associated with the transition metal catalyzed cross-coupling methods. Inspired by the needs for green and sustainable chemistry, transition metal catalyzed dehydrogenative and dehydrative coupling methods have been recognized as environmentally sustainable and atom economical synthetic routes for the new C-C bond formation. The catalytic activation of C-H and C-O bonds allows the formation of coupling products from ubiquitous hydrocarbon substrates by releasing hydrogen or water byproduct. However, these novel protocols require relatively harsh conditions due to their low reactivity of C-H and C-O bonds, and difficulty in controlling regioselectivity. The development of new catalytic C-H bond activation methods is highly desirable for the selective C-C formation reactions.

The cationic ruthenium-hydride complex was found to be a highly effective catalyst for the dehydrogenative and dehydrative C-H coupling reactions of simple arenes with alcohols and carbonyl compounds. The dehydrogenative coupling reaction of phenols with aldehydes formed the 2-acylphenols without using any metal oxidant or forming wasteful byproducts. The mechanistic studies suggested that the aldehyde substrate was served as both the coupling partner and hydrogen acceptor. The coupling method was successfully extended to the synthesis of 2*H*-chromene derivatives by using α,β -unsaturated aldehydes. The cationic ruthenium-hydride complex was found to exhibit uniquely high activity for the coupling reaction of phenols with ketones to form synthetically useful 2-vinylphenols. The coupling of phenols with linear ketones led to a highly (*Z*)-selective formation of trisubstituted olefins. We also developed the catalytic synthesis of biologically important indole and quinoline derivatives from the coupling reaction of arylamines with diols. A broad range of substrates was demonstrated to afford the regioselective *N*-heteroannulated products. The deuterium labeling study and control experiments were performed to discern the mechanistic pathway.

ACKNOWLEDGMENTS

Hanbin Lee, B.Sc., M.Sc.

I give my deepest gratitude to all those people who enriched my graduate study at Marquette university. I would like to thank the most influential person, Dr. Chae Sung Yi, for the tremendous support, motivation, and mentorship. I consider myself very fortunate to have him as my dissertation advisor. I would like to thank my committee members, Dr. Chieu D. Tran, Dr. James R. Gardinier, and Dr. Christopher Dockendorff for their insightful comments and supports.

I would like to thank my group members, Pandula Kirinde Arachchige, Nuwan Pannilawithana, Dulanjali Thennakoon, and the former group members, Dr. Dong-Hwan Lee, Dr. Kwang-Min Choi, Dr. Nishantha Kumara Kalutharage, and Dr. Junghwa Kim for being such a good friend and mentor.

I am deeply grateful to my father, the greatest person in my life, who inspired me to be a scientist. I always want to be a father, mentor, and scientist like him. To my wife Xuchan, I would like to express my deepest gratitude for her encouragement, love and sacrifice. I thank my son Albert for bringing happiness and joy to our lives.

TABLE OF CONTENTS

ACKNOWLEDGMENTS.....	i
LIST OF TABLES	vii
LIST OF FIGURES	ix
LIST OF SCHEMES.....	x
CHAPTER 1	1
Introduction.....	1
1.1 Catalytic Dehydrogenative Cross-Coupling Methods via C-H Activation.....	2
1.1.1 Dehydrogenative Heck-Type Cross-Coupling Reactions.....	3
1.1.2 Catalytic Dehydrogenative Biaryl C-C Bond Formation Reactions.....	12
1.1.3 Catalytic Oxidative Coupling of Aldehydes via C-H Bond Activation.....	19
1.2 Catalytic Dehydrative Cross-Coupling Reactions via C-H and C-O Bond Activation	24
1.2.1 Catalytic Dehydrative Reaction of Allylic Alcohols	25
1.2.2 Catalytic Dehydrative Coupling Reaction of Aliphatic Alcohols.....	31
1.2.3 Dehydrative Arene C-H Coupling Reactions	34
CHAPTER 2	37
Ruthenium Catalyzed Dehydrogenative ortho-Acylation of Phenols with Aldehydes via C-H Activation.....	37
2.1 Backgrounds.....	37
2.1.1 Traditional Acylation Methods	37

2.1.2	Transition Metal-Catalyzed Acylation Methods.....	39
2.2	Results and Discussion.....	40
2.3	Optimization Studies.....	45
2.3.1	Additive Effect.....	45
2.3.2	Solvent and Temperature Effects.....	47
2.3.3	Catalyst Survey.....	48
2.4	Reaction Scope.....	50
2.4.1	Dehydrogenative <i>ortho</i> -Acylation of Phenols with Aldehydes.....	50
2.4.2	Formation of Flavene Derivatives for the Dehydrative Coupling of Phenols with α,β -Unsaturated Aldehydes.....	53
2.4.3	Dehydrogenative <i>ortho</i> -Acylation of Estrone with Aldehydes.....	58
2.5	Mechanistic Studies.....	59
2.5.1	Deuterium Labeling Study.....	59
2.5.2	Deuterium Isotope Effect Study.....	60
2.5.3	Hammett Study.....	62
2.5.4	Proposed Mechanism.....	63
2.6	Conclusions.....	65
CHAPTER 3.....		66
Synthesis of Alkenylated Phenols from Ruthenium-Catalyzed Dehydrative C-H Coupling of Phenols with Ketones.....		66
3.1	Backgrounds.....	66
3.1.1	Synthetic Application of 2-Vinylphenols.....	66

3.1.2	Traditional Carbonyl Olefination Methods.....	67
3.2	Catalytic Reactions for the Formation of 2-Vinylphenols	70
3.3	Optimization Studies	73
3.3.1	Solvent Screening	73
3.3.2	Catalyst Screening	74
3.4	Reaction Scope and Applications.....	76
3.4.1	Scope of Dehydrative C-H Alkenylation of Phenols with Ketones.....	76
3.4.2	Synthetic Applications for the Catalytic Method for the Coupling of Phenols with Ketones	80
3.5	Mechanistic Studies.....	82
3.5.1	Deuterium Labeling Study	82
3.5.2	Deuterium Isotope Effect Study.....	83
3.5.3	Proposed mechanism	85
3.6	Conclusions	87
CHAPTER 4		88
Catalytic Synthesis of Substituted Indoles and Quinolines from the Dehydrative C-H Coupling of Arylamines with 1,2- and 1,3-Diols		88
4.1	Introduction	88
4.2	Results and Discussion.....	90
4.3	Catalyst Screening and Optimization Studies	93
4.4.1	Scope of Dehydrative C-H Coupling Reaction of Arylamines with 1,2-Diols	95

4.4.2	Scope of Dehydrative C-H Coupling Reaction of Arylamines with 1,3-Diols	99
4.4.3	Ru-Catalyzed C-C Bond Activation Reactions of 1,3-Diols	101
4.4.4	Ru-Catalyzed ortho-C-H Alkylation of Arylamines with 1,4-Diols.....	103
4.5	Mechanistic Study for the Ru Catalyzed Coupling of Aniline with 1,2-Diols	105
4.5.1	Deuterium Labeling Study	105
4.5.2	Control Experiments	106
4.5.3	Proposed Mechanism	108
4.6	Conclusions	110
CHAPTER 5		111
Experimental Section		111
5.1	General Information	111
5.2	Synthesis of Ruthenium Catalysts.....	112
5.2.1	Synthesis of [(PCy ₃) ₂ (CO)RuH] ₄ (μ ₄ -O)(μ ₃ -OH)(μ ₂ -OH) (79).....	112
5.2.2	Synthesis of [(η ⁶ -C ₆ H ₆)(PCy ₃)(CO)RuH] ⁺ BF ₄ ⁻ (26).....	113
5.3	Experimental Procedures and Data for the Chapter 2	114
5.3.1	General Procedures for the Coupling Reaction of Phenol with Aldehydes	114
5.3.2	General Procedures for the Mechanistic Studies	115
5.3.3	X-Ray Crystallographic Determination of 81v , 83t , and 84b	116
5.3.4	Characterization Data of the Products	118
5.3.5	X-ray Crystal Data and Structure Refinements	133

5.4	Experimental Procedures and Data for the Chapter 3	136
5.4.1	General Procedures for the Catalytic C-H Coupling reaction of Phenols with Ketones	136
5.4.2	General Procedures for the Mechanistic Studies	136
5.4.3	X-Ray Crystallographic Determination of 98k and 101	137
5.4.4	Characterization Data of the Products	139
5.4.5	X-ray Crystal Data and Structure Refinements	146
5.5	Experimental Procedures and Data for the Chapter 4.....	148
5.5.1	General Procedures for the Catalytic Synthesis of Indole and Quinoline Products	148
5.5.2	General Procedures for the Deuterium Labeling Study and Control Experiments.....	148
5.5.3	Characterization Data of the Products	151
	BIBLIOGRAPHY.....	164

LIST OF TABLES

Table 2.1 Additive effect on the reaction of 3-methoxyphenol and benzaldehyde.....	46
Table 2.2 Solvent and temperature effects for the reaction of 3-methoxyphenol and benzaldehyde.....	47
Table 2.3 Catalyst and additive survey for the reaction of 3-methoxyphenol and benzaldehyde.....	48
Table 2.4 Dehydrogenative acylation of phenols with aldehydes.....	50
Table 2.5 Formation of flavene derivatives from the dehydrative coupling reaction of phenols with α,β -unsaturated aldehydes	54
Table 3.1 Synthetic applications of 2-vinylphenols	67
Table 3.2 Solvent screening for the coupling reaction of 3,5-dimethoxyphenol with cyclohexanone.....	73
Table 3.3 Catalyst screening for the coupling reaction of 3,5-dimethoxyphenol with cyclohexanone.....	75
Table 3.4 Dehydrative C-H alkenylation of phenols with ketones	77
Table 3.5 Dehydrative coupling of 3,5-dimethoxyphenol with biologically active ketones	80
Table 4.1 Catalyst and additive screening for the coupling reaction of aniline with 1-phenyl-1,2-ethanediol	94
Table 4.2 Dehydrative coupling of arylamines with 1,2-diols.....	95
Table 4.3 Dehydrative coupling of anilines with 1-phenyl-1,2-ethanediol.....	98
Table 4.4 Dehydrative coupling of arylamines with 1,3-diols.....	99
Table 4.5 Ruthenium catalyzed C-C bond activation reaction of 1,3-diols	102
Table 5.1 X-ray crystal data for 81v	133
Table 5.2 X-ray crystal data for 83t	134
Table 5.3 X-ray crystal data for 84b	135

Table 5.4 X-ray crystal data for 98k	146
Table 5.5 X-ray crystal data for 110	147

LIST OF FIGURES

Figure 1.1 ORTEP diagram of anionic Ru-amido-hydride complex	9
Figure 1.2 ORTEP plot of dimeric Pd complex 49	17
Figure 1.3 Cationic palladium(II) complex 70	27
Figure 2.1 Molecular geometry of cationic ruthenium-hydride complex 26	41
Figure 2.2 Common structures of flavonoids.....	53
Figure 2.3 Molecular structure of 81v	57
Figure 2.4 Molecular structure of 83t	57
Figure 2.5 Molecular structure of 84b	59
Figure 2.6 ^1H and ^2H NMR spectra of benzyl alcohol byproduct isolated from the reaction of 3,5-dimethoxyphenol with benzaldehyde- α - d_1	60
Figure 2.7 Deuterium isotope effect study for the reaction of 3,5-dimethoxyphenol with benzaldehyde and benzaldehyde- α - d_1	61
Figure 2.8 Hammett plot from the reaction of 3,5-dimethoxyphenol with p -X-C ₆ H ₄ CHO (X = Me, H, F, Cl, CF ₃)	62
Figure 3.1 Molecular structure of 98k	79
Figure 3.2 Molecular structure of 101	82
Figure 3.3 ^1H and ^2H NMR spectra of the product 98a-d isolated from the reaction of 3,5-methoxyphenol with cyclohexanone-2,2,6,6- d_4	83
Figure 3.4 The pseudo-first order plots for the reaction of 3,5-dimethoxyphenol with cyclohexanone and cyclohexanone-2,2,6,6- d_4	84
Figure 4.1 ^1H and ^2H NMR spectra of the product 106a-d isolated from the reaction of aniline-2,3,4,5,6- d_5 with 1-phenyl-1,2-ethanediol	106

LIST OF SCHEMES

Scheme 1.1 Transition metal catalyzed cross-coupling reactions	2
Scheme 1.2 Transition metal catalyzed oxidative cross-coupling reactions via C-H activation.....	3
Scheme 1.3 Oxidative Heck-type alkenylation via C-H activation.....	4
Scheme 1.4 Proposed mechanism of the Pd-catalyzed oxidative ortho-alkenylation of anilides	6
Scheme 1.5 Proposed mechanism for Ru-catalyzed oxidative arene-alkene olefination ...	7
Scheme 1.6 Proposed mechanism for Ru-catalyzed oxidative α -alkenylation of cyclic amines	9
Scheme 1.7 Proposed mechanism of oxidative cross-coupling reaction of benzamide and cyclopentene	11
Scheme 1.8 Proposed mechanism of Pd-catalyzed oxidative cross-coupling of naphthalene with arenes.....	13
Scheme 1.9. Two possible metalation pathways. (a) The electrophilic aromatic metalation pathway, and (b) concerted proton transfer metallation pathway	14
Scheme 1.10 Proposed mechanism for Pd-catalyzed oxidative <i>ortho</i> -arylation.....	16
Scheme 1.11 Cyclo-dehydrogenative arylation of 1,2,3-triazoles	17
Scheme 1.12 Dehydrogenative polyheterocyclization 4-aniline substituted coumarins, quinolinones, and pyrones	18
Scheme 1.13 Proposed mechanism for Pd-catalyzed oxidative <i>ortho</i> -acylation of 2-phenylpyridines with aryl aldehydes	20
Scheme 1.14 Pd-catalyzed cross-coupling of aryl ketone <i>O</i> -methyl oximes with aldehydes.....	21
Scheme 1.15 Proposed mechanism for Pd-catalyzed ortho-acylation of aryl oxime with aldehydes.....	22
Scheme 1.16 Proposed mechanism for Cu-catalyzed intramolecular acylation of formyl- <i>N</i> -arylformamides	23
Scheme 1.17 Transition metal catalyzed cross-dehydrative coupling reactions	24

Scheme 1.18 Pd-catalyzed dehydrative coupling of allyl alcohols with alkynes	26
Scheme 1.19 Proposed mechanism for the dehydrative coupling of terminal alkynes with allylic alcohols	26
Scheme 1.20 Pd-catalyzed dehydrative coupling of allyl alcohols with styrenes	27
Scheme 1.21 Co-catalyzed dehydrative C-H ortho-allylation of arenes	28
Scheme 1.22 Proposed mechanism for the dehydrative C-H allylation of 6-arylpurines	29
Scheme 1.23 Ru-catalyzed dehydrative C-H allylation of indoles.....	30
Scheme 1.24 Ru-catalyzed dehydrative alkylation of alkenes with alcohols.....	31
Scheme 1.25 A plausible mechanism for the dehydrative C-H alkylation of alkenes	32
Scheme 1.26 Ru-catalyzed dehydrative synthesis of ortho-alkylated phenols and benzofurans	33
Scheme 1.27 Ru/ L2 -catalyzed dehydrative biarylation of arenes with phenols	34
Scheme 1.28 Proposed transition states for the <i>ortho</i> -arene arylations.....	35
Scheme 1.29 Ru-catalyzed dehydrative biarylation of arenes with phenols	35
Scheme 2.1 Reaction mechanism of the Friedel-Crafts acylation.....	38
Scheme 2.2 The reaction pathway of the Houben-Hoesch reaction.....	38
Scheme 2.3 Synthesis of cationic ruthenium-hydride complex 26	41
Scheme 2.4 Dehydrogenative and dehydrative coupling reactions mediated by Ru catalyst	42
Scheme 2.5 Oxidative C-H acylation and aldol condensation of estrone with aldehydes	58
Scheme 2.6 Proposed mechanism for the dehydrogenative <i>ortho</i> -acylation of phenols with aldehydes	63
Scheme 3.1 Mechanism for the Wittig olefination reaction.....	68
Scheme 3.2 The reaction pathways for the Peterson olefination.....	69
Scheme 3.3 The olefination of carbonyl compounds by using the Tebbe's reagent	69

Scheme 3.4 Rh-catalyzed coupling reaction of <i>N</i> -phenoxyacetamides with <i>N</i> -tosylhydrazones.....	70
Scheme 3.5 Mechanistic rationale for the C-H alkenylation of phenols	85
Scheme 3.6 Mechanistic rationale for the (<i>Z</i>)-selective formation of 2-alkynylphenols .	86
Scheme 4.1 Ruthenium-hydride catalyzed syntheses of unsymmetrical ethers	91
Scheme 4.2 The coupling reaction of 1-naphthylamine with 1,4-diols.....	104
Scheme 4.3 Plausible mechanistic pathway for the dehydrative coupling of aniline with 1,2-diol	109

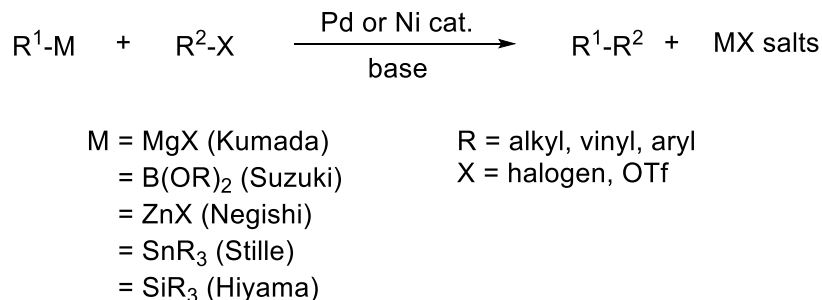
CHAPTER 1

Introduction

Hydrocarbons are ubiquitous constituents present in organic and petroleum products. It is very important to develop efficient processes for the transformation of inexpensive hydrocarbons to more valuable products such as pharmaceuticals, natural products, and polymers. Since carbon-hydrogen (C-H) and carbon-carbon (C-C) bonds are the most fundamental linkage for these substances, the development of catalytic methods for efficient and selective C-H bond activation and C-C bond formation reactions remains one of the most critical challenges in organic chemistry.

To overcome shortcomings of classical C-C coupling methods such as Grignard and Friedel-Crafts reactions, transition metal catalyzed cross-coupling reactions have emerged as highly effective methods for C-C bond formation. Since Heck's pioneering work on the palladium-catalyzed cross coupling of aryl halides and olefins in late 1960s, extensive research has been directed to the development of transition metal catalyzed cross-coupling reactions.¹ Many types of transition metal catalyzed C-C coupling methods (Kumada, Suzuki-Miyaura, Negishi, Stille, and Hiyama) have led to indispensable tools for chemical synthesis.² However, in spite of outstanding achievements on these catalytic C-C bond formation methods, these processes commonly require prefunctionalized starting materials and a stoichiometric amount of base.³ The requirement of preformed functional groups is an inherent disadvantage because the substrate availability is often limited or multiple functionalization steps are needed to synthesize these starting materials. Moreover,

the formation of stoichiometric amount of undesirable salt byproduct is inevitable from the use of base (Scheme 1.1).



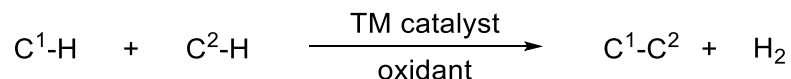
Scheme 1.1 Transition metal catalyzed cross-coupling reactions

In this regards, the development of catalytic methods which can lead to the direct formation of C-C bonds through the selective cleavage of unreactive C-H bonds would be highly desirable. Thus, the transition metal catalyzed C-H activation methods have attracted much interest in synthetic chemistry.⁴ In particular, dehydrogenative and dehydrative C-C cross-coupling methods via C-H activation have been found to be highly atom economical ways that do not form any harmful byproducts. This chapter will mainly discuss the recent developments on the synthetic and mechanistic aspects of transition metal mediated C-C bond formation methods via C-H bond activation.

1.1 Catalytic Dehydrogenative Cross-Coupling Methods via C-H Activation

Considerable efforts have been devoted to the development of catalytic C-C bond formation methods via unfunctionalized C-H bond activation, which are inspired by the needs for green and sustainable chemistry.⁵ The cross-dehydrogenative-coupling (CDC) of two C-H bonds is not only advantageous in terms of eliminating byproduct formation but

also from the viewpoint of reducing the reaction steps. Both starting hydrocarbon substrates do not need to be prefunctionalized, which reduces costly chemical steps and the wasteful byproducts (Scheme 1.2).



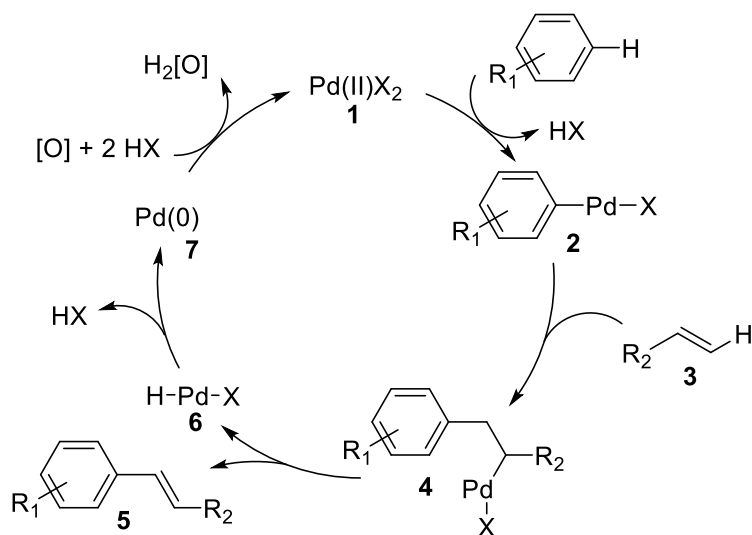
Scheme 1.2 Transition metal catalyzed oxidative cross-coupling reactions via C-H activation

Although CDC method can be a powerful tool for the selective formation of new C-C bonds, certain obstacles still remain to be resolved. First, the generation of C-C bonds with loss of hydrogen gas might not be thermodynamically favored under normal reaction conditions. Thus, the reaction may require an external driving force such as a hydrogen acceptor and/or elevated temperature. Second, the selective activation of two different C-H bonds is required on the starting materials. In case of benzene derivatives, the difference in reactivity between the C-H bonds is generally less ascertained. The use of directing groups is commonly employed to improve both regioselectivity and reactivity, because the C-H bond near the directing group would promote the access to metal catalysts.⁶ Despite such challenges, various oxidative C-C bond formation methods have been achieved by using CDC strategy including alkenylations⁷, arylations, alkylations⁸, and acylation reactions.

1.1.1 Dehydrogenative Heck-Type Cross-Coupling Reactions

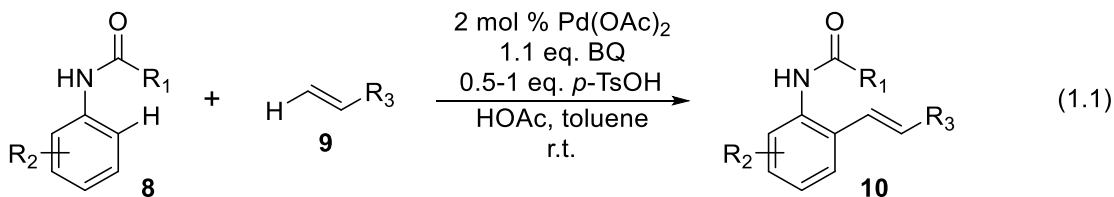
Olefins are fundamental building blocks for a variety of important reactions in organic synthesis. In a pioneering study, Fujiwara reported a Mizoroki-Heck-type reaction

of Pd-catalyzed oxidative cross-coupling between aryl C-H bonds and olefins to generate arylalkenes.⁹ The proposed mechanism as shown in Scheme 1.3 involves arene-C-H bond activation and transmetalation by Pd(II) complex **1** to generate arylpalladium intermediate **2**, which undergoes carbopalladation of olefin (**3**) to form new C-C bond of alkylpalladium complex **4**. The β -H elimination yields styrenyl product **5** and Pd(II)-hydride species **6**. The subsequent reductive elimination gives Pd(0) species **7**, and reoxidation of Pd(0) to Pd(II) **1** completes the catalytic cycle.¹⁰ There are two major problems for this reaction. First, the reaction requires a large excess of arene substrate. Second, poor regioselectivity was observed for monosubstituted benzene substrates.

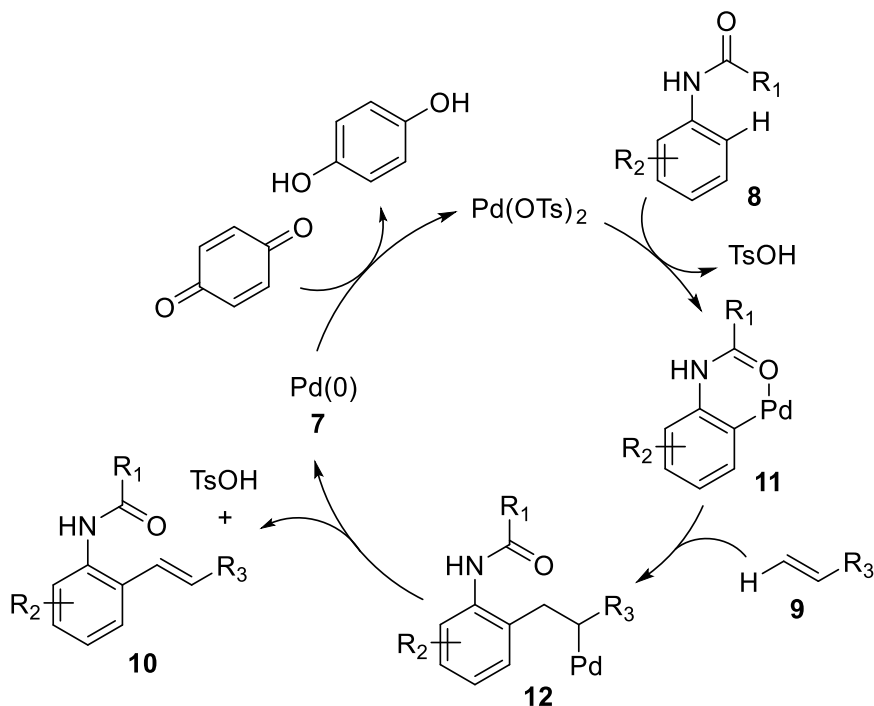


Scheme 1.3 Oxidative Heck-type alkenylation via C-H activation

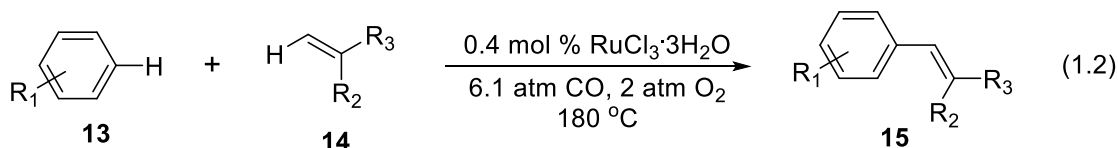
To address this regioselectivity problem, de Vries and van Leeuwen adopted chelate assisted regioselective oxidative cross-coupling between anilides (**8**) and olefins (**9**) under mild conditions (eq 1.1).¹¹



The Pd(II) catalyst was found to be most effective for the coupling reaction, whereas other metal complexes such as $\text{Ru}_3(\text{CO})_{12}$, $[\text{RuCl}_2(p\text{-cymene})]_2$, PtCl_2 , and $\text{Ni}(\text{OAc})_2$ showed no activity. The reaction was found to exhibit a large electronic dependence as measured from the competitive experiments of a series of *para*-substituted anilides ($\rho^+ = 2.2$). A large deuterium isotope effect was measured on the *ortho*-C-H bond of anilides, indicating the C-H activation is the slow step ($k_{\text{H}}/k_{\text{D}} = 3$). The authors proposed a mechanism involving the electrophilic cyclopalladation of anilides **8** as the rate-limiting step to generate palladacycle **11**. Then, carbopalladation of olefin **9** generates *ortho*-alkylpalladium complex **12**, which undergoes β -H elimination to yield the *ortho*-alkenylation product **10**. Stoichiometric amount of benzoquinone (BQ) was found to be the optimal oxidant. *p*-Toluenesulfonic acid (TsOH) also showed beneficial effect for improving the product yields.

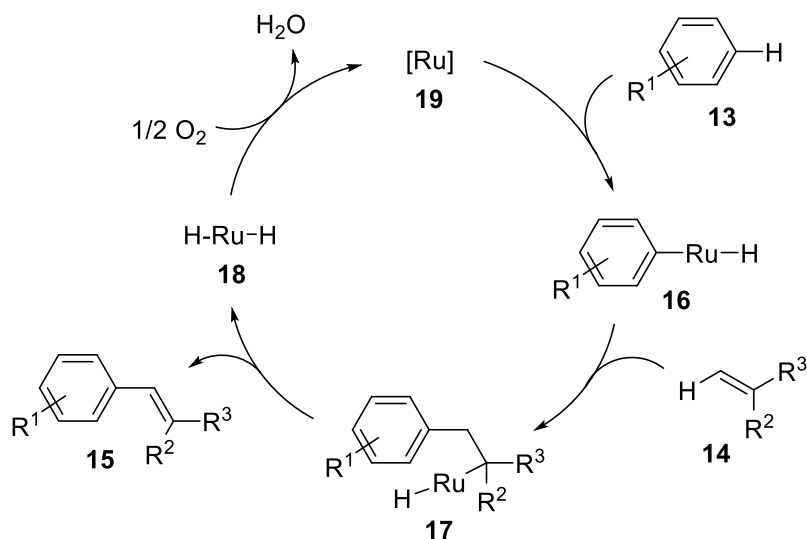


Scheme 1.4 Proposed mechanism of the Pd-catalyzed oxidative ortho-alkenylation of anilides



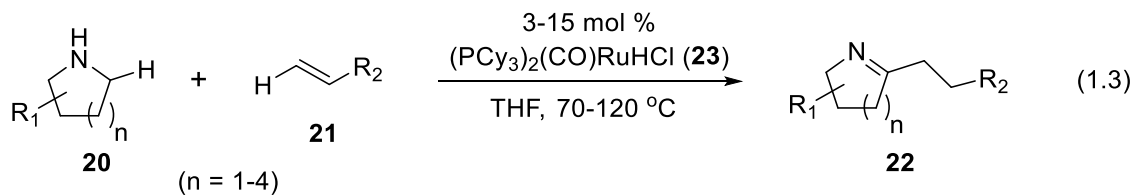
In 2001, Milstein and co-workers reported the oxidative olefination of arenes catalyzed by ruthenium complexes (eq 1.2).¹² A number of ruthenium complexes such as $\text{RuCl}_3\cdot 3\text{H}_2\text{O}$, $[\text{Ru}(\text{CO})_3\text{Cl}_2]_2$, $[(\eta^6\text{-C}_6\text{H}_6)\text{RuCl}_2]_2$, $\text{Ru}(\text{NO})\text{Cl}_3\cdot 5\text{H}_2\text{O}$, and $\text{Ru}(\text{CF}_3\text{COCH}_2\text{COCF}_3)_3$ showed similar catalytic activity. The authors found that O_2 can be directly used as the oxidant, but olefins can also serve as the oxidant in the absence of O_2 to yield a 1:1 ratio of alkenylation and the alkylation products. The Hammett type of competitive experiment indicated that electron-donating substituents on the arene react faster than electron-deficient arenes ($\rho^+ = -1.16$). The authors proposed a possible mechanism as shown in Scheme 1.5. First, C-H activation of **13** forms an arylruthenium

intermediate **16**. The insertion of olefin **14** into metal-aryl bond forms alkylruthenium complex **17**, which undergoes β -H elimination to yield the product **15** and ruthenium-hydride species **18**. Regeneration of electrophilic ruthenium species **19** by oxidation with O_2 completes the catalytic cycle. The product yield increases under CO atmosphere (6.1 atm) by stabilizing the electrophilic ruthenium species. In support of this, ruthenium-carbonyl peaks (2054 and 1983 cm^{-1}) are observed by IR spectroscopy in the reaction mixture.



Scheme 1.5 Proposed mechanism for Ru-catalyzed oxidative arene-alkene olefination

The selective activation of sp^3 -C-H bonds of simple alkanes has proven to be much more challenging because it is both kinetically and thermodynamically less favored than sp^2 -C-H bonds. However, sp^3 -C-H bonds with neighboring α -heteroatom could be selectively activated by late transition metal complexes.¹³



Previously, our research group developed a highly regioselective dehydrogenative coupling reaction between cyclic amines and alkenes by using the Ru-H catalyst $(\text{PCy}_3)_2(\text{CO})\text{RuHCl}$ (**23**) (eq 1.3).¹⁴ The reaction occurred without any additives, and H_2 is the only byproduct consumed by excess alkene starting material. A normal deuterium isotope effect was observed from the coupling reaction of $\text{C}_4\text{H}_8\text{N}-\text{H}$ and $\text{C}_4\text{H}_8\text{N}-\text{D}$ ($k_{\text{H}}/k_{\text{D}} = 1.9$), whereas no significant carbon isotope effect was measured. The authors were able to isolate an anionic ruthenium-amido complex as a sodium salt. The X-ray crystallographic analysis (Figure 1.1) supports that the isolated complex is an active species for the reaction. The proposed mechanism starts with coordination of **20** to ruthenium complex **23**, followed by α -C-H activation and olefin insertion to form the alkyruthenium intermediate **24** (Scheme 1.6). The subsequent β -H elimination liberates an equivalent of alkane, which was detected by NMR in the reaction mixture. Another α -C-H activation of cyclic imine forms α -ruthenated imine complex **25**. Insertion of second olefin **21** followed by reductive elimination gives the product **22** with the regenerated Ru catalyst.

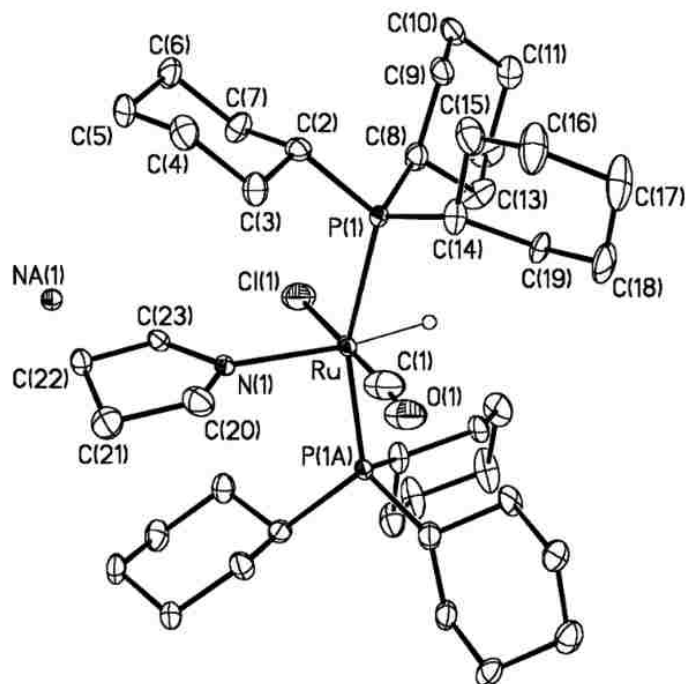
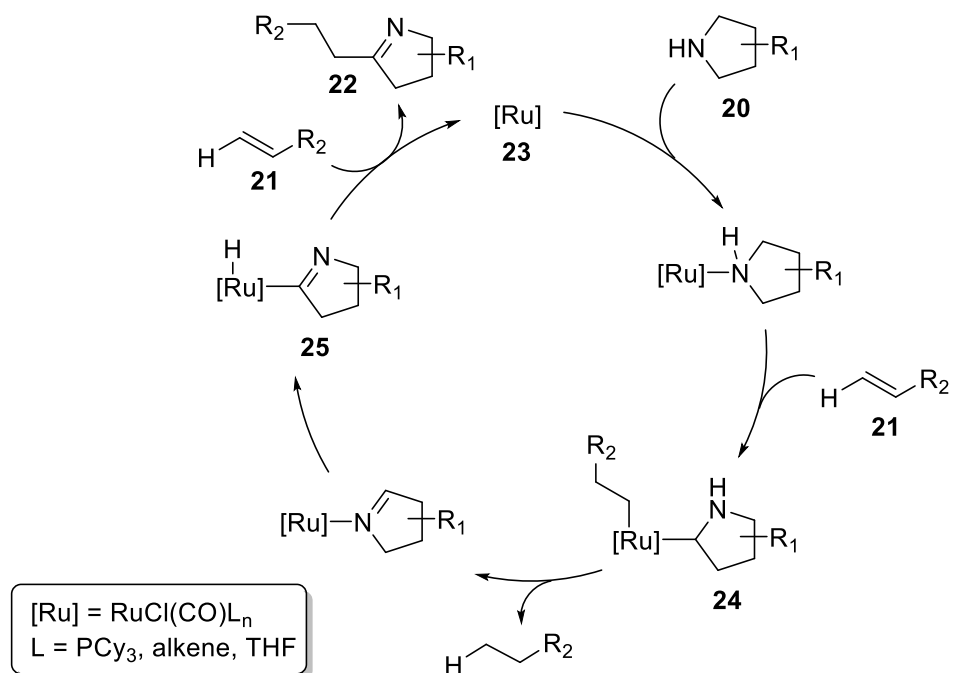
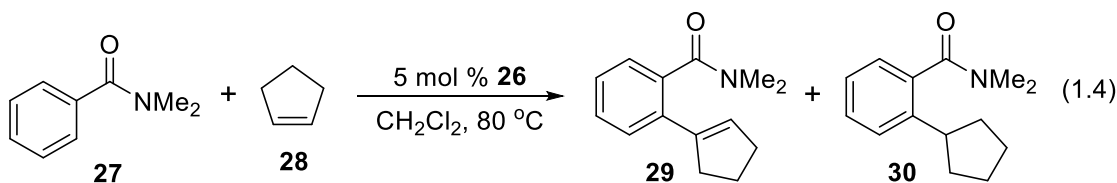


Figure 1.1 ORTEP diagram of anionic Ru-amido-hydride complex

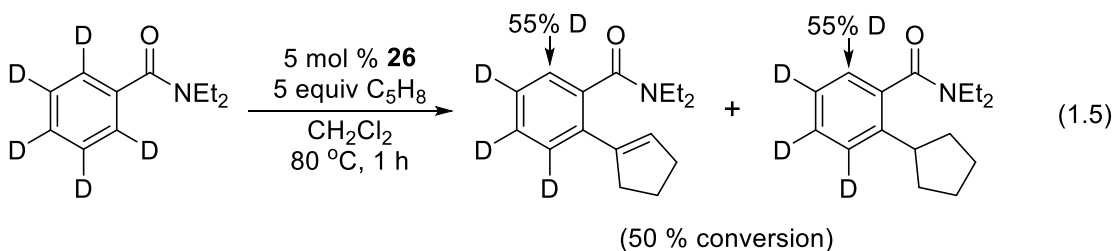


Scheme 1.6 Proposed mechanism for Ru-catalyzed oxidative α -alkenylation of cyclic amines

In 2010, our group also reported a chelate-assisted oxidative coupling reaction of arylamides and unactivated alkenes by using the well-defined cationic ruthenium-hydride complex $[(C_6H_6)(CO)(PCy_3)RuH]^+BF_4^-$ (**26**) (eq 1.4).¹⁵ Compared to other oxidative Heck-type C-H alkenylations, the coupling reaction is environmentally beneficial because it does not employ any hazardous external metal oxidants or additives.

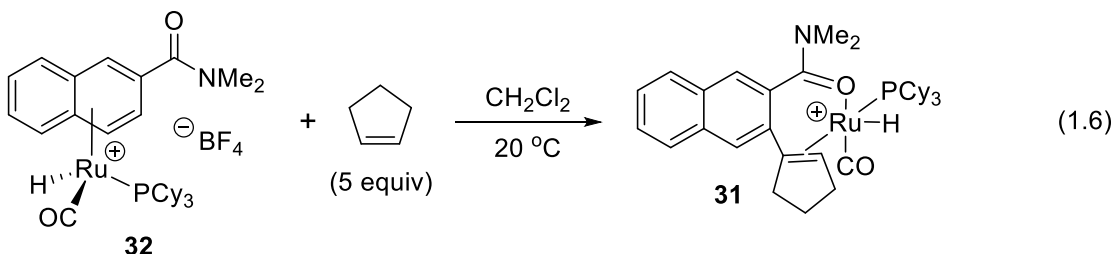


The reaction between $C_6D_5CONEt_2$ and cyclopentene showed an extensive *ortho*-H/D exchange pattern (55% D) on both products at 50 % conversion. A rapid and reversible *ortho*-C-H bond activation of the amide substrate was also observed (eq 1.5). The carbon isotope effect revealed a pronounced ^{13}C ratio on the *ortho*-carbon ($^{13}C(\text{recovered})/^{13}C(\text{virgin}) = 1.023$), when recovered amide at 80% conversion and virgin sample are compared. These results suggest that C-C bond formation step is the rate-limiting step.

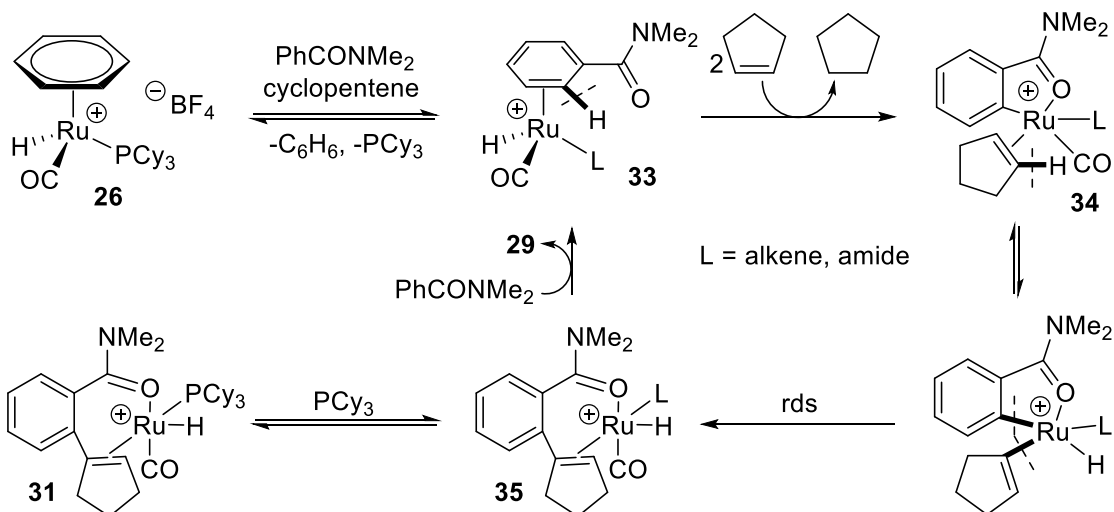


A stable Ru-H complex **31** was isolated from the reaction of cyclopentene and naphthylamide-coordinated complex **32**, which is prepared from the reaction of tetranuclear ruthenium complex $[RuH(CO)(PCy_3)]_4(O)(OH)_2$, *N,N*-dimethyl-2-

naphthamide, and $\text{HBF}_4 \cdot \text{OEt}_2$ (eq 1.6).¹⁶ The cationic ruthenium complex **31** showed the same activity as the catalyst **26** for the coupling reaction between naphthylamide and cyclopentene.



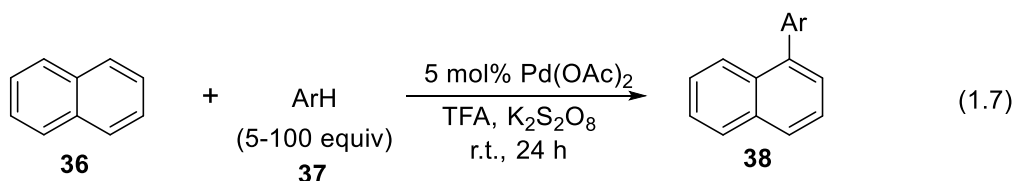
The proposed mechanism involves an initial arene exchange from **26** to form arylamide-coordinated cationic ruthenium-hydride species **33**. The subsequent chelate-directed *ortho*-C-H activation and dehydrogenation steps generate the *ortho*-metalated species **34**. The vinyl C-H activation of alkenes, followed by aryl-to-vinyl reductive elimination steps produce cationic ruthenium hydride complex **35**. Liberation of the product **29** and coordination of another arylamide completes the catalytic cycle.



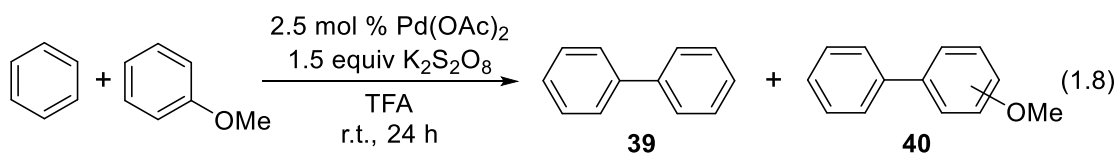
Scheme 1.7 Proposed mechanism of oxidative cross-coupling reaction of benzamide and cyclopentane

1.1.2 Catalytic Dehydrogenative Biaryl C-C Bond Formation Reactions

Biaryls are common structural motifs in pharmaceutical products, liquid crystals, and chiral ligands. Although the synthesis of biaryls has its roots in the pioneering work of Ullmann and Goldberg over a century ago,¹⁷ the development of broadly applicable Pd-catalyzed aryl-aryl bond formation methods (Kumada, Suzuki, Negishi, Stille, Hiyama) still require aryl halides and appropriate organometallic reagents. Recently, direct C-H oxidative coupling of two unfunctionalized arenes has emerged as a promising synthetic strategy for the formation of biaryl products.¹⁸

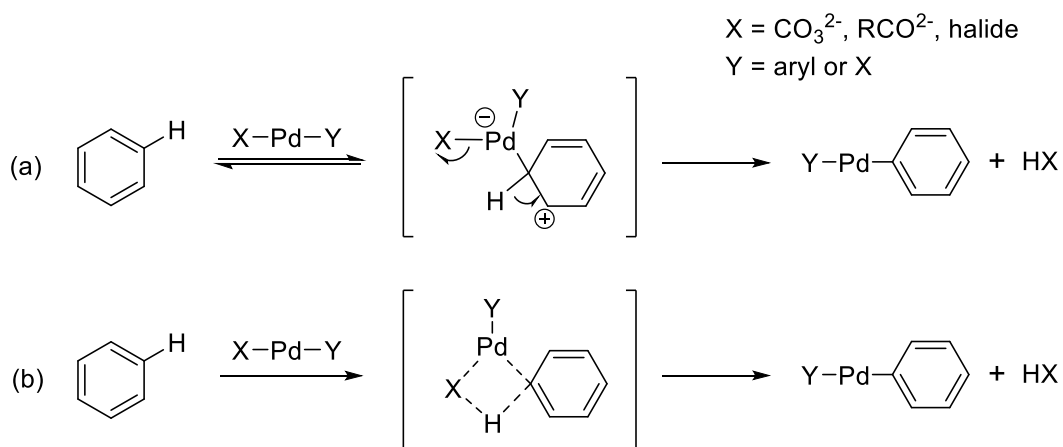


In 2006, Lu and co-workers published oxidative cross-coupling of naphthalene with various arenes (eq 1.7).¹⁹ The biaryl formation reaction was achieved with a palladium(II) catalyst, $\text{K}_2\text{S}_2\text{O}_8$, and CF_3COOH (TFA), which is the same catalytic system used for the carboxylation of arenes.²⁰ The authors found that the ratio between homo-coupling and unsymmetrical biaryl products from the reaction of benzene and anisole can be controlled by changing the relative concentration of TFA (eq 1.8).



When TFA = 6.3 equiv, **39/40** = 56/44
 When TFA = 0.63 equiv, **39/40** = 21/79

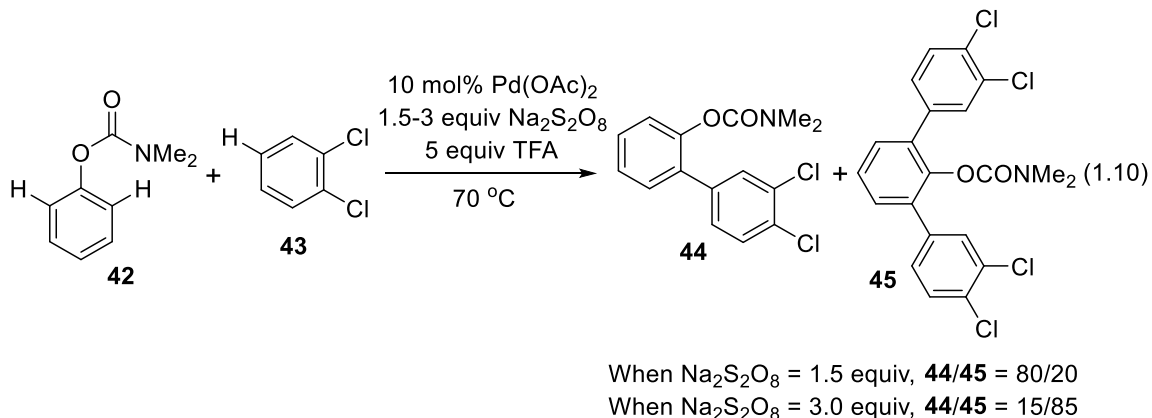
Fagnou and co-workers reported a palladium catalyzed C3-arylation of *N*-acetylindoles with simple arenes by using $\text{Cu}(\text{OAc})_2$ as the oxidant (eq 1.9).²¹ Optimal catalytic reactivity was discovered with palladium trifluoroacetate $[\text{Pd}(\text{TFA})_2]$ complex, 3-nitropyridine, cesium pivalate, and pivalic acid as the solvent. Addition of pyridine presumably acts to stabilize the palladium(0), thereby preventing the formation of palladium black precipitates before reoxidation. The authors believed that a complete inversion of catalyst selectivity occurred in a single catalytic cycle by using two different arenes as starting materials, because no homo-coupling products are detected in the crude reaction mixture. They hypothesized that two potential arene palladation pathways could be involved in the mechanism for the formation of unsymmetrical biaryl products (Scheme 1.9).



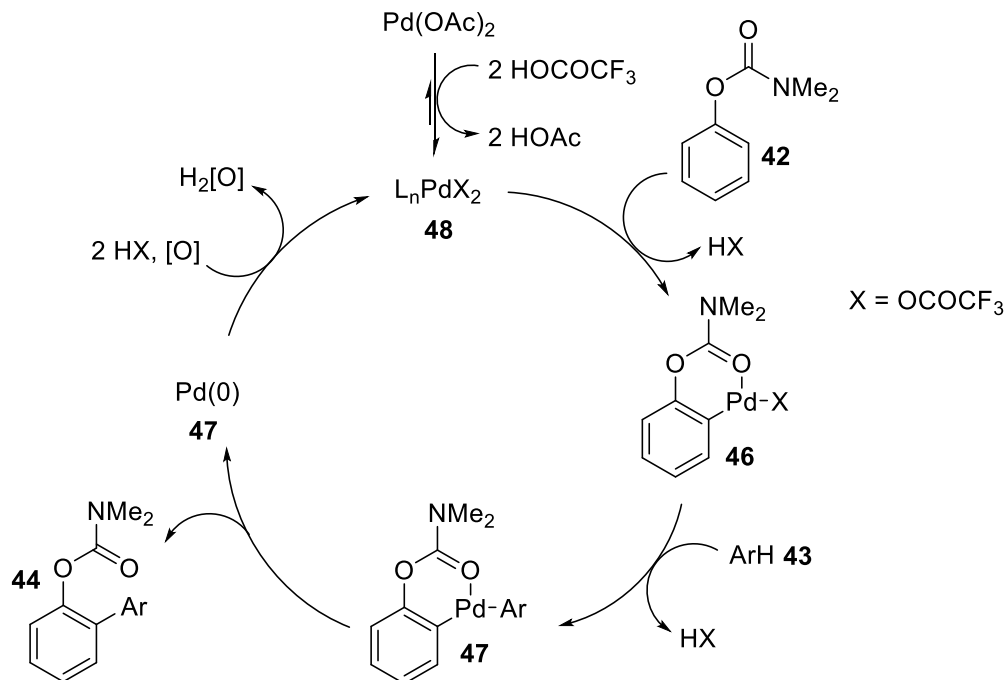
Scheme 1.9. Two possible metalation pathways. (a) The electrophilic aromatic metalation pathway, and (b) concerted proton transfer metalation pathway

Fagnou group also showed that changing the oxidant from $\text{Cu}(\text{OAc})_2$ to AgOAc results in regioselective C2 arylation of indoles (eq 1.9).²² Although the rationale of the

C2/C3 regioselectivity has not been settled, they explained that the formation of mixed Pd-Cu clusters may promote pronounced C3 selectivity.



More recently, Dong and co-workers reported *O*-carbamate directed *ortho*-selective oxidative arylation by using palladium catalyst.²³ Sodium persulfate (Na₂S₂O₈) was found to be an optimal oxidant, whereas Cu(OAc)₂ and AgOAc were ineffective. The authors observed that either products **44** and **45** can be selectively produced by controlling the relative concentration of the oxidant (eq 1.10). Also, *ortho*- or *meta*-substituted *O*-phenylcarbamates readily underwent to form the monoarylation products. The addition of TFA was found to be critical for achieving highly efficient oxidative cross-coupling reactions. The authors proposed that TFA enhances the electrophilic metalation of the palladium catalyst center toward arene substrates.²⁴



Scheme 1.10 Proposed mechanism for Pd-catalyzed oxidative *ortho*-arylation

The authors proposed a possible mechanism is proposed as shown in Scheme 1.10. Carbamate-assisted cyclopalladation of **42** forms the arylpalladium **46**. The subsequent C-H bond activation of electron-deficient arene **43** by electrophilic metalation, followed by reductive elimination to yield the product **44** (or **45** for the second cycle) and Pd(0) **47**. The reoxidation of Pd(0) **47** with Na₂S₂O₈ forms active Pd(II) species **48**. In order to support the first C-H bond activation by cyclopalladation,²⁵ Pd complex **49** was prepared by treatment of *m*-tolyl dimethylcarbamate with Pd(OAc)₂ in the presence of TFA (eq 1.11). The Pd complex **49** was characterized by NMR spectroscopy and X-ray crystallography (Figure 1.2). The treatment of obtained dimeric Pd complex **49** with benzene produced *ortho*-phenylated *O*-phenylcarbamate in excellent yield. The molecular structure of **49** suggests the formation of palladacycle intermediate **46**.

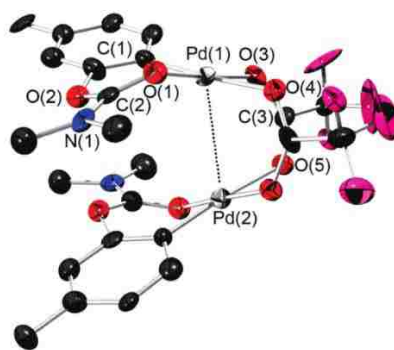
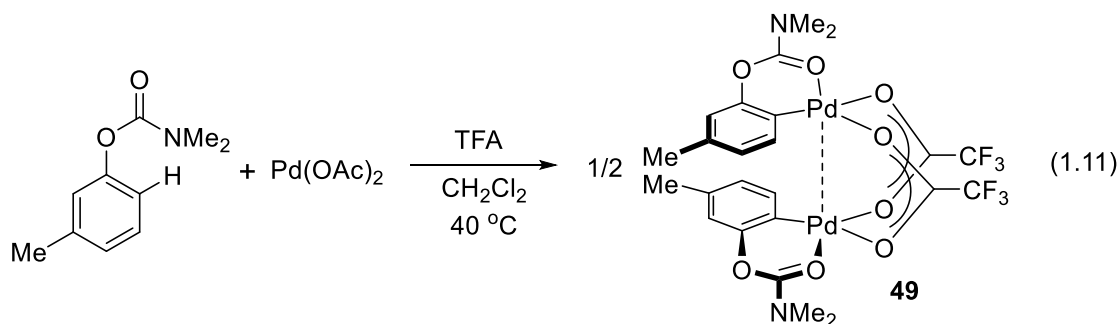
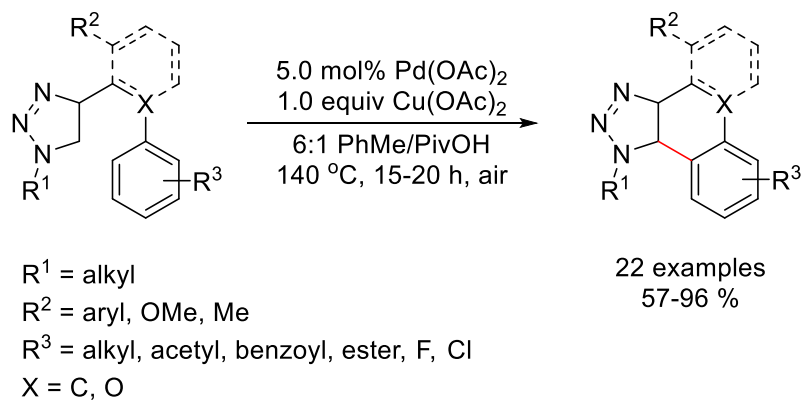


Figure 1.2 ORTEP plot of dimeric Pd complex **49**

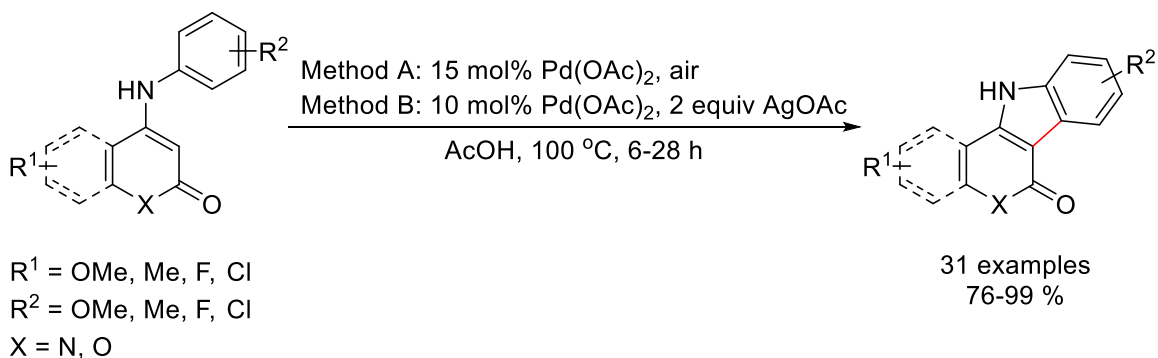


Scheme 1.11 Cyclo-dehydrogenative arylation of 1,2,3-triazoles

Heterocyclic products have been synthesized by applying intramolecular dehydrogenative C-C bond formation protocol. Ackermann and co-workers reported intramolecular arylation of 1,2,3-triazoles via two different sp^2 C-H bond activation by using Pd(OAc)₂ catalyst (Scheme 1.11).²⁶ The heteroannulated triazoles could be formed

by intramolecular C-C bond formation with 6:1 toluene/pivalic acid solvent system in air, but there was no distinct advantage on using molecular oxygen as the oxidant. The addition of the stoichiometric amount of $\text{Cu}(\text{OAc})_2$ was found to be the most optimal among a variety of screened terminal oxidants. The authors were able to expand the scope of this method to synthesize π -conjugated heteroannulated phenanthrenes.

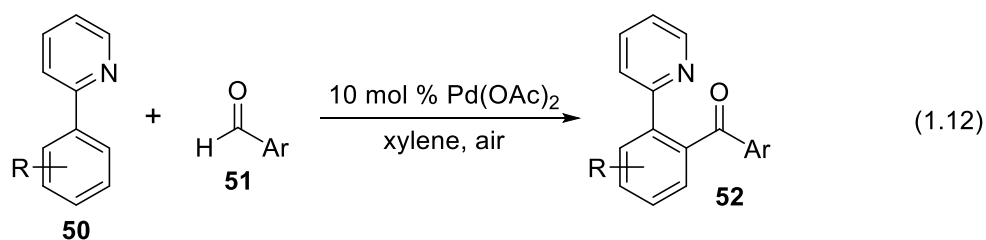
Recently, Xu and co-workers reported $\text{Pd}(\text{OAc})_2$ catalyzed intramolecular heterocyclization of 4-aniline substituted coumarins, quinolinones, and pyrones (Scheme 1.12).²⁷ A wide range of indole-fused polyheterocycles such as indolo[3,2-*c*]coumarins, indolo[3,2-*c*]quinolinones, and indolo[3,2-*c*]pyrones can be produced by atom economical dehydrogenative C-C bond connection. The authors devised base-free reaction conditions by changing catalyst loading and the oxidant. Since replacing AgOAc (method B) with air (method A) is environmentally beneficial, method A was employed for the heterocyclization of 4-arylamino coumarines with a longer reaction time (> 24 h). These methods readily afforded biologically valuable polyheterocycle compounds in good to excellent yields while avoiding prefunctionalization or *N*-protection of substrates.



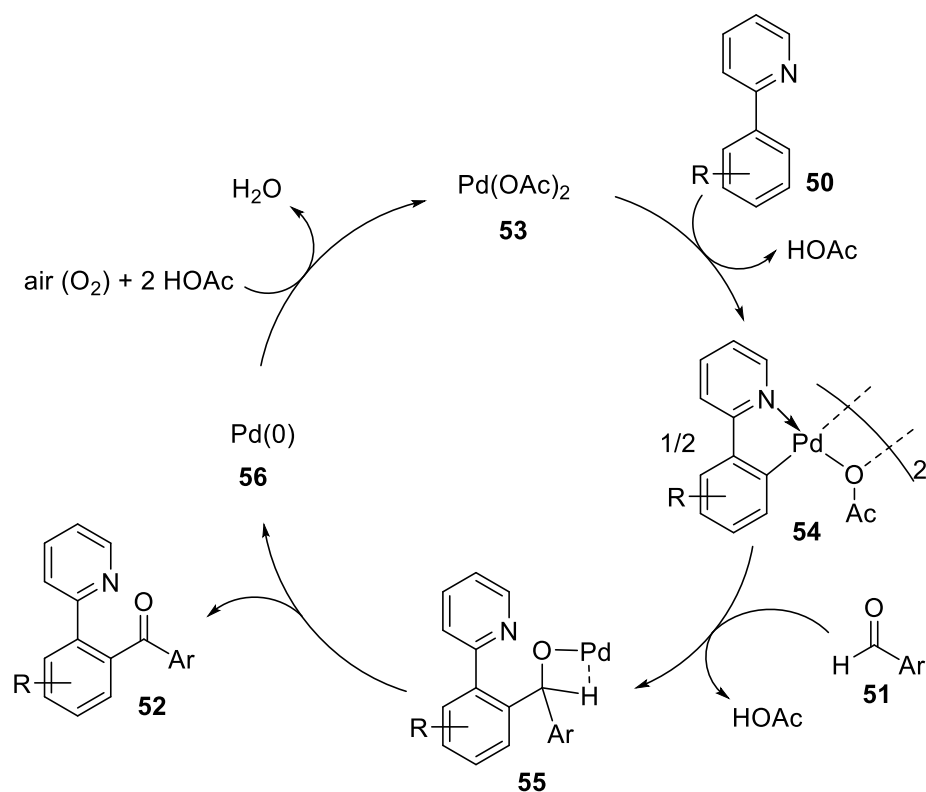
Scheme 1.12 Dehydrogenative polyheterocyclization 4-aniline substituted coumarins, quinolinones, and pyrones

1.1.3 Catalytic Oxidative Coupling of Aldehydes via C-H Bond Activation

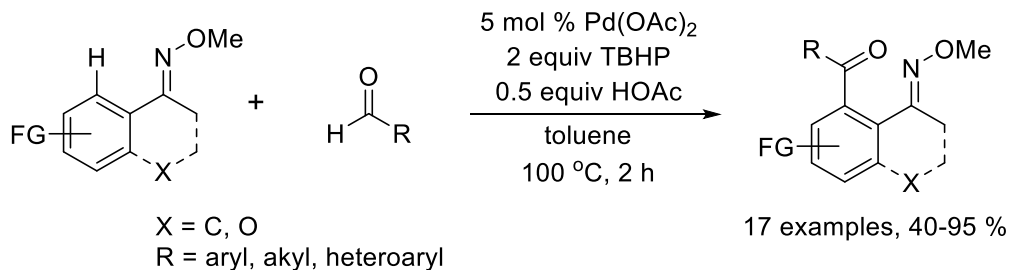
Transition metal catalyzed direct carbonylation via C-H bond activation is an attractive synthetic method in organic chemistry. In a pioneering study, Murai and co-workers developed $\text{Ru}_3(\text{CO})_{12}$ catalyzed acylation of imidazoles with CO and olefins.²⁸ In 2013, Beller and co-workers reported $[\text{RuCl}_2(\text{cod})]_n$ catalyzed C-C coupling of 2-phenylpyridine with CO and aryl halides to form benzophenones.²⁹ In both cases, the authors applied high pressure of CO gas (20-40 atm) to proceed their reactions. Recently, the acylation of arenes via direct aldehydic C-H bond activation has been developed, but most of the applications are limited to aromatic aldehydes.³⁰ For example, Cheng and co-workers reported palladium-catalyzed *ortho*-selective C-H acylation of arenes with aldehydes (eq 1.12).³¹ The reaction was carried out with 10 mol % of $\text{Pd}(\text{OAc})_2$ as the catalyst, 1:2 mol ratio of 2-phenylpyridine derivatives and aryl aldehydes in dry xylene at 120 °C using air as the optimal oxidant. The authors found a high degree of functional group tolerance on both starting materials. The electronic effect was not observed on 2-arylpyridines for both electron-donating and electron-withdrawing substituents. However, the reaction efficiency was sensitive to the electronic nature on aryl aldehyde substituents. Electron-withdrawing groups on the phenyl ring of benzaldehyde gave higher yields than benzaldehydes with electron-donating groups.



The proposed mechanism involves a chelate-directed C-H activation of 2-phenylpyridine to form a cyclopalladated complex **54**. To support this initial step, the authors were able to isolate and characterize the palladacycle complex **54**, which showed the same catalytic activity as Pd(OAc)₂ catalyst **53**. Insertion of C=O bond of aldehyde into C-Pd bond gives palladium complex **55**, and the consequent β -H elimination forms the product **52** and Pd(0) species **56**. The Pd(0) species is reoxidized by air to regenerate the Pd(II) catalyst **53**.

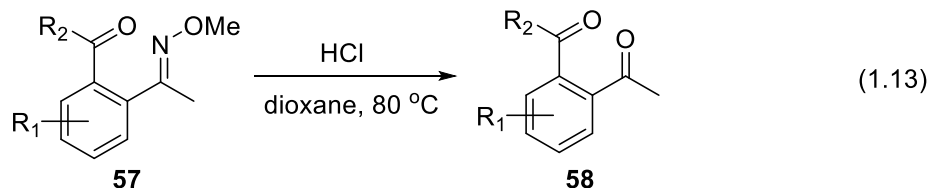


Scheme 1.13 Proposed mechanism for Pd-catalyzed oxidative *ortho*-acylation of 2-phenylpyridines with aryl aldehydes

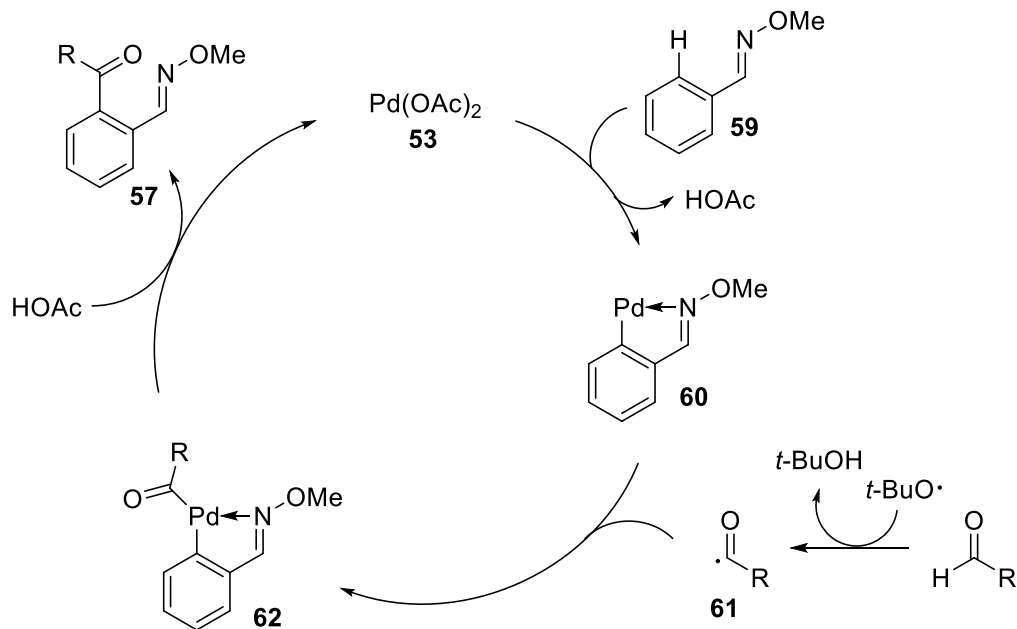


Scheme 1.14 Pd-catalyzed cross-coupling of aryl ketone *O*-methyl oximes with aldehydes

In 2010, Yu and co-workers reported Pd-catalyzed *ortho*-acylation of aryl-substituted oximes with aldehydes (Scheme 1.14).³² The reaction was carried out with 5 mol % of Pd(OAc)₂, 0.5 equivalent of acetic acid (HOAc), and 2 equivalents of *tert*-butyl hydroperoxide (TBHP) in toluene at 100 °C for 2 h. The oxime was found to be an effective directing group for the *ortho*-acylation reaction. Moreover, the treatment of *ortho*-acylated product **57** with HCl/dioxane provided oxime deprotected 1,4-diketone product **58** (eq 1.13).

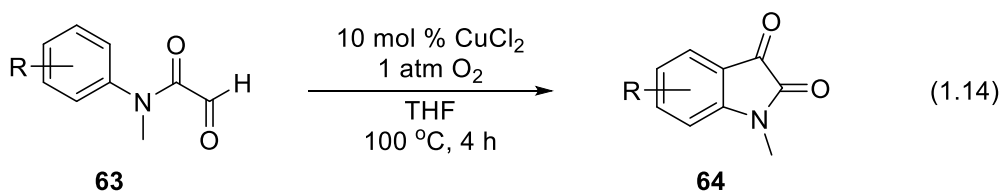


tert-Butyl hydroperoxide (TBHP) was found to be an optimal oxidant. The authors proposed a radical pathway involving hydrogen abstraction from the aldehyde, because dramatic decrease in reaction yields was observed in the presence of a radical scavenger such as ascorbic acid. Also, the reaction did not produce the product in the absence of TBHP.



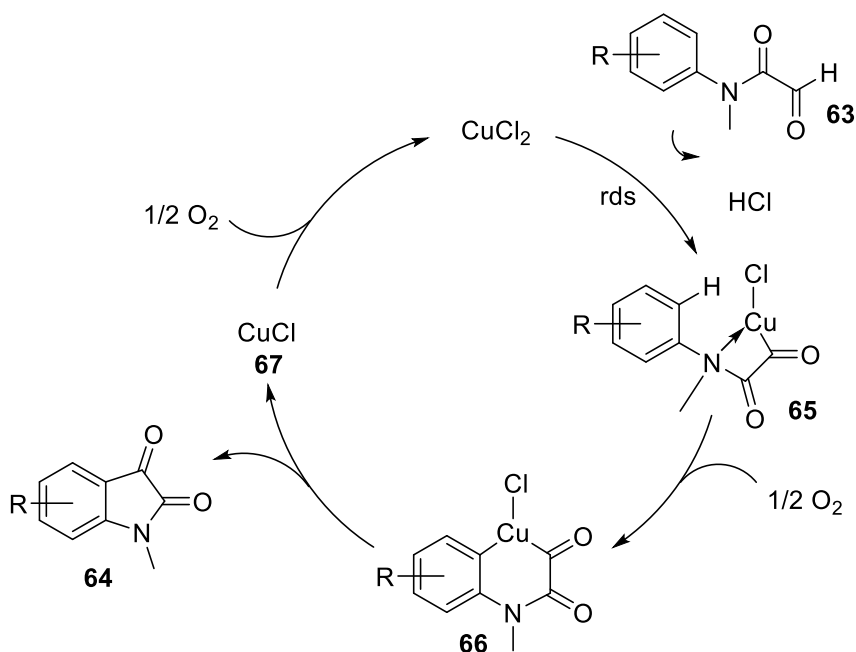
Scheme 1.15 Proposed mechanism for Pd-catalyzed *ortho*-acylation of aryl oxime with aldehydes

A proposed mechanism involving radical pathway is shown in Scheme 1.15. The reaction is initiated by chelate-assisted *ortho*-selective cyclopalladation on the substrate **59** by Pd(OAc)₂ catalyst. The palladacycle intermediate **60** reacts with acyl radical **61** to produce putative Pd(III) or Pd(IV) complex **62**. The acyl radical is generated in situ by hydrogen abstraction of aldehyde by using TBHP. The Pd complex intermediate **62** undergoes reductive elimination to form the active catalyst **53**.



Recently, Li and co-workers demonstrated Cu-catalyzed intramolecular oxidative acylation of formyl-*N*-arylformamides (**63**) to produce indoline-2,3-diones (**64**) using O₂

as the terminal oxidant (eq 1.14).³³ A 10 mol % of CuCl₂ with 1 atm of O₂ offered the optimal reaction condition at 100 °C for 4 h. Substrates with a variety of functional substituents on aromatic ring were tolerated under the reaction conditions. The electron density of the substituents at the para position was found to affect the reaction. The desired products were obtained when the electron-donating or weak electron-withdrawing group is attached to the aromatic ring.



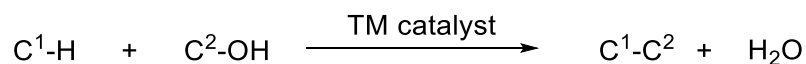
Scheme 1.16 Proposed mechanism for Cu-catalyzed intramolecular acylation of formyl-*N*-arylformamides

The authors proposed a possible mechanism as shown in Scheme 1.16. First, C-H bond activation of aldehyde generates copper(II) complex intermediate **65** by releasing HCl. Subsequent arene C-H activation produces Cu(III) intermediate **66**. The intermediate then undergoes reductive elimination to yield heterocyclic product **64** and Cu(I) species **67**. The formation of intermediate **65** and **66** was supported by the detection of C=O peak from FTIR spectroscopy. Based on the kinetic isotope effect study (k_H/k_D (monodeuterated

aldehyde) = 2.4), the authors suggested that the aldehyde C-H bond activation is the rate-limiting step.

1.2 Catalytic Dehydrative Cross-Coupling Reactions via C-H and C-O Bond Activation

From the viewpoint of green and sustainable chemistry, atom economical C-C bond formation methods have emerged as an attractive strategy in terms of minimizing reagents and corresponding waste products. Transition metal catalyzed cross-dehydrogenative coupling (CDC) method has become one of the most active area in research, which renders the formation of C-C bond from two different C-H bond activations, with H₂ as the only byproduct. Despite the significant advances in eco-friendly chemistry, many oxidative C-C formation methods still require stoichiometric oxidants or hydrogen acceptors. One of the ideal scenarios would be to employ catalytic cross-dehydrative coupling via C-H and C-OH bond activations. The attractive features of this method are the direct use of inexpensive and broadly available alcohols as coupling partner, and water is the only byproduct (Scheme 1.17). Although the transition metal catalyzed cross-dehydrative coupling reaction has been recognized as environmentally and economically impeccable strategy in recent years, this novel protocol has been rarely explored in synthetic chemistry.³⁴

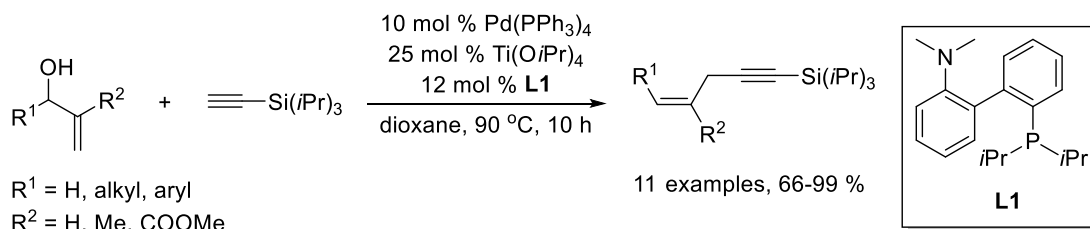


Scheme 1.17 Transition metal catalyzed cross-dehydrative coupling reactions

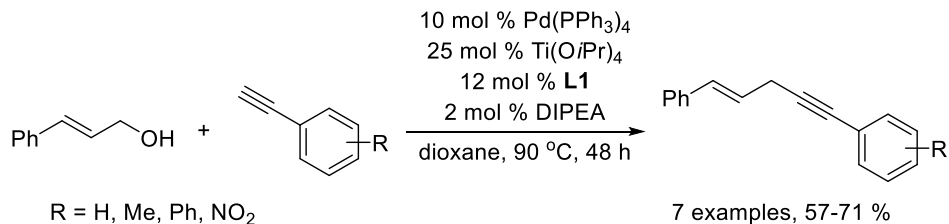
1.2.1 Catalytic Dehydrative Reaction of Allylic Alcohols

The palladium catalyzed allylation of carbon nucleophiles with allylic compounds (Tsuji-Trost reaction) is an important synthetic method in organic chemistry.³⁵ However, very few articles have been reported on using allylic alcohols in Tsuji-Trost reaction because the alcohol hydroxy group has very poor leaving ability.³⁶ Ozawa and co-workers reported allylation of anilines with allyl alcohols by using the π -allyl palladium complexes bearing diphosphinidene-cyclobutene ligands (DPCB-Y).³⁷ Mechanistic studies revealed that the C-O bond cleavage is the rate-determining step in these reactions. Li and co-workers have developed a palladium catalyzed direct dehydrative coupling of terminal alkynes with allylic alcohols.³⁸ A series of 1,4-enyne derivatives could be obtained from the reaction of (triisopropylsilyl)acetylene with Morita-Baylis-Hillman (MBH) alcohols in the presence of Pd(PPh₃)₄, N,P-ligand **L1**, and Ti(OiPr)₄ (Scheme 1.18a). For the reaction between cinnamyl alcohol and arylacetylenes, catalytic amount of diisopropylethylamine (DIPEA) was employed to activate the alkynyl C-H bond (Scheme 1.18b). The authors proposed a plausible mechanism for this reaction as shown in Scheme 1.19. The initial activation of allylic alcohol by Ti(OiPr)₄ generates allylic titanate **67**, which reacts with Pd(0)/**L1** species to give π -allylpalladium intermediate **68**. The subsequent deprotonation of terminal alkyne by assistance of **L1** and base forms an intermediate **69** and water. The reductive elimination of **69** furnishes the 1,4-enyne product and regenerates the palladium catalyst for the next catalytic cycle.

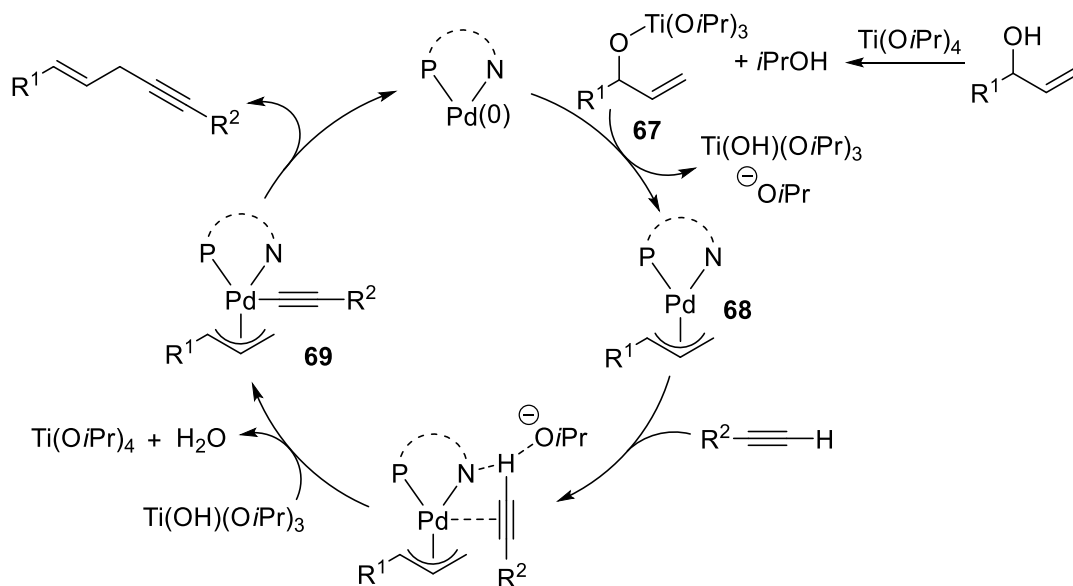
(a) Reaction between MBH alcohols and (triisopropylsilyl)acetylene



(b) Reaction between cinnamyl alcohol and arylacetylenes



Scheme 1.18 Pd-catalyzed dehydrative coupling of allyl alcohols with alkynes



Scheme 1.19 Proposed mechanism for the dehydrative coupling of terminal alkynes with allylic alcohols

Reek and co-workers reported palladium catalyzed dehydrative cross-coupling reaction between allylic alcohols and styrenes without using any stoichiometric additives.³⁹

The cationic palladium(II) complex **70** was identified as an effective catalyst to form π -

allyl palladium species (Figure 1.3), while other neutral palladium(II) or palladium(0) complexes failed to show any activities. The treatment of cinnamyl alcohol with styrene derivatives in the presence of 3 mol % Pd complex **70** in dioxane at 120 °C formed the corresponding linear 1,4-diene products (Scheme 1.20a). In case of the coupling reaction between methyl substituted aliphatic allyl alcohols and styrene derivatives, two regioisomers were formed depending on the allyl alcohol substrates (Scheme 1.20b). The authors explained that these two products were generated by the isomerization of π -allyl palladium intermediate involving β -hydride elimination.

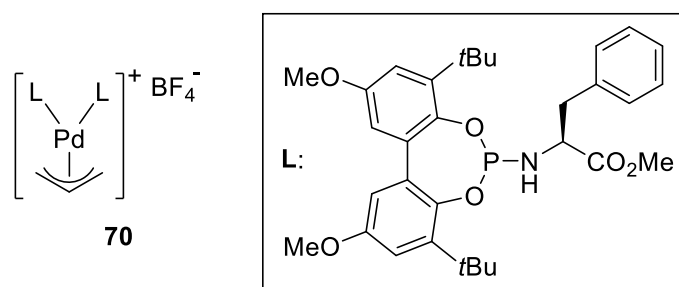
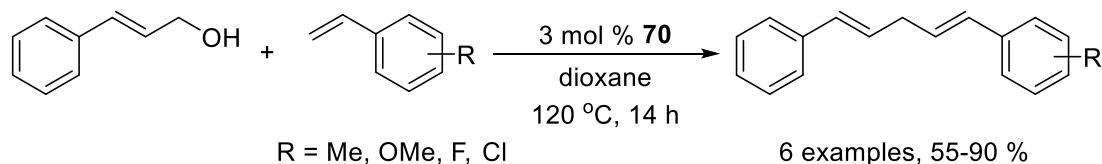
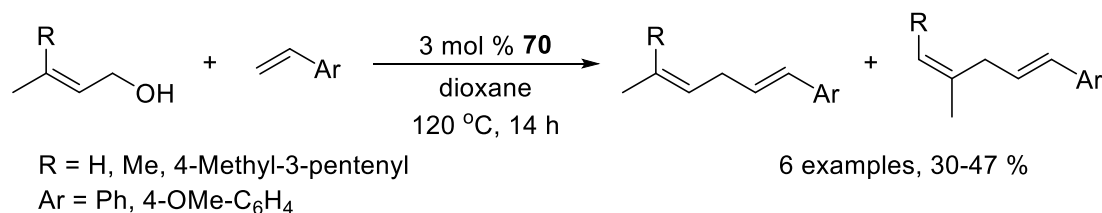


Figure 1.3 Cationic palladium(II) complex **70**

(a) Cross-coupling of cinnamyl alcohol with styrenes



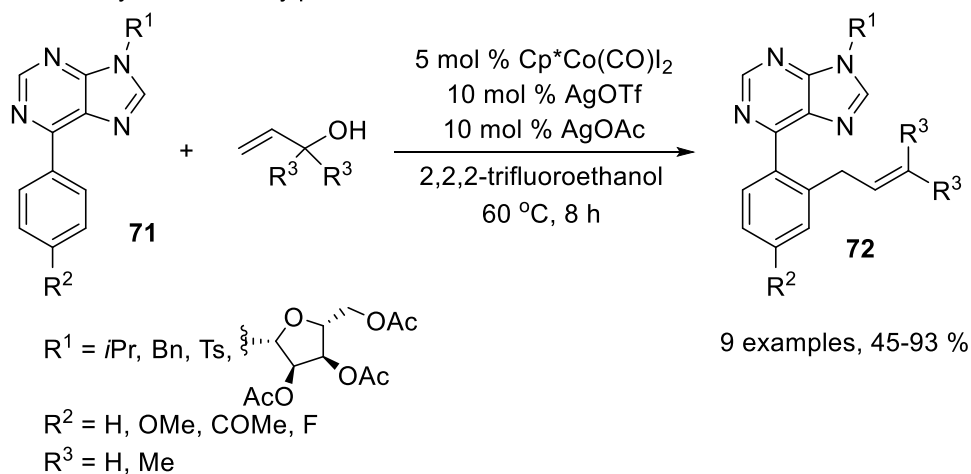
(b) Cross-coupling of aliphatic allyl alcohol with styrenes



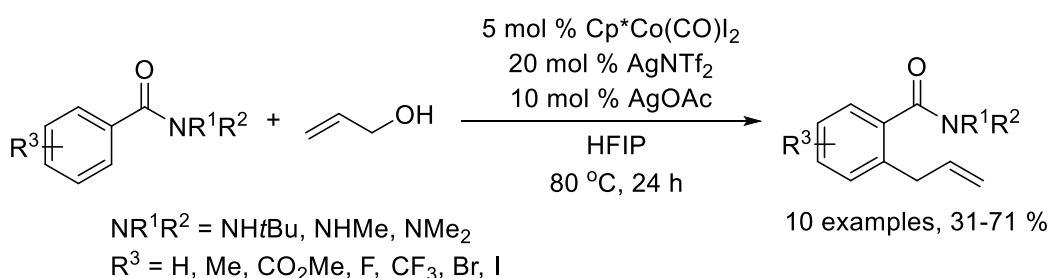
Scheme 1.20 Pd-catalyzed dehydrative coupling of allyl alcohols with styrenes

Although the Pd-catalyzed C-O activation of allyl alcohol via formation of π -allylpalladium species has been shown to be an efficient method, the catalytic cross-dehydrative C-H allylation reactions can also be achieved by different transition metals such as cobalt and ruthenium. In these cases, the C-O activation occurs through β -hydroxy elimination rather than the formation of π -allylmetal species.

(a) Dehydrative allylation of 6-arylpurines



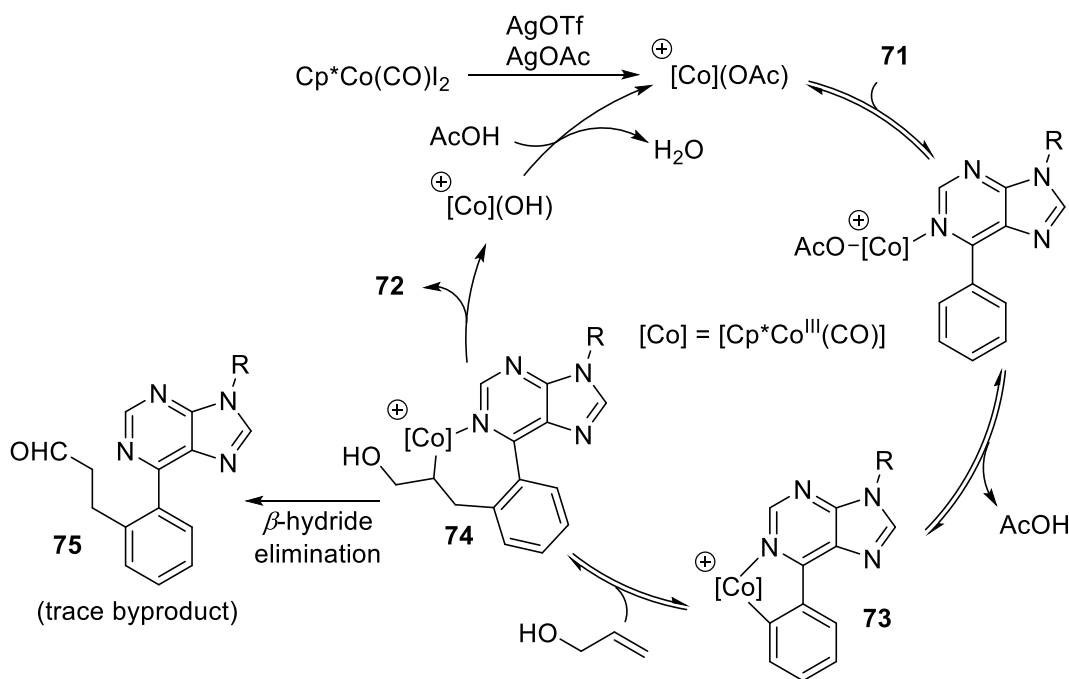
(a) Dehydrative allylation of benzamides



Scheme 1.21 Co-catalyzed dehydrative C-H *ortho*-allylation of arenes

Very recently, Yoshino and Matsunaga reported cobalt catalyzed C-H allylation of 6-arylpurines and aryl amides with allyl alcohols.⁴⁰ The reaction of purinyl arenes or benzamides with allyl alcohols catalyzed by $Cp^*Co(CO)I_2$, silver salt and base afforded *ortho*-allylated arenes in good yields at a moderate temperature (Scheme 1.21). During the

solvent screening, the authors found that fluorinated alcohols, 2,2,2-trifluoroethanol (TFE) and 1,1,1,3,3,3-hexafluoro-2-propanol (HFIP), are the most effective solvents for this catalytic system. A broad range of benzamides and *N*9-substituted purinyl derivatives (including fully acetylated 6-phenylpurine riboside) afforded the allylation product for this method.

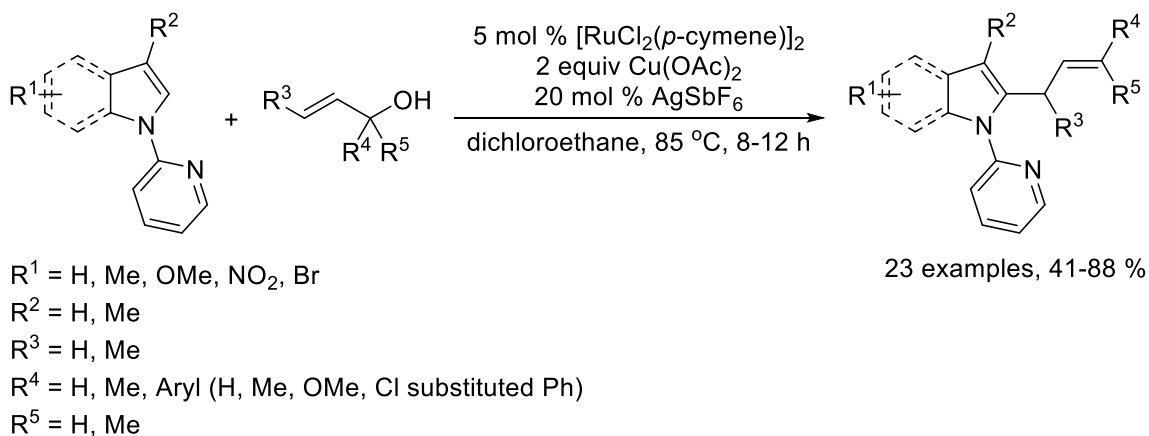


Scheme 1.22 Proposed mechanism for the dehydrative C-H allylation of 6-arylpurines

A plausible mechanism for the allylation of 6-arylpurine **71** is shown in Scheme 1.22. The active cationic cobalt species would be generated from $\text{Cp}^*\text{Co}(\text{CO})\text{I}_2$, AgOTf , and AgOAc . Coordination of **71** followed by acetate-assisted sp^2 -C-H activation gives 5-membered metallacycle complex **73**. Subsequent alkene insertion of allyl alcohol forms 7-membered metallacycle intermediate **74**. At this stage, β -hydroxy elimination is favored over the competing β -hydride elimination to release the desired allylation product **72** with

cationic cobalt hydroxo complex. The authors also observed a trace amount of aldehyde byproduct **75**, which was resulted from β -hydride elimination process.

Kapur and co-workers reported ruthenium catalyzed dehydrative C-H allylation of indoles with allyl alcohols.⁴¹ Coupling reaction of *N*-pyridinyl indoles with allyl alcohols in the presence of $[\text{RuCl}_2(p\text{-cymene})]_2$, $\text{Cu}(\text{OAc})_2$, and AgSbF_6 afforded C2-arylated indoles. In this protocol, pyridine served as a directing group for the regioselective C-H activation of indoles. The authors also demonstrated the removal of the pyridinyl directing group of the coupling products by simple reaction with MeOTf followed by base solution treatment. The proposed mechanism similarly follows Yoshino and Matsunaga's cobalt catalyzed allylation process.⁴⁰ Pyridine directed C-H activation of indole generates C2-metallated indole intermediate. Alkene insertion of allyl alcohol followed by β -hydroxy elimination gives the product.

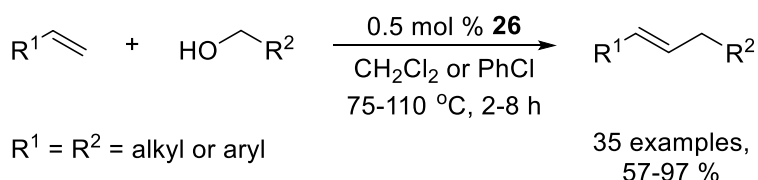


Scheme 1.23 Ru-catalyzed dehydrative C-H allylation of indoles

1.2.2 Catalytic Dehydrative Coupling Reaction of Aliphatic Alcohols

Catalytic dehydrative C-C coupling reactions involving C-O bond cleavage of unactivated aliphatic alcohols are very difficult to achieve because it is thermodynamically less favorable than alkoxylation or dehydrogenation of alcohols (C-O bond dissociation energy = 85 to 91 kcal·mol⁻¹).⁴² Recently, a number of ruthenium complexes have been successfully employed for the selective activation of challenging sp³ C-O bond activation of alcohols.

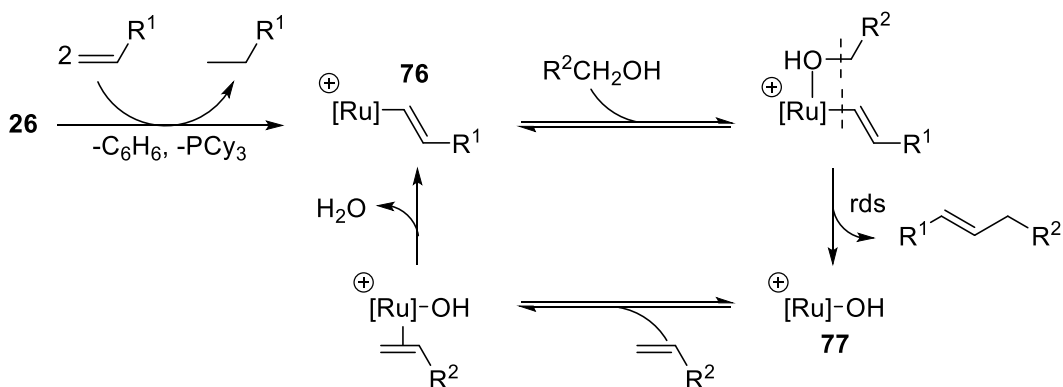
In 2011, our group reported ruthenium catalyzed dehydrative C-H alkylation of alkenes with alcohols.⁴³ The coupling reaction employed 0.5 mol % cationic Ru-H complex [(C₆H₆)(PCy₃)(CO)RuH]⁺BF₄⁻ (**26**) at 75-110 °C without using any additives. The catalytic method tolerated a broad range of alcohol and alkene (including cycloalkenes, indene, *N*-methylindole, 2,3-dihydrobenzofuran, and styrene derivatives) substrates with high product yields. The catalytic method was successfully applied to several biologically active alkenes to demonstrate high regioselectivity and functional group tolerance.



Scheme 1.24 Ru-catalyzed dehydrative alkylation of alkenes with alcohols

The preliminary mechanistic studies were inconsistent with the Friedel-Crafts-type electrophilic substitution reactions. For example, an opposite trend in reactivity of alcohols (1° > 2° > 3°) was observed from the initial rate comparison study of the alkylation reaction of primary, secondary, and tertiary alcohols. A plausible mechanism is proposed in Scheme

1.25. A cationic Ru-alkenyl species **76** is generated by the initial alkene insertion, vinylic C-H activation, and alkane elimination sequence. Coordination of an alcohol to the ruthenium center followed by oxidative addition of the C-O bond would give cationic Ru(IV)-alkenyl-alkyl species, which liberates the alkene alkylation product to form the coupling product and forms Ru-hydroxo intermediate **77** by reductive elimination. Another vinylic C-H activation and subsequent water elimination regenerates the Ru-alkenyl species **76**.

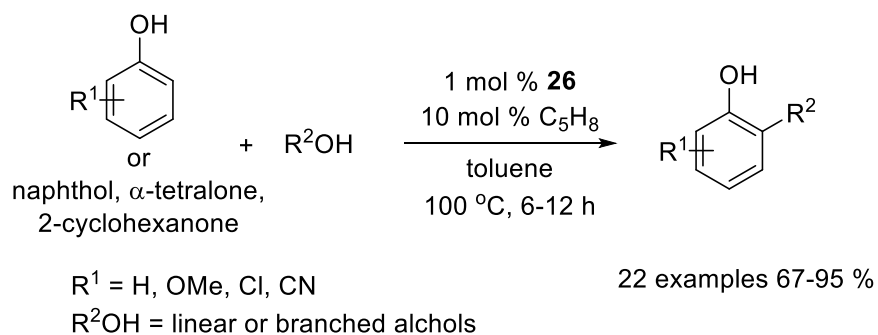


Scheme 1.25 A plausible mechanism for the dehydrative C-H alkylation of alkenes

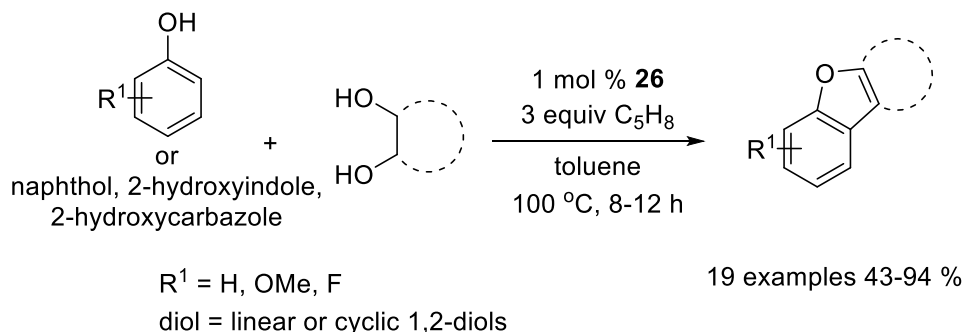
The well-defined cationic ruthenium hydride complex $[(C_6H_6)(PCy_3)(CO)RuH]^+BF_4^-$ complex (**26**) has been found to exhibit exceptional catalytic activity for C-O bond activation of alcohols. Our group also developed the ruthenium catalyzed dehydrative C-H alkylation and alkenylation of phenols with alcohols without using any expensive or toxic metal oxides.⁴⁴ The initial reaction of 3-methoxyphenol with cyclohexanol in the presence of 1 mol % **26** and a catalytic amount (10 mol %) of cyclopentene in toluene at 100 °C resulted in the formation of highly regioselective *ortho*-cyclohexylphenol product along with a trace amount of *ortho*-cyclohexenylphenol product. Notably, synthetically more useful *ortho*-alkenylated phenols

can also be obtained as the major product in this catalytic protocol by simply adding excess (3.0 equivalents) amount of cyclopentene. A series of benzofuran derivatives was formed when 1,2-diol was used as the coupling partner (Scheme 1.26b). The catalytic method was successfully extended to bioactive phenol and alcohol substrates such as cholesterol, estrone, coumarine derivatives to produce the corresponding *ortho*-alkylated phenol or benzofuran compounds in good to excellent yields (67-91 %).

(a) Dehydrative *ortho*-C-H alkylation of pheols with alcohols



(a) Dehydrative *ortho*-C-H alkenylation and cyclization of pheols with diols

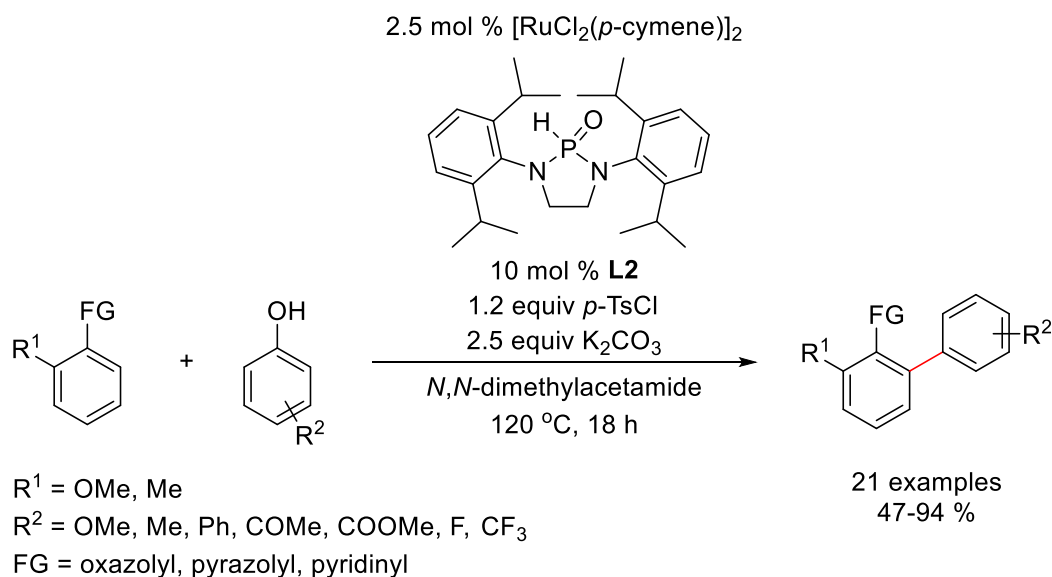


Scheme 1.26 Ru-catalyzed dehydrative synthesis of *ortho*-alkylated phenols and benzofurans

The possible mechanistic pathway of the dehydrative *ortho*-alkylation of phenols involves the initial formation of cationic *ortho*-ruthenated phenol species by *ortho*-C-H activation of phenol. Subsequent C-O bond oxidative addition of alcohol followed by

reductive elimination of product to form the Ru-hydroxo species, which then reacts another phenol and releases water. The deuterium labeling experiment, Hammett plot, and kinetic isotope effect studies were conducted, and these results supported the proposed mechanism.

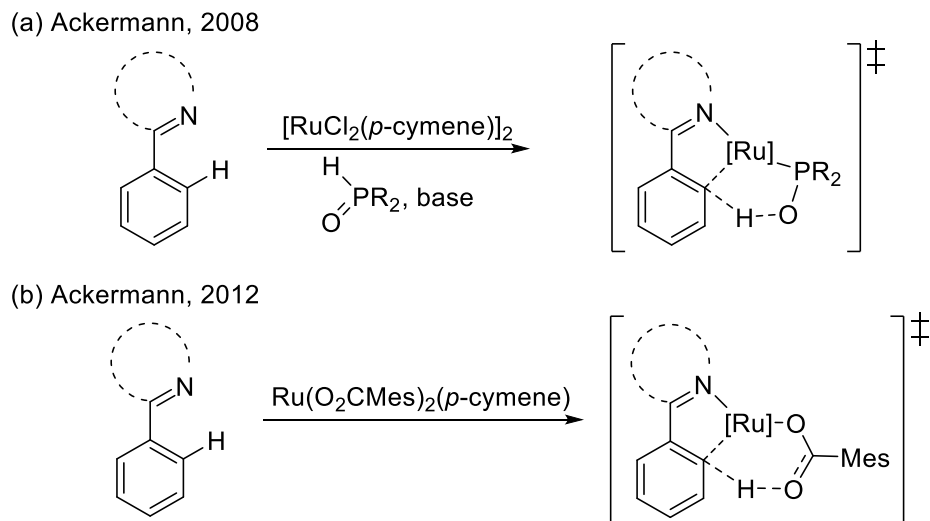
1.2.3 Dehydrative Arene C-H Coupling Reactions



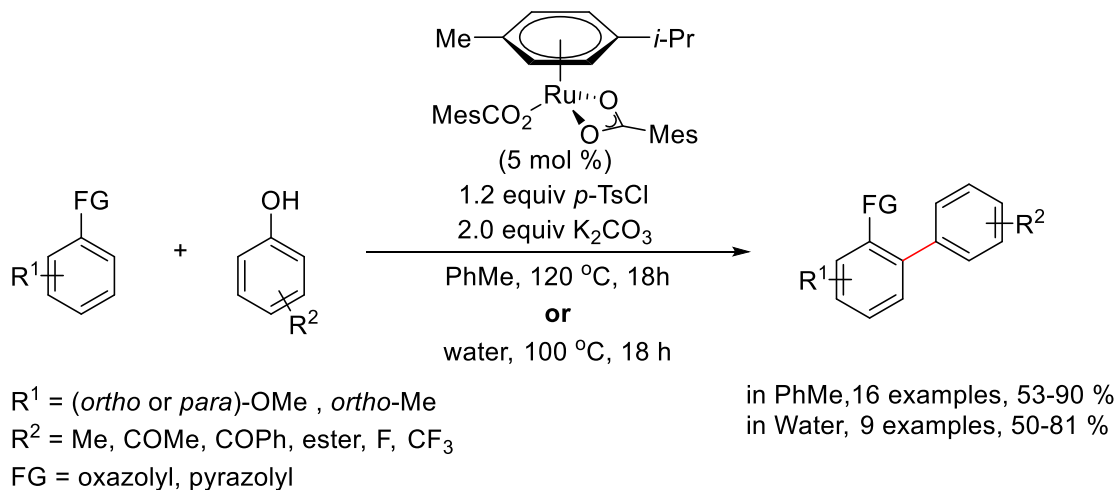
Scheme 1.27 Ru/**L2**-catalyzed dehydrative biarylation of arenes with phenols

In 2008, Ackermann and co-workers have developed the ruthenium catalyzed cross-dehydrative biarylation reactions by using inexpensive phenols as the starting materials.⁴⁵ As shown in Scheme 1.27, chelate-assisted C-H arylation of *ortho*-oxazolyl and pyrazolyl arenes with a variety of substituted phenols was achieved in the presence of $[\text{RuCl}_2(p\text{-cymene})]_2$, ligand **L2**, K_2CO_3 , and 4-toluenesulfonyl chloride (*p*-TsCl). In this study, the air-stable ligand precursor, heteroatom-substituted secondary phosphine oxide (HASPO, **L2**), was shown to be more efficient than simple tertiary phosphine ligands. To explain high catalytic efficacy of HASPO, the authors proposed base-assisted

cyclometalation-deprotonation model in the C-H bond activation transition state (scheme 1.28a).^{5(f)} The catalytic system was successful with a wide range of phenol substrates bearing ether, ester, alkyl, and fluorides.



Scheme 1.28 Proposed transition states for the *ortho*-arene arylations



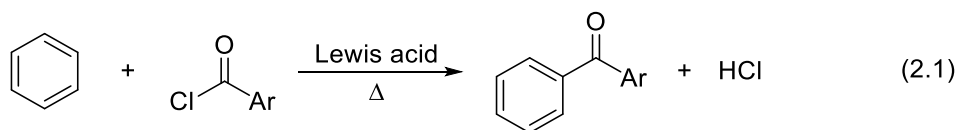
Scheme 1.29 Ru-catalyzed dehydrative biarylation of arenes with phenols

Ackermann's group later modified this dehydrative *ortho*-arene arylation by employing the well-defined $\text{Ru}(\text{O}_2\text{CMes})_2(p\text{-cymene})$ catalyst without using any external ligands (Scheme 1.29).⁴⁶ They have found that ruthenium(II) carboxylates are powerful

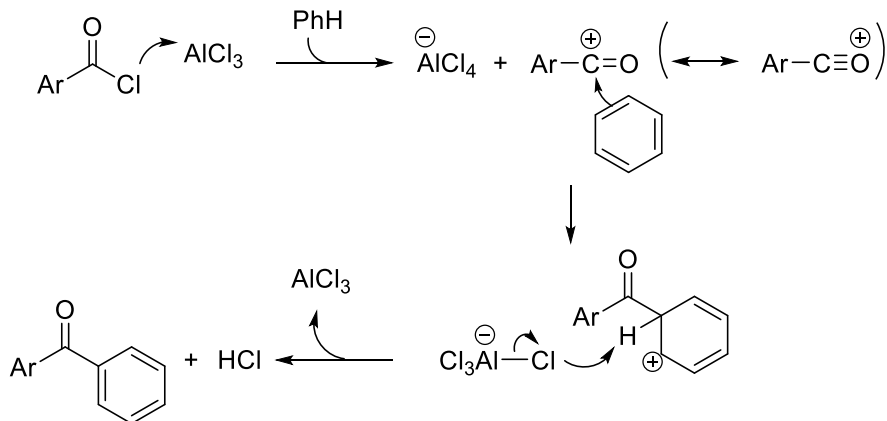
catalysts for the direct C-H arylation reaction,^{5(f),47} which could successfully replace the *in situ* generated ruthenium complexes derived from HASPO ligand (Scheme 1.28b). Notably, this catalytic system could also be performed in water at a lower reaction temperature.

In conclusion, transition metal-catalyzed dehydrogenative and dehydrative coupling reactions have received considerable interest in recent years. A number of catalytic methods have greatly advanced synthetic strategies for the economically and environmentally sustainable formation of the C-C coupling products. Although the direct activation of C-H and C-O bond allows a broad range of available substrates without preforming reactive functional groups, these methods often require relatively harsh conditions and a stoichiometric amount of additives. Thus, the development of efficient catalytic methods with high regioselectivity remains a long term challenge to subjugate. In this context, our research group have developed a number of dehydrogenative and dehydrative C-H coupling reaction by using well-defined cationic ruthenium-hydride catalyst **26**. The recent synthetic and mechanistic studies of dehydrogenative and dehydrative coupling reactions will be presented in the following chapters.

CHAPTER 2

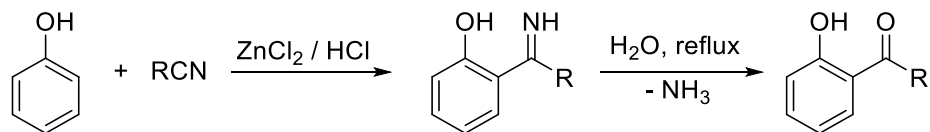
**Ruthenium Catalyzed Dehydrogenative *ortho*-Acylation of Phenols with Aldehydes
via C-H Activation****2.1 Backgrounds****2.1.1 Traditional Acylation Methods**

Aryl ketones are common structural motifs present in biologically active compounds and pharmaceutical agents. Traditionally, Friedel-Crafts acylation method has been commonly used for installing acyl groups to aromatic rings by using strong Lewis acid catalysts (AlCl_3 , FeCl_3).⁴⁸ The general reaction conditions of the Friedel-Crafts acylation facilitates the coupling of arene with acyl chloride in the presence of Lewis acid to give an acylated arene product along with a hydrochloric acid byproduct (eq 2.1). The reaction mechanism involves the initial formation of the acyl cation by the Lewis acid-mediated halide dissociation. The acyl cation can be stabilized by its acylium ion resonance structure, thus other acylium sources such as acid anhydrides can also be used for this reaction. The nucleophilic attack of π -electrons on the benzene to the electrophilic acyl cation forms the cyclohexadienyl cation intermediate by breaking aromaticity. The subsequent dehydrogenation by tetrachloroaluminate provides acylated product and HCl.



Scheme 2.1 Reaction mechanism of the Friedel-Crafts acylation

Hoesch and Houben have reported the formation of 2-acylphenols from the reaction of phenols with nitriles by using ZnCl_2 catalyst and HCl (Scheme 2.2).⁴⁹ This is similar to Friedel-Crafts acylation reaction, and the ketimine can be isolated as an intermediate product via nucleophilic attack on the nitrile electrophile by π -electrons of phenols. The ketimine is subsequently hydrolyzed by aqueous workup to afford 2-acylphenols.

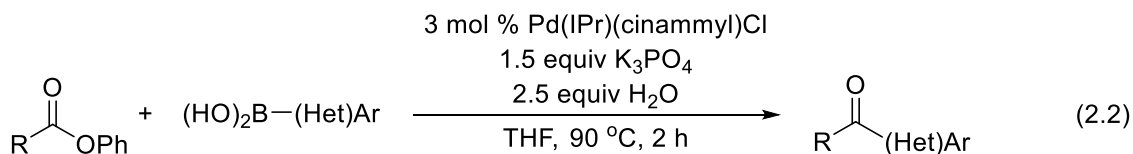


Scheme 2.2 The reaction pathway of the Houben-Hoesch reaction

Despite of its convenient process to produce acylated arenes, these Friedel-Crafts type of coupling methods possess a number of drawbacks and limitations. The reaction is problematic in controlling product regioselectivity and often results in multiple addition of electrophiles. Also, the reaction works only with benzene or activated arenes for the formation of dearomatized intermediate. Furthermore, employing toxic acyl halide or nitrile starting materials yields the corresponding wasteful byproducts.

2.1.2 Transition Metal-Catalyzed Acylation Methods

Much research has been devoted to the development of transition metal catalyzed carbonyl functionalization of arenes via C-H bond activation. In particular, Pd-catalyzed arene carbonylation methods have greatly advanced synthetic potency for forming acyl-substituted arene compounds.⁵⁰ Recently, Newman and Houk reported Suzuki-Miyaura coupling of aryl esters with arylboronic acids (eq 2.2).⁵¹ The NHC-based Pd catalyst enabled the formation of acylated products via C(aryl)-O activation. However, these catalytic methods typically require prefunctionalized starting materials, which lead to the formation of wasteful byproducts.

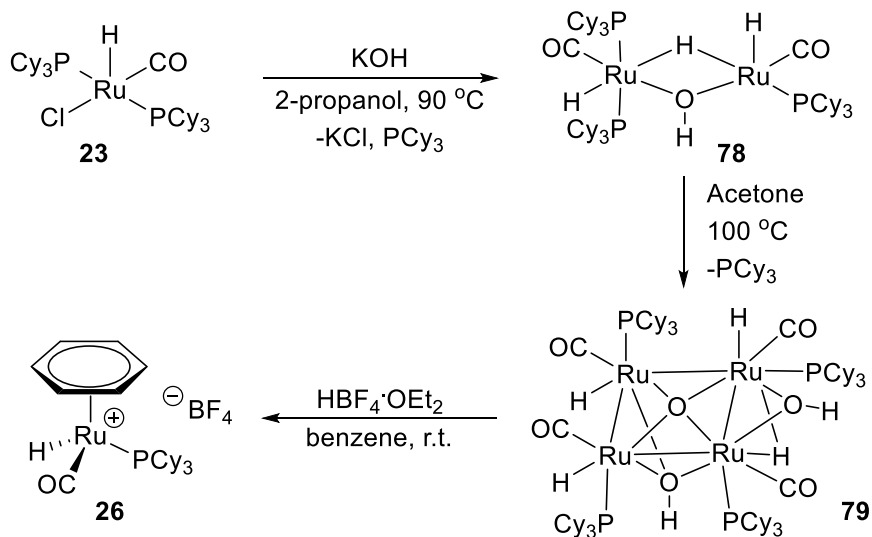


From the viewpoint of step efficient and environmentally compatible synthesis, catalytic C-H oxidative coupling reaction of unactivated arenes with aldehydes is a promising method for the synthesis of aryl ketones. Li and co-workers reported Cu-catalyzed intramolecular arene-to-aldehyde coupling reaction to form indoline-2,3-diones.³³ Cheng³¹ and Yu³² reported intermolecular C-H oxidative arene-aldehyde coupling reactions. These coupling methods are facilitated by directing groups for the regioselective C-H activation of arenes. In 2012, Wang and co-workers reported Cu-catalyzed *ortho*-acylation of a simple directing group phenol with aldehydes,⁵² but the scope of aldehyde substrates is limited to aromatic aldehydes.

2.2 Results and Discussion

Recently, our research group developed the synthesis of a well-defined cationic ruthenium-hydride complex $[(\eta^6\text{-C}_6\text{H}_6)(\text{PCy}_3)(\text{CO})\text{RuH}]^+\text{BF}_4^-$ (**26**). The complex **26** was found to be a highly effective catalyst precursor for a number of dehydrogenative and dehydrative C-C bond formation reactions. The cationic ruthenium-hydride complex was synthesized in three steps from ruthenium-hydride complex $(\text{PCy}_3)_2(\text{CO})\text{RuHCl}$ (**23**) as described in Scheme 2.3.^{15,53} Treatment of **23** with KOH in 2-propanol at 90 °C formed the dinuclear Ru complex **78**, which was isolated in 85% yield after recrystallization in hexane. The tetranuclear Ru complex $\{[(\text{PCy}_3)(\text{CO})\text{RuH}]_4(\mu\text{-O})(\mu\text{-OH})_2\}$ (**79**) was obtained in 80% yield as brown-red solid from the reaction of **78** with wet acetone at 100 °C. Subsequent treatment of **79** with one equivalent of $\text{HBF}_4\cdot\text{OEt}_2$ in benzene at room temperature cleanly afforded the cationic ruthenium-hydride complex **26**, which was isolated as an ivory solid in 90% yield.

The molecular structure of the cationic ruthenium-hydride complex was elucidated by NMR spectroscopy and X-ray crystallography (Figure 2.1). In ^1H NMR, the metal-hydride signal was observed at δ -10.39 (d, $J_{\text{PH}} = 25.9$ Hz) in CD_2Cl_2 , and a single phosphine signal was detected by ^{31}P NMR at δ 72.9 ppm. The X-ray crystallography showed a three legged piano-stool geometry, which is capped by a η^6 -benzene moiety.



Scheme 2.3 Synthesis of cationic ruthenium-hydride complex **26**

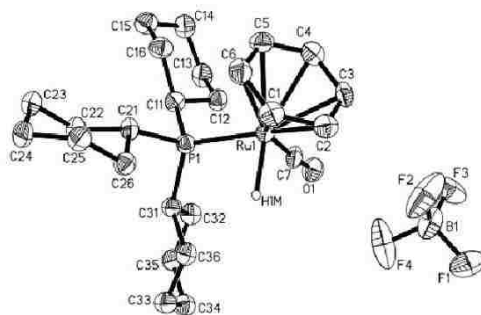
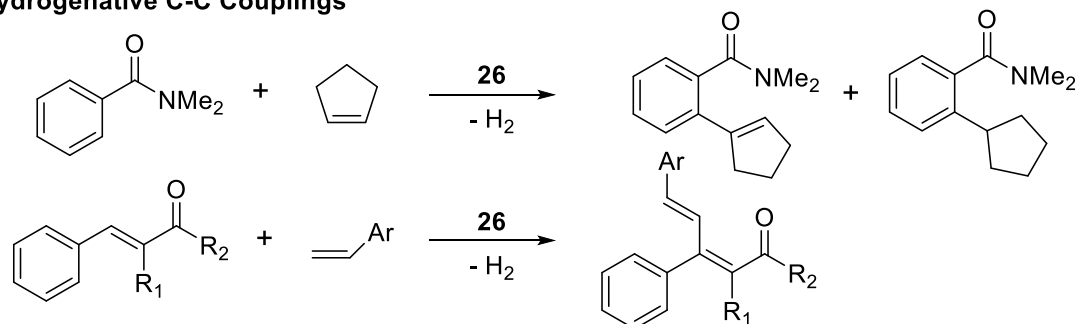


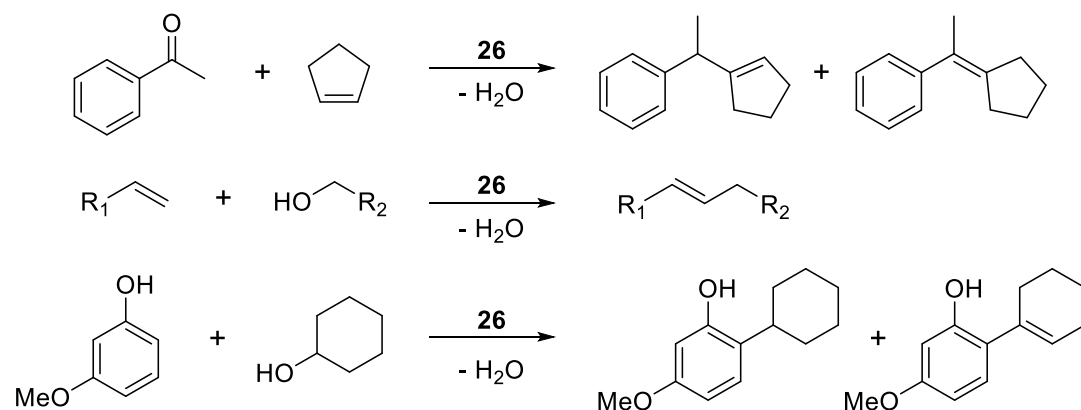
Figure 2.1 Molecular geometry of cationic ruthenium-hydride complex **26**

We found that the cationic ruthenium-hydride complex **26** is a highly effective catalyst for a number of dehydrogenative and dehydrative coupling reactions involving C-H and C-O bond activation. By using the cationic ruthenium-hydride complex **26**, we achieved the chelate-assisted oxidative coupling reaction of arylamides and with unactivated alkenes,¹⁵ the coupling reaction of α,β -unsaturated carbonyl compounds with alkenes,⁵⁴ the coupling reaction of aryl ketones with cyclic alkenes,⁵³ selective catalytic alkylation of alkenes with alcohols,⁴³ and the C-H alkylation and alkenylation of phenols with alcohols⁴⁴ (Scheme 2.4).

Dehydrogenative C-C Couplings

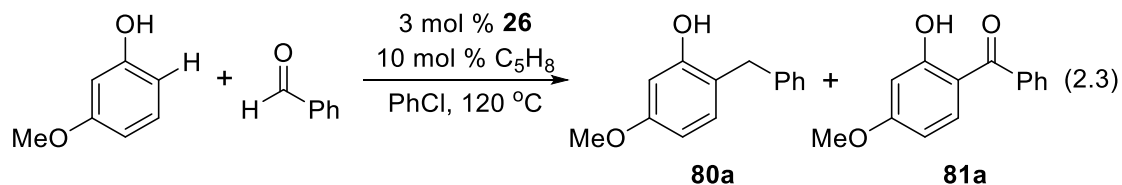


Dehydrative C-C Couplings

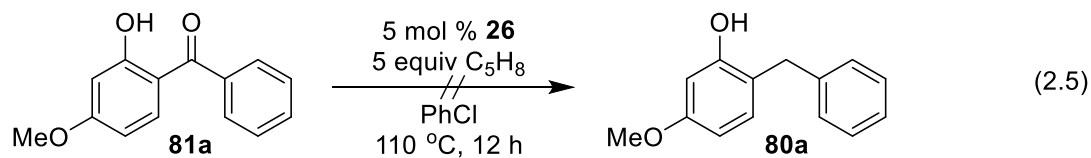
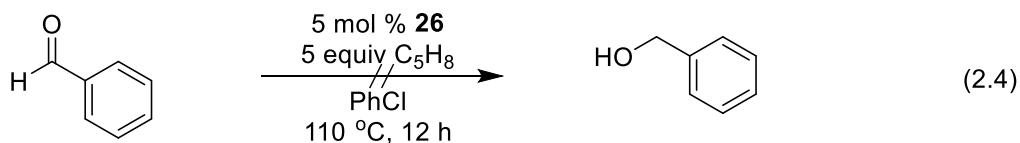


Scheme 2.4 Dehydrogenative and dehydrative coupling reactions mediated by Ru catalyst

We next explored its catalytic activity for the dehydrogenative coupling reaction of phenols and aldehydes. Initially, we found that $[(\eta^6\text{-C}_6\text{H}_6)(\text{PCy}_3)(\text{CO})\text{RuH}]^+\text{BF}_4^-$ (**26**) catalyzes the reaction of 3-methoxyphenol with benzaldehyde in the presence of catalytic amount (10 mol %) of cyclopentene in chlorobenzene at 120 °C to form a 1:1 mixture of 2-benzyl-3-methoxyphenol (**80a**) and 2-hydroxy-4-methoxybenzophenone (**81a**), but with only ca. 20 % of the combined yield (eq 2.3).



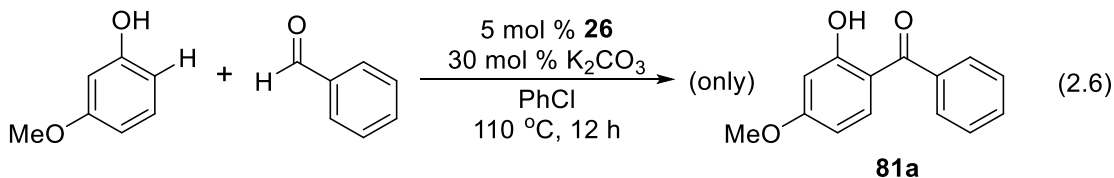
The *ortho*-alkylated phenol **80a** was formed apparently from the elimination of an equivalent of water molecule. Two catalytic *ortho*-phenol C-H activation pathways can be proposed to explain the formation of the alkylated product **80a**. Our group has demonstrated a broad scope of the dehydrative alkylation of phenols with alcohols as indicated above (Scheme 2.4).⁴⁴ One possible path involves the reduction of benzaldehyde to benzyl alcohol, followed by the dehydrative benzylation of phenol with newly generated alcohol. Second, we recently observed the hydrogenolysis of ketones or aldehydes by using cationic ruthenium-hydride complex **26** and phenol ligands with H₂.⁵⁵ The reaction is more environmentally friendly than the conventional Clemmensen reduction or Wolff-Kishner reduction methods. For this deoxygenation method, a catalytic amount of phenol was found to be an effective additive to promote the reaction. Similarly, the hydrogenolysis of ketone to alkane pathway might be feasible for the acylated product **81a** in the catalytic system. However, the hydrogen source was unclear in this case because both pathways require the same equivalent of H₂ to lose a water molecule. We performed the following experiments in order to discern the formation of **80a** (eq 2.4 and 2.5).



The treatment of benzaldehyde (0.5 mmol) with an excess amount of cyclopentene (5 equiv) in the presence of cationic ruthenium-hydride complex **26** (5 mol%) did not form

benzyl alcohol (eq 2.4). Also, the treatment of the acylated product **81a** (0.5 mmol) did not produce its deoxygenated product **80a** under the same reaction condition (eq 2.5). These results indicate that cyclopentene is not the hydrogen source. We believe that two products **80a** and **81a** were formed simultaneously in this case because a 1:1 ratio between two products was observed, and that the alkylation product **80a** was resulted from the coupling with the alcohol formed from the hydrogenation of aldehyde.

The *ortho*-acylated phenol product **81a** was obtained (11 % GC-MS yield) (eq. 2.3) from the dehydrogenative direct C-H acylation of aldehydes. Rather than consuming acyl halide and generating a stoichiometric amount of wastes, this catalytic method directly combines simple phenols and aldehydes to form the acylated product. Due to its synthetic importance for the oxidative C-C formation reactions via double C-H activation of two starting materials, we devoted much efforts to optimize the reactivity and selectivity pattern of acylated phenol product **81a**. First, the amount of cyclopentene was increased up to 10 equivalents from 3 equivalents, but there was no significant improvement on either reactivity or selectivity. Also, other alkenes such as cyclohexene, 1,4-cyclohexadiene, and 3,3-methyl-1-butene were found to be ineffective.



Instead, high selectivity for the *ortho*-acylation product was observed from the addition of an inorganic base K_2CO_3 (eq 2.6). With the addition of catalytic amount of K_2CO_3 (30 mol%), only the acylated product **81a** was obtained in a moderate yield (39 %

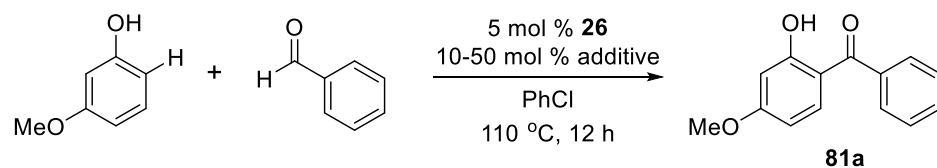
GC-MS yield). Although K_2CO_3 has a poor solubility in chlorobenzene, the addition of water did not improve the efficiency of the reaction. Since the catalytic dehydrogenative C-H acylation reaction of phenols with aliphatic aldehydes has not been reported, we further investigated the reaction scope of phenols with aliphatic aldehydes.

2.3 Optimization Studies

2.3.1 Additive Effect

The additive effect was found to be critical for increasing the reactivity and selectivity of the catalytic C-H acylation reaction. A variety of inorganic bases was screened for the reaction of 3-methoxyphenol (0.5 mmol) and benzaldehyde (1.0 mmol) in the presence of the cationic ruthenium-hydride complex **26** in chlorobenzene at 110 °C for 12 h (Table 2.1). The product yield was determined by GC-MS.

We found that inorganic bases K_2CO_3 , Cs_2CO_3 , and KOH exhibit similar effect in promoting the selective formation of *ortho*-acylated phenol product **81a**, whereas other inorganic bases and triethylamine were ineffective. We have chosen K_2CO_3 as an appropriate additive over KOH due to a slightly increased yield. Also, K_2CO_3 was chosen rather than Cs_2CO_3 for this catalytic reaction due to its cost. The relative additive concentration effect was surveyed by changing the amount of base in the reaction mixture (entries 1, 10-12). About 30 mol % of K_2CO_3 was found to be optimal, as no significant increase in yield was observed when the additive loading was increased above 30 mol % (entry 12). Significantly less than a stoichiometric amount of base needed for the reaction suggests that the base takes role of activating the ruthenium catalyst.

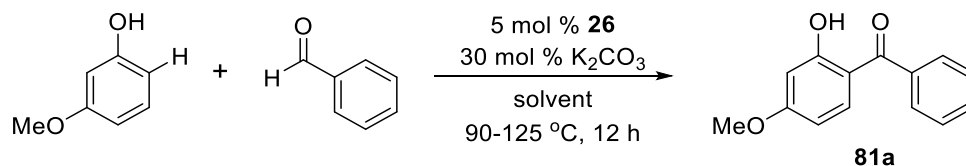
Table 2.1 Additive effect on the reaction of 3-methoxyphenol and benzaldehyde^a

entry	additive	loading (mol%)	81a ^b (%)
1	K ₂ CO ₃	30	39
2	Cs ₂ CO ₃	30	38
3	Na ₂ CO ₃	30	< 3
4	KHCO ₃	30	0
5	NaHCO ₃	30	0
6	NaOMe	30	0
7	NaOAc	30	0
8	KOH	30	33
9	NEt ₃	30	0
10	K ₂ CO ₃	10	16
11	K ₂ CO ₃	20	31
12	K ₂ CO ₃	50	38

^a Reaction conditions: 3-methoxyphenol (0.5 mmol), benzaldehyde (1.0 mmol), **26** (5 mol %), additive (10-50 mol %), chlorobenzene (2 mL), 110 °C, 12 h. ^b The product yield of **81a** was determined by GC-MS using hexamethylbenzene as an internal standard.

2.3.2 Solvent and Temperature Effects

Table 2.2 Solvent and temperature effects for the reaction of 3-methoxyphenol and benzaldehyde^a



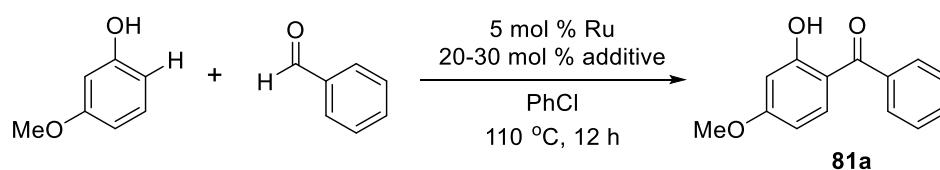
entry	solvent	temperature (°C)	81a ^b (%)
1	toluene	110	29
2	chlorobenzene	110	39
3	1,4-dioxane	110	0
4	water	110	0
5	chlorobenzene	90	12
6	chlorobenzene	100	28
7	chlorobenzene	125	43

^a Reaction conditions: 3-methoxyphenol (0.5 mmol), benzaldehyde (1.0 mmol), **26** (5 mol %), K₂CO₃ (30 mol %), solvent (2 mL), 90-125 °C, 12 h. ^b The product yield of **81a** was determined by GC-MS using hexamethylbenzene as an internal standard.

The choice of solvent was surveyed as shown in Table 2.2. The use of chlorobenzene gave the best yield among the screened solvents (entries 1-4). Dioxane and water did not form any products, presumably because oxygen-containing solvent could coordinate to the Ru center to inhibit the coordination of benzaldehyde. The effect of temperature was investigated by running reactions at different temperatures using chlorobenzene as the solvent (entries 2, 5-7). The reaction of 3-methoxyphenol with benzaldehyde effectively occurred at above 100 °C, and 110 °C was found to be the most optimal temperature for the coupling reaction.

2.3.3 Catalyst Survey

Table 2.3 Catalyst and additive survey for the reaction of 3-methoxyphenol and benzaldehyde^a



entry	catalyst	additive ^b	yield 81a (%) ^c
1	26	---	trace
2	26	K ₂ CO ₃	34
3	26	PPh ₃	0
4	26	K ₂ CO ₃ , PPh ₃	47
5	RuCl ₃ ·3H ₂ O	K ₂ CO ₃	0
6	RuCl ₃ ·3H ₂ O	K ₂ CO ₃ , PPh ₃	21
7	[RuH(CO)(PCy ₃) ₄ (O)(OH) ₂]	K ₂ CO ₃ , PPh ₃	40
8	RuCl ₂ (PPh ₃) ₃	K ₂ CO ₃	28
9	[(<i>p</i> -cymene)RuCl ₂] ₂	K ₂ CO ₃	0
10	Ru ₃ (CO) ₁₂	K ₂ CO ₃	0
11	---	K ₂ CO ₃	0
12	---	PPh ₃	0

^a Reaction conditions: 3-methoxyphenol (0.5 mmol), benzaldehyde (1.0 mmol), additive (20-30 mol %), chlorobenzene (2 mL), catalyst (5 mol % Ru), 110 °C, 12 h. ^b Amount of additives: PPh₃ (20 mol %), K₂CO₃ (30 mol %). ^c The product yield of **81a** was determined by ¹H NMR using hexamethylbenzene as an internal standard.

Initially, we used the reaction of 3-methoxyphenol (0.5 mmol) with benzaldehyde (1.0 mmol) to screen the activity of ruthenium catalysts (Table 2.3). The product yields were analyzed by GC-MS at 110 °C after 12 h. The cationic ruthenium-hydride complex **26** exhibits the best catalytic activity for the C-C coupling reaction with additives. In the

absence of any additives, the cationic Ru complex **26** gave only a trace amount of product (entry 1). The inorganic base K_2CO_3 was found to be critical for obtaining acylated phenol product **81a** selectively. The data for the other ruthenium complexes without K_2CO_3 are not included in the table due to the absence of any catalytic activity for this transformation. Moreover, we subsequently observed that the addition of 20 mol % of PPh_3 further promoted the reactivity of the catalytic system (entries 4, 6). No product was formed either K_2CO_3 or PPh_3 were used in the absence of ruthenium complexes (entries 11, 12). On the basis of these screening of ruthenium catalysts and additives, the cationic ruthenium complex **26**, K_2CO_3 , and PPh_3 were found to be the most effective catalytic system for the dehydrogenative acylation of phenols with aldehydes (entry 4).

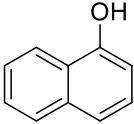
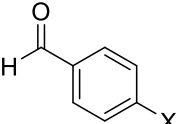
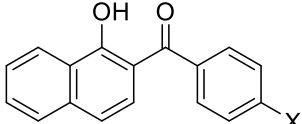
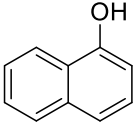
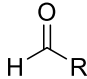
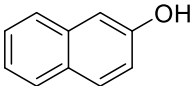
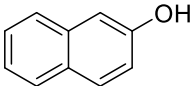
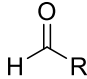
2.4 Reaction Scope

2.4.1 Dehydrogenative *ortho*-Acylation of Phenols with Aldehydes

Table 2.4 Dehydrogenative acylation of phenols with aldehydes^a

entry	phenol	aldehyde	product(s)	time (h)	yield ^b (%)
1		X = H	81a	12	47
2		X = 4-Me	81b	12	43
3		X = 4-F	81c	12	53
4		X = 2-Br	81d	12	58
5		R = Et	81e	12	56
6		R = <i>n</i> -Pr	81f	12	44
7		R = <i>i</i> -Bu	81g	12	58
8		R = Cy	81h	12	50
9		R = CH(Me)Ph	81i	12	67
10		X = H	81j	16	65
11		X = Me	81k	16	51
12		X = F	81l	16	73
13		X = Cl	81m	16	70
14		X = CF ₃	81n	16	74
15		R = Et	81o	8	74
16		R = <i>i</i> -Bu	81p	12	69
17		R = Cy	81q	12	71
18		R = CH(Me)Ph	81r	12	78

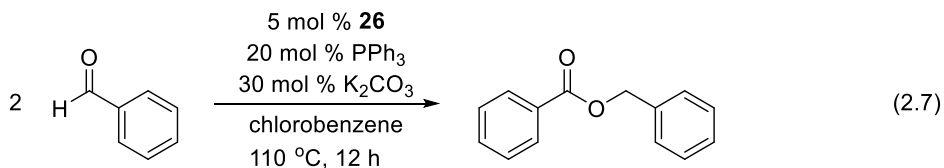
Table 2.4 Dehydrogenative acylation of phenols with aldehydes^a (continued)

entry	phenol	aldehyde	product(s)	time (h)	yield ^b (%)
19				8	48
20					
		X = H	81s		
		X = F	81t	8	35
					
21	R = Et	81u		8	47
22	R = Cy	81v		8	40
23	R = 3-cyclohexenyl	81w		12	33
24	R = CH(Me)Ph	81x		12	61
					
25				R = Ph	81y
26	R = Cy	81z	20	38	

^a Reaction conditions: phenol (0.5 mmol), aldehyde (1.0 mmol), **26** (5 mol %), PPh₃ (20 mol %), K₂CO₃ (30 mol %), chlorobenzene (2 mL), 110 °C. ^b Isolated yields.

We found that the cationic ruthenium-hydride complex **26** is a highly effective catalyst for the direct dehydrogenative coupling of phenols and aldehydes to afford *ortho*-acylated phenol products. As mentioned in the previous section, the addition of catalytic amount of K₂CO₃ (30 mol %) and PPh₃ (20 mol %) was found to be critical for the selective formation of *ortho*-acylated phenols over the *ortho*-alkylated phenol products. We explored the reaction scope with various phenols and aldehydes by using the optimized conditions (Table 2.4). The electron-rich 3-methoxyphenol, 3,5-dimethoxyphenol, and 1- and 2-naphthol were found to be suitable substrates for the *ortho*-acylation reactions. However, relatively electron-deficient phenols such as a phenol or 3-chlorophenol gave

undesired benzyl benzoates as the major product resulted from Tishchenko-type reaction of benzaldehydes (eq 2.7).⁵⁶



We first examined the substituent effect of aromatic aldehydes such as *ortho*- and *para*-substituted benzaldehydes. These benzaldehydes readily reacted with 3-methoxyphenol to produce 2-hydroxy-4-methoxybenzophenone products **81a-81d**. Among *para*-substituted benzaldehydes, 4-fluorobenzaldehyde showed higher product yield than simple benzaldehyde and 4-methylbenzaldehyde (entries 1-3). The results indicate that the benzaldehydes with electron-withdrawing group promote the coupling reaction. We observed that the reaction of 3-methoxyphenol and electron-rich 4-methoxybenzaldehyde gave less than 10% yield as analyzed by GC-MS. Notably, sterically hindered 3,5-dimethoxyphenol was found to be a better substrate than 3-methoxyphenol in forming the *ortho*-acylphenol products. A similar substituent dependence trend was also observed from the reactions of 3,5-dimethoxyphenol with *para*-substituted benzaldehydes (entries 10-14). The coupling of phenols with linear or branched aliphatic aldehydes also gave the corresponding *ortho*-acylphenol products (entries 5-9, 15-18).

Aliphatic aldehydes are generally not suitable for the catalytic C-C coupling reactions because they can be easily converted to homo-aldol products. We have not found any reports on the catalytic dehydrogenative *ortho*-acylation of phenols with aliphatic aldehydes. We successfully demonstrated that the reaction of phenols with aliphatic aldehydes proceeds to form *ortho*-acylated phenols without forming aldol byproducts.

Among the screened aliphatic aldehydes, 2-phenylpropionaldehyde as a coupling partner showed the highest product yields. Steric environment on the α -carbon adjacent to aldehyde group was found to be less important because no significant difference in reactivity was observed between linear and branched aldehydes by comparing the product yields. Both 1-naphthol and 2-naphthol also readily reacted with aliphatic and aryl-substituted aldehydes to give 2-acylated (**81s-81x**) and 1-acylated (**81y-81z**) products respectively (entries 19-26). Although the crude mixture typically contained a negligible amount of alkylation product along with unidentified oligomeric side products (5-10 % combined), analytically pure *ortho*-acylphenol products were isolated by silica gel column chromatography.

2.4.2 Formation of Flavene Derivatives for the Dehydrative Coupling of Phenols with α,β -Unsaturated Aldehydes

Flavonoids are a large family of polyphenolic compounds with a wide range of its biological activities such as antioxidant, cancer prevention, and antibacterial agents.⁵⁷ Flavonoids can be classified as flavanones, flavenes, flavones, and anthocyanidins according to their chemical structures (Figure 2.2).

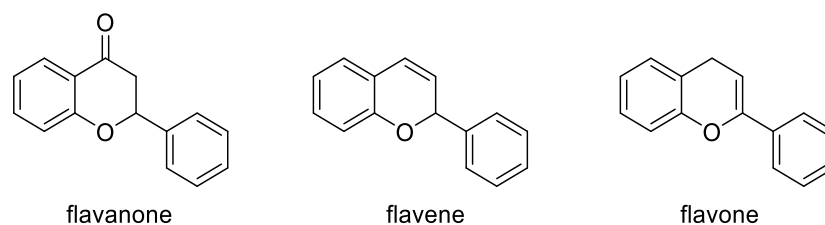


Figure 2.2 Common structures of flavonoids

Table 2.5 Formation of flavene derivatives from the dehydrative coupling reaction of phenols with α,β -unsaturated aldehydes^a

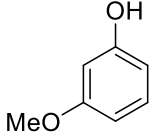
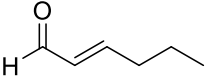
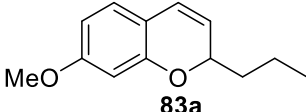
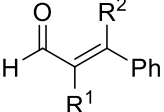
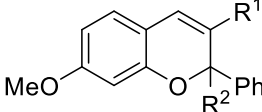
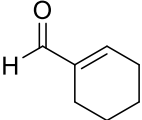
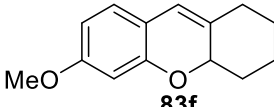
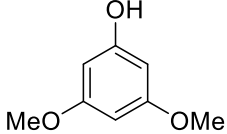
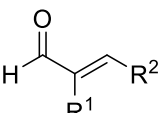
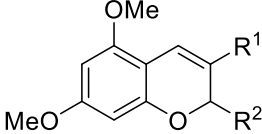
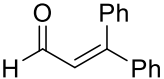
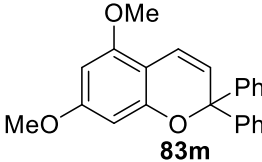
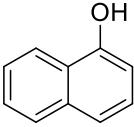
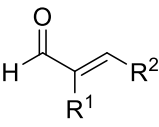
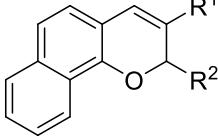
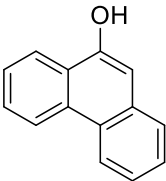
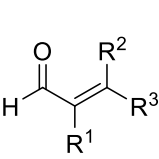
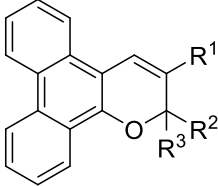
entry	phenol	aldehyde	product(s)	T (°C)	t (h)	yield ^b (%)
1			 83a	110	24	37
2			 83b	130	16	23
3		R ¹ = H R ² = H	83b	130	16	43
4		R ¹ = Me R ² = H	83c	130	16	63
5		R ¹ = <i>n</i> -hexyl R ² = H	83d	130	16	40
6		R ¹ = H R ² = Ph	83e	130	16	40
6			 83f	130	16	53
7			 83g	120	16	54
8		R ¹ = H R ² = <i>n</i> -Pr	83g	120	16	47
9		R ¹ = Me R ² = Et	83h	120	16	52
10		R ¹ = H R ² = Ph	83i	120	16	55
11		R ¹ = H R ² = 4-FC ₆ H ₄	83j	120	16	72
12		R ¹ = Me R ² = Ph	83k	120	16	88
13		R ¹ = <i>n</i> -hexyl R ² = Ph	83l	120	16	88
13			 83m	130	16	63

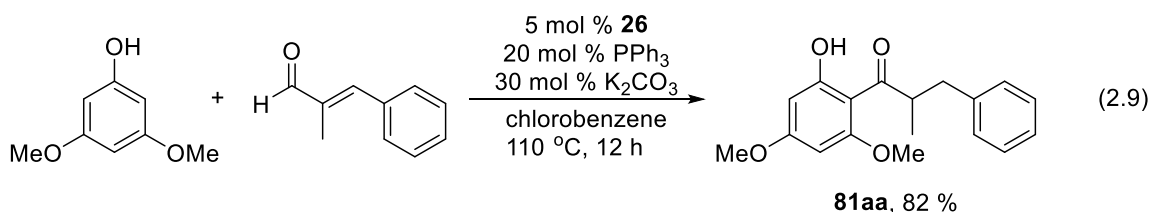
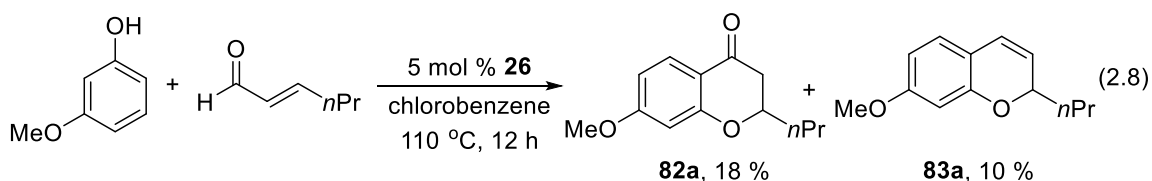
Table 2.5 Formation of flavene derivatives from the dehydrative coupling reaction of phenols with α,β -unsaturated aldehydes^a (continued)

entry	phenol	aldehyde	product(s)	T (°C)	t (h)	yield ^b (%)
						
14		R ¹ = H R ² = <i>n</i> -Pr	83n	130	20	40
15		R ¹ = H R ² = Ph	83o	130	12	46
16		R ¹ = Me R ² = Ph	83p	130	12	42
17		R ¹ = <i>n</i> -hexyl R ² = Ph	83q	130	12	59
						
18		R ¹ = H R ² = H R ³ = <i>n</i> -Pr	83r	120	16	71
19		R ¹ = Me R ² = H R ³ = Ph	83s	120	16	60
20		R ¹ = H R ² = Ph R ³ = Ph	83t	120	16	56

^a Reaction conditions: phenol (0.5 mmol), aldehyde (1.0 mmol), **26** (5 mol %), PPh₃ (20 mol %), chlorobenzene (2 mL), 110 °C. ^b Isolated yields.

To extend the synthetic utility of the catalytic method, we explored the coupling reaction of phenol substrates with α,β -unsaturated aldehydes (Table 2.5). We initially investigated the cationic ruthenium-hydride complex **26** catalyzed coupling reaction of 3-methoxyphenol with *trans*-2-hexenal, which gave a mixture of heterocyclic annulated compounds 2,3-dihydrochromone **82a** and 2*H*-chromene **83a** (eq 2.8). In the course of additive screening, we have found that the same reaction in the presence of 20 mol % of PPh₃ formed only the 2*H*-chromene-type product **83a** selectively (entry 1). Since 2*H*-Chromene is known to be a core structure of naturally occurring flavene compounds, we next aimed to expand the substrate scope of the formation of flavene derivatives. The reaction was carried out with 0.5 mmol of phenols, 1.0 mmol of α,β -unsaturated aldehydes,

5 mol% of cationic ruthenium-hydride complex **26**, and 20 mol % of PPh₃ in the absence of base additive. The addition of K₂CO₃ reliably produced the acylated phenols. For example, the coupling reaction of 3,5-dimethoxyphenol with α -methylcinnamaldehyde in the presence of **26**, PPh₃, and K₂CO₃ gave the *ortho*-acylphenol product **81aa** in 82 % yield without forming any byproduct (eq 2.9).



The coupling reaction of 3-methoxyphenol with α -substituted cinnamaldehydes smoothly occurred to give the 3-substituted flavene derivatives (entries 2-4). The reaction of 3-methoxyphenol with β -phenylcinnamaldehyde resulted in selective formation 2,2-diphenyl-2*H*-chromene compound **83e**, which indicates that the intramolecular heterocyclization of phenol and alkene was not inhibited by sterically demanding phenyl groups (entry 5). The coupling with 1-cyclohexene-1-carboaldehyde also gave polycyclic 2*H*-chromene product **83f** (entry 6). Higher product yields were obtained from the reaction of 3,5-dimethoxyphenol substrate with disubstituted enals (entries 7-13). Other electron-rich phenol derivatives, including 1-naphthol and 9-phenanthrol, afforded the corresponding polycyclic enol ether products **83n-83t** (entries 14-20). The formation of

flavene derivatives **83** can be rationalized by *ortho*-C-H acylation followed by conjugate addition and dehydrative annulation, and water is the only byproduct in this reaction.

The structure of 2-acylphenols **81** and 2*H*-chromenes **83** was completely established by NMR analysis. In the acylated phenol products, characteristic phenolic OH signal was shown at δ 12-14 ppm in ^1H NMR, due to the hydrogen bond with adjacent carbonyl group. We also confirmed the molecular structure of the products **81v** and **83t** by X-ray crystallography (Figure 2.3 and 2.4).

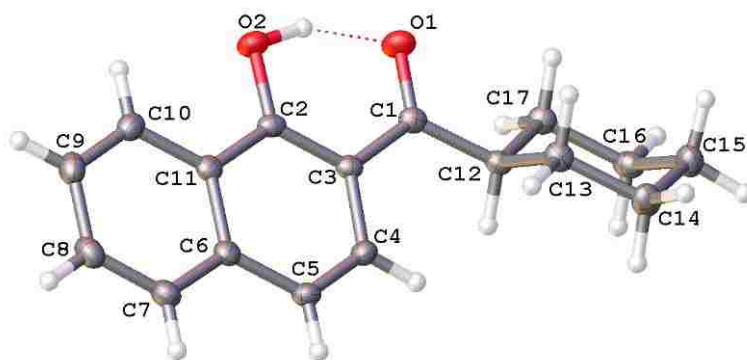


Figure 2.3 Molecular structure of **81v**

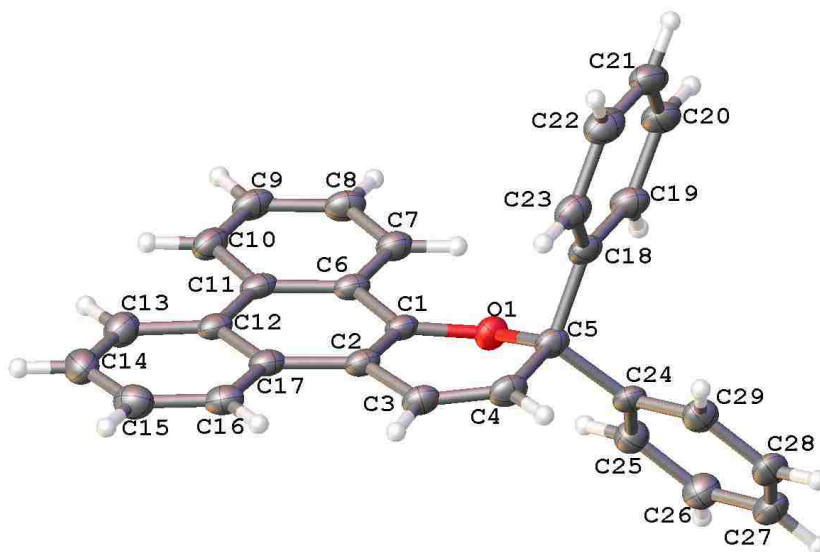
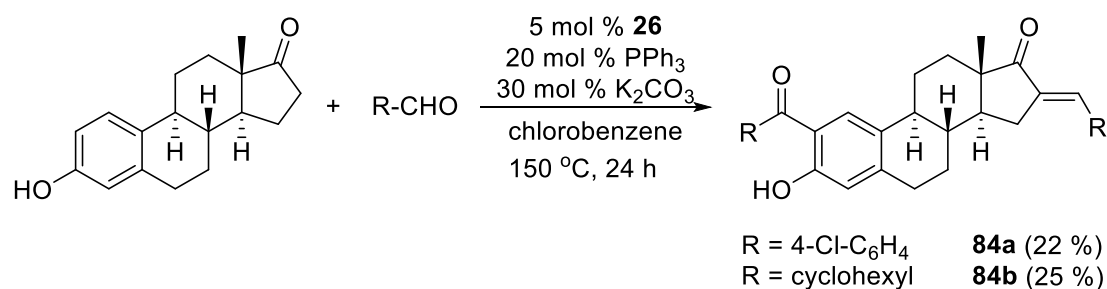


Figure 2.4 Molecular structure of **83t**

2.4.3 Dehydrogenative *ortho*-Acylation of Estrone with Aldehydes

We further demonstrated the synthetic utility of *ortho*-acylation by using bioactive phenol substrates with aliphatic- and aryl-substituted aldehydes (Scheme 2.5). The treatment of estrone with 4-chlorobenzaldehyde and cyclohexanecarboxaldehyde in the presence of **26**, PPh₃, and K₂CO₃ at 150 °C gave 1:2 coupling products **84a** and **84b**, respectively. In this case, both arene C-H acylation and aldol condensation-type couplings occurred on the estrone substrate. Our efforts on the formation of C-H acylated 1:1 coupling product was unsuccessful. Instead, a small amount of aldol condensation-type coupling product were detected as the byproduct, which indicates that the aldol formation is faster than the C-H acylation for these substrates. The molecular structure of **84a** and **84b** were established by NMR spectroscopy, and (E)-enone configuration was confirmed by X-ray crystallography (**84b**) (Figure 2.5).



Scheme 2.5 Oxidative C-H acylation and aldol condensation of estrone with aldehydes

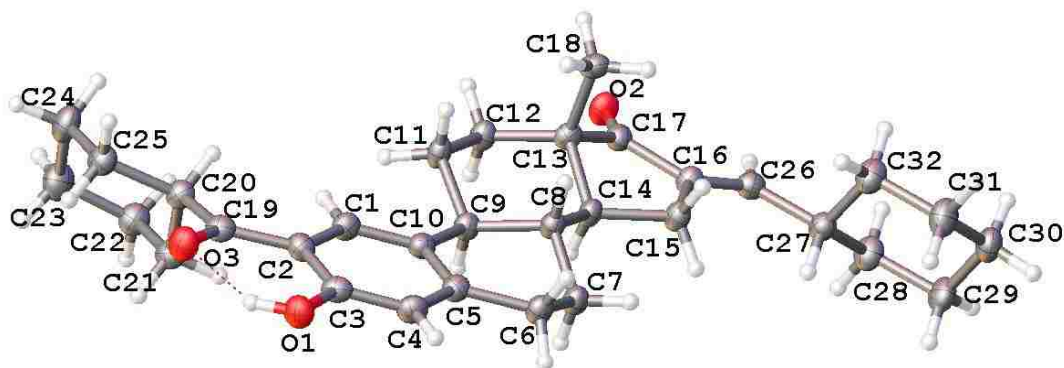
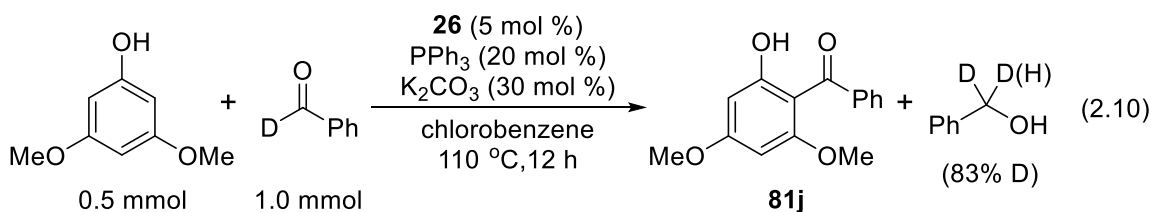


Figure 2.5 Molecular structure of **84b**

2.5 Mechanistic Studies

2.5.1 Deuterium Labeling Study



We conducted the deuterium labeling experiment to obtain mechanistic insights on the acylation reaction. To probe the possible hydrogen-deuterium exchange pattern, we performed the reaction of 3,5-dimethoxyphenol (0.5 mmol) with PhCDO (> 95 % D, 1.0 mmol) in the presence of **26** (5 mol %), PPh₃ (20 mol %), and K₂CO₃ (30 mol %) in chlorobenzene (2 mL) at 110 °C for 12 h (eq 2.10). After the reaction (86 % conversion by GC-MS), analytically pure product **81j** and unreacted phenol substrate were isolated by a simple column chromatography on silica gel. The deuterium content of these was determined by NMR and GC-MS spectroscopic methods. The ¹H, and ²H NMR showed that 83% deuterium was incorporated to the α-CH₂ of benzyl alcohol byproduct while no

H/D exchange was observed on the either recovered phenol or acylphenol product (Figure 2.6). This result suggests that the aldehyde coupling partner also serves as an internal oxidant via hydrogenation to the corresponding alcohol. Thus, the oxidative C-H acylation reaction could be achieved in the absence of any external oxidants.

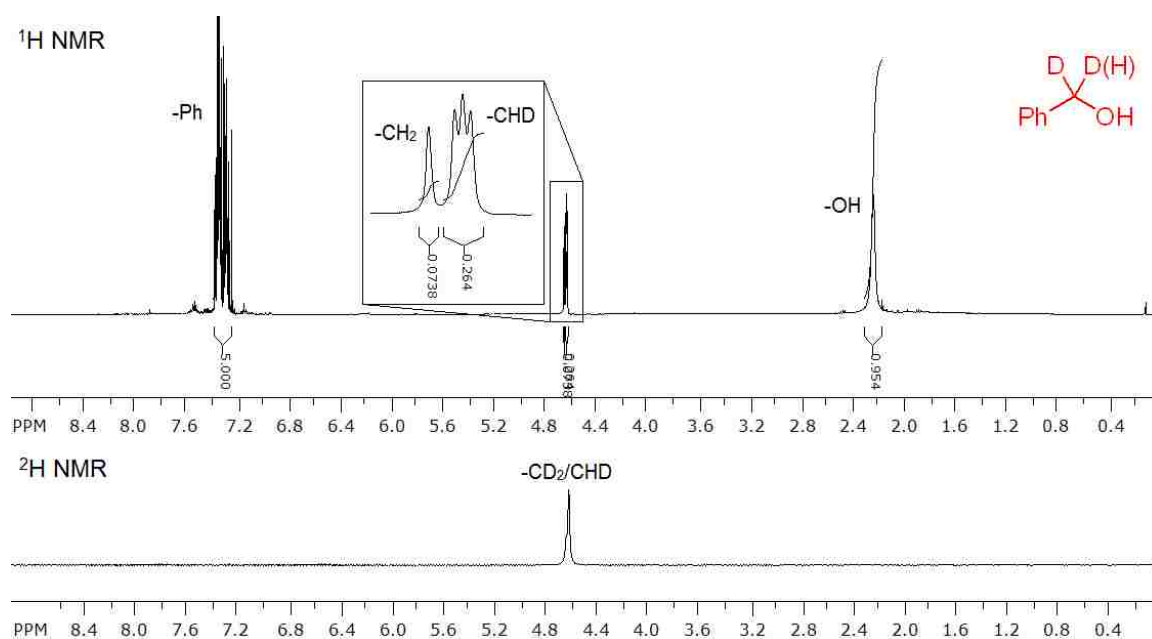
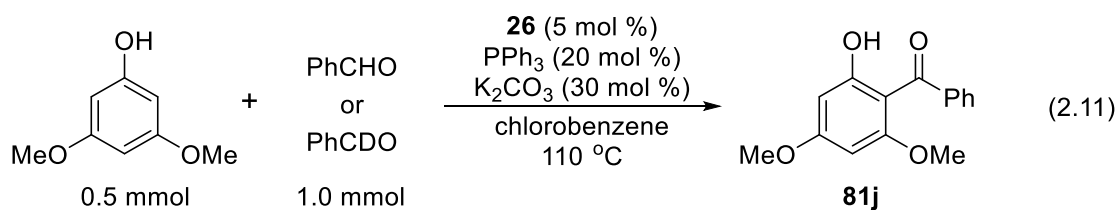


Figure 2.6 ^1H and ^2H NMR spectra of benzyl alcohol byproduct isolated from the reaction of 3,5-dimethoxyphenol with benzaldehyde- α - d_1

2.5.2 Deuterium Isotope Effect Study



To discern the rate-determining step of the catalytic reaction, we measured the deuterium isotope effect of aldehyde by comparing the initial reaction rate of 3,5-dimethoxyphenol with PhCHO and PhCDO at 110 °C (eq 2.11). The k_{obs} value of for each substrate was obtained as $k_{\text{obs}} = 1.80 \times 10^{-3} \text{ min}^{-1}$ (PhCHO) and $k_{\text{obs}} = 5.43 \times 10^{-4} \text{ min}^{-1}$ (PhCDO) from the pseudo-first order plot of the formation of **81j**, which led a normal deuterium isotope effect of $k_{\text{H}}/k_{\text{D}} = 3.3 \pm 0.3$ (Figure 2.7). A relatively high $k_{\text{H}}/k_{\text{D}}$ value indicates that the cleavage of aldehydic C-H bond is the rate-determining step of the coupling reaction.

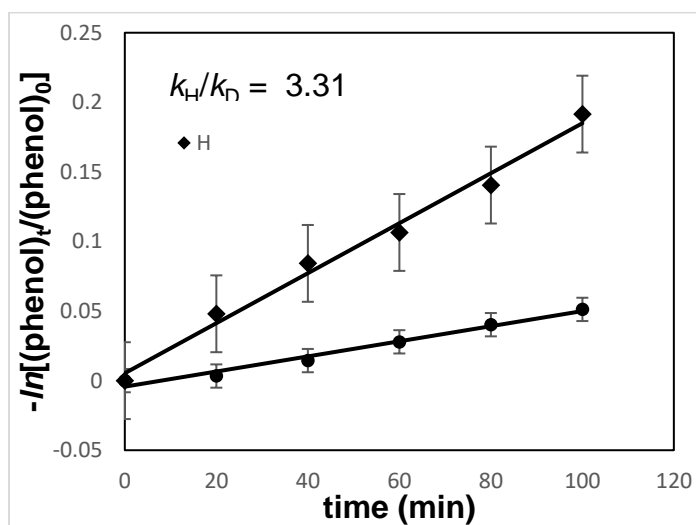
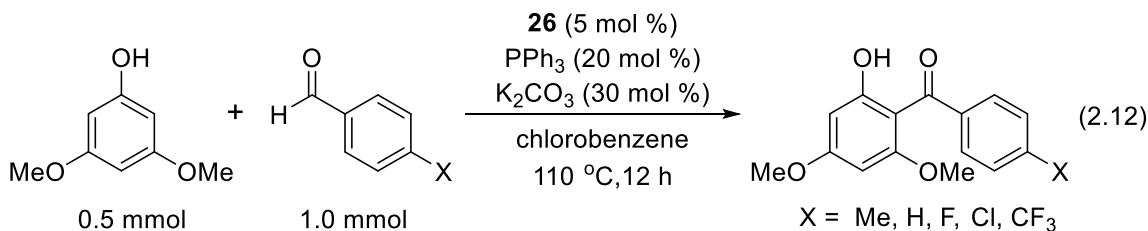


Figure 2.7 Deuterium isotope effect study for the reaction of 3,5-dimethoxyphenol with benzaldehyde and benzaldehyde- α - d_1

2.5.3 Hammett Study



To probe the electronic influence on the aldehyde substrate, a Hammett plot is constructed from the reaction of 3,5-dimethoxyphenol with a series of *para*-substituted benzaldehydes $p\text{-X-C}_6\text{H}_4\text{CHO}$ (X = Me, H, F, Cl, CF₃) (eq 2.12). A positive ρ value of $+0.69 \pm 0.05$ was obtained from a linear correlation of the relative rate vs. Hammett σ_p constant (Figure 2.8). This result indicates that the negative charge is built-up in the transition state, which is stabilized by electron-withdrawing inductive effect on the aldehyde. Thus, the aldehyde C-H activation can be promoted by electron withdrawing substituents in forming Ru-acyl species. Similar Hammett ρ values have been observed in the catalytic coupling reactions of benzaldehydes and related arenes.⁵⁸

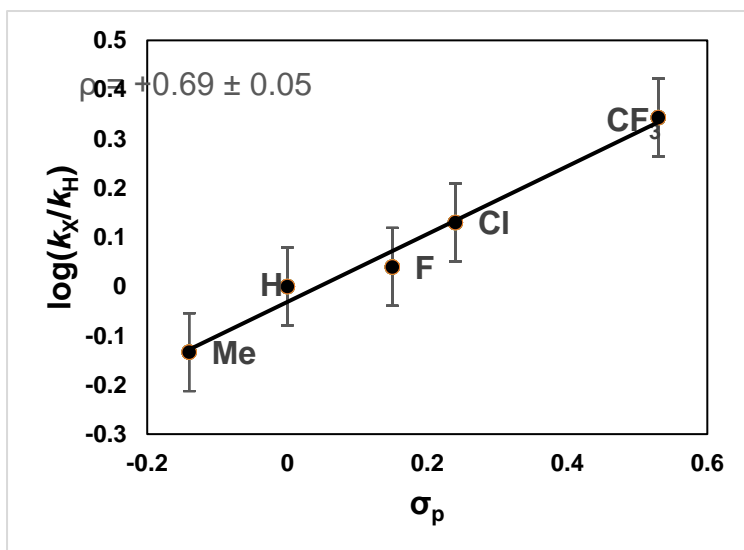
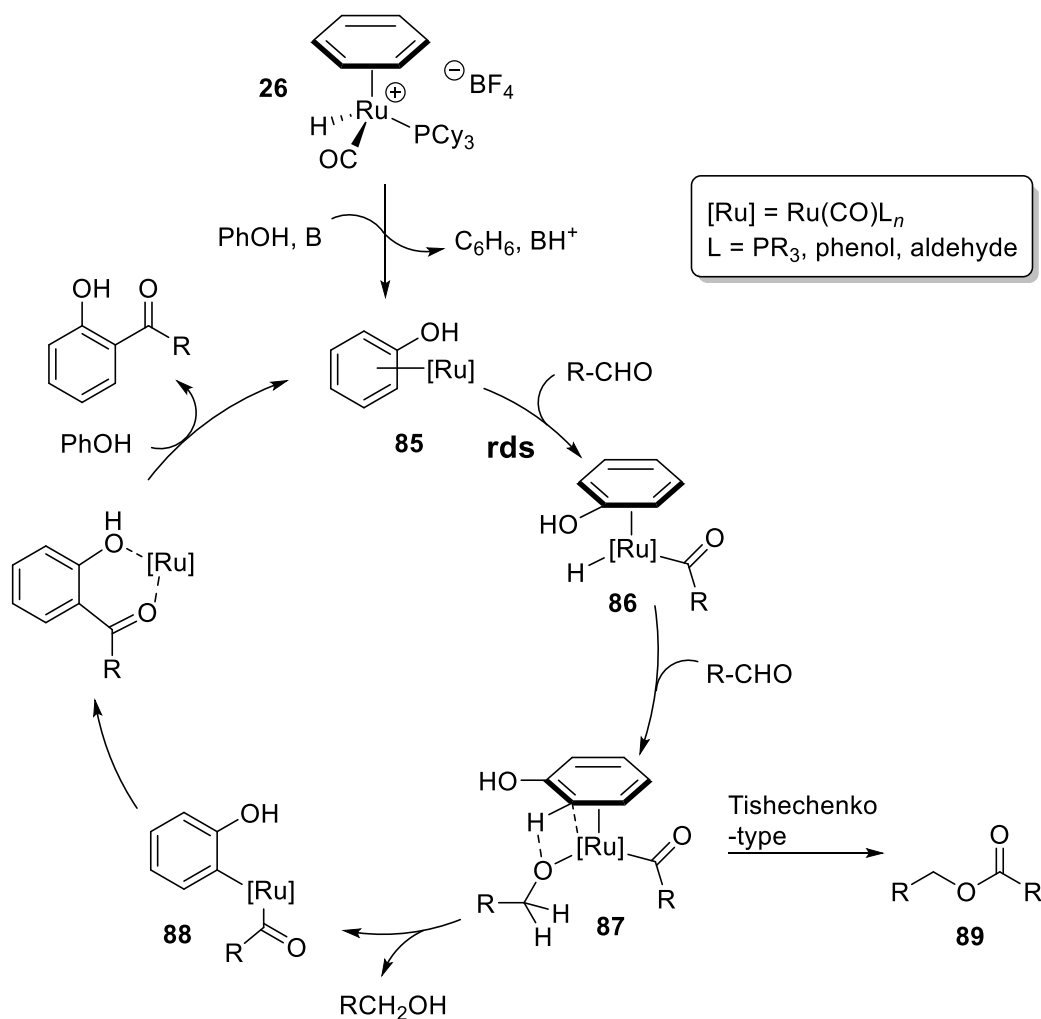


Figure 2.8 Hammett plot from the reaction of 3,5-dimethoxyphenol with $p\text{-X-C}_6\text{H}_4\text{CHO}$ (X = Me, H, F, Cl, CF₃)

2.5.4 Proposed Mechanism

Although detail of the reaction mechanism remains unclear at the present time, we present a mechanistic hypothesis for the formation of *ortho*-acylated phenols on the basis of mechanistic experimental results. A plausible mechanism is compiled as shown in Scheme 2.6.



Scheme 2.6 Proposed mechanism for the dehydrogenative *ortho*-acylation of phenols with aldehydes

Initially, the cationic ruthenium hydride complex **26** would be transformed to an active neutral Ru-arene species **85** via a base-assisted deprotonation and the benzene ligand exchange with the phenol substrate. In support of this notion, we previously reported a facile arene exchange reaction of **26** at room temperature.^{15,55} The C-H activation of the first equivalent of aldehyde generates Ru-acyl intermediate **86**. Both Hammett study and the normal kinetic isotope effect (k_H/k_D 3.3 ± 0.3) indicate that the aldehyde C-H activation is the rate-limiting step. The subsequent carbonyl insertion of the second aldehyde into Ru-H bond forms alkoxy Ru-acyl species **87**. The alkoxy-assisted *ortho*-C-H activation of phenol substrate and the liberation of benzyl alcohol would give the *ortho*-metallated phenol species **88**, which is followed by reductive elimination of the coupling product **73** and the regeneration of **85**. The electron-rich phenols were found to be suitable for the *ortho*-C-H activation because we observed the formation of Tishchenko-type byproduct **89** with relative electron-deficient phenol substrates. We rationalized the formation of **89** from the reductive coupling of Ru-acyl with alkoxy via the intermediate **87**.

2.6 Conclusions

We have successfully developed an *ortho*-selective C-H acylation method for simple phenol substrates. The cationic Ru-H catalyst exhibits a uniquely high catalytic activity for the dehydrogenative coupling reaction of phenols with aldehydes without using any external oxidants. Deuterium labeling study showed that the aldehyde substrate served as both the coupling partner and hydrogen acceptor. The reaction tolerates electron withdrawing and donating group substituted aryl aldehydes as well as aliphatic aldehydes without forming aldol byproducts. The coupling method can be extended to the step-efficient synthesis of bioactive flavene derivatives by using α,β -unsaturated aldehydes. A portion of this work was published in *European Journal of Organic Chemistry* **2015**, 2015, 1899-1904. DOI: 10.1002/ejoc.201403518

CHAPTER 3

Synthesis of Alkenylated Phenols from Ruthenium-Catalyzed Dehydrative C-H

Coupling of Phenols with Ketones

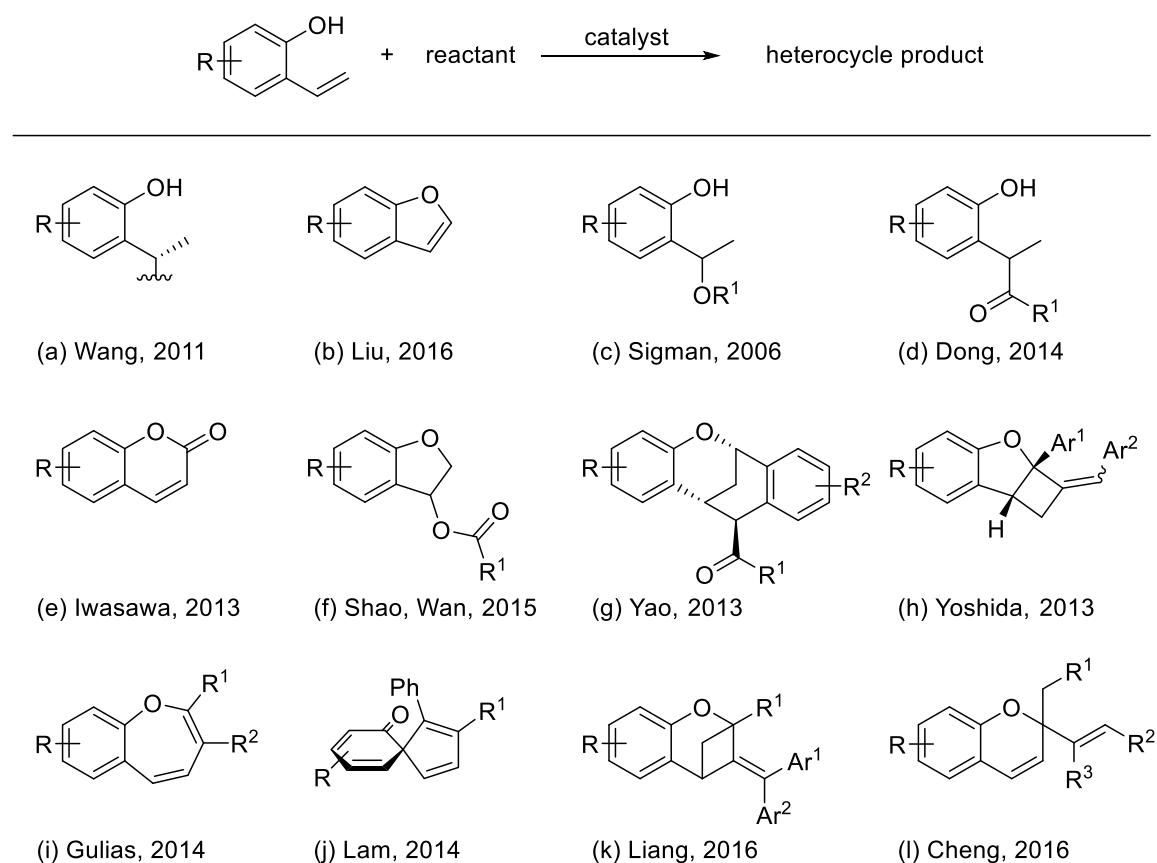
3.1 Backgrounds

3.1.1 Synthetic Application of 2-Vinylphenols

2-Vinylphenol compounds comprise versatile synthetic intermediates in forming various pharmaceutically active compounds (Table 3.1).⁵⁹⁻⁷⁰ A number of catalytic reactions including asymmetric hydrogenation,⁵⁹ dehydrogenative intramolecular cyclization,⁶⁰ hydroalkoxylation,⁶¹ and hydroacylation⁶² have been explored for using 2-vinylphenol as the starting material. Iwasawa reported Pd-catalyzed direct synthesis of coumarin derivatives under atmospheric pressure of CO₂.⁶³ Recently, a number of coupling reactions have been shown to provide biologically active heterocycles through cycloaddition of alkynes with 2-vinylphenols.⁶⁵⁻⁶⁹ Yao reported Pd-catalyzed asymmetric cascade annulation between 2-alkynylbenzaldehydes and 2-vinylphenols, which led to the formation of naturally occurring tetrahydronaphthalene derivatives.⁶⁵ Analogous alkyne coupling reactions have been successfully developed for the formation of structurally diverse oxygen-containing heterocycles, such as tetrahydrocyclobuta[*b*]benzofuran,⁶⁶ benzoxepin,⁶⁷ spirocyclic enons,⁶⁸ and 3,4-dihydro-2*H*-2,4-methanochromans.⁶⁹ Besides, Cheng's group reported Co-catalyzed synthesis of alkene-substituted 2*H*-chromenes from

2-vinylphenols with allenes.⁷⁰ The authors proposed a reaction mechanism via a vinylic C-H activation and [5+1] annulation with the allene acting as a one-carbon source.

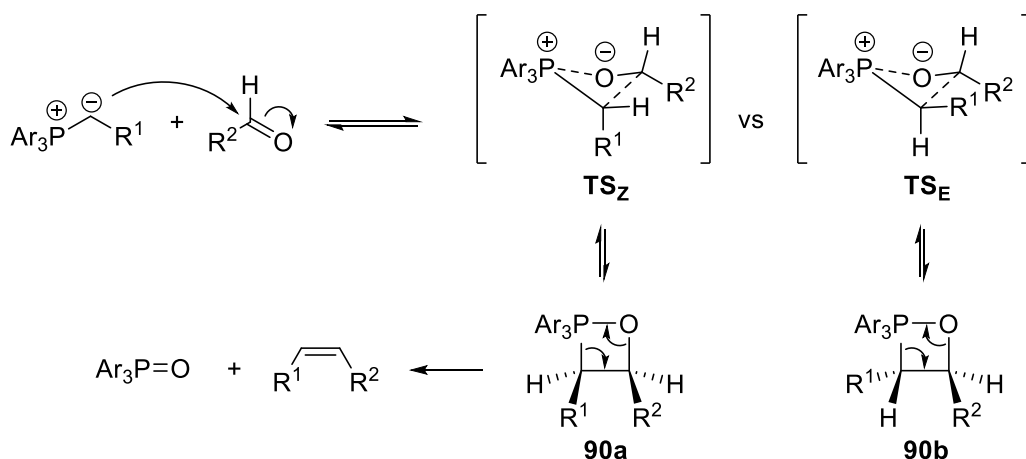
Table 3.1 Synthetic applications of 2-vinylphenols



3.1.2 Traditional Carbonyl Olefination Methods

Traditionally, 2-vinylphenol starting materials have been prepared by using carbonyl olefination methods from 2-acylphenols compounds.⁵⁹⁻⁷⁰ The Wittig reaction has been used as the standard tool for the synthesis of olefin natural products.⁷¹ The reaction of carbonyl compounds with a phosphonium ylide produced alkene products with concomitant formation of phosphine oxide byproduct. The reaction mechanism involves

the formation of oxaphosphetane intermediate **90** by nucleophilic addition of ylide to the carbonyl carbon (Scheme 3.1). The subsequent decomposition of the intermediate led to the formation of alkene and phosphine oxide by breaking C-P and C-O bonds. The stereoselectivity of the olefin products is influenced by many factors including the type of phosphorus and carbonyl starting materials, solvent, and reaction conditions. In general, (*Z*)-selectivity (typically ~9:1) can be expected when nonstabilized ylide reacts to aldehydes because **TS_Z** is believed to be kinetically favored over **TS_E**. Much effort has been devoted to controlling the stereoselectivity of alkene products.⁷²

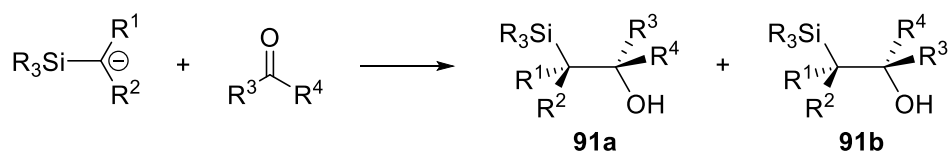


Scheme 3.1 Mechanism for the Wittig olefination reaction

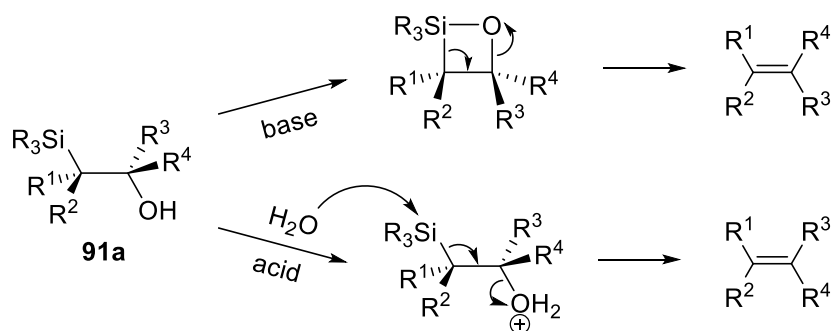
The Peterson olefination has been found to be a highly effective method for the stereoselective formation of alkenes from the reaction of α -silylcarbanions with carbonyl compounds (Scheme 3.2).⁷³ The nucleophilic addition of a silylcarbanion to a carbonyl substrate generates a set of diastereomers of β -hydroxysilane intermediate **91**, where the diastereoselectivity can be modulated by the choice of starting materials and reaction conditions. The β -hydroxysilane intermediate can be isolated or can be prepared in

different pathways including reduction of α -silyl ketones and nucleophilic opening of silyl epoxides. Decomposition of β -hydroxysilane **91** leads to the olefin and silanol products under acidic or basic conditions. Notably, the acid and base treatments of β -hydroxysilane proceed different eliminations to give the opposite stereoselectivity for alkenes (Scheme 3.2b).

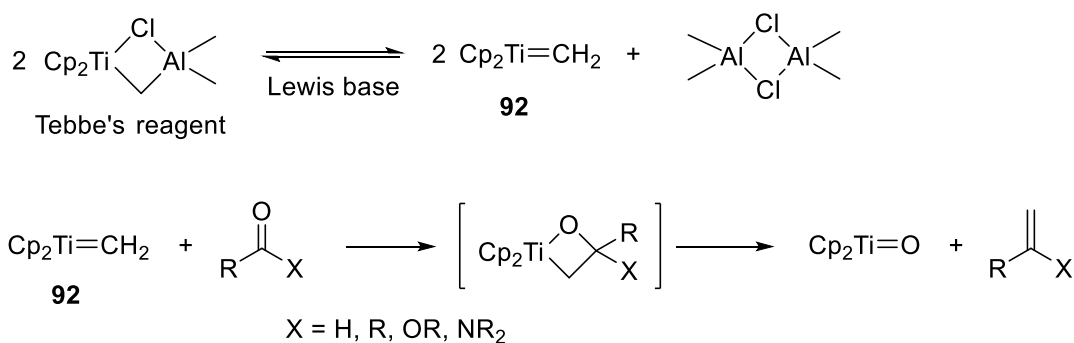
(a) Formation of the β -hydroxysilane intermediate diastereomers



(b) Acid- and base-induced eliminations



Scheme 3.2 The reaction pathways for the Peterson olefination



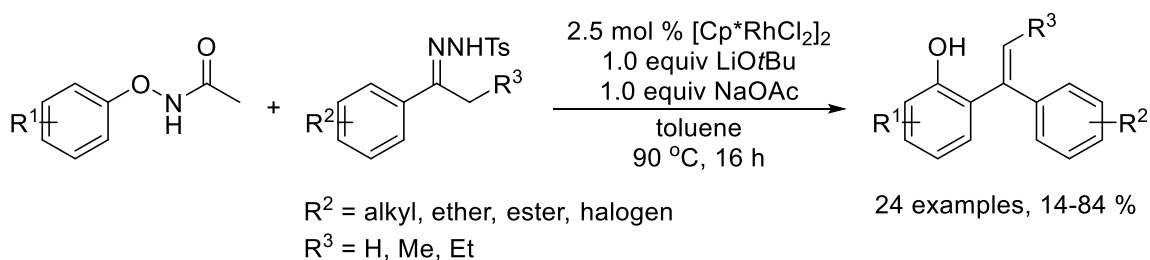
Scheme 3.3 The olefination of carbonyl compounds by using the Tebbe's reagent

The Tebbe's reagent also allows efficient synthesis of olefins from various types of carbonyl compounds including aldehydes, ketones, esters, and amides (Scheme 3.3).⁷⁴ The

treatment of the Tebbe's reagent with a mild Lewis base generates the active titanium carbene **92** with $\text{Al}_2\text{Cl}_2(\text{CH}_3)_4$. The *in situ* formed titanium carbene **92** reacts with carbonyl compounds to yield the olefin product and Cp_2TiO . Even though these methods have been widely used for the alkene synthesis, these methods commonly employ stoichiometric amount of reagents, thus the formation of copious amount of wasteful byproducts remains as an inherent drawback.

3.2 Catalytic Reactions for the Formation of 2-Vinylphenols

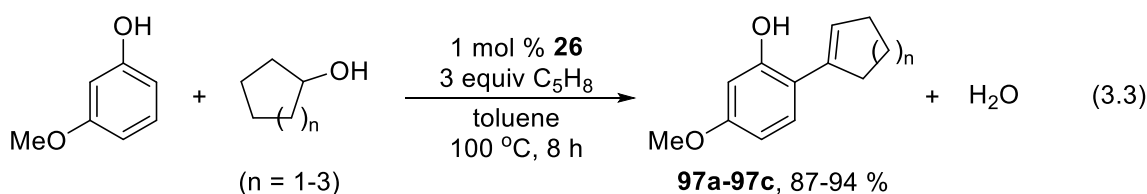
A number of catalytic methods have been developed for the formation of bioactive compounds using 2-vinylphenols as the starting material.⁵⁹⁻⁷⁰ However, in most cases, 2-vinylphenols are still prepared from the traditional stoichiometric carbonyl olefination methods. To solve the problems associated with the wasteful byproducts, the development of environmentally sustainable green catalytic methods for the synthesis of 2-vinylphenols has attracted considerable attentions in synthetic and catalysis communities.



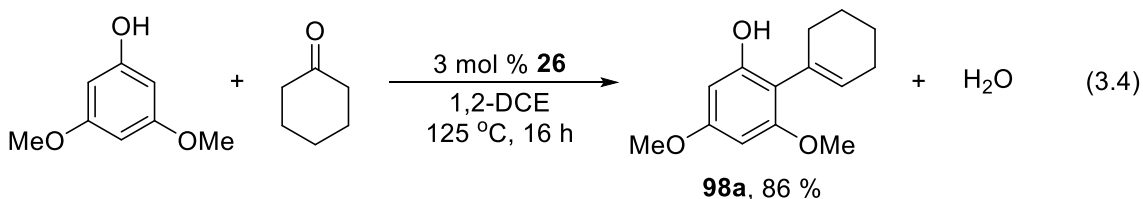
Scheme 3.4 Rh-catalyzed coupling reaction of *N*-phenoxyacetamides with *N*-tosylhydrazones

In recent years, considerable efforts have been devoted to the development of new catalytic approaches involving arene-C-H activation for the formation of 2-vinylphenols. Wang and co-workers reported Rh-catalyzed C-H *ortho*-alkenylation of *N*-

formed cationic ruthenium-hydride complex gave a 2:3 mixture of the indene derivative **93** and the *ortho*-C-H insertion product **94** (eq 3.1).⁷⁷ Similarly, the coupling reaction of acetophenone with cyclopentene in the presence of 5 mol % **26** and HBF₄·OEt₂ produced nearly 1:1 ratio of double bond isomers of the olefination products **95** and **96** (eq 3.2).⁵³ The common features of these reactions are the carbonyl insertion after the requisite C-H activation, and subsequent dehydration of alkoxy-Ru species in forming the alkene products.



Our group also reported dehydrative C-H alkylation and alkenylation of phenols with alcohols (Scheme 1.26).⁴⁴ The treatment of 3-methoxyphenol with cycloalkanol in the presence of **26** and excess cyclopentene (3 equiv) yielded *ortho*-cycloalkenylphenol products **97a-97c** and water (eq 3.3). Inspired by these environmentally friendly dehydrative alkenylation methods, we explored the analogous coupling reaction of phenols with simple ketones. We initially discovered that the treatment of 3,5-dimethoxyphenol with cyclohexanone in the presence of cationic ruthenium-hydride complex **26** in 1,2-dichloroethane led to the formation of *ortho*-alkenylated phenol product **98a** (eq 3.4).



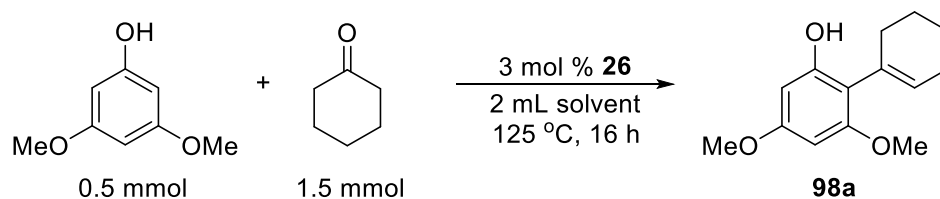
The salient features of the catalytic method are that synthetically valuable 2-vinylphenols are formed from readily available phenol and ketone substrates. In particular,

the reaction does not require any stoichiometric amount of additives or activating reagents, and water is the only byproduct. To the best of our knowledge, the catalytic synthesis of 2-vinylphenols from the coupling reaction of phenols with ketones has not been achieved before.

3.3 Optimization Studies

3.3.1 Solvent Screening

Table 3.2 Solvent screening for the coupling reaction of 3,5-dimethoxyphenol with cyclohexanone^a



entry	solvent	yield ^b (%)
1	1,2-dichloroethane	92
2	chlorobenzene	72
3	toluene	90
4	benzene	87
5	n-hexane	55
6	1,4-dioxane	24
7	<i>tert</i> -amyl alcohol	< 3

^a Reaction conditions: **26** (3 mol %), phenol (0.5 mmol), cyclohexanone (1.5 mmol), solvent (2 mL), 125 °C, 16 h. ^b The product yield of **98a** was determined by ¹H NMR using methylsulfonylmethane as an internal standard.

We first screened a number of different solvents to attain optimized reaction conditions for the coupling reaction of phenols with ketones (Table 3.2). The reaction

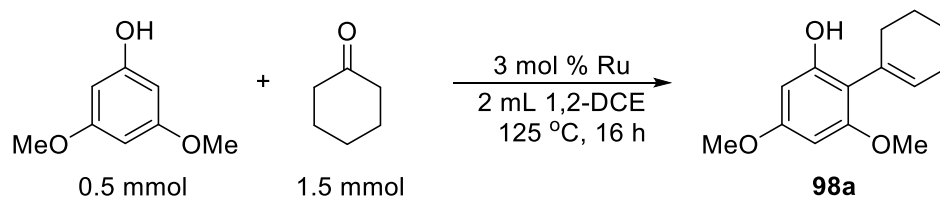
progress of 3,5-dimethoxyphenol (0.5 mmol) with cyclohexanone (1.5 mmol) in the presence of ruthenium-hydride catalyst **26** (3 mol %) in different solvents was analyzed by GC-MS and ^1H NMR using methylsulfonylmethane as an internal standard. The use of 1,2-dichloroethane showed the highest product yield (entry 1), while other non-polar aprotic solvents were found to be acceptable solvents for this coupling method (entries 1-5). A poor solubility of the catalyst and phenol substrate in *n*-hexane resulted a relatively low activity among the selected non-polar solvents (entry 5). 1,4-Dioxane was not a suitable solvent, which might inhibit the coordination of ketone to the ruthenium center (entry 6). The use of a polar protic solvent, *tert*-amyl alcohol yielded a trace amount of product (entry 7).

3.3.2 Catalyst Screening

We next surveyed the activity of commonly available ruthenium catalysts for the reaction of 3,5-dimethoxyphenol with cyclohexanone in 1,2-dichloroethane (Table 3.3). Among the screened ruthenium catalysts, cationic ruthenium-hydride complex **26** exhibited the highest activity in forming the coupling product **98a** (entry 1). The tetranuclear ruthenium-hydride complex **79** also showed a moderate activity while other ruthenium complexes did not proceed the reaction efficiently. The *in situ* generated cationic ruthenium-hydride **26** from the treatment of **79** with $\text{HBF}_4\cdot\text{OEt}_2$ gave the undesired *2H*-chromene derivative **99** as the major product (entry 3) (eq 3.5), Wu and co-workers reported similar acid-catalyzed synthesis of chromenes from ketones and phenols.⁷⁸ The acid-catalyzed *2H*-chromene formation was also observed when only $\text{HBF}_4\cdot\text{OEt}_2$ was employed as the catalyst (entry 12). Additive effects of phosphine ligands (PPh_3 , PCy_3)

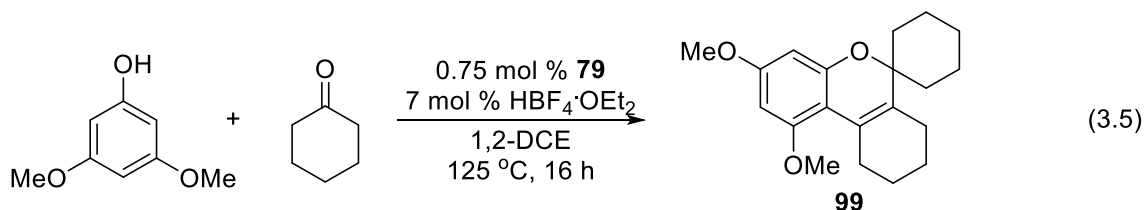
and base (K_2CO_3) were also investigated, but none of the tested additives was found to be effective in improving the product yields.

Table 3.3 Catalyst screening for the coupling reaction of 3,5-dimethoxyphenol with cyclohexanone^a



entry	catalyst	yield ^b (%)
1	$[(\text{C}_6\text{H}_6)(\text{PCy}_3)(\text{CO})\text{RuH}]\text{BF}_4$ (26)	91
2	$[(\text{PCy}_3)(\text{CO})\text{RuH}]_4(\mu\text{-O})(\mu\text{-OH})_2$ (79)	52
3	79 / $\text{HBF}_4\cdot\text{OEt}_2$	< 3
4	$[\text{RuCl}_2(p\text{-cymene})]_2$	14
5	$[\text{Ru}(\text{COD})\text{Cl}_2]_n$	< 3
6	$[(\text{PCy}_3)(\text{CH}_3\text{CN})(\text{CO})\text{RuH}]\text{BF}_4$	< 3
7	$\text{RuCl}_2(\text{PPh}_3)_3$	11
8	$\text{RuHCl}(\text{CO})(\text{PCy}_3)_2$	< 3
9	$\text{RuH}_2(\text{CO})(\text{PPh}_3)_3$	18
10	$\text{RuCl}_3\cdot 3\text{H}_2\text{O}$	6
11	$\text{Ru}_3(\text{CO})_{12}$	15
12	$\text{HBF}_4\cdot\text{OEt}_2$	< 3

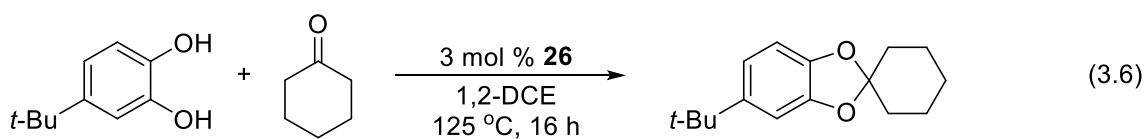
^a Reaction conditions: catalyst (3 mol % Ru equivalents), phenol (0.5 mmol), cyclohexanone (1.5 mmol), 1,2-dichloroethane (2 mL), 125 °C, 16 h. ^b The product yield of **98a** was determined by ¹H NMR using methylsulfonylmethane as an internal standard.



3.4 Reaction Scope and Applications

3.4.1 Scope of Dehydrative C-H Alkenylation of Phenols with Ketones

The substrate scope of the phenol *ortho*-alkenylation reaction was explored by using the optimized conditions (Table 3.4). The electron-releasing group substituted phenols and 1-naphthol were found to be suitable substrates for the coupling reaction. Phenols with electron-withdrawing group including simple phenol, 3-fluorophenol, 3-chlorophenol, and 3-nitrophenol did not form the desired coupling product with ketones. The coupling reaction of catechol with phenols gave the undesired 1,3-benzodioxole derivatives in excellent yields (< 90 %) (eq 3.6), wherein several synthetic approaches have already been reported.⁷⁹



The coupling reaction of 3,5-dimethoxyphenol with cycloalkanones cleanly formed cycloalkenylated phenol products **98a-98c** (entries 1-3). The coupling reaction of 3,5-dimethoxyphenol with 2-Indanone and 2-tetralone led to the formation of benzocycloalkenylated phenol products **98d** and **98f**, respectively (entries 4, 5). 3-Methoxyphenol and 1-naphthol also reacted with cycloalkanones to form 2-vinylphenol products (entries 6-8).

Table 3.4 Dehydrative C-H alkenylation of phenols with ketones^a

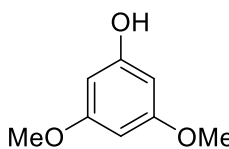
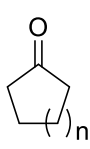
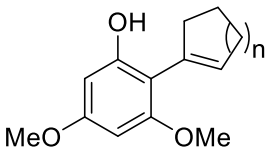
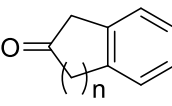
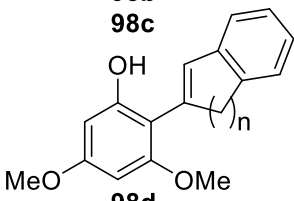
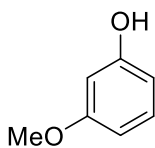
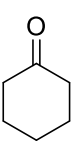
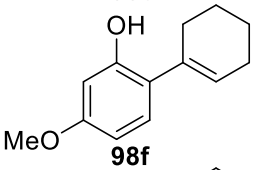
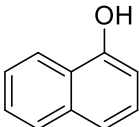
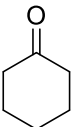
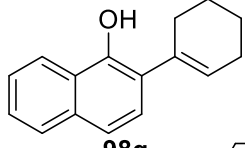
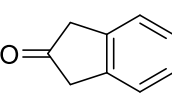
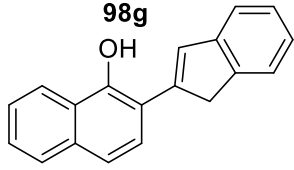
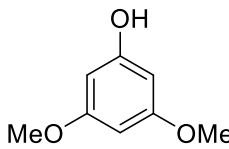
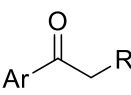
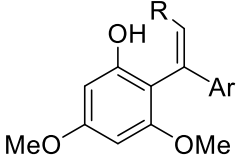
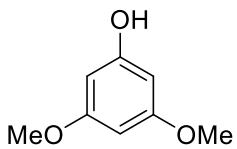
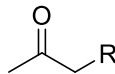
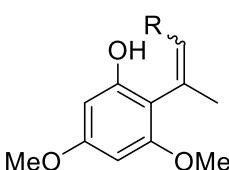
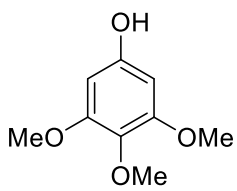
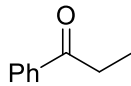
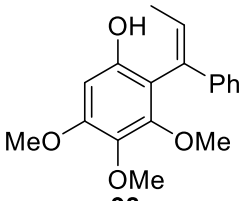
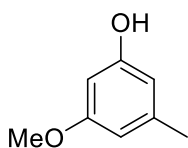
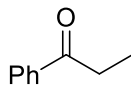
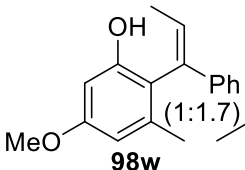
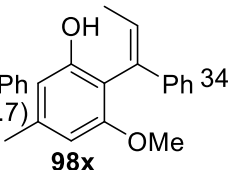
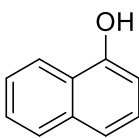
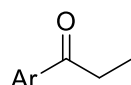
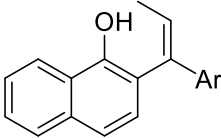
entry	phenol	ketone	product(s)	yield ^b (%)
1 ^c				83
2 ^c		n = 1	98b	92
3		n = 4	98c	63
4				78
5		n = 1	98d	80
5		n = 2	98e	80
6 ^c				55
7 ^c				59
8				62
9				55
10		Ar = Ph	98i	79
11		Ar = <i>p</i> -Cl-C ₆ H ₄	98j	95
12		Ar = Ph	98k	79
13		Ar = Ph	98l	96
14		Ar = <i>p</i> -F-C ₆ H ₄	98m	76
15		Ar = <i>p</i> -Cl-C ₆ H ₄	98n	84
16		Ar = <i>p</i> -OMe-C ₆ H ₄	98o	83
17		Ar = <i>p</i> -Me-C ₆ H ₄	98p	72

Table 3.4 Dehydrative C-H alkenylation of phenols with ketones^a (continued)

entry	phenol	ketone	product(s)	yield ^b (%)
18				
19		R = Ph	98r (Z:E > 95:5)	72
20		R = Bn	98s (Z:E = 4:1)	55
21		R = Et	98t (Z:E = 3:1)	70
21		R = Me	98u (Z:E = 1.4:1)	77
22				58
			98v	
23			 	34
			98w (1:1.7)	
			98x	
24				85
25		Ar = Ph	98y	85
		Ar = <i>p</i> -Cl-C ₆ H ₄	98z	70

^a Reaction conditions: phenol (0.5 mmol), ketone (1.0 mmol), **26** (3 mol %), 1,2-dichloroethane (2 mL), 125 °C. ^b Isolated yields. ^c 1.5 mmol ketone substrate used.

In a similar fashion, we next examined the substrate scope of linear ketones. Acetophenone and 4'-chloroacetophenone readily reacted with 3,5-dimethoxyphenol to give 2-vinylphenol products **98i** and **98j**, respectively (entries 9, 10). The coupling reaction of 3,5-dimethoxyphenol with a series of 2-substituted acetophenones afforded trisubstituted alkene products **98k-98m** (entries 11-13). To our surprise, the stereochemistry of the trisubstituted alkene products was determined to be (Z)-alkenes by nuclear Overhauser effect spectroscopy (NOESY) analysis. To support this, we were able to obtain the X-ray

crystal structure for **98k** (Figure 3.1). The X-ray structure of **98k** showed a (*Z*)-configuration, where the phenolic group is rotated out of conjugation (dihedral angle 69.8°).

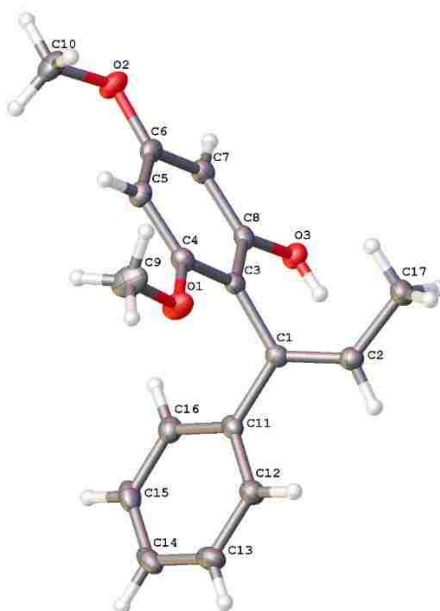


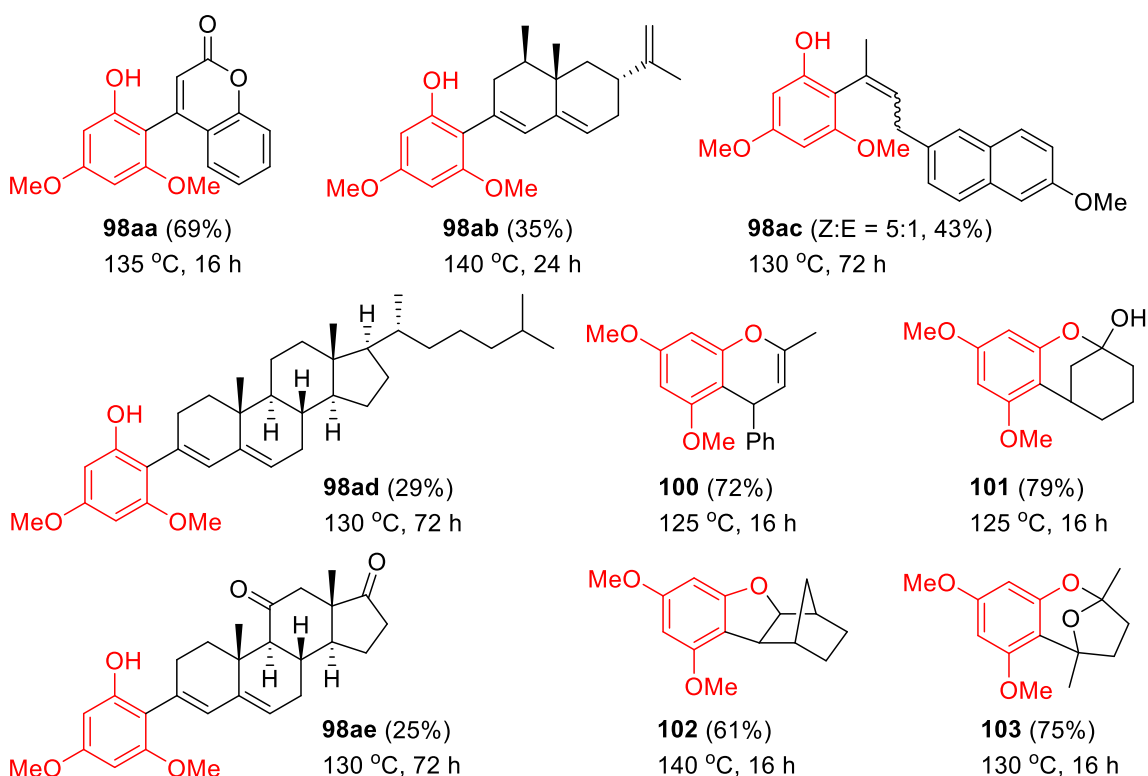
Figure 3.1 Molecular structure of **98k**

Propiophenones with both electron-withdrawing and -donating group also afforded trisubstituted (*Z*)-alkenes exclusively from the coupling reaction with 3,5-dimethoxyphenols (entries 14-17). For these benzoyl-type substrates, a highly (*Z*)-selective formation of *ortho*-alkenylated phenol products were observed. However, the stereoselectivity of the coupling products from alkyl substituted ketone substrates were found to depend on the substituents. The treatment of 3,5-dimethoxyphenol with 4-phenyl-2-butanone gave a 4:1 mixture of *Z/E*-stereoisomers **98s**, while the reaction with 2-butanone gave less selective 1.4:1 mixture of **98u** (entries 19 and 21). These results suggest that the stereoselectivity of the coupling product would be influenced by steric environments around the carbonyl group of the ketone substrate. 3,4,5-Trimethoxyphenol also reacted with propiophenone to form (*Z*)-alkenylphenol product **98v** (entry 22). In case

of 3-methoxy-5-methylphenol, two regioisomers **98w** and **98x** were obtained from the reaction with propiophenone (entry 23). The analogous treatment of 1-naphthol with propiophenones led to the (Z)-selective formation of 2-alkenylated-1-naphthol products (entries 24, 25).

3.4.2 Synthetic Applications for the Catalytic Method for the Coupling of Phenols with Ketones

Table 3.5 Dehydrative coupling of 3,5-dimethoxyphenol with biologically active ketones^a



^a Reaction conditions: 3,5-dimethoxyphenol (0.5 mmol), ketone (1.0 mmol), **26** (3 mol %), 1,2-dichloroethane (2 mL). Isolated yields in parenthesis.

To further illustrate synthetic versatility of the catalytic coupling method, we next surveyed the coupling reaction of biologically active ketone substrates with 3,5-

dimethoxyphenol (Table 3.5). The dehydrative coupling reaction of 3,5-dimethoxyphenol with 4-hydroxycoumarin yielded 4-arylated coumarin product **98aa**. The reaction of 3,5-dimethoxyphenol with (+)-nootkatone led to the alkenylated coupling product **98ab**, and the structure of **98ab** was completely established by two-dimensional NMR spectroscopy (HMQC and HMBC). An anti-inflammatory drug nabumetone also readily reacted with 3,5-dimethoxyphenol to afford a 5:1 mixture of alkenylated phenol products **98ac**. Analogous treatment of 3,5-dimethoxyphenol with (+)-4-cholesten-3-one and adrenosterone gave the corresponding coupling products **98ad** and **98ae**, respectively.

In an effort to extend the substrate scope, we next explored the coupling reaction with α,β -unsaturated ketones. The treatment of 3,5-dimethoxyphenol with 4-phenyl-3-buten-2-one led to the formation of 4*H*-chromene product **100**, which is likely resulted from the Michael addition followed by dehydrative annulation.⁸⁰ In case of 2-cyclohexenone as a coupling partner, a bicyclic hemiketal compound **101** was obtained, and the molecular structure of **101** was also confirmed by X-ray crystallography (Figure 3.2). Bicyclic ketone 2-norbornanone also smoothly reacted with 3,5-dimethoxyphenol to give dihydrobenzofuran product **102**. The coupling reaction of 3,5-dimethoxyphenol with 2,5-hexanedione yielded bicyclic ketal compound **103** under the standard conditions. The analytically pure coupling products **98-103** were isolated by simple column chromatography, and their molecular structure was completely established by NMR spectroscopy.

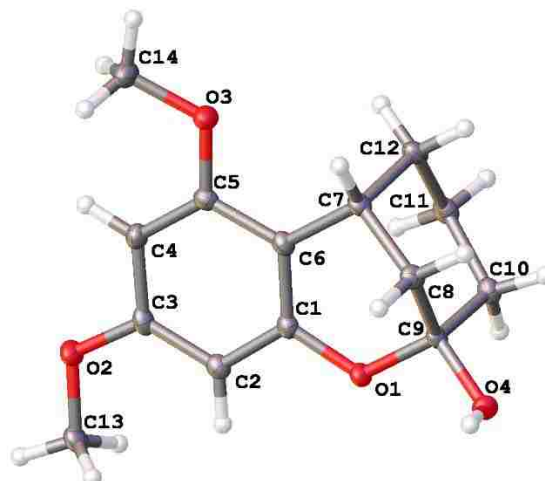
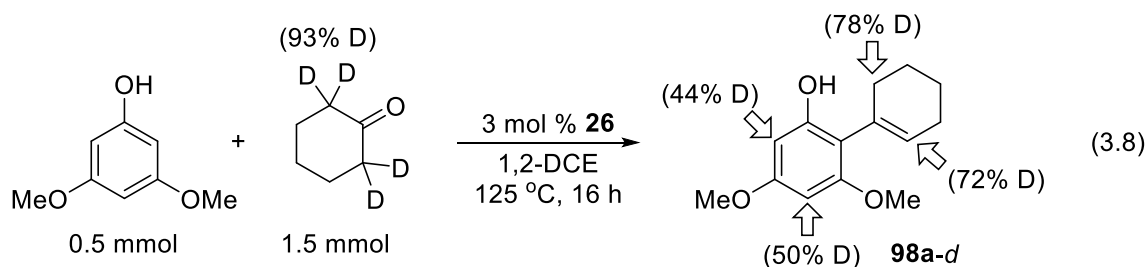


Figure 3.2 Molecular structure of **101**

3.5 Mechanistic Studies

3.5.1 Deuterium Labeling Study



We conducted the deuterium labeling experiment to probe the possible H/D exchange pattern on the coupling product. The treatment of 3,5-dimethoxyphenol (0.5 mmol) with 2,2,6,6-deuterated cyclohexanone (93% D, 1.5 mmol) in the presence of **26** (3 mol %) in 1,2-dichloroethane (2 mL) was heated at 125 °C for 16 h (eq 3.8). The analytically pure product **98a-d** was isolated by silica gel column chromatography, and was analyzed by ^1H and ^2H NMR spectroscopic methods. The ^1H and ^2H NMR spectra of

isolated 2-cyclohexenylphenol showed a selective H/D exchange on *ortho* (44% D) and *para* (50% D) positions on phenol as well as C2 (72% D) and C6 (78% D) of cyclohexenyl group (Figure 3.3). The observed H/D exchange pattern suggests that both reversible C-H activation on phenol and tautomerization of ketone are mediated by the Ru catalyst during the course of the coupling product formation.

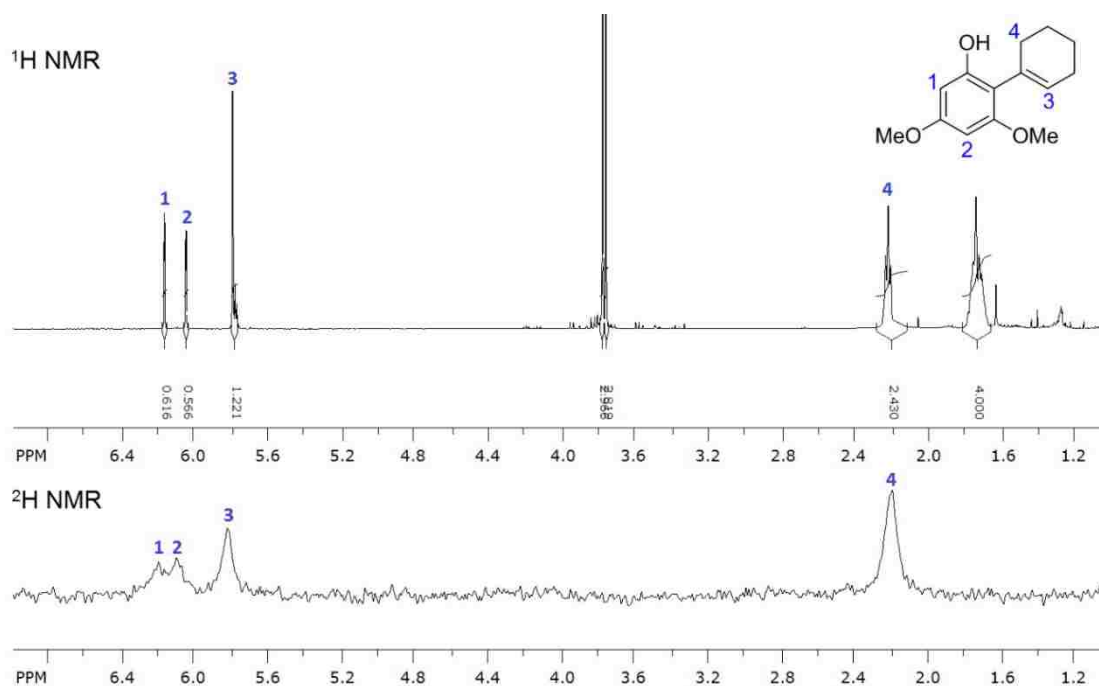
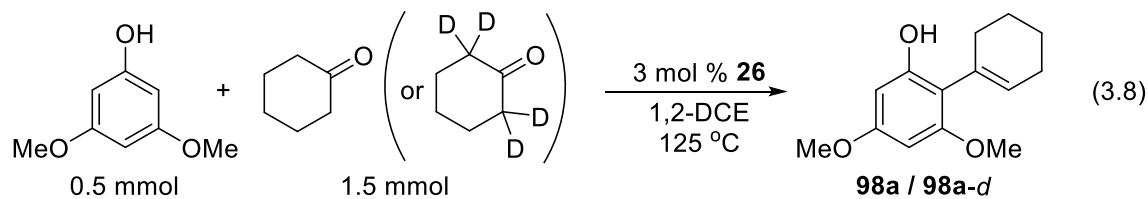


Figure 3.3 ^1H and ^2H NMR spectra of the product **98a-d** isolated from the reaction of 3,5-methoxyphenol with cyclohexanone-2,2,6,6- d_4

3.5.2 Deuterium Isotope Effect Study



To discern the rate-determining step of the catalytic reaction, we performed the deuterium isotope effect on the α -C-H bond of cyclohexanone by comparing the initial reaction rate of 3,5-dimethoxyphenol with cyclohexanone and 2,2,6,6-deuterated cyclohexanone (93% D) at 125 °C in separate reaction tubes (eq 3.8). The k_{obs} value of for each substrate was obtained as $k_{\text{obs}} = 1.86 \times 10^{-3} \text{ min}^{-1}$ (cyclohexanone) and $k_{\text{obs}} = 1.75 \times 10^{-3} \text{ min}^{-1}$ (cyclohexanone- d_4) from the pseudo-first order plot of the formation of **98a**, which led a normal kinetic isotope effect of $k_{\text{H}}/k_{\text{D}} = 1.07 \pm 0.05$ (Figure 3.4). The experimentally determined kinetic isotope effect value indicates that there is no significant initial reaction rate difference between two reactions in forming alkenylated product. These results indicate that the cleavage of α -C-H bond of ketone substrate is not likely the rate-determining step of the coupling reaction.

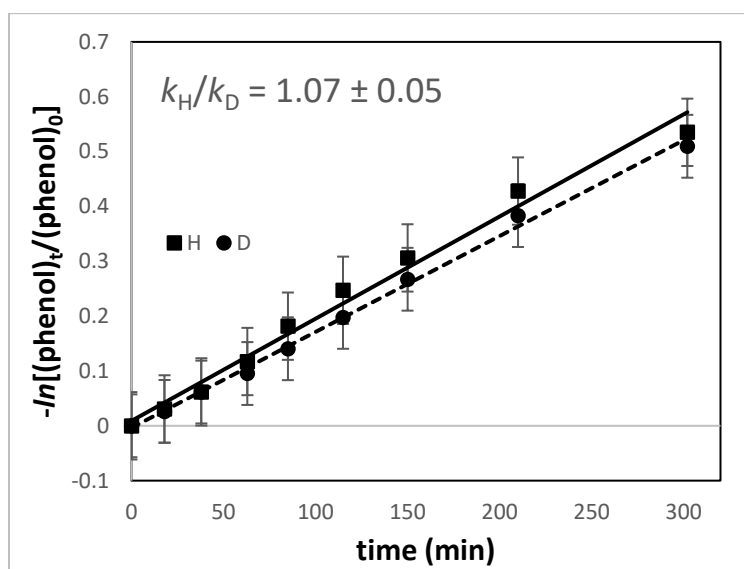
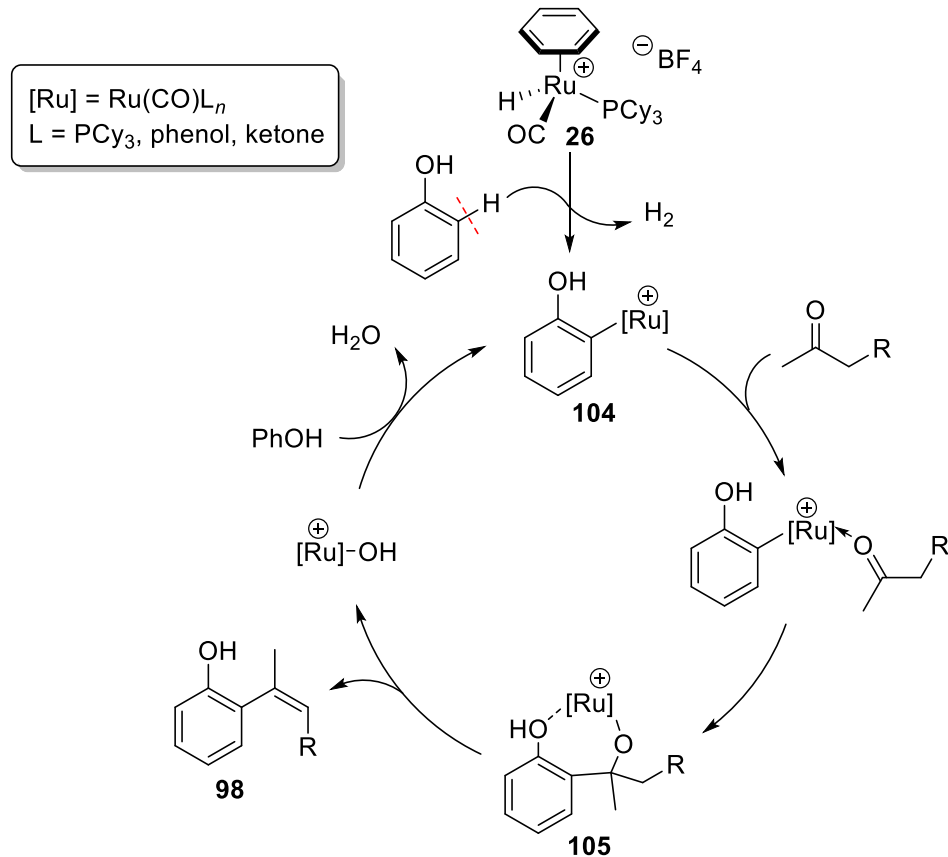


Figure 3.4 The pseudo-first order plots for the reaction of 3,5-dimethoxyphenol with cyclohexanone and cyclohexanone-2,2,6,6- d_4

3.5.3 Proposed mechanism

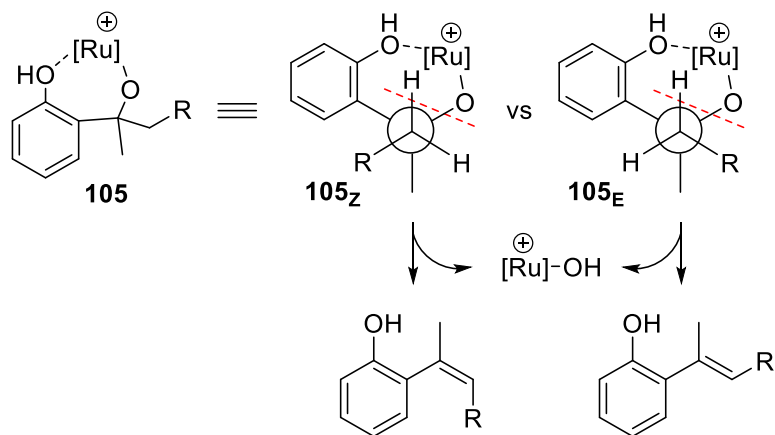


Scheme 3.5 Mechanistic rationale for the C-H alkenylation of phenols

Although details for the C-H alkenylation of phenols still remains unclear at this stage, a plausible reaction mechanism is compiled in Scheme 3.5. We propose that the *ortho*-ruthenated phenol species **104** is initially generated from the dehydrogenative *ortho*-C-H activation of the phenol substrate by cationic ruthenium-hydride catalyst **26**. The observed H/D exchange pattern suggested that the rapid and reversible C-H activation occurs adjacent to the phenol directing groups. The ketone substrate would coordinate to the electrophilic ruthenium center, and the subsequent carbonyl insertion into the Ru-phenyl bond generates 6-membered ruthenacyclic intermediate **105**. The *syn*-elimination of **105** would form the ruthenium-hydroxo species and liberate the *ortho*-alkenylated

phenol product. Dehydrative C-H activation of another phenol substrate would regenerate *ortho*-metalated Ru species **104** for the next catalytic cycle.

The (*Z*)-selective formation of the alkene products **98** can be rationalized by the geometrically preferred formation of the intermediate **105_Z** over **105_E** due to the steric hindrance between R group and ruthenium center (Scheme 3.6). We observed that the (*Z*)-selectivity of the products increases with respect to the steric bulkiness of R group on the ketone substrate (Table 3.3, entries 15-18).



Scheme 3.6 Mechanistic rationale for the (*Z*)-selective formation of 2-alkynylphenols

3.6 Conclusions

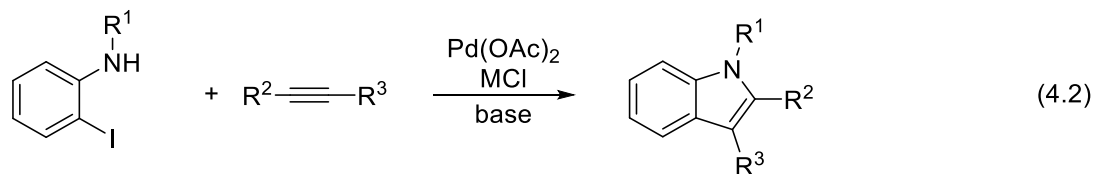
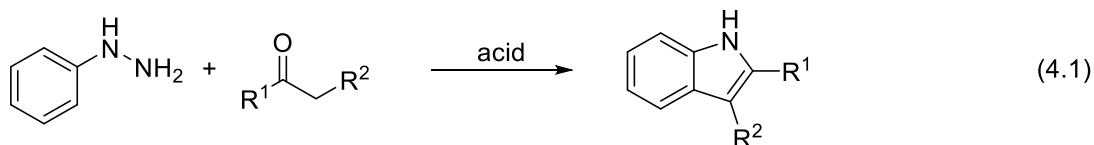
We have successfully developed a highly regio- and stereoselective dehydrative *ortho*-alkenylation method of phenols with ketones. The well-defined ruthenium-hydride catalyst **26** exhibits high activity and a broad substrate scope in promoting the coupling reaction to give (*Z*)-selective olefinated products. The catalytic method employs readily available phenols and ketone substrates to produce synthetically useful 2-vinylphenols without using any additives or activating reagents. The mechanistic rationale has been presented for the (*Z*)-selective formation of coupling product. Efforts to investigate the detailed mechanistic pathway are currently underway.

CHAPTER 4

Catalytic Synthesis of Substituted Indoles and Quinolines from the Dehydrative C-H Coupling of Arylamines with 1,2- and 1,3-Diols

4.1 Introduction

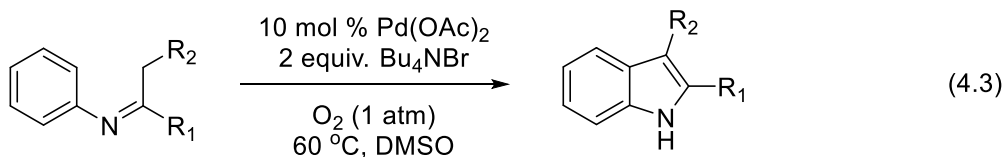
Indole and quinoline derivatives are common structural motifs present in many bioactive natural products and pharmaceutical compounds. The synthesis of these biologically important nitrogen-containing heterocyclic compounds has been studied with a large number of different synthetic methods over the decades.^{81,82} Since, Fischer pioneered the synthesis of indole products from arylhydrazines with ketones/aldehydes under acidic conditions (eq 4.1), various modifications on the classical Fischer indole synthesis have been applied including transition metal-based catalytic methods.⁸³



Larock's indole synthesis is another effective heteroannulation protocol which mediates the coupling of *ortho*-haloaniline with alkynes by using palladium catalysis (eq 4.2).⁸⁴ However, these catalytic methods generally require prefunctionalized starting materials such as hydrazines and *ortho*-haloanilines. Also, the consumption or substitution

of these reactive functional group leads to the inevitable formation of corresponding byproducts.

Recently, a number of oxidative catalytic C-H coupling methods have been developed as viable synthetic methods for indole and related nitrogen heterocyclic compounds. These catalytic methods alleviate inherent problems associated with the classical methods such as requiring prefuctionalized substrates and wasteful byproduct formation.^{85,86} Very recently, the analogous C-H coupling reactions have been achieved by using earth-abundant Co and Ni catalysts.⁸⁷ Notably, a number of oxidative C-H cross-coupling methods have been successfully used to promote the intramolecular annulation of *N*-arylimines and enamines.⁸⁸ Yoshikai and co-workers reported Pd-catalyzed aerobic oxidative cyclization *N*-arylimines (eq 4.3).⁸⁹ This process allowed an atom-economical assembly of indole derivatives from readily available anilines and ketones.



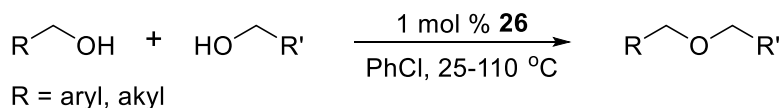
From both environmental and economic points of view, catalytic C-H annulation of simple anilines with diols would be an attractive method to afford *N*-heterocyclic compounds because such method would generate water as the only byproduct. The pioneering work on this protocol was first reported by Watanabe with $\text{RuCl}_3 \cdot n\text{H}_2\text{O}/\text{PBu}_3$ system.⁹⁰ Shim later demonstrated $\text{RuCl}_3 \cdot n\text{H}_2\text{O}/\text{SnCl}_2 \cdot 2\text{H}_2\text{O}$ system for indole and quinoline synthesis from anilines with ethylene glycols or trialkanolammonium salts.⁹¹ Using the $\text{IrCl}_3/\text{BINAP}$ catalyst system, Ishii achieved a highly regioselective coupling of naphthylamines with 1,2- and 1,3-diols to give indole and quinoline products.⁹² Recently, Madsen described 2,3-disubstituted indole and quinoline synthesis from anilines with diols

in the presence of RuCl₃ catalyst.⁹³ However, the synthetic utility of these C-H dehydrative coupling methods has been limited because of the requirement of an excess amount of arylamine substrate, difficulty in controlling regioselectivity as well as the lack of functional group tolerance, and relatively harsh reaction conditions (> 170 °C).

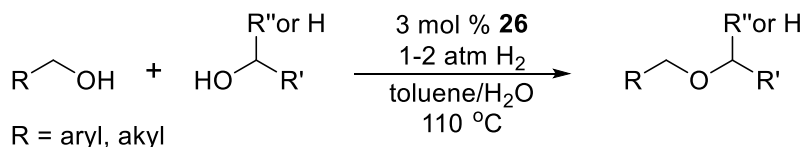
4.2 Results and Discussion

From both environmental and economical points of view, alcohols are highly attractive substrates because they can be readily obtained from natural sources. However, they have been rarely employed for the catalytic C-H coupling reactions because C-O bond cleavage of alcohol is energetically less favored than alkoxylation or dehydrogenation reactions. Our research group recently has shown that the cationic ruthenium-hydride complex **26** is a highly active catalyst for the C-O bond activation reactions, as demonstrated in the C-H alkylation of alkenes with alcohols (Scheme 1.24)⁴³ and C-H alkylation and alkenylation of phenols with alcohols (Scheme 1.26).⁴⁴ More recently, we also reported unsymmetrical etherification of two different alcohols (Scheme 4.1a)⁹⁴ and reductive coupling of aldehydes and ketones with alcohols in aqueous solution (Scheme 4.1b).⁹⁵ A common feature of these catalytic methods involves the formation of ruthenium-hydroxo species as the key intermediate for the C-O bond activation. Late metal-hydroxo and -phenoxo complexes have been found to mediate a number of C-O cleavage reactions.⁹⁶

(a) Catalytic unsymmetrical etherification of two different alcohols

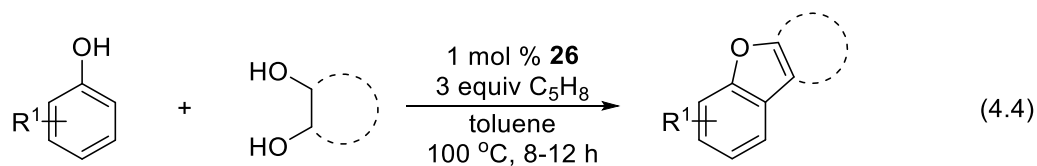


(b) Catalytic reductive coupling of aldehyde and ketones with alcohols



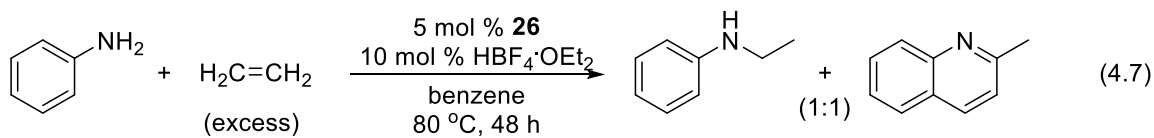
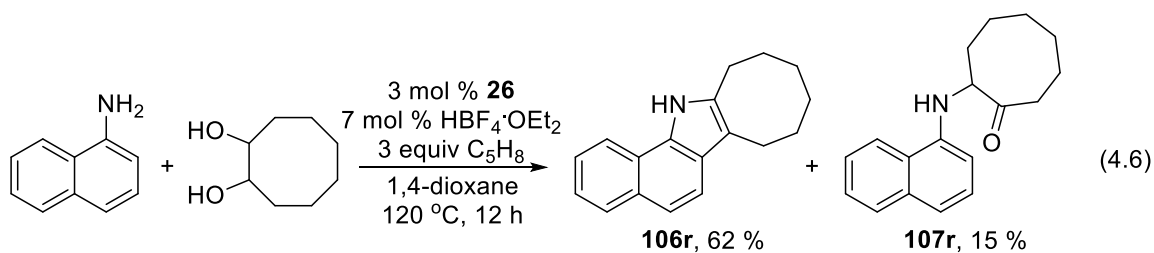
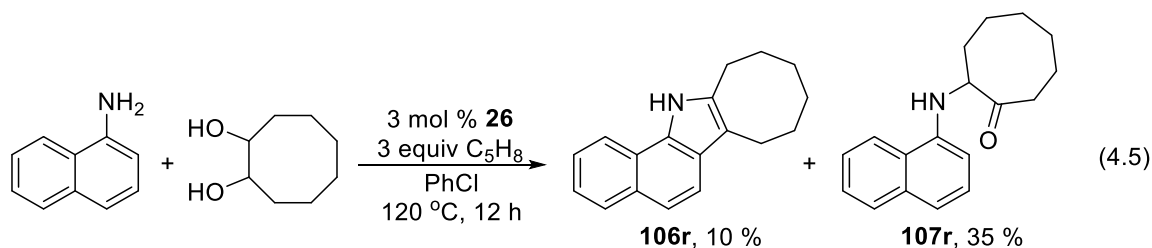
Scheme 4.1 Ruthenium-hydride catalyzed syntheses of unsymmetrical ethers

Glycols and polyols are organic compounds containing more than two hydroxyl groups, which can be easily obtained from the oxidation of alkenes or the dehydration of natural carbohydrates. In the catalytic dehydrative C-O bond activation reactions, they can also be used as the substrates having multiple activation sites. Our group has been able to devise the coupling reaction of phenols with vicinal 1,2-diols to form benzofuran derivatives (eq 4.4).⁴⁴



The success in the heterocyclic annulation of phenols led us to explore the synthesis of nitrogen-containing heterocyclic compounds. Our studies began with the exploration of coupling reactions of arylamines with 1,2-diols. Initially, we have chosen the coupling reaction of 1-naphthylamine with 1,2-cyclooctanediol to produce indole product under the previously reported conditions. The reaction was performed in the presence of the ruthenium catalyst **26** (3 mol %) and cyclopentene (3 equiv.) in chlorobenzene at 120 °C.

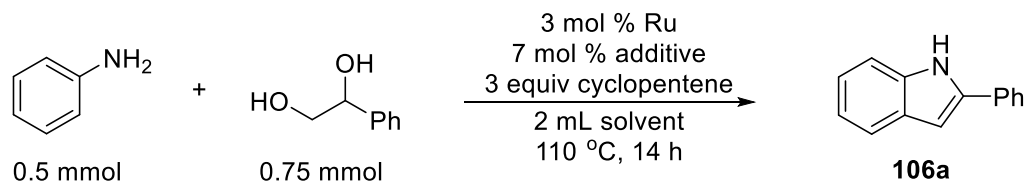
However, under these conditions, the desired indole **106r** was obtained only 10 % isolated yield along with α -ketoamine **107r** as the major product (35 %) (eq 4.5). The undesired α -ketoamine was formed apparently from the dehydrative *N*-alkylation of 1-naphthol with the dehydrogenation of alcohol, which was favored over the dehydrative C-H annulation. In an effort to improve the catalytic efficacy, we were pleased to find that the coupling reaction in the presence of the catalytic amount of $\text{HBF}_4 \cdot \text{OEt}_2$ (7 mol %) additive in 1,4-dioxane afforded 62 % of the polycyclic indole **106r** as the major product and 15 % of byproduct **107r** (eq 4.6). These results indicate that the addition of $\text{HBF}_4 \cdot \text{OEt}_2$ promotes the activity of the Ru catalyst **26** for the both *ortho*-C-H activation of arylamine and C-O bond activation of alcohols. Our previous study showed that the **26**/ $\text{HBF}_4 \cdot \text{OEt}_2$ system effectively catalyzed the coupling reaction of anilines with ethylenes to produce *N*-ethylanilines and 2-methylquinolines (eq 4.7).⁹⁷



Our catalytic method efficiently forms the indole derivatives from the coupling reaction of readily available anilines with 1,2-diols. The catalytic method does not require any stoichiometric amount of base and does not generate any toxic byproducts. For these reasons, we have decided to further investigate both synthetic utility and the mechanism of the catalytic method.

4.3 Catalyst Screening and Optimization Studies

To attain the optimized conditions, we next screened both Ru catalysts and additives for the coupling reaction of aniline with 1-phenyl-1,2-ethanediol (Table 4.1). The treatment of aniline (0.5 mmol) with 1-phenyl-1,2-ethanediol (0.75 mol) in the presence of a ruthenium catalyst (3 mol %) and cyclopentene (1.5 mmol) dioxane was heated at 110 °C for 14 h. The conversion of the indole product **106c** was analyzed by both GC-MS and NMR methods. We found that the addition of catalytic amount of $\text{HBF}_4 \cdot \text{OEt}_2$ has led to the dramatic improvement of the product yield. The cationic Ru-H complex, either in isolated form of the complex **26** or *in situ* generated from a tetranuclear Ru complex **79** exhibited uniquely high catalytic activity with $\text{HBF}_4 \cdot \text{OEt}_2$ (entries 3, 8). No reaction occurred when only $\text{HBF}_4 \cdot \text{OEt}_2$ was employed without Ru complex (entry 22). Among the screened ruthenium complexes and additives, tetranuclear ruthenium hydride complex $\{[(\text{PCy}_3)(\text{CO})\text{RuH}]_4(\mu_4\text{-O})(\mu_3\text{-OH})(\mu_2\text{-OH})\}$ (**79**) with $\text{HBF}_4 \cdot \text{OEt}_2$ was found to be the most effective catalyst for the selective formation of 2-phenylindole product **106a** (entry 3), and 1,4-dioxane was found to be the most suitable solvent for the coupling reaction (entries 3-6).

Table 4.1 Catalyst and additive screening for the coupling reaction of aniline with 1-phenyl-1,2-ethanediol^a

entry	catalyst	additive	solvent	yield (%) ^b
1	[RuH(CO)(PCy ₃) ₄ (O)(OH) ₂ (79)	---	1,4-dioxane	0
2	[RuH(CO)(PCy ₃) ₄ (O)(OH) ₂ (79)	NH ₄ PF ₆	1,4-dioxane	18
3	[RuH(CO)(PCy ₃) ₄ (O)(OH) ₂ (79)	HBF ₄ ·Et ₂ O	1,4-dioxane	96
4	[RuH(CO)(PCy ₃) ₄ (O)(OH) ₂ (79)	HBF ₄ ·Et ₂ O	chlorobenzene	46
5	[RuH(CO)(PCy ₃) ₄ (O)(OH) ₂ (79)	HBF ₄ ·Et ₂ O	toluene	42
6	[RuH(CO)(PCy ₃) ₄ (O)(OH) ₂ (79)	HBF ₄ ·Et ₂ O	dichloroethane	17
7	[RuH(C ₆ H ₆)(CO)(PCy ₃) ⁺ BF ₄ ⁻	---	1,4-dioxane	19
8	[RuH(C ₆ H ₆)(CO)(PCy ₃) ⁺ BF ₄ ⁻	HBF ₄ ·Et ₂ O	1,4-dioxane	83
9	[RuH(CO)(CH ₃ CN) ₂ (PCy ₃) ₂] ⁺ BF ₄ ⁻	---	1,4-dioxane	0
10	RuHCl(CO)(PCy ₃) ₂	---	1,4-dioxane	0
11	RuHCl(CO)(PCy ₃) ₂	HBF ₄ ·Et ₂ O	1,4-dioxane	23
12	RuCl ₂ (PPh ₃) ₃	---	1,4-dioxane	< 3
13	RuCl ₂ (PPh ₃) ₃	HBF ₄ ·Et ₂ O	1,4-dioxane	42
14	RuCl ₃ ·3H ₂ O	---	1,4-dioxane	0
15	[Ru(COD)Cl ₂] ₂	HBF ₄ ·Et ₂ O	1,4-dioxane	< 3
16	[RuCl ₂ (<i>p</i> -cymene)] ₂	---	1,4-dioxane	0
17	[RuCl ₂ (<i>p</i> -cymene)] ₂	HBF ₄ ·Et ₂ O	1,4-dioxane	0
18	Ru ₃ (CO) ₁₂	---	1,4-dioxane	0
19	Ru ₃ (CO) ₁₂	NH ₄ PF ₆	1,4-dioxane	0
20	RuH ₂ (CO)(PPh ₃) ₃	---	1,4-dioxane	0
21	PCy ₃	HBF ₄ ·Et ₂ O	1,4-dioxane	0
22	---	HBF ₄ ·Et ₂ O	1,4-dioxane	0

^a Reaction conditions: catalyst (3 mol % Ru equivalents), additive (7 mol %), aniline (0.5 mmol), 1-phenyl-1,2-ethanediol (0.75 mmol), cyclopentene (1.5 mmol), 1,4-dioxane (2 mL), 110 °C, 14 h. ^b The product yield of **106a** was determined by ¹H NMR using hexamethylbenzene as an internal standard.

4.4 Reaction Scope and Applications

4.4.1 Scope of Dehydrative C-H Coupling Reaction of Arylamines with 1,2-Diols

Table 4.2 Dehydrative coupling of arylamines with 1,2-diols^a

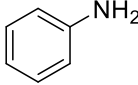
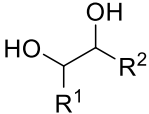
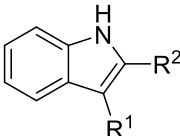
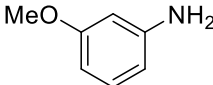
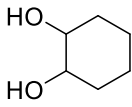
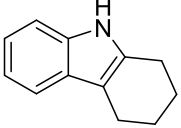
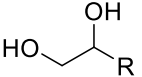
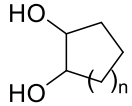
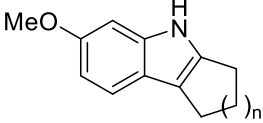
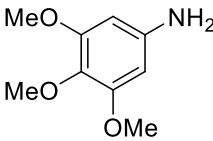
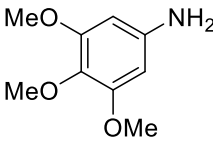
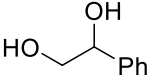
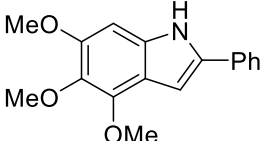
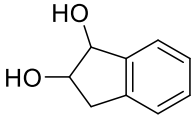
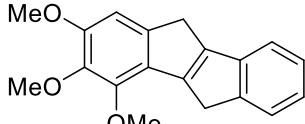
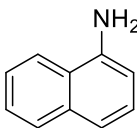
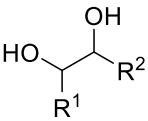
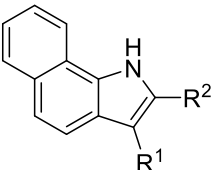
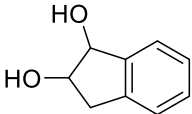
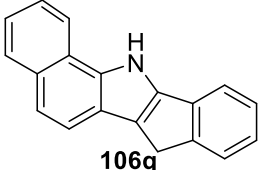
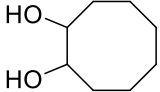
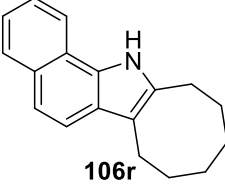
entry	amine	diol	product(s)	temp (°C)	yield ^b (%)
1					
2		R ¹ = H R ² = Ph	106a	110	94
3		R ¹ = H R ² = <i>n</i> -Bu	106b	120	74
4		R ¹ = H R ² = Me	106c	140	61
5		R ¹ = Me R ² = Me	106d	130	60
6				110	56
7			106e		
8		R = <i>n</i> -Bu	106f	110	80
9		R = Ph	106g	130	91
10					
11		n = 1	106h	110	62
12		n = 2	106i	110	85
13		n = 4	106j	140	57 ^c
14				135	94
15			106k		
16				140	62
17			106l		

Table 4.2 Dehydrative coupling of arylamines with 1,2-diols^a (continued)

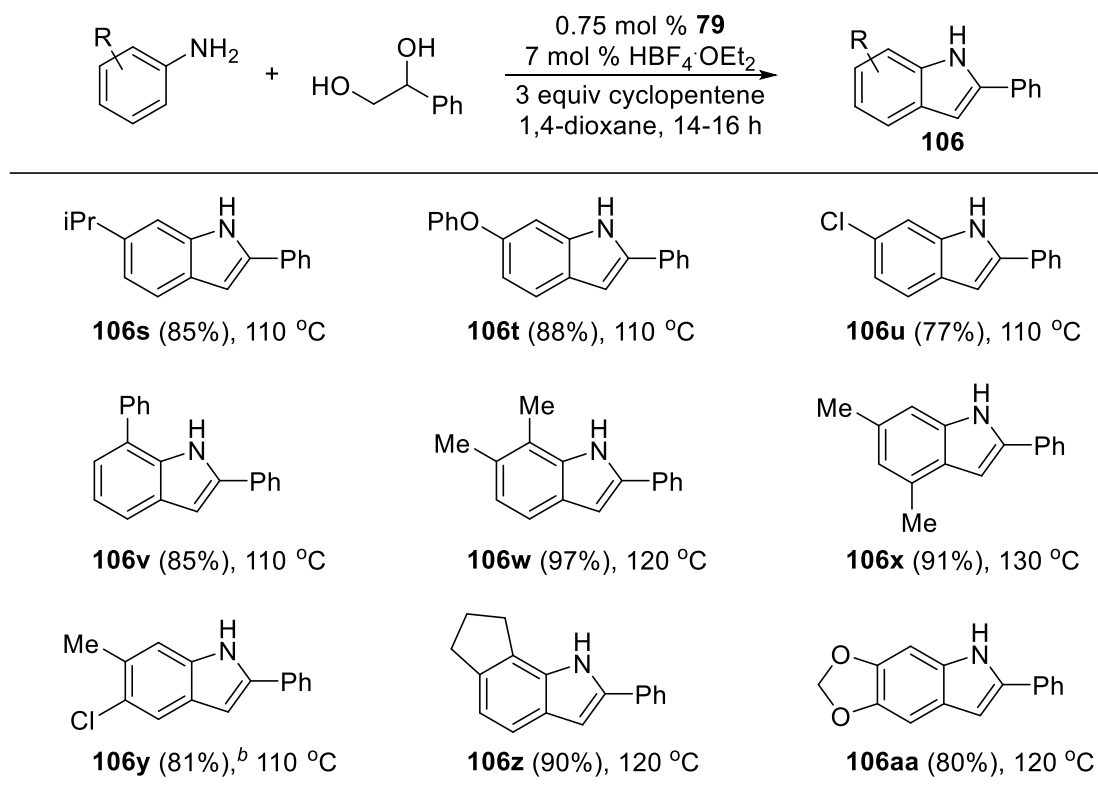
entry	amine	diol	product(s)	temp (°C)	yield ^b (%)
					
13		R ¹ = H R ² = <i>n</i> -Bu	106m	130	63
14		R ¹ = H R ² = Ph	106n	100	74
15		R ¹ = Me R ² = Me	106o	130	72
16		R ¹ = Ph R ² = Ph	106p	130	42
17			 106q	130	63
18			 106r	120	85

^a Reaction conditions: amine (1.0 mmol), 1,2-diol (1.5 mmol), **79** (0.75 mol %), HBF₄·OEt₂ (7 mol %), cyclopentene (3.0 mmol), 1,4-dioxane (3 mL), 14–16 h. ^b Isolated yields. ^c ¹H NMR yield.

With these optimized reaction conditions in hand, we explored the substrate scope of the coupling reaction of anilines with 1,2-diol substrates (Table 4.2). Both aliphatic and aryl-substituted primary-secondary diols readily reacted with aniline to give regioselective 2-substituted indole products **106a–106c** (entries 1–3). A secondary diol 2,3-butanediol afforded 2,3-disubstituted indole product **106d** (entry 4), but with a lower yield than primary-secondary diols. 1,2-Cyclohexanediol also successfully gave the coupling product **106e**, and no difference in reactivity was observed between *cis*- and *trans*-cyclohexanediol. For the coupling of 3-methoxyanilines, 6-methoxyindoles **106f–106j** were obtained regioselectively along with a negligible amount of 4-methoxyindole products by forming

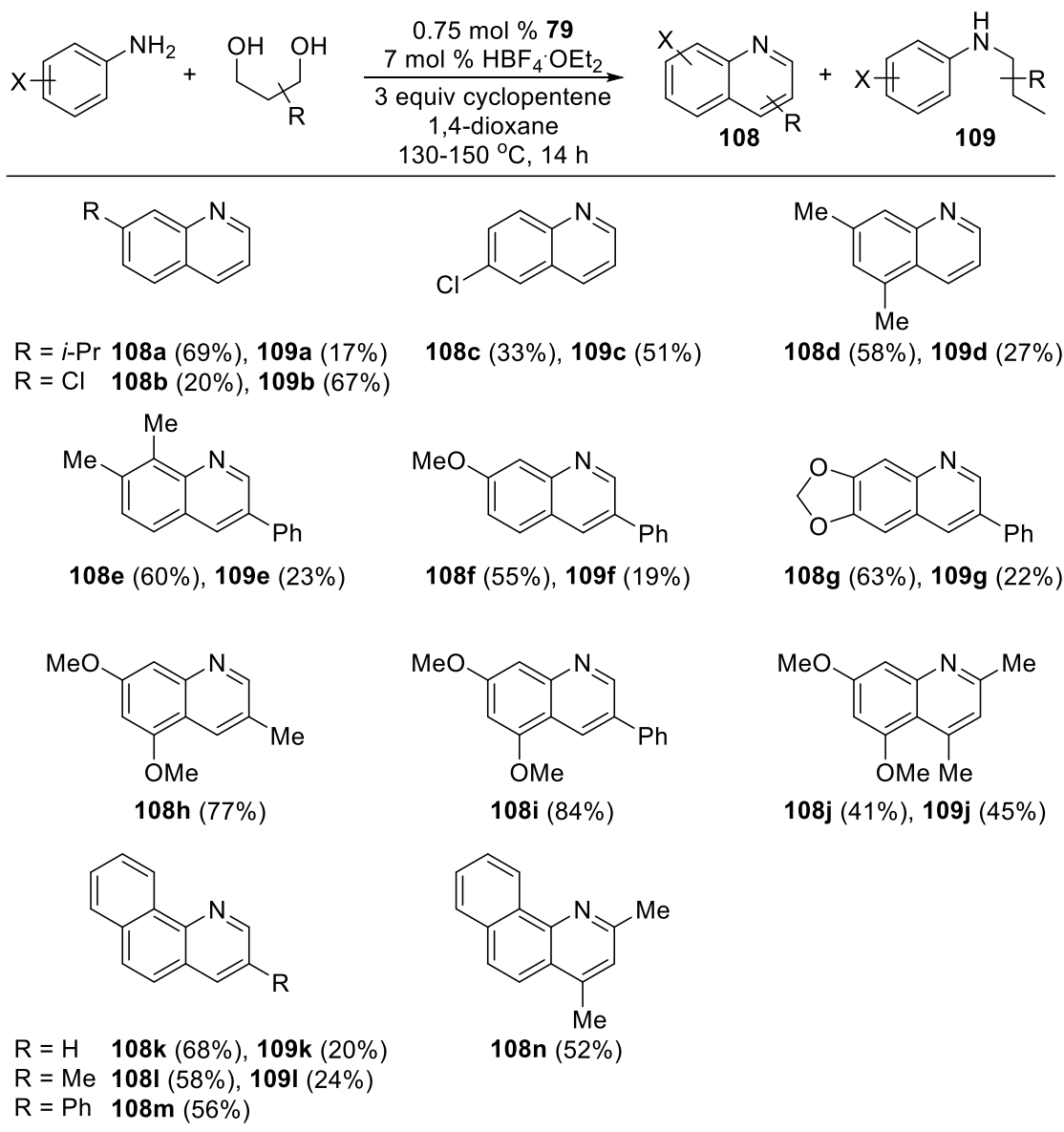
a new C-C bond at *para* to the methoxy group. A series of 1,2-cycloalkanediols effectively proceeded to form tricyclic indoles **106h-106j** (entries 8-10). The coupling of electron-rich 3,4,5-trimethoxyaniline with 1,2-diols also gave the indole products **106k** and **106l** (entries 11, 12). We found that a range of polycyclic indole derivatives can be obtained from the coupling reaction of 1-naphthylamine with 1,2-diols (entries 13-18). Both primary-secondary and secondary-secondary 1,2-diols afforded the corresponding 2-substituted and 2,3-disubstituted 1*H*-benzo[*g*]indoles **106m-106p** in moderate to good yields (entries 13-16). The coupling reaction of 1-naphthylamine with 1,2-indandiol and 1,2-cyclooctanediol gave polycyclic indole products **106q** and **106r**, respectively (entries 17, 18). Among the tested 1,2-diols, 1-phenyl-1,2-ethanediol was found to be the most efficient diol substrate to give 2-substituted indoles for this coupling reaction. The catalytic method achieves the regioselective synthesis of indole derivatives from the direct coupling between arylamines and 1,2-diols without forming any harmful byproducts.

We next surveyed the scope of substituted anilines with 1-phenyl-1,2-diols (Table 4.3). Mono- and disubstituted anilines readily reacted with the diol substrate to form the 2-phenylindole products in good to excellent yields. Both electron-withdrawing and -donating groups were found to be compatible, but we observed the relatively electron-deficient 3-substituted aniline (**106u**) generally gave lower yield than the ones with electron-releasing group (**106g**, **106s**, **106t**). The reaction also tolerates sterically demanding *ortho*-substituted anilines (**106v**, **106w**) and 4-aminoindan (**106z**) in the formation of corresponding indole products. The coupling reaction of 3,4-(methylenedioxy)aniline with diol afforded the heterocyclic indole product **106aa** in 80 % yield.

Table 4.3 Dehydrative coupling of anilines with 1-phenyl-1,2-ethanediol^a

^a Reaction conditions: aniline (1.0 mmol), 1-phenyl-1,2-ethanediol (1.5 mmol), **79** (0.75 mol %), HBF₄·OEt₂ (7 mol %), cyclopentene (3.0 mmol), 1,4-dioxane (3 mL), 14-16 h. Isolated yields in parenthesis. ^b Combined yield of two regioisomers.

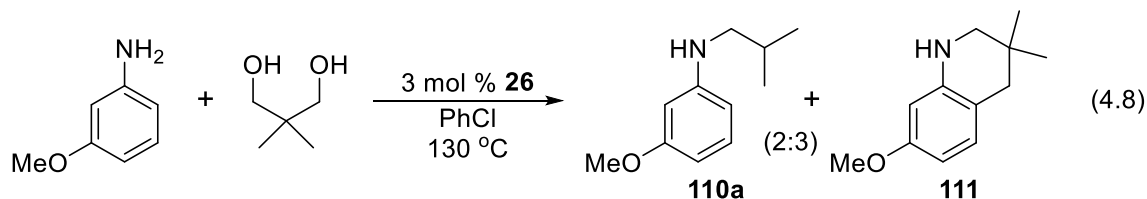
4.4.2 Scope of Dehydrative C-H Coupling Reaction of Arylamines with 1,3-Diols

Table 4.4 Dehydrative coupling of arylamines with 1,3-diols^a

^a Reaction conditions: amine (1.0 mmol), 1,3-diol (1.5 mmol), **79** (0.75 mol %), HBF₄·OEt₂ (7 mol %), cyclopentene (3.0 mmol), 1,4-dioxane (3 mL), 130-150 °C, 14 h. Isolated yields in parenthesis.

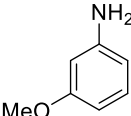
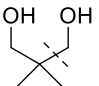
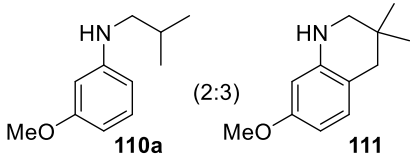


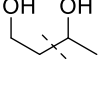
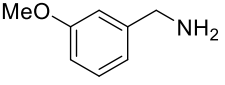
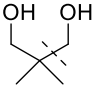
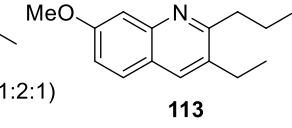
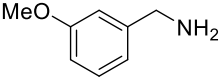
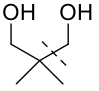
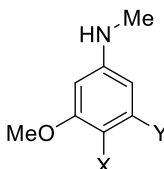
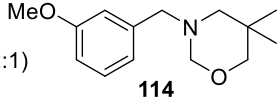
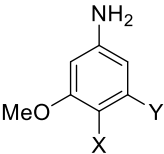
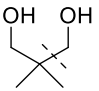

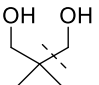

We have been able to extend the synthetic utility to the C-H annulation of anilines with 1,3-diols to produce quinoline derivatives (Table 4.4). The coupling reaction of anilines with 1,3-diols readily afforded quinoline product **108** by using the same catalytic system. However, these reactions required higher temperature (130-150 °C) for the optimal conversion and selectivity in forming the quinoline products. In most cases, significant amount of *N*-alkylated aniline **109** was obtained as the byproduct. We reasoned that the byproduct **109** was formed by the dehydrative hydrogenolysis of the other hydroxyl group over the requisite *ortho*-C-H coupling and annulation process. Anilines bearing electron-withdrawing and -donating group readily reacted with 1,3-propanediols to give the substituted quinoline derivatives (**108a-108d**) with *N*-alkylated anilines (**109a-109d**). In contrast to the anilines with electron-donating group, electron-deficient 3- and 4-chloroanilines gave *N*-alkylated anilines as the major product. Electron-donating group disubstituted anilines smoothly reacted with 2-phenyl-1,3-propanediols to form quinolines as the major product (**108e-108g**). We found that the coupling reaction of 3,5-dimethoxyaniline with 2-substituted 1,3-propanediol gave quinoline product **108h** and **108i** selectively among the screened reactions, as only a trace amount of *N*-alkylated aniline byproduct was detected from the GC-MS analysis of the crude mixture. However, the coupling of 3,5-dimethoxyaniline with secondary 1,3-diol 2,4-pentanediol led to nearly 1:1 mixture of the quinoline product **108j** and *N*-alkylated aniline **109j**. The analogous treatment of 1-naphthylamine with 1,3-diols formed the corresponding polycyclic quinoline derivatives **108k-108n**. Both quinoline and *N*-alkylaniline products **108** and **109** were readily separated by silica gel column chromatography and were analyzed by ¹H and ¹³C NMR spectroscopy.

4.4.3 Ru-Catalyzed C-C Bond Activation Reactions of 1,3-Diols



To examine the coupling reaction of arylamines with 2,2-disubstituted-1,3-diols by using **26**, we initially tested the coupling of 3-methoxyphenol with 2,2-dimethyl-1,3-propanediol in chlorobenzene at 130 °C (eq 4.8). To our surprise, the C-C cleavage product *N*-isobutylaniline **110a** was obtained along with tetrahydroquinoline derivative **111**. This unexpected formation of **110a** was apparently resulted from the dehydrative *N*-alkylation and the cleavage of C-C bond adjacent to the hydroxyl group. To the best of our knowledge, catalytic methods for the selective activation of unstrained sp³-sp³ C-C bond are very rare and difficult, because the C-C bond activation of unstrained saturated hydrocarbons is both kinetically and thermodynamically less favored than that of the C-H bonds.⁹⁸

Table 4.5 Ruthenium catalyzed C-C bond activation reaction of 1,3-diols^a

entry	amine	1,3-diol	product(s)	yield (%)
1				75
2				82
3				80
4 ^b				68
5 ^b				78
6 ^b				74

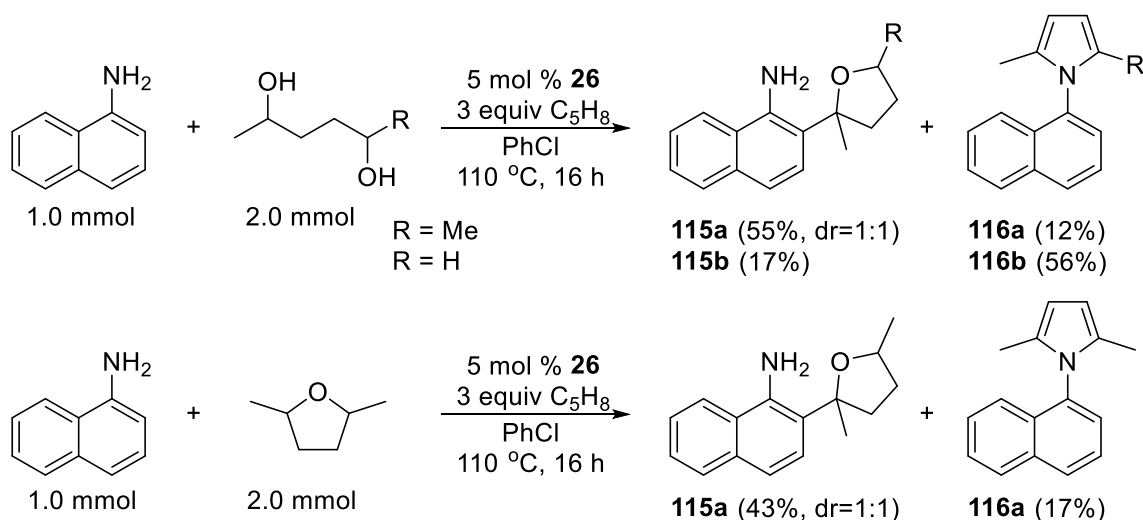
^a Reaction conditions: amine (0.5 mmol), 1,3-diol (1.0 mmol), **26** (5 mol %), chlorobenzene (2 mL), 130 °C. ^b Cs₂CO₃ (20 mol %) was added.

We next explored several other coupling reactions to investigate the pattern of this C-C bond activation method (Table 3.5). The coupling of 3-methoxyaniline with 1,3-butanediol yielded a mixture of the products *N*-ethylaniline **110b**, *N*-butylaniline **112**, and quinoline **113** (entry 2). Again, the coupling product **110b** was formed from the regioselective C-C bond cleavage next to the secondary alcohol. The formation of quinoline product **113** can be explained from the competitive dehydrative *ortho*-C-H alkylation and annulation of two equivalents 1,3-diols. We also observed a similar C-C cleavage pattern from the coupling reaction of 3-methoxybenzylamine with 2,2-dimethyl-1,3-propanediol. In this case, a 2:1 mixture of *N*-isobutylbenzylamine **110c** and tetrahydro-

1,3-oxazine **114** was formed (entry 3). The exact reaction pathways is still not clear at this stage, but we presumed that the byproduct formaldehyde, might have coupled with benzylamine and diol in forming tetrahydro-1,3-oxazine **114**. The product selectivity control is generally difficult in this coupling reaction, often gave a complex mixture of *N,N*-disubstituted products at a higher temperature. Interestingly, the addition of catalytic amount of base completely switched the product formation of the C-C bond cleavage reaction. The coupling reaction of anilines with 2,2-dimethyl-1,3-propanediol in the presence of **26** (5 mol %) and Cs₂CO₃ (20 mol %) in chlorobenzene at 130 °C led to the selective formation of *N*-methylanilines **110d-110f** (entries 4-6).

4.4.4 Ru-Catalyzed *ortho*-C-H Alkylation of Arylamines with 1,4-Diols

During the course of extending this methodology to 1,4-diol substrates, we observed an interesting product formation. The reaction of 1-naphthylamine with 2,5-hexanediol in the presence of **26** (5 mol %), cyclopentene (3 equivalents) in chlorobenzene at 110 °C afforded a 1:1 diastomeric mixture of *ortho*-alkylated arylamine products **115a** along with pyrrole **116a** (Scheme 4.2). Each diastereomer of **115a** was cleanly separated by column chromatography and analyzed by both GC-MS and NMR spectroscopy. For the formation of **115a**, we suspected that a 2,5-dimethyltetrahydrofuran intermediate might have been formed initially via intramolecular dehydration, which subsequently reacted with 1-naphthylamine to give the *ortho*-alkylated product. To discern this hypothesis, we next performed the coupling of 1-naphthylamine with 2,5-dimethyltetrahydrofuran under the same reaction conditions, and the resulting product mixture was similar to the reaction between 1-naphthylamine and 2,5-diol (Scheme 4.2).

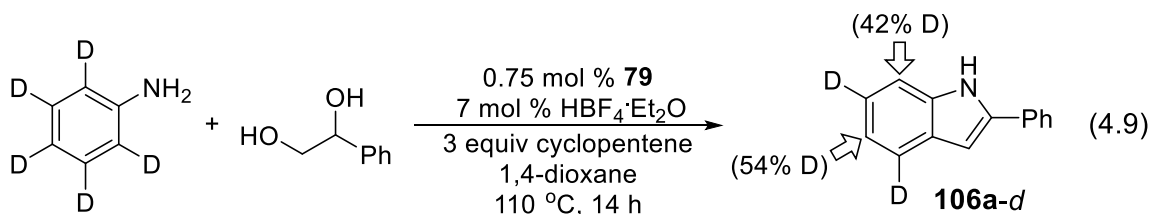


Scheme 4.2 The coupling reaction of 1-naphthylamine with 1,4-diols

The coupling method can accommodate a variety of electron-rich anilines such as 3-methoxyaniline, 3-isopropylaniline, 3-phenoxyaniline, and 4-ethylaniline. However, the scope of 1,4-diol substrates is limited to 2,5-hexanediol or 1,4-pentanediol thus far. The coupling reaction with 1,4-diphenyl-1,4-butanediol gave only intramolecular cyclization product 2,5-diphenyltetrahydrofuran with the recovered aniline starting material, while other primary-primary diols 1,4-butanediol and 1,5-pentanediol gave only corresponding *N*-heterocycles under the catalytic system.

4.5 Mechanistic Study for the Ru Catalyzed Coupling of Aniline with 1,2-Diols

4.5.1 Deuterium Labeling Study



To probe the possible H/D exchange pattern on the coupling product, we examined the reaction of a deuterium-labeled aniline with a 1,2-diol. A mixture of deuterium-labeled aniline-2,3,4,5,6-*d*₅ (0.5 mmol) with 1-phenyl-1,2-ethanediol (0.75 mmol) in the presence of **79** (0.75 mol %), HBF₄·OEt₂ (7 mol %), cyclopentene (3 equivalents) in 1,4-dioxane was heated at 110 °C for 14 hours (eq 4.9). The isolated 2-phenylindole product **106a-d** showed a selective deuterium incorporation to both *ortho* (42% D) and *para* (54% D) arene positions as measured by ¹H and ²H NMR analysis. The observed extensive H/D exchange pattern suggests a rapid and reversible *ortho*- and *para*-C-H bond activations by the Ru catalyst. Our group previously observed a similar H/D exchange pattern on the *para*-arene position from the coupling reaction of arylamines with terminal alkynes from using the same Ru catalytic system.⁹⁹

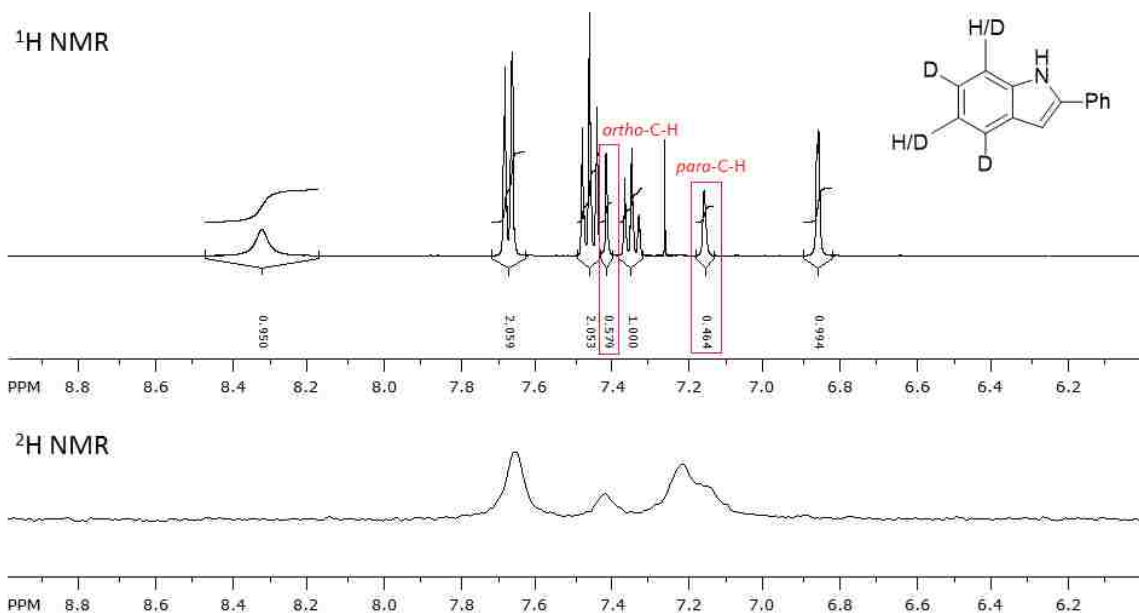
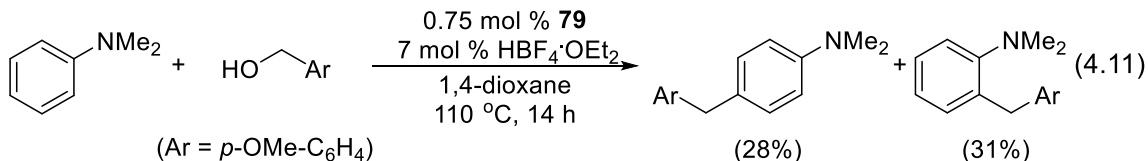
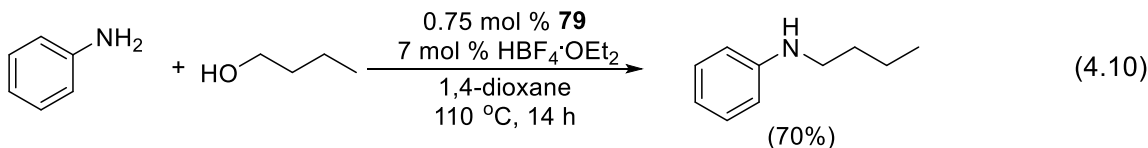


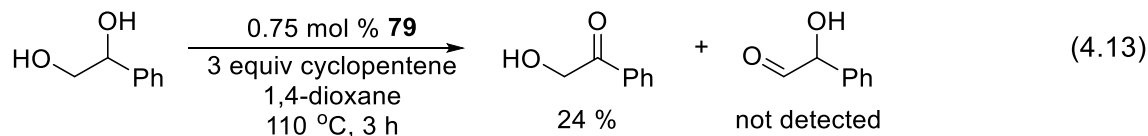
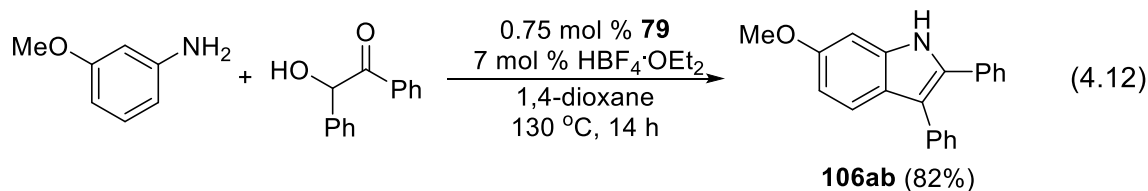
Figure 4.1 ¹H and ²H NMR spectra of the product **106a-d** isolated from the reaction of aniline-2,3,4,5,6-*d*₅ with 1-phenyl-1,2-ethanediol

4.5.2 Control Experiments

We conducted a series of control experiments to distinguish the possible mechanistic pathways. Since the deuterium labeling study showed the selective H/D exchange on *ortho*- and *para*-positions of the aniline substrate, this result indicates the aniline substrate possesses two different potential sites for the C-H activation. However, *para*-alkylated aniline had not been detected under the catalytic conditions, which led us to hypothesize that the coupling reaction might be proceeded by the initial generation of C-N bond with the subsequent intramolecular *ortho*-C-H activation.



To test this hypothesis, we first employed an aliphatic alcohol under the similar reaction conditions. The coupling reaction of aniline with *n*-butanol selectively formed *N*-butylaniline in 70 % yield (eq 4.10). In this case, *N*-alkylation product was formed preferentially over the *ortho*-alkylated aniline product. This result is in sharp contrast to the previously reported coupling reaction of phenol with alcohols, where the *ortho*-alkylation product was exclusively formed.⁴⁴ In a separate experiment, the coupling reaction of *N,N*-dimethylaniline with 4-methoxybenzyl alcohol afforded both *ortho*- and *para*-alkylated *N,N*-dimethylanilines (eq 4.11). These experimental results support a reaction sequence involving the initial C-N bond followed by intramolecular *ortho*-C-H annulation.

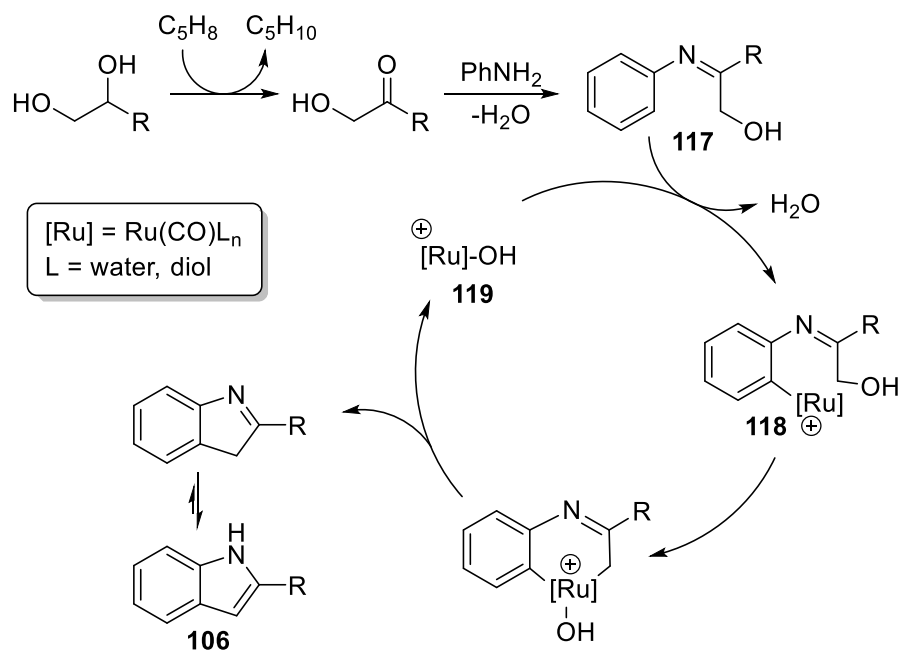


We discovered that the reaction of 3-methoxyaniline with benzoin provides corresponding indole product **106ab** in 82 % yield under the standard conditions. For this reaction, no difference in product yield was made even in the absence of hydrogen acceptor (cyclopentene) (eq 4.12). To explain the observed regioselectivity of the indole product, we hypothesized that the 1,2-diol substrate could undergo dehydrogenation to form a α -hydroxyketone intermediate prior to the dehydrative C-N bond formation. In support of this initial formation of α -hydroxyketone and the regioselectivity of the indole product, 2-hydroxyacetophenone was cleanly formed when 1-phenyl-1,2-ethanediol was treated with **79** and cyclopentene (24 % conversion in 3 hours) (eq 4.13). The similar chemoselective oxidation of the secondary alcohols over the primary alcohols was reported by using transition metal catalysts.¹⁰⁰

4.5.3 Proposed Mechanism

On the basis of these results, we present a possible mechanism for the dehydrative coupling reaction of aniline with 1,2-diol (Scheme 4.3). We propose that the dehydrogenation of diol would initially generate α -hydroxyketone, which could react with aniline to give α -hydroxyimine **111** by releasing water. We believe that the chemoselective oxidation of the secondary alcohol at this stage is the key step for the regioselective formation of the 2-substituted indole products. The subsequent chelate-assisted *ortho*-C-H activation would form *ortho*-ruthenated imine species **118**, in a similar fashion to the dehydrative C-H insertion reaction of phenols.⁴⁴ The intramolecular C-O bond activation of alcohol followed by reductive elimination would liberate the indole product **106** and generate cationic Ru-hydroxo species **119**. In support of this proposal, we recently showed

that Ru-hydroxo complexes are a key intermediate species in ketone hydrogenolysis reaction.⁵⁵ In addition, the formation of N-alkylated product **108** can be explained by a competitive hydrogenolysis pathway especially in case of for the coupling of an electron-deficient aniline with 1,3-diols.



Scheme 4.3 Plausible mechanistic pathway for the dehydrative coupling of aniline with 1,2-diol

4.6 Conclusions

We have successfully developed an effective catalytic protocol for the coupling of inexpensive and readily available arylamines and diols substrates to produce biologically important indole and quinoline derivatives. A wide range of substrates has been demonstrated to form the regioselective *N*-heteroannulated products without forming any toxic byproducts. The tetrameric Ru-hydride **79** with $\text{HBF}_4 \cdot \text{OEt}_2$ was found to be an effective catalyst precursor, which exhibits uniquely high catalytic activity for the dehydrative coupling reaction of arylamines with diols. We have performed the deuterium labeling study and control experiments, which support our proposed mechanism for the regioselective formation of indoles. A part of this work was published in *Organometallics* **2016**, 35, 1973-1977. DOI: 10.1021/acs.organomet.6b00273

CHAPTER 5

Experimental Section

5.1 General Information

All operations were carried out in a nitrogen-filled glove box or by using standard high vacuum and Schlenk techniques unless otherwise noted. Solvents were freshly distilled over appropriate drying reagents. Benzene, toluene, and n-hexane were distilled from purple solutions of sodium and benzophenone, and dichloromethane was dried over calcium hydride prior to use. All organic substrates were received from commercial sources and were used without further purification. Column chromatography was performed on Dynamic Absorbents silica gel 60A (32-63 μm particle size), and thin layer chromatography was performed on Agela glass back TLC plates pre-coated with silica gel MF254. The ^1H , ^2H , ^{13}C , ^{19}F and ^{31}P NMR spectra were recorded on a Varian 300 or 400 MHz FT-NMR spectrometer, and the data are reported in parts per million (ppm) relative to TMS, with the residual solvent peak as an internal reference. Multiplicities are reported as: s = singlet, d = doublet, t = triplet, q = quartet, m = multiplet, br = broad; coupling constant(s) in Hz. Mass spectra were recorded from Agilent 6850 GC-MS spectrometer with a HP-5 (5% phenylmethylpolysiloxane) column (30 m, 0.32 mm, 0.25 μm). High resolution mass spectra (HRMS) were obtained at the Mass Spectrometry/ICP Lab, Department of Chemistry and Biochemistry, University of Wisconsin Milwaukee, Milwaukee, WI and the Center of Mass Spectrometry, Washington University, St. Louis, MO. Elemental analyses were performed at the Midwest Microlab, Indianapolis, IN.

5.2 Synthesis of Ruthenium Catalysts

5.2.1 Synthesis of [(PCy₃)₂(CO)RuH]₄(μ₄-O)(μ₃-OH)(μ₂-OH) (**79**)

The tetranuclear Ru-hydride complex **79** was synthesized in two steps from the 5-coordinated Ru-hydride complex (PCy₃)₂(CO)RuHCl (**23**) (Scheme 2.3). In a glovebox, a 25 mL Schlenk tube equipped with a magnetic stirring bar and Teflon stopcock was charged with (PCy₃)₂(CO)RuHCl (**2**) (726 mg, 1.0 mmol), KOH (6.5 mmol), and 2-propanol (5 mL). The reaction tube was brought out of the box and was stirred in an oil bath at 90 °C for 8 h. The solvent was removed under high vacuum, and the residue was washed with 2-propanol and benzene to obtain the dinuclear Ru complex **78**.

In the glove box, the obtained Ru complex **78** (500 mg, 0.46 mmol) and acetone (5 mL) were added to a 25 mL Schlenk tube equipped with a magnetic stirring bar and Teflon stopcock. The reaction tube was brought out of the glovebox and stirred in an oil bath at 100 °C for 4 h. After the tube was cooled to room temperature, the resulting red solid was filtered, washed with cold acetone (5 mL, 3 times), and recrystallized in dichloromethane to obtain product **79** in 90 % yield. Spectroscopic data for **78**: ¹H NMR (300 MHz, CD₂Cl₂) δ 2.25-1.15 (m, PCy₃), -2.50 and -2.60 (s, μ-OH), -14.56 (d, *J*_{PH} = 19.2 Hz, Ru-H), -15.02 (d, *J*_{PH} = 18.0 Hz, Ru-H), -15.28 (d, *J*_{PH} = 34.8 Hz, Ru-H), -18.64 (dt, *J*_{PH} = 13.2, 4.8 Hz, Ru-H-Ru); ³¹P{¹H} NMR (CDCl₃, 121.6 MHz) δ 82.13 (s, PCy₃), 79.01 (d, *J*_{PP} = 14.0 Hz (PCy₃)), 71.96 (s, (PCy₃)), 68.89 (d, *J*_{PP} = 14.0 Hz, (PCy₃)); IR (CH₂Cl₂) ν_{OH} = 2926, 2849 cm⁻¹, ν_{CO} = 1925, 1912, 1894, 1868 cm⁻¹. Anal. Calcd for **79** C₇₆H₁₃₈O₇P₄-Ru₄: C 53.95; H 8.22. Found: C 55.03; H 8.14.

5.2.2 Synthesis of $[(\eta^6\text{-C}_6\text{H}_6)(\text{PCy}_3)(\text{CO})\text{RuH}]^+\text{BF}_4^-$ (**26**)

The cationic Ru-hydride **26** was synthesized from the tetranuclear Ru-H complex **79** (Scheme 2.3). Under N_2 atmosphere (glove box), the complex **79** (400 mg, 0.24 mmol) was dissolved in benzene (15 mL) in a 25 mL Schlenk tube equipped with a Teflon screw-cap stopcock and a magnetic stirring. Then $\text{HBF}_4 \cdot \text{OEt}_2$ (128 μL , 0.96 mmol) was added to the tube via syringe under N_2 stream. The color of the solution was changed from brown-red to pale yellow immediately. After stirring for 1 h at room temperature, the solvent was removed under vacuum, and the residue was crashed by adding hexanes (20 mL). Filtering the resulting solid through a fritted funnel and recrystallization from CH_2Cl_2 /hexanes yielded the product as a pale yellow powder (524 mg, 95% yield). Single crystals of **26** suitable for X-ray crystallography were obtained from a slow evaporation of benzene and hexanes solution. Spectroscopic data for **26**: ^1H NMR (CD_2Cl_2 , 400 MHz) δ 6.53 (s, C_6H_6), 2.0-1.2 (m, PCy_3), -10.39 (d, $J_{\text{PH}} = 25.9$ Hz, Ru-H); $^{13}\text{C}\{^1\text{H}\}$ NMR (CD_2Cl_2 , 100 MHz), δ 196.4 (d, $J_{\text{CP}} = 19.3$ Hz, CO), 100.0 (C_6H_6), 38.4, 38.2, 30.2, 29.9, 27.4, 27.3 and 26.2 (PCy_3); $^{31}\text{P}\{^1\text{H}\}$ NMR (CD_2Cl_2 , 162 MHz) δ 72.9 (PCy_3); IR (KBr) $\nu_{\text{CO}} = 1991$ cm^{-1} ; Anal. Calcd for **26** $\text{C}_{25}\text{H}_{40}\text{BF}_4\text{OPRu}$: C, 52.18; H, 7.01. Found: C, 51.73; H, 6.91.

5.3 Experimental Procedures and Data for the Chapter 2

5.3.1 General Procedures for the Coupling Reaction of Phenol with Aldehydes

General Procedure for the C-H Acylation of Phenol with Aldehyde. In a glove box, a phenol (0.5 mmol), an aldehyde (1.0 mmol), K_2CO_3 (30 mol %), PPh_3 (20 mol %) and complex **26** (14 mg, 5 mol %) were dissolved in chlorobenzene (2 mL) in a 25 mL Schlenk tube equipped with a Teflon stopcock and a magnetic stirring bar. The tube was brought out of the glove box, and was stirred in an oil bath set at 70-110 °C for 8-16 h. The reaction tube was taken out of the oil bath, and was cooled to room temperature. After the tube was open to air, the solution was filtered through a short silica gel column by eluting with CH_2Cl_2 (10 mL), and the filtrate was analyzed by GC-MS. Analytically pure product was isolated by a simple column chromatography on silica gel (280-400 mesh, hexanes/EtOAc). The product was completely characterized by NMR and GC-MS spectroscopic methods.

General Procedure for the C-H Acylation of Phenol with α,β -Unsaturated Aldehyde. In a glove box, a phenol (0.5 mmol), an α,β -unsaturated aldehyde (1.0 mmol), K_2CO_3 (30 mol %), PPh_3 (20 mol %) and complex **26** (14 mg, 5 mol %) were dissolved in chlorobenzene (2 mL) in a 25 mL Schlenk tube equipped with a Teflon stopcock and a magnetic stirring bar. The tube was brought out of the glove box, and was stirred in an oil bath set at 110-130 °C for 12-24 h. The reaction tube was taken out of the oil bath, and was cooled to room temperature. After the tube was open to air, the solution was filtered through a short silica gel column by eluting with CH_2Cl_2 (10 mL), and the filtrate was analyzed by GC-MS. Analytically pure product was isolated by a simple column

chromatography on silica gel (280-400 mesh, hexanes/EtOAc). The product was completely characterized by NMR and GC-MS spectroscopic methods.

5.3.2 General Procedures for the Mechanistic Studies

Deuterium Labeling Study. In a glove box, 3,5-dimethoxyphenol (0.77 g, 5.0 mmol), benzaldehyde- α - d_1 (>95 % D, 1.0 mmol), K_2CO_3 (30 mol %), PPh_3 (20 mol %) and complex **26** (5 mol %) were dissolved in chlorobenzene (2 mL) in a 25 mL Schlenk tubes equipped with a Teflon screw cap stopcock. The tube were brought out of the box, and immersed in an oil bath preset at 110 °C for 12 h. The reaction tube was taken out of the oil bath, and was cooled to room temperature. After the tube was open to air, the solution was filtered through a short silica gel column by eluting with CH_2Cl_2 (10 mL), and the filtrate was analyzed by GC-MS. Analytically pure products and unreacted phenol substrate were isolated by a simple column chromatography on silica gel (280-400 mesh, hexanes/EtOAc = 100:1 to 1:1), then were completely characterized by 1H , 2H NMR and GC-MS spectroscopic methods.

Deuterium Isotope Effect Study. In a glove box, 3,5-methoxyphenol (0.5 mmol), benzaldehyde- α - d_1 (1.0 mmol), K_2CO_3 (30 mol %), PPh_3 (20 mol %) and complex **26** were dissolved in chlorobenzene (2 mL) in five separate 25 mL Schlenk tubes equipped with a Teflon screw cap stopcock. The tubes were brought out of the box, and immersed in an oil bath preset at 110 °C. The reaction rate was measured by monitoring the appearance of the product signals on 1H NMR, which were normalized against the internal standard hexamethylbenzene in 20 min intervals for 100 min of the reaction time. The experiment

was repeated by using benzaldehyde. The k_{obs} was determined from a first-order plot of $-\ln[(3,5\text{-methoxyphenol})_t/(3,5\text{-methoxyphenol})_0]$ vs time.

Hammett Study. In a glove box, 3,5-dimethoxyphenol (0.5 mmol), $p\text{-X-C}_6\text{H}_4\text{CHO}$ (1.0 mmol), K_2CO_3 (30 mol %), PPh_3 (20 mol %) and complex **26** were dissolved in chlorobenzene (2.0 mL) in five separate 25 mL Schlenk tubes equipped with a Teflon screw cap stopcock. The tubes were brought out of the box, and immersed in an oil bath preset at 110 °C. The reaction rate was measured by monitoring the appearance of the product signals on ^1H NMR, which were normalized against the internal standard hexamethylbenzene peak in 20 min intervals for 100 min of the reaction time. The k_{obs} was determined from a first-order plot of $-\ln[(3,5\text{-dimethoxyphenol})_t/(3,5\text{-dimethoxyphenol})_0]$ vs time. The Hammett plot of $\log(k_{\text{X}}/k_{\text{H}})$ vs σ_p is shown in Figure 2.9.

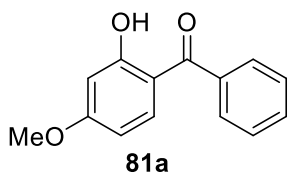
5.3.3 X-Ray Crystallographic Determination of **81v**, **83t**, and **84b**

For **81v**: Colorless single crystals of **81v** were grown in CH_2Cl_2 at room temperature. A suitable crystal with the dimension of $0.28 \times 0.14 \times 0.11 \text{ mm}^3$ was selected and mounted on an Oxford SuperNova diffractometer equipped with dual microfocus Cu/Mo X-ray sources, X-ray mirror optics, and Atlas CCD area detector. A total of 15224 reflection data were collected by using $\text{MoK}\alpha$ ($\lambda = 0.71073$) radiation while the crystal sample was cooled at 100.05 K during the data collection. Using Olex2, the molecular structure was solved with the ShelXS structure solution program by using Direct Methods, and the data was refined with the XL refinement package using Least Squares minimization. The molecular structure of **81v** is shown in Figure 2.4.

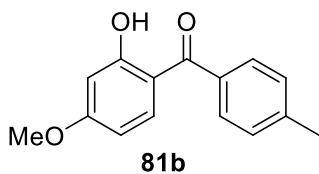
For **83t**: Colorless single crystals of **83t** were grown in CH₂Cl₂ at room temperature. A suitable crystal with the dimension of 0.42 × 0.35 × 0.18 mm³ was selected and mounted on an Oxford SuperNova diffractometer equipped with dual microfocus Cu/Mo X-ray sources, X-ray mirror optics, and Atlas CCD area detector. A total of 18380 reflection data were collected by using CuKα (λ = 1.54184) radiation while the crystal sample was cooled at 100.00 K during the data collection. Using Olex2, the molecular structure was solved with the ShelXS structure solution program by using Direct Methods, and the data was refined with the XL refinement package using Least Squares minimization. The molecular structure of **83t** is shown in Figure 2.5.

For **84b**: Colorless single crystals of **84b** were grown in CH₂Cl₂/Hexane at room temperature. A suitable crystal with the dimension of 0.18 × 0.14 × 0.02 mm³ was selected and mounted on an Oxford SuperNova diffractometer equipped with dual microfocus Cu/Mo X-ray sources, X-ray mirror optics, and Atlas CCD area detector. A total of 11892 reflection data were collected by using CuKα (λ = 1.54184) radiation while the crystal sample was cooled at 99.8 K during the data collection. Using Olex2, the molecular structure was solved with the ShelXS structure solution program by using Direct Methods, and the data was refined with the XL refinement package using Least Squares minimization. The molecular structure of **84b** is shown in Figure 2.6.

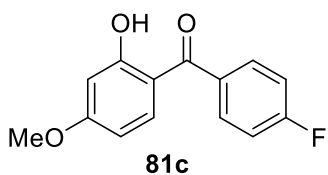
5.3.4 Characterization Data of the Products



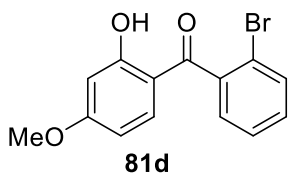
Data for **81a**: ^1H NMR (400 MHz, CDCl_3) δ 12.70 (s, 1H), 7.65-7.62 (m, 2H), 7.59-7.54 (m, 1H), 7.52-7.47 (m, 3H), 7.50 (d, $J = 9.0$, 1H), 6.52 (d, $J = 2.5$ Hz, 1H), 6.41 (dd, $J = 9.0, 2.5$ Hz, 1H), 3.86 (s, 3H) ppm; $^{13}\text{C}\{^1\text{H}\}$ NMR (100 MHz, CDCl_3) δ 200.0, 166.3, 166.2, 138.2, 135.2, 131.4, 128.8, 128.3, 113.1, 107.4, 101.0, 55.6 ppm; GC-MS $m/z = 228$ (M^+); Anal. Calcd for $\text{C}_{14}\text{H}_{12}\text{O}_3$: C, 73.67; H, 5.30. Found: C, 73.56; H, 5.25.



Data for **81b**: ^1H NMR (400 MHz, CDCl_3) δ 12.73 (s, 1H), 7.55 (d, $J = 8.1$ Hz, 2H), 7.53 (d, $J = 8.9$ Hz, 1H), 7.29 (d, $J = 8.1$ Hz, 2H), 6.52 (d, $J = 2.5$ Hz, 1H), 6.41 (dd, $J = 8.9, 2.5$ Hz, 1H), 3.86 (s, 3H), 2.44 (s, 3H) ppm; $^{13}\text{C}\{^1\text{H}\}$ NMR (100 MHz, CDCl_3) δ 199.8, 166.2, 166.0, 142.1, 135.5, 135.2, 129.1, 128.9, 113.2, 107.2, 101.0, 55.6, 21.5 ppm; GC-MS $m/z = 242$ (M^+); Anal. Calcd for $\text{C}_{15}\text{H}_{14}\text{O}_3$: C, 74.36; H, 5.82. Found: C, 74.29; H, 5.94.

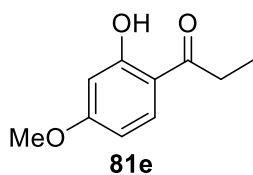


Data for **81c**: ^1H NMR (400 MHz, CDCl_3) δ 12.58 (s, 1H), 7.69-7.64 (m, 2H), 7.47 (d, $J = 9.0$ Hz, 1H), 7.20-7.14 (m, 2H), 6.52 (d, $J = 2.5$ Hz, 1H), 6.42 (dd, $J = 9.0, 2.5$ Hz, 1H), 3.86 (s, 3H) ppm; $^{13}\text{C}\{^1\text{H}\}$ NMR (100 MHz, CDCl_3) δ 198.4, 166.3, 166.2, 164.7 (d, $J_{\text{CF}} = 252.7$ Hz), 134.9, 134.4 (d, $J_{\text{CF}} = 3.4$ Hz), 131.4 (d, $J_{\text{CF}} = 9.0$ Hz), 115.5 (d, $J_{\text{CF}} = 21.7$ Hz), 112.9, 107.5, 101.1, 55.6 ppm; Anal. Calcd for $\text{C}_{14}\text{H}_{11}\text{FO}_3$: C, 68.29; H, 4.50. Found: C, 68.23; H, 4.47.



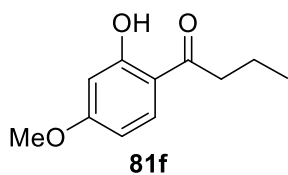
Data for **81d**: ^1H NMR (400 MHz, CDCl_3) δ 12.45 (s, 1H), 7.64 (dd, $J = 7.9, 1.2$ Hz, 1H), 7.41 (td, $J = 7.4, 1.2$ Hz, 1H), 7.34 (td, $J = 7.9, 1.8$ Hz, 1H), 7.30 (dd, $J = 7.4, 1.8$ Hz, 1H), 7.10 (d, $J =$

9.0 Hz, 1H), 6.50 (d, $J = 2.5$ Hz, 1H), 6.36 (dd, $J = 9.0, 2.5$ Hz, 1H), 3.84 (s, 3H) ppm; $^{13}\text{C}\{^1\text{H}\}$ NMR (100 MHz, CDCl_3) δ 199.0, 166.8, 166.1, 139.5, 135.1, 133.0, 131.0, 128.4, 127.2, 119.1, 113.2, 108.0, 100.8, 55.6 ppm; GC-MS $m/z = 306$ (M^+); Anal. Calcd for $\text{C}_{14}\text{H}_{11}\text{BrO}_3$: C, 54.75; H, 3.61. Found: C, 54.68; H, 3.70.



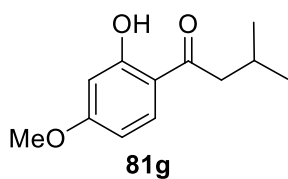
Data for **81e**: ^1H NMR (400 MHz, CDCl_3) δ 12.83 (s, 1H), 7.64 (d, $J = 10.5$ Hz, 1H), 6.42 (dd, $J = 10.5, 2.5$ Hz, 1H), 6.40 (d, $J = 2.5$ Hz, 1H), 3.81 (s, 3H), 2.93 (q, $J = 7.3$ Hz, 2H), 1.21 (t, $J = 7.3$ Hz, 3H)

ppm; $^{13}\text{C}\{^1\text{H}\}$ NMR (100 MHz, CDCl_3) δ 205.3, 165.7, 165.1, 131.3, 113.2, 107.4, 100.8, 55.4, 31.0, 8.4 ppm; GC-MS $m/z = 180$ (M^+); Anal. Calcd for $\text{C}_{10}\text{H}_{12}\text{O}_3$: C, 66.65; H, 6.71. Found: C, 66.57; H, 6.68.



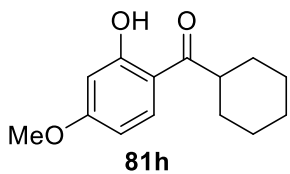
Data for **81f**: ^1H NMR (400 MHz, CDCl_3) δ 12.91 (s, 1H), 7.66 (d, $J = 9.2$ Hz, 1H), 6.44 (dd, $J = 9.2, 2.5$ Hz, 1H), 6.42 (d, $J = 2.5$ Hz, 1H), 3.84 (s, 3H), 2.88 (t, $J = 7.4$ Hz, 2H), 1.76 (sextet, $J =$

7.4 Hz, 2H), 1.01 (t, $J = 7.4$ Hz, 3H) ppm; $^{13}\text{C}\{^1\text{H}\}$ NMR (100 MHz, CDCl_3) δ 205.0, 165.9, 165.4, 131.6, 113.5, 107.5, 100.9, 55.5, 39.8, 18.2, 13.9 ppm; GC-MS $m/z = 194$ (M^+); Anal. Calcd for $\text{C}_{11}\text{H}_{14}\text{O}_3$: C, 68.02; H, 7.27. Found: C, 67.81; H, 7.19.

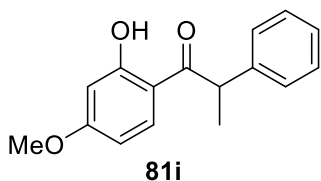


Data for **81g**: ^1H NMR (400 MHz, CDCl_3) δ 12.99 (s, 1H), 7.63 (d, $J = 9.3$ Hz, 1H), 6.41 (dd, $J = 9.3, 2.5$ Hz, 1H), 6.40 (d, $J = 2.5$ Hz, 1H), 3.81 (s, 3H), 2.74 (d, $J = 6.9$ Hz, 2H), 2.25 (m, 1H), 0.99

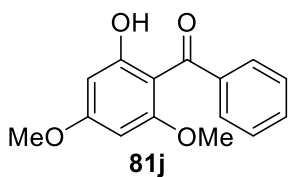
(d, $J = 6.7$ Hz, 6H) ppm; $^{13}\text{C}\{^1\text{H}\}$ NMR (100 MHz, CDCl_3) δ 204.8, 165.8, 165.5, 131.7, 113.7, 107.4, 100.8, 55.5, 46.7, 25.8, 22.7 ppm; GC-MS $m/z = 208$ (M^+); Anal. Calcd for $\text{C}_{12}\text{H}_{16}\text{O}_3$: C, 69.21; H, 7.74. Found: C, 69.08; H, 7.59.



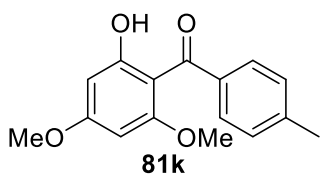
Data for **81h**: ^1H NMR (400 MHz, CDCl_3) δ 13.10 (s, 1H), 7.68 (d, $J = 8.4$ Hz, 1H), 6.44 (dd, $J = 8.4, 2.4$ Hz, 1H), 6.42 (d, $J = 2.4$ Hz, 1H), 3.83 (s, 3H), 3.19 (tt, $J = 11.6, 2.9$ Hz, 1H), 1.90-1.17 (m, 10H) ppm; $^{13}\text{C}\{^1\text{H}\}$ NMR (100 MHz, CDCl_3) δ 208.3, 166.0, 165.8, 131.3, 112.3, 107.5, 101.1, 55.5, 45.0, 29.6, 25.8, 25.8 ppm; GC-MS $m/z = 234$ (M^+); Anal. Calcd for $\text{C}_{14}\text{H}_{18}\text{O}_3$: C, 71.77; H, 7.74. Found: C, 71.53; H, 7.58.



Data for **81i**: ^1H NMR (400 MHz, CDCl_3) δ 12.99 (s, 1H), 7.72 (d, $J = 9.0$ Hz, 1H), 7.35-7.21 (m, 5H), 6.42 (d, $J = 2.5$ Hz, 1H), 6.37 (dd, $J = 9.0, 2.5$ Hz, 1H), 4.66 (q, $J = 6.9$ Hz, 1H), 3.78 (s, 3H), 1.56 (d, $J = 6.9$ Hz, 3H) ppm; $^{13}\text{C}\{^1\text{H}\}$ NMR (100 MHz, CDCl_3) δ 204.6, 166.1, 166.1, 141.5, 132.0, 129.0, 127.5, 127.1, 107.6, 101.0, 101.0, 55.5, 46.9, 19.2 ppm; GC-MS $m/z = 256$ (M^+); Anal. Calcd for $\text{C}_{16}\text{H}_{16}\text{O}_3$: C, 74.98; H, 6.29. Found: C, 74.82; H, 6.16.

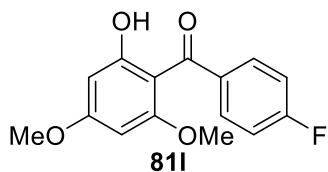


Data for **81j**: ^1H NMR (400 MHz, CDCl_3) δ 12.27 (s, 1H), 7.54-7.51 (m, 2H), 7.48-7.44 (m, 1H), 7.41-7.36 (m, 2H), 6.17 (d, $J = 2.3$ Hz, 1H), 5.92 (d, $J = 2.3$ Hz, 1H), 3.85 (s, 3H), 3.45 (s, 3H) ppm; $^{13}\text{C}\{^1\text{H}\}$ NMR (100 MHz, CDCl_3) δ 199.1, 166.4, 166.0, 161.9, 141.7, 130.8, 127.8, 127.5, 105.6, 93.6, 91.3, 55.6, 55.1 ppm; GC-MS $m/z = 258$ (M^+); Anal. Calcd for $\text{C}_{15}\text{H}_{14}\text{O}_4$: C, 69.76; H, 5.46. Found: C, 69.44; H, 5.44.



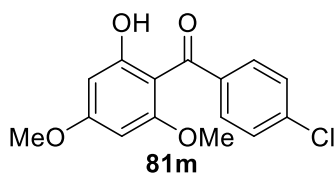
Data for **81k**: ^1H NMR (400 MHz, CDCl_3) δ 12.11 (s, 1H), 7.46 (d, $J = 8.1$ Hz, 2H), 7.18 (m, $J = 8.1$ Hz, 2H), 6.16 (d, $J = 2.3$ Hz, 1H), 5.94 (d, $J = 2.3$ Hz, 1H), 3.85 (s, 3H), 3.48 (s, 3H), 2.40 (s, 3H) ppm; $^{13}\text{C}\{^1\text{H}\}$ NMR (100 MHz, CDCl_3) δ 198.7, 166.1, 165.6, 161.8, 141.6,

138.7, 128.3, 128.2, 105.7, 93.6, 91.3, 55.6, 55.1, 21.6 ppm; GC-MS $m/z = 272$ (M^+); Anal. Calcd for $C_{16}H_{16}O_4$: C, 70.58; H, 5.92. Found: C, 70.57; H, 5.95.



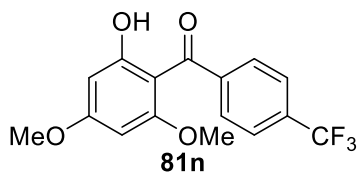
Data for **81l**: 1H NMR (400 MHz, $CDCl_3$) δ 12.09 (s, 1H), 7.58-7.53 (m, 2H), 7.09-7.03 (m, 2H), 6.16 (d, $J = 2.3$ Hz, 1H), 5.93 (d, $J = 2.3$ Hz, 1H), 3.85 (s, 3H), 3.48 (s, 3H) ppm; $^{13}C\{^1H\}$

NMR (100 MHz, $CDCl_3$) δ 197.4, 166.4, 165.8, 164.4 (d, $J_{CF} = 251.8$ Hz), 161.7, 137.7 (d, $J_{CF} = 3.5$ Hz), 130.4 (d, $J_{CF} = 9.0$ Hz), 114.5 (d, $J_{CF} = 21.9$ Hz), 105.4, 93.7, 91.3, 55.7, 55.1 ppm; GC-MS $m/z = 276$ (M^+); Anal. Calcd for $C_{15}H_{13}FO_4$: C, 65.21; H, 4.74. Found: C, 62.17; H, 4.76.



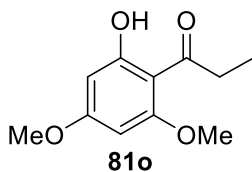
Data for **81m**: 1H NMR (400 MHz, $CDCl_3$) δ 12.17 (s, 1H), 7.47 (d, $J = 8.4$ Hz, 2H), 7.35 (d, $J = 8.4$ Hz, 2H), 6.16 (d, $J = 2.3$ Hz, 1H), 5.92 (d, $J = 2.3$ Hz, 1H), 3.85 (s, 3H), 3.48 (s, 3H)

ppm; $^{13}C\{^1H\}$ NMR (100 MHz, $CDCl_3$) δ 197.6, 166.6, 166.0, 161.7, 140.0, 136.9, 129.3, 127.8, 105.3, 93.7, 91.3, 55.6, 55.1 ppm; GC-MS $m/z = 292$ (M^+); Anal. Calcd for $C_{15}H_{13}ClO_4$: C, 61.55; H, 4.48. Found: C, 61.20; H, 4.34.

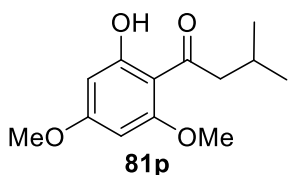


Data for **81n**: 1H NMR (400 MHz, $CDCl_3$) δ 12.41 (s, 1H), 7.65 (d, $J = 8.1$ Hz, 2H), 7.58 (d, $J = 8.1$ Hz, 2H), 6.16 (d, $J = 2.3$ Hz, 1H), 5.91 (d, $J = 2.3$ Hz, 1H), 3.85 (s, 3H), 3.42 (s,

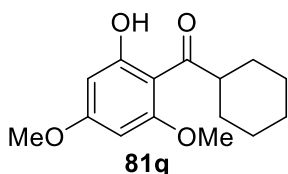
3H) ppm; $^{13}C\{^1H\}$ NMR (100 MHz, $CDCl_3$) δ 197.8, 167.1, 166.6, 161.9, 145.3 (q, $J_{CF} = 1.2$ Hz), 131.9 (q, $J_{CF} = 32.4$ Hz), 127.6, 124.5 (q, $J_{CF} = 3.8$ Hz), 123.8 (q, $J_{CF} = 272.6$ Hz), 105.2, 93.7, 91.3, 55.7, 55.0 ppm; GC-MS $m/z = 326$ (M^+); Anal. Calcd for $C_{16}H_{13}F_3O_4$: C, 58.90; H, 4.02. Found: C, 58.81; H, 3.94.



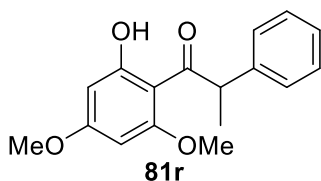
Data for **81o**: ^1H NMR (400 MHz, CDCl_3) δ 14.10 (s, 1H), 6.04 (d, $J = 2.3$ Hz, 1H), 5.90 (d, $J = 2.3$ Hz, 1H), 3.83 (s, 3H), 3.79 (s, 3H), 3.00 (q, $J = 7.2$ Hz, 2H), 1.13 (t, $J = 7.2$ Hz, 3H) ppm; $^{13}\text{C}\{^1\text{H}\}$ NMR (100 MHz, CDCl_3) δ 206.3, 167.4, 165.7, 162.7, 105.6, 93.5, 90.6, 55.4, 55.4, 37.3, 8.5 ppm; GC-MS $m/z = 210$ (M^+); Anal. Calcd for $\text{C}_{11}\text{H}_{14}\text{O}_4$: C, 62.85; H, 6.71. Found: C, 62.45; H, 6.66.



Data for **81p**: ^1H NMR (400 MHz, CDCl_3) δ 14.15 (s, 1H), 6.04 (d, $J = 2.4$ Hz, 1H), 5.89 (d, $J = 2.4$ Hz, 1H), 3.83 (s, 3H), 3.79 (s, 3H), 2.83 (d, $J = 6.7$ Hz, 2H), 2.18 (nonet, $J = 6.7$ Hz, 1H), 0.95 (d, $J = 6.7$ Hz, 6H) ppm; $^{13}\text{C}\{^1\text{H}\}$ NMR (100 MHz, CDCl_3) δ 205.5, 167.7, 165.7, 162.5, 105.8, 93.6, 90.7, 55.4, 55.4, 53.0, 25.2, 22.8 ppm; GC-MS $m/z = 238$ (M^+); Anal. Calcd for $\text{C}_{13}\text{H}_{18}\text{O}_4$: C, 65.53; H, 7.61. Found: C, 65.59; H, 7.62.

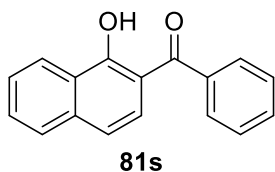


Data for **81q**: ^1H NMR (400 MHz, CDCl_3) δ 14.14 (s, 1H), 6.04 (d, $J = 2.4$ Hz, 1H), 5.90 (d, $J = 2.4$ Hz, 1H), 3.84 (s, 3H), 3.79 (s, 3H), 3.43 (tt, $J = 11.0, 2.9$ Hz, 1H), 1.89-1.78 (m, 4H), 1.73-1.67 (m, 1H), 1.45-1.19 (m, 5H) ppm; $^{13}\text{C}\{^1\text{H}\}$ NMR (100 MHz, CDCl_3) δ 209.2, 167.9, 165.6, 162.3, 105.1, 93.7, 90.8, 55.6, 55.4, 50.0, 29.4, 26.2, 26.1 ppm; GC-MS $m/z = 264$ (M^+); Anal. Calcd for $\text{C}_{15}\text{H}_{20}\text{O}_4$: C, 68.16; H, 7.63. Found: C, 67.86; H, 7.46.

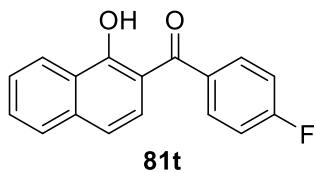


Data for **81r**: ^1H NMR (400 MHz, CDCl_3) δ 14.07 (s, 1H), 7.32-7.24 (m, 4H), 7.22-7.18 (m, 1H), 6.06 (d, $J = 2.4$ Hz, 1H), 5.84 (d, $J = 2.4$ Hz, 1H), 5.00 (q, $J = 6.9$ Hz, 1H), 3.77 (s, 3H), 3.74 (s, 3H), 1.49 (d, $J = 6.9$ Hz, 3H) ppm; $^{13}\text{C}\{^1\text{H}\}$ NMR (100 MHz, CDCl_3) δ 205.8, 168.0, 165.9, 162.1, 142.4, 128.3, 127.7, 126.3, 105.4, 93.6, 90.8, 55.4, 55.1, 50.8, 19.7

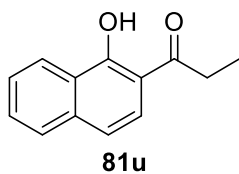
ppm; GC-MS $m/z = 286$ (M^+); Anal. Calcd for $C_{17}H_{18}O_4$: C, 71.31; H, 6.34. Found: C, 71.26; H, 6.34.



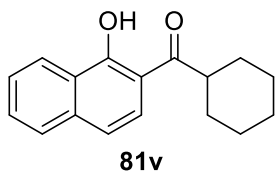
Data for **81s**: 1H NMR (400 MHz, $CDCl_3$) δ 13.96 (s, 1H), 8.55-8.52 (m, 1H), 7.80-7.76 (m, 1H), 7.74-7.71 (m, 2H), 7.69-7.64 (m, 1H), 7.63-7.51 (m, 5H), 7.23 (d, $J = 8.8$ Hz, 1H) ppm; $^{13}C\{^1H\}$ NMR (100 MHz, $CDCl_3$) δ 201.4, 163.9, 138.2, 137.3, 131.6, 130.4, 129.1, 128.3, 127.4, 127.3, 126.0, 125.3, 124.5, 117.8, 112.5 ppm; GC-MS $m/z = 248$ (M^+); Anal. Calcd for $C_{17}H_{12}O_2$: C, 82.24; H, 4.87. Found: C, 82.01; H, 4.89.



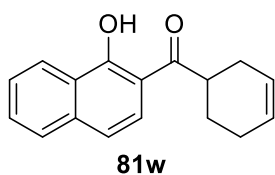
Data for **81t**: 1H NMR (400 MHz, $CDCl_3$) δ 13.84 (s, 1H), 8.54-8.51 (m, 1H), 7.79-7.74 (m, 3H), 7.69-7.64 (m, 1H), 7.59-7.55 (m, 1H), 7.52 (d, $J = 8.9$ Hz, 1H), 7.26-7.19 (m, 3H) ppm; $^{13}C\{^1H\}$ NMR (100 MHz, $CDCl_3$) δ 199.8, 164.8 (d, $J_{CF} = 253.4$ Hz), 163.9, 137.3, 134.3 (d, $J_{CF} = 3.3$ Hz), 131.7 (d, $J_{CF} = 9.0$ Hz), 130.4, 127.4, 127.0, 126.1, 125.2, 124.5, 118.0, 115.5 (d, $J_{CF} = 22.0$ Hz), 112.4 ppm; GC-MS $m/z = 266$ (M^+); Anal. Calcd for $C_{17}H_{11}FO_2$: C, 76.68; H, 4.16. Found: C, 76.46; H, 4.36.



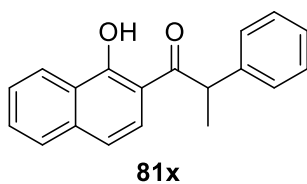
Data for **81u**: 1H NMR (400 MHz, $CDCl_3$) δ 14.09 (s, 1H), 8.46 (dd, $J = 8.3, 1.3$ Hz, 1H), 7.75 (d, $J = 8.1$ Hz, 1H), 7.67 (d, $J = 8.9$ Hz, 1H), 7.62 (ddd, $J = 8.1, 6.9, 1.3$ Hz, 1H), 7.52 (ddd, $J = 8.3, 6.9, 1.2$ Hz, 1H), 7.26 (d, $J = 8.9$ Hz, 1H) 3.10 (q, $J = 7.3$ Hz, 2H), 1.29 (t, $J = 7.3$ Hz, 3H) ppm; $^{13}C\{^1H\}$ NMR (100 MHz, $CDCl_3$) δ 206.9, 162.3, 137.2, 129.9, 127.3, 125.8, 125.3, 124.4, 124.2, 118.2, 112.7, 31.9, 8.2 ppm; GC-MS $m/z = 200$ (M^+); Anal. Calcd for $C_{13}H_{12}O_2$: C, 77.98; H, 6.04. Found: C, 78.16; H, 6.05.



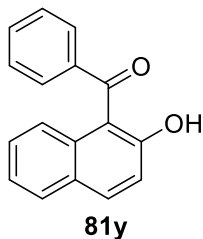
Data for **81v**: ^1H NMR (400 MHz, CDCl_3) δ 14.40 (s, 1H), 8.47 (dd, $J = 8.4, 1.3$ Hz, 1H), 7.75 (d, $J = 8.1$ Hz, 1H), 7.69 (d, $J = 8.9$ Hz, 1H), 7.62 (ddd, $J = 8.1, 6.9, 1.3$ Hz, 1H), 7.52 (ddd, $J = 8.4, 6.9, 1.3$ Hz, 1H), 7.26 (d, $J = 8.9$ Hz, 1H), 3.35 (tt, $J = 11.4, 3.1$ Hz, 1H), 1.99-1.86 (m, 4H), 1.82-1.75 (m, 1H), 1.65-1.54 (m, 2H), 1.50-1.38 (m, 2H), 1.36-1.25 (m, 1H) ppm; $^{13}\text{C}\{^1\text{H}\}$ NMR (100 MHz, CDCl_3) δ 209.8, 163.3, 137.2, 129.9, 127.3, 125.8, 125.6, 124.4, 124.2, 118.0, 111.8, 45.3, 29.4, 25.9, 25.8 ppm; GC-MS $m/z = 254$ (M^+); Anal. Calcd for $\text{C}_{17}\text{H}_{18}\text{O}_2$: C, 80.28; H, 7.13. Found: C, 80.22; H, 7.15.



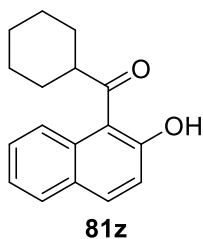
Data for **81w**: ^1H NMR (400 MHz, CDCl_3) δ 14.32 (s, 1H), 8.48 (dd, $J = 8.4, 1.3$ Hz, 1H), 7.76 (d, $J = 8.1$ Hz, 1H), 7.71 (d, $J = 8.9$ Hz, 1H), 7.63 (ddd, $J = 8.1, 6.9, 1.3$ Hz, 1H), 7.53 (ddd, $J = 8.4, 6.9, 1.3$ Hz, 1H), 7.27 (d, $J = 8.9$ Hz, 1H), 5.82-5.78 (m, 2H), 3.68-3.59 (m, 1H), 2.50-2.40 (m, 1H), 2.32-2.17 (m, 3H), 2.09-2.02 (m, 1H), 1.89-1.78 (m, 1H) ppm; $^{13}\text{C}\{^1\text{H}\}$ NMR (100 MHz, CDCl_3) δ 209.3, 163.4, 137.2, 130.0, 127.3, 126.6, 125.9, 125.6, 125.5, 124.4, 124.1, 118.2, 111.9, 41.2, 27.9, 25.8, 24.9 ppm; GC-MS $m/z = 252$ (M^+); Anal. Calcd for $\text{C}_{17}\text{H}_{16}\text{O}_2$: C, 80.93; H, 6.39. Found: C, 80.95; H, 6.47.



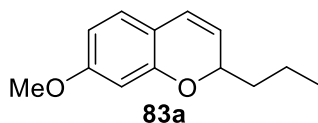
Data for **81x**: ^1H NMR (400 MHz, CDCl_3) δ 14.20 (s, 1H), 8.46-8.43 (m, 1H), 7.71-7.67 (m, 2H), 7.61-7.57 (m, 1H), 7.52-7.47 (m, 1H), 7.36-7.29 (m, 4H), 7.25-7.20 (m, 1H), 7.16 (d, $J = 9.0$ Hz, 1H), 4.80 (q, $J = 6.9$ Hz, 1H), 1.60 (t, $J = 6.9$ Hz, 3H) ppm; $^{13}\text{C}\{^1\text{H}\}$ NMR (100 MHz, CDCl_3) δ 206.2, 163.4, 141.3, 137.1, 130.1, 129.0, 127.6, 127.3, 127.1, 125.9, 125.4, 124.5, 124.4, 118.2, 112.3, 47.5, 19.2 ppm; GC-MS $m/z = 276$ (M^+); Anal. Calcd for $\text{C}_{19}\text{H}_{16}\text{O}_2$: C, 82.58; H, 5.84. Found: C, 82.27; H, 5.81.



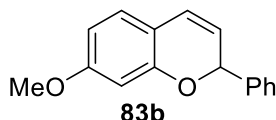
Data for **81y**: ^1H NMR (400 MHz, CDCl_3) δ 11.24 (s, 1H), 7.94 (d, $J = 9.0$ Hz, 1H), 7.76 (d, $J = 8.0$ Hz, 1H), 7.65-7.62 (m, 2H), 7.56 (tt, $J = 7.5$, 1.3 Hz, 1H), 7.43-7.39 (m, 2H), 7.33-7.26 (m, 2H), 7.25 (d, $J = 9.0$ Hz, 1H), 7.16 (dd, $J = 7.0$, 1.5 Hz, 1H) ppm; $^{13}\text{C}\{^1\text{H}\}$ NMR (100 MHz, CDCl_3) δ 200.4, 161.4, 140.3, 136.3, 132.6, 132.3, 129.4, 128.5, 128.5, 128.4, 126.7, 126.3, 123.7, 119.1, 114.3 ppm; GC-MS $m/z = 248$ (M^+); Anal. Calcd for $\text{C}_{17}\text{H}_{12}\text{O}_2$: C, 82.24; H, 4.87. Found: C, 81.97; H, 4.67.



Data for **81z**: ^1H NMR (400 MHz, CDCl_3) δ 11.95 (s, 1H), 7.91-7.88 (m, 1H), 7.86 (d, $J = 9.0$ Hz, 1H), 7.80-7.77 (m, 1H), 7.58-7.53 (m, 1H), 7.42-7.37 (m, 1H), 7.14 (d, $J = 9.0$ Hz, 1H), 3.49 (tt, $J = 11.5$, 3.2 Hz, 1H), 1.99-1.91 (m, 2H), 1.88-1.81 (m, 2H), 1.77-1.62 (m, 3H), 1.40-1.24 (m, 3H) ppm; $^{13}\text{C}\{^1\text{H}\}$ NMR (75.5 MHz, CDCl_3) δ 212.0, 161.1, 136.1, 131.6, 129.2, 128.6, 127.8, 124.2, 123.8, 119.4, 115.5, 50.2, 29.9, 25.7, 25.6 ppm; GC-MS $m/z = 254$ (M^+); Anal. Calcd for $\text{C}_{17}\text{H}_{18}\text{O}_2$: C, 80.28; H, 7.13. Found: C, 79.97; H, 6.99.

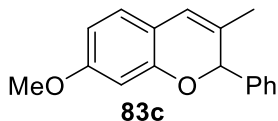


Data for **83a**: ^1H NMR (400 MHz, CDCl_3) δ 6.86 (d, $J = 8.2$ Hz, 1H), 6.40 (dd, $J = 8.2$, 2.5 Hz, 1H), 6.37 (d, $J = 2.5$ Hz, 1H), 6.34 (dd, $J = 9.9$, 1.6 Hz, 1H), 5.54 (dd, $J = 9.9$, 3.3 Hz, 1H), 4.85-4.80 (m, 1H), 3.77 (s, 3H), 1.83-1.74 (m, 1H), 1.67-1.42 (m, 3H), 0.95 (t, $J = 7.3$, 3H) ppm; $^{13}\text{C}\{^1\text{H}\}$ NMR (100 MHz, CDCl_3) δ 160.5, 154.8, 127.0, 123.5, 123.0, 115.3, 106.6, 101.8, 75.1, 55.3, 37.5, 18.1, 14.0 ppm; GC-MS $m/z = 204$ (M^+); Anal. Calcd for $\text{C}_{13}\text{H}_{16}\text{O}_2$: C, 76.44; H, 7.90. Found: C, 76.52; H, 7.89.

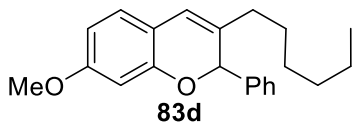


Data for **83b**: ^1H NMR (400 MHz, CDCl_3) δ 7.48-7.45 (m, 2H), 7.41-7.31 (m, 3H), 6.94 (d, $J = 8.2$, 1H), 6.50 (dd, $J = 9.8$, 1.8 Hz,

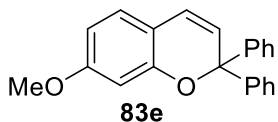
1H), 6.44 (dd, $J = 8.2, 2.5$ Hz, 1H), 6.40 (d, $J = 2.5$ Hz, 1H), 5.90 (dd, $J = 3.4, 1.8$ Hz, 1H), 5.67 (dd, $J = 9.8, 3.4$ Hz, 1H), 3.76 (s, 3H) ppm; $^{13}\text{C}\{^1\text{H}\}$ NMR (100 MHz, CDCl_3) δ 160.8, 154.3, 140.9, 128.6, 128.3, 127.2, 127.0, 123.6, 121.8, 114.6, 107.0, 101.8, 77.3, 55.3 ppm; GC-MS $m/z = 238$ (M^+). ^1H and ^{13}C NMR spectral data are in good agreement with the literature data.¹⁰¹



Data for **83c**: ^1H NMR (400 MHz, CDCl_3) δ 7.41-7.31 (m, 5H), 6.89 (d, $J = 8.3$, 1H), 6.42 (dd, $J = 8.3, 2.5$ Hz, 1H), 6.33 (d, $J = 2.5$ Hz, 1H), 6.31 (s, 1H), 5.64 (s, 1H), 3.73 (s, 3H), 1.69 (s, 3H) ppm; $^{13}\text{C}\{^1\text{H}\}$ NMR (100 MHz, CDCl_3) δ 160.1, 152.6, 139.3, 129.4, 128.6, 128.5, 127.5, 126.1, 119.4, 115.2, 106.6, 101.6, 81.2, 55.2, 19.8 ppm; GC-MS $m/z = 252$ (M^+); HRMS (APCI) Calcd for $\text{C}_{17}\text{H}_{17}\text{O}_2$ ($[\text{M}+\text{H}]^+$): 253.1223. Found: 253.1229.

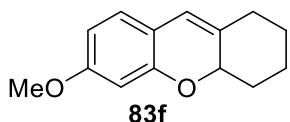


Data for **83d**: ^1H NMR (400 MHz, CDCl_3) δ 7.40-7.36 (m, 2H), 7.34-7.29 (m, 3H), 6.90 (d, $J = 8.3$ Hz, 1H), 6.41 (dd, $J = 8.3, 2.5$ Hz, 1H), 6.32 (s, 1H), 6.30 (d, $J = 2.5$ Hz, 1H), 5.66 (s, 1H), 3.72 (s, 3H), 1.97-1.91 (m, 2H), 1.54-1.40 (m, 2H), 1.33-1.19 (m, 6H), 0.87 (t, $J = 6.9$ Hz, 3H) ppm; $^{13}\text{C}\{^1\text{H}\}$ NMR (100 MHz, CDCl_3) δ 160.1, 152.7, 139.4, 133.7, 128.6, 128.5, 127.7, 126.3, 118.3, 115.5, 106.7, 101.7, 80.2, 55.2, 33.0, 31.6, 28.9, 27.0, 22.5, 14.1 ppm; GC-MS $m/z = 322$ (M^+); HRMS (ESI) Calcd for $\text{C}_{22}\text{H}_{26}\text{O}_2$ (M^+): 322.1927. Found: 322.1903.

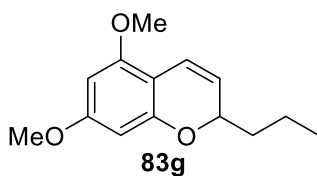


Data for **83e**: ^1H NMR (400 MHz, CDCl_3) δ 7.46-7.43 (m, 4H), 7.35-7.24 (m, 6H), 6.92 (d, $J = 8.3$ Hz, 1H), 6.58 (d, $J = 9.8$ Hz, 1H), 6.53 (d, $J = 2.5$ Hz, 1H), 6.41 (dd, $J = 8.3, 2.5$ Hz, 1H), 6.03 (d, $J = 9.8$ Hz, 1H), 3.77 (s, 3H) ppm; $^{13}\text{C}\{^1\text{H}\}$ NMR (100 MHz, CDCl_3) δ 160.9, 153.7, 145.0, 128.1, 127.4, 127.2,

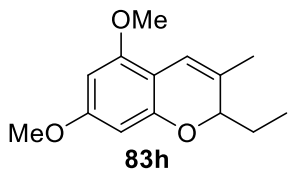
127.0, 125.9, 123.0, 114.4, 107.1, 102.1, 82.8, 55.3 ppm; GC-MS $m/z = 314$ (M^+); HRMS (ESI) Calcd for $C_{22}H_{18}O_2$ (M^+): 314.1301. Found: 314.1289.



Data for **83f**: 1H NMR (400 MHz, $CDCl_3$) δ 6.74 (d, $J = 8.2$ Hz, 1H), 6.33 (dd, $J = 8.2, 2.5$ Hz, 1H), 6.29 (d, $J = 2.5$ Hz, 1H), 5.97-5.95 (m, 1H), 4.94-4.88 (m, 1H), 3.74 (s, 3H), 2.43-2.36 (m, 1H), 2.23-2.16 (m, 1H), 2.08-1.98 (m, 1H), 1.92-1.85 (m, 1H), 1.80-1.68 (m, 2H), 1.51-1.39 (m, 1H), 1.38-1.27 (m, 1H) ppm; $^{13}C\{^1H\}$ NMR (100 MHz, $CDCl_3$) δ 159.8, 154.0, 134.7, 126.0, 115.8, 114.8, 106.0, 100.9, 77.4, 55.3, 35.1, 32.9, 26.7, 24.4 ppm; GC-MS $m/z = 216$ (M^+); HRMS (APCI) Calcd for $C_{14}H_{17}O_2$ ($[M+H]^+$): 217.1223. Found: 217.1229.

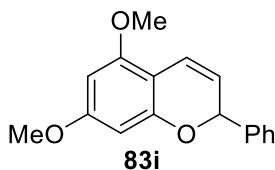


Data for **83g**: 1H NMR (400 MHz, $CDCl_3$) δ 6.64 (dd, $J = 9.9, 1.6$ Hz, 1H), 6.04 (d, $J = 2.3$ Hz, 1H), 6.01 (d, $J = 2.3$ Hz, 1H), 5.49 (dd, $J = 9.9, 3.4$ Hz, 1H), 4.80-4.75 (m, 1H), 3.78 (s, 3H), 3.76 (s, 3H), 1.84-1.74 (m, 1H), 1.68-1.42 (m, 3H), 0.95 (t, $J = 7.3$ Hz, 3H) ppm; $^{13}C\{^1H\}$ NMR (100 MHz, $CDCl_3$) δ 160.9, 156.1, 155.3, 120.9, 118.4, 104.9, 93.7, 91.5, 74.9, 55.5, 55.3, 37.2, 18.1, 13.9 ppm; GC-MS $m/z = 234$ (M^+); HRMS (ESI) Calcd for $C_{14}H_{18}O_3$ (M^+): 234.1250. Found: 234.1239; Anal. Calcd for $C_{14}H_{18}O_3$: C, 71.77; H, 7.74. Found: C, 71.78; H, 7.89.

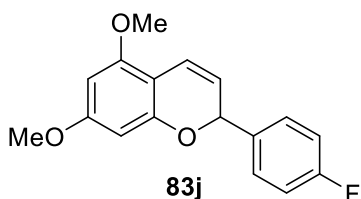


Data for **83h**: 1H NMR (400 MHz, $CDCl_3$) δ 6.39-6.37 (m, 1H), 6.06 (d, $J = 2.3$ Hz, 1H), 6.01 (d, $J = 2.3$ Hz, 1H), 4.51 (dd, $J = 8.7, 3.5$ Hz, 1H), 3.78 (s, 3H), 3.76 (s, 3H), 1.82-1.81 (m, 3H), 1.78-1.56 (m, 2H), 1.01 (t, $J = 7.4$ Hz, 3H) ppm; $^{13}C\{^1H\}$ NMR (100 MHz, $CDCl_3$) δ 160.1, 155.3, 153.1, 129.5, 113.2, 105.3, 93.8, 91.4, 80.1, 55.5, 55.3, 25.4, 19.7, 9.7 ppm; GC-

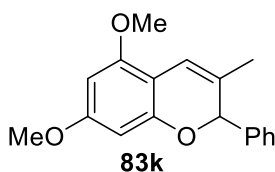
MS $m/z = 234$ (M^+); HRMS (APCI) Calcd for $C_{14}H_{19}O_3$ ($[M+H]^+$): 235.1329. Found: 235.1339.



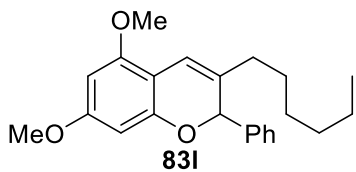
Data for **83i**: 1H NMR (400 MHz, $CDCl_3$) δ 7.51-7.47 (m, 2H), 7.42-7.32 (m, 3H), 6.84 (dd, $J = 9.9, 1.9$ Hz, 1H), 6.09 (d, $J = 2.1$ Hz, 1H), 6.06 (d, $J = 2.1$ Hz, 1H), 5.86 (dd, $J = 3.5, 1.9$ Hz, 1H), 5.64 (dd, $J = 9.9, 3.5$ Hz, 1H), 3.82 (s, 3H), 3.76 (s, 3H) ppm; $^{13}C\{^1H\}$ NMR (100 MHz, $CDCl_3$) δ 161.2, 156.2, 154.8, 140.8, 128.5, 128.2, 127.1, 119.7, 118.7, 104.3, 93.7, 91.7, 77.1, 55.5, 55.3 ppm; GC-MS $m/z = 268$ (M^+). 1H and ^{13}C NMR spectral data are in good agreement with the literature data.¹⁰²



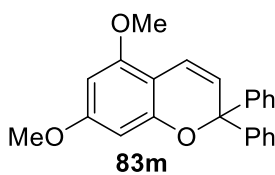
Data for **83j**: 1H NMR (400 MHz, $CDCl_3$) δ 7.47-7.42 (m, 2H), 7.08-7.02 (m, 2H), 6.84 (dd, $J = 9.9, 1.8$ Hz, 1H), 6.04 (s, 2H), 5.82 (dd, $J = 3.5, 1.8$ Hz, 1H), 5.59 (dd, $J = 9.9, 3.5$ Hz, 1H), 3.81 (s, 3H), 3.75 (s, 3H) ppm; $^{13}C\{^1H\}$ NMR (100 MHz, $CDCl_3$) δ 162.6 (d, $J_{CF} = 246.8$ Hz), 161.3, 156.2, 154.6, 136.6 (d, $J_{CF} = 3.2$ Hz), 129.0 (d, $J_{CF} = 8.3$ Hz), 119.3, 119.0, 115.4 (d, $J_{CF} = 21.5$ Hz), 104.3, 93.7, 91.8, 76.3, 55.5, 55.3 ppm; GC-MS $m/z = 286$ (M^+); Anal. Calcd for $C_{17}H_{15}FO_3$: C, 71.32; H, 5.28. Found: C, 71.18; H, 5.05.



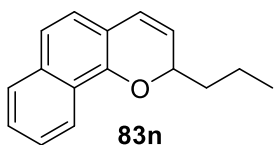
Data for **83k**: 1H NMR (400 MHz, $CDCl_3$) δ 7.42-7.39 (m, 2H), 7.36-7.30 (m, 3H), 6.64-6.62 (m, 1H), 6.03 (d, $J = 2.3$ Hz, 1H), 5.99 (d, $J = 2.3$ Hz, 1H), 5.62 (br s, 1H), 3.82 (s, 3H), 3.71 (s, 3H), 1.72-1.71 (m, 3H) ppm; $^{13}C\{^1H\}$ NMR (100 MHz, $CDCl_3$) δ 160.3, 155.3, 153.1, 139.3, 128.6, 128.5, 127.6, 127.4, 114.1, 104.6, 93.6, 91.6, 81.0, 55.5, 55.2, 19.9 ppm; GC-MS $m/z = 282$ (M^+); HRMS (APCI) Calcd for $C_{18}H_{19}O_3$ ($[M+H]^+$): 283.1329. Found: 283.1334.



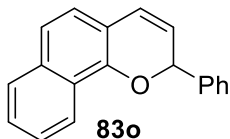
Data for **83l**: ^1H NMR (400 MHz, CDCl_3) δ 7.41-7.37 (m, 2H), 7.34-7.28 (m, 3H), 6.63-6.61 (m, 1H), 6.02 (d, $J = 2.3$ Hz, 1H), 5.96 (d, $J = 2.3$ Hz, 1H), 5.63 (br s, 1H), 3.82 (s, 3H), 3.70 (s, 3H), 2.04-1.89 (m, 2H), 1.54-1.39 (m, 2H), 1.33-1.18 (m, 6H), 0.86 (t, $J = 7.0$, 3H) ppm; $^{13}\text{C}\{^1\text{H}\}$ NMR (100 MHz, CDCl_3) δ 160.3, 155.5, 153.1, 139.4, 131.8, 128.5, 128.4, 127.8, 113.0, 104.9, 93.7, 91.6, 80.0, 55.5, 55.3, 33.3, 31.6, 29.0, 27.2, 22.5, 14.1 ppm; GC-MS $m/z = 352$ (M^+); HRMS (ESI) Calcd for $\text{C}_{23}\text{H}_{28}\text{O}_3$ (M^+): 352.2033. Found: 352.2014.



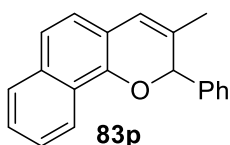
Data for **83m**: ^1H NMR (400 MHz, CDCl_3) δ 7.46-7.43 (m, 4H), 7.35-7.23 (m, 6H), 6.89 (dd, $J = 9.9, 0.6$ Hz, 1H), 6.19 (dd, $J = 2.2, 0.6$ Hz, 1H), 6.00 (d, $J = 2.2$ Hz, 1H), 5.96 (d, $J = 9.9$ Hz, 1H), 3.77 (s, 3H), 3.76 (s, 3H) ppm; $^{13}\text{C}\{^1\text{H}\}$ NMR (100 MHz, CDCl_3) δ 161.3, 156.2, 154.1, 145.0, 128.0, 127.3, 126.9, 123.9, 118.0, 104.2, 94.0, 91.7, 82.6, 55.4, 55.3 ppm; GC-MS $m/z = 344$ (M^+); HRMS (APCI) Calcd for $\text{C}_{23}\text{H}_{21}\text{O}_3$ ($[\text{M}+\text{H}]^+$): 345.1485. Found: 345.1491.



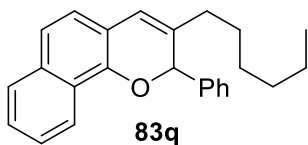
Data for **83n**: ^1H NMR (400 MHz, CDCl_3) δ 8.22-8.15 (m, 1H), 7.77-7.73 (m, 1H), 7.48-7.41 (m, 2H), 7.36 (d, $J = 8.3$ Hz, 1H), 7.15 (d, $J = 8.3$ Hz, 1H), 6.52 (dd, $J = 9.7, 1.6$ Hz, 1H), 5.73 (dd, $J = 9.7, 3.5$ Hz, 1H), 5.10-5.05 (m, 1H), 2.00-1.90 (m, 1H), 1.74-1.53 (m, 3H), 1.00 (t, $J = 7.2$ Hz, 3H) ppm; $^{13}\text{C}\{^1\text{H}\}$ NMR (100 MHz, CDCl_3) δ 148.7, 134.4, 127.6, 126.1, 125.3, 124.7, 124.6, 124.6, 124.3, 121.8, 120.0, 116.3, 75.4, 37.3, 18.1, 13.9 ppm; GC-MS $m/z = 224$ (M^+); HRMS (ESI) Calcd for $\text{C}_{16}\text{H}_{16}\text{O}$ (M^+): 224.1196. Found: 224.1202. Anal. Calcd for $\text{C}_{16}\text{H}_{16}\text{O}$: C, 85.68; H, 7.19. Found: C, 85.86; H, 7.49.



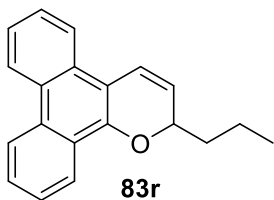
Data for **83o**: ^1H NMR (400 MHz, CDCl_3) δ 8.22-8.19 (m, 1H), 7.77-7.73 (m, 1H), 7.56-7.53 (m, 2H), 7.45-7.33 (m, 6H), 7.19 (d, $J = 8.3$ Hz, 1H), 6.67 (dd, $J = 9.7, 1.7$ Hz, 1H), 6.15 (dd, $J = 3.6, 1.7$ Hz, 1H), 5.90 (dd, $J = 9.7, 3.6$ Hz, 1H) ppm; $^{13}\text{C}\{^1\text{H}\}$ NMR (100 MHz, CDCl_3) δ 148.4, 141.0, 134.5, 128.6, 128.2, 127.5, 126.7, 126.3, 125.4, 124.6, 124.5, 124.5, 123.2, 121.9, 120.3, 115.6, 77.1 ppm; GC-MS $m/z = 258$ (M^+); HRMS (ESI) Calcd for $\text{C}_{19}\text{H}_{14}\text{O}$ (M^+): 258.1039. Found: 258.1038.



Data for **83p**: ^1H NMR (400 MHz, CDCl_3) δ 8.13-8.09 (m, 1H), 7.74-7.70 (m, 1H), 7.50-7.46 (m, 2H), 7.40-7.30 (m, 6H), 7.18 (d, $J = 8.3$ Hz, 1H), 6.50 (s, 1H), 5.92 (s, 1H), 1.83 (s, 3H) ppm; $^{13}\text{C}\{^1\text{H}\}$ NMR (100 MHz, CDCl_3) δ 146.5, 139.4, 134.0, 131.2, 128.6, 128.5, 127.4, 127.4, 125.7, 125.2, 124.4, 124.2, 121.7, 120.3, 120.2, 116.2, 81.2, 20.0 ppm; GC-MS $m/z = 272$ (M^+); HRMS (APCI) calcd for $\text{C}_{20}\text{H}_{17}\text{O}$ ($[\text{M}+\text{H}]^+$): 273.1274. Found: 273.1279.

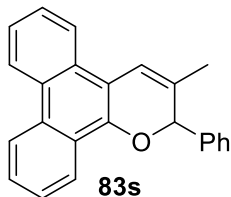


Data for **83q**: ^1H NMR (400 MHz, CDCl_3) δ 8.19-8.15 (m, 1H), 7.78-7.74 (m, 1H), 7.55-7.52 (m, 2H), 7.44-7.32 (m, 6H), 7.25 (d, $J = 8.3$ Hz, 1H), 6.57 (s, 1H), 6.00 (s, 1H), 2.19-2.09 (m, 2H), 1.71-1.55 (m, 2H), 1.46-1.32 (m, 6H), 0.98 (t, $J = 7.0$ Hz, 3H) ppm; $^{13}\text{C}\{^1\text{H}\}$ NMR (100 MHz, CDCl_3) δ 146.5, 139.4, 135.4, 134.0, 128.5, 128.5, 127.6, 127.4, 125.7, 125.2, 124.5, 124.3, 121.7, 120.2, 119.2, 116.4, 80.1, 33.3, 31.7, 29.0, 27.0, 22.6, 14.1 ppm; GC-MS $m/z = 342$ (M^+); HRMS (ESI) Calcd for $\text{C}_{25}\text{H}_{26}\text{O}$ (M^+): 342.1978. Found: 342.1979.

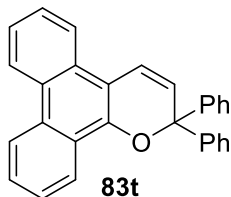


Data for **83r**: ^1H NMR (400 MHz, CDCl_3) δ 8.70-8.66 (m, 2H), 8.47-8.43 (m, 1H), 8.09-8.05 (m, 1H), 7.72-7.63 (m, 2H), 7.61-7.56 (m, 1H), 7.42-7.40 (m, 1H), 7.18 (dd, $J = 9.9, 1.6$ Hz, 1H), 5.90

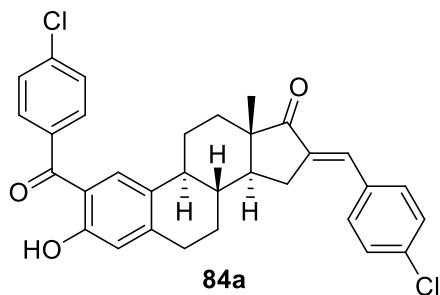
(dd, $J = 9.9, 3.7$ Hz, 1H), 5.12-5.07 (m, 1H), 2.11-2.02 (m, 1H), 1.82-1.60 (m, 3H), 1.07 (t, $J = 7.2$ Hz, 3H) ppm; $^{13}\text{C}\{^1\text{H}\}$ NMR (100 MHz, CDCl_3) δ 147.3, 131.0, 129.2, 127.0, 126.9, 126.5, 126.3, 125.5, 124.1, 123.9, 122.9, 122.5, 122.4, 121.8, 120.4, 111.5, 75.0, 36.6, 18.2, 13.9 ppm; HRMS (ESI) Calcd for $\text{C}_{20}\text{H}_{18}\text{O}$ (M^+): 274.1352. Found: 274.1366; Anal. Calcd for $\text{C}_{20}\text{H}_{18}\text{O}$: C, 87.56; H, 6.61. Found: C, 87.56; H, 6.69.



Data for **83s**: ^1H NMR (400 MHz, CDCl_3) δ 8.69-8.62 (m, 2H), 8.37-8.34 (m, 1H), 8.19-8.16 (m, 1H), 7.70-7.54 (m, 6H), 7.37-7.31 (m, 3H), 7.18 (s, 1H), 5.97 (s, 1H), 2.00 (s, 3H) ppm; $^{13}\text{C}\{^1\text{H}\}$ NMR (100 MHz, CDCl_3) δ 144.8, 138.9, 130.9, 130.6, 129.0, 128.5, 128.4, 127.5, 126.8, 126.6, 126.5, 126.4, 125.4, 124.0, 123.0, 122.3, 121.7, 116.2, 111.0, 80.5, 20.5 ppm; GC-MS $m/z = 322$ (M^+); HRMS (APCI) Calcd for $\text{C}_{24}\text{H}_{19}\text{O}$ ($[\text{M}+\text{H}]^+$): 323.1430. Found: 323.1444.

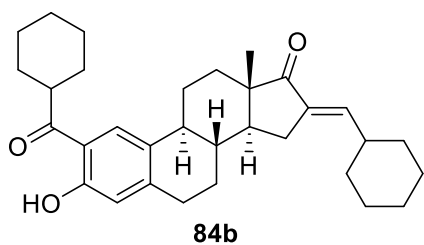


Data for **83t**: ^1H NMR (400 MHz, CDCl_3) δ 8.64-8.54 (m, 2H), 8.07-8.03 (m, 1H), 7.69-7.64 (m, 2H), 7.61-7.56 (m, 5H), 7.54-7.49 (m, 1H), 7.41-7.30 (m, 5H), 7.27-7.23 (m, 2H) 6.35 (d, $J = 9.9$ Hz, 1H) ppm; $^{13}\text{C}\{^1\text{H}\}$ NMR (100 MHz, CDCl_3) δ 146.2, 144.9, 131.3, 129.0, 128.1, 127.5, 127.2, 127.0, 126.9, 126.8, 126.7, 126.5, 125.5, 124.3, 123.0, 122.7, 122.5, 121.9, 120.1, 110.9, 82.8 ppm; GC-MS $m/z = 384$ (M^+); Anal. Calcd for $\text{C}_{29}\text{H}_{20}\text{O}$: C, 90.60; H, 5.24. Found: C, 90.44; H, 5.34.



Data for **84a**: ^1H NMR (400 MHz, CDCl_3) δ 11.74 (s, 1H), 7.63 (d, $J = 8.7$ Hz, 2H), 7.51 (d, $J = 8.7$ Hz, 2H), 7.48 (d, $J = 8.5$ Hz, 2H), 7.45 (s, 1H), 7.41 (s, 1H), 7.39 (d, $J = 8.5$ Hz, 2H), 6.83 (s, 1H), 3.01-2.91 (m, 3H), 2.52 (ddd, $J = 15.5, 12.6, 2.9$ Hz, 1H), 2.30-2.01

(m, 3H), 1.78-1.23 (m, 6H), 0.99 (s, 3H) ppm; $^{13}\text{C}\{^1\text{H}\}$ NMR (100 MHz, CDCl_3) δ 208.9, 199.7, 161.0, 147.0, 138.3, 136.4, 136.1, 135.2, 133.9, 132.0, 131.4, 130.8, 130.5, 129.9, 129.0, 128.7, 117.9, 117.0, 48.4, 47.6, 43.6, 37.6, 31.4, 29.8, 29.0, 26.3, 25.7, 14.5 ppm; HRMS (ESI) Calcd for $\text{C}_{32}\text{H}_{29}\text{Cl}_2\text{O}_3$ ($[\text{M}+\text{H}]^+$): 531.1488. Found: 531.1485.



Data for **84b**: ^1H NMR (400 MHz, CDCl_3) δ 12.38 (s, 1H), 7.65 (s, 1H), 6.70 (s, 1H), 6.49 (ddd, $J = 9.6, 2.6, 1.8$ Hz, 1H), 3.30-3.22 (m, 1H), 2.96-2.84 (m, 2H), 2.67 (ddd, $J = 15.2, 6.4, 1.7$ Hz, 1H), 2.43-2.37 (m, 1H),

2.30-1.99 (m, 5H), 1.91-1.81 (m, 4H), 1.80-1.14 (m, 21H), 0.92 (s, 3H) ppm; $^{13}\text{C}\{^1\text{H}\}$ NMR (100 MHz, CDCl_3) δ 209.6, 209.2, 160.8, 146.4, 142.5, 134.6, 130.7, 126.2, 117.9, 116.2, 48.1, 47.9, 45.0, 43.6, 38.9, 37.6, 31.7, 31.4, 29.7, 29.6, 26.3, 26.0, 25.9, 25.8, 25.7, 25.5, 25.5, 14.4 ppm; HRMS (ESI) Calcd for $\text{C}_{32}\text{H}_{43}\text{O}_3$ ($[\text{M}+\text{H}]^+$): 475.3207. Found: 474.3209.

5.3.5 X-ray Crystal Data and Structure Refinements

Table 5.1 X-ray crystal data for **81v**

Empirical formula	C ₁₇ H ₁₈ O ₂
Formula weight	254.31
Temperature/K	100.05(10)
Crystal system	monoclinic
Space group	P2 ₁ /c
a/Å	7.08927(18)
b/Å	10.1152(2)
c/Å	18.6070(5)
α/°	90.00
β/°	96.927(2)
γ/°	90.00
Volume/Å ³	1324.56(6)
Z	4
ρ _{calc} /mg/mm ³	1.275
m/mm ⁻¹	0.082
F(000)	544.0
Crystal size/mm ³	0.28 × 0.14 × 0.11
Radiation	MoKα (λ = 0.71073)
2θ range for data collection	5.78 to 58.8°
Index ranges	-9 ≤ h ≤ 9, -13 ≤ k ≤ 13, -25 ≤ l ≤ 24
Reflections collected	15224
Independent reflections	3372 [R _{int} = 0.0343, R _{sigma} = 0.0279]
Data/restraints/parameters	3372/0/176
Goodness-of-fit on F ²	1.076
Final R indexes [I >= 2σ (I)]	R ₁ = 0.0467, wR ₂ = 0.1265
Final R indexes [all data]	R ₁ = 0.0592, wR ₂ = 0.1374
Largest diff. peak/hole / e Å ⁻³	0.38/-0.23

Table 5.2 X-ray crystal data for **83t**

Empirical formula	C ₂₉ H ₂₀ O
Formula weight	384.45
Temperature/K	100.00(10)
Crystal system	triclinic
Space group	P-1
a/Å	11.6412(4)
b/Å	11.9623(5)
c/Å	14.3355(6)
α/°	94.336(3)
β/°	103.650(3)
γ/°	90.068(3)
Volume/Å ³	1933.99(12)
Z	4
ρ _{calc} /mg/mm ³	1.320
m/mm ⁻¹	0.605
F(000)	808.0
Crystal size/mm ³	0.42 × 0.35 × 0.18
Radiation	CuKα (λ = 1.54184)
2θ range for data collection	6.36 to 147.4°
Index ranges	-14 ≤ h ≤ 10, -14 ≤ k ≤ 14, -17 ≤ l ≤ 17
Reflections collected	18380
Independent reflections	7504 [R _{int} = 0.0657, R _{sigma} = 0.0456]
Data/restraints/parameters	7504/0/541
Goodness-of-fit on F ²	1.044
Final R indexes [I ≥ 2σ (I)]	R ₁ = 0.0743, wR ₂ = 0.2135
Final R indexes [all data]	R ₁ = 0.0827, wR ₂ = 0.2229
Largest diff. peak/hole / e Å ⁻³	0.45/-0.35

Table 5.3 X-ray crystal data for **84b**

Empirical formula	C ₃₂ H ₄₂ O ₃
Formula weight	474.66
Temperature/K	99.8(5)
Crystal system	triclinic
Space group	P1
a/Å	6.6192(2)
b/Å	6.9546(2)
c/Å	14.6658(7)
α/°	99.503(3)
β/°	96.444(3)
γ/°	95.740(3)
Volume/Å ³	656.79(4)
Z	1
ρ _{calc} /cm ³	1.200
μ/mm ⁻¹	0.581
F(000)	258.0
Crystal size/mm ³	0.18 × 0.14 × 0.02
Radiation	CuKα (λ = 1.54184)
2θ range for data collection/°	13 to 146.86
Index ranges	-8 ≤ h ≤ 8, -8 ≤ k ≤ 8, -17 ≤ l ≤ 18
Reflections collected	11892
Independent reflections	4532 [R _{int} = 0.0521, R _{sigma} = 0.0369]
Data/restraints/parameters	4532/3/321
Goodness-of-fit on F ²	1.127
Final R indexes [I ≥ 2σ (I)]	R ₁ = 0.0644, wR ₂ = 0.1789
Final R indexes [all data]	R ₁ = 0.0667, wR ₂ = 0.1804
Largest diff. peak/hole / e Å ⁻³	0.29/-0.30
Flack parameter	-0.1(4)

5.4 Experimental Procedures and Data for the Chapter 3

5.4.1 General Procedures for the Catalytic C-H Coupling reaction of Phenols with Ketones

In a glove box, a phenol (0.5 mmol), a ketone (1.0-1.5 mmol), and complex **26** (9 mg, 3 mol %) were dissolved in 1,2-dichloroethane (2 mL) in a 25 mL Schlenk tube equipped with a Teflon stopcock and a magnetic stirring bar. The tube was brought out of the glove box, and was stirred in an oil bath set at 125-140 °C for 16-72 h. The reaction tube was taken out of the oil bath, and was cooled to room temperature. After the tube was open to air, the solution was filtered through a short silica gel column by eluting with CH₂Cl₂ (10 mL), and the filtrate was analyzed by GC-MS. Analytically pure product was isolated by a simple column chromatography on silica gel (280-400 mesh, hexanes/EtOAc). The product was completely characterized by NMR and GC-MS spectroscopic methods.

5.4.2 General Procedures for the Mechanistic Studies

Deuterium Labeling Study. In a glove box, 3,5-dimethoxyphenol (0.77 g, 5.0 mmol), cyclohexanone-2,2,6,6-*d*₄ (93 % D, 1.5 mmol), and complex **26** (3 mol %) were dissolved in 1,2-dichloroethane (2 mL) in a 25 mL Schlenk tubes equipped with a Teflon screw cap stopcock. The tube were brought out of the box, and immersed in an oil bath preset at 125 °C for 16 h. The reaction tube was taken out of the oil bath, and was cooled to room temperature. After the tube was open to air, the solution was filtered through a short silica gel column by eluting with CH₂Cl₂ (10 mL), and the filtrate was analyzed by GC-MS. Analytically pure was isolated by a simple column chromatography on silica gel

(280-400 mesh, hexanes/EtOAc = 100:1 to 10:1), then were completely characterized by ^1H , ^{13}C NMR and GC-MS spectroscopic methods.

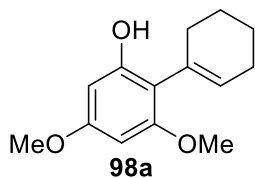
Deuterium Isotope Effect Study. In a glove box, 3,5-methoxyphenol (0.5 mmol), cyclohexanone-2,2,6,6- d_4 (1.5 mmol), and complex **26** were dissolved in 1,2-dichlorobenzene (2 mL) in 25 mL Schlenk tubes equipped with a Teflon screw cap stopcock. The tubes were brought out of the box, and immersed in an oil bath preset at 125 °C. The reaction rate was measured by monitoring the appearance of the product signals on ^1H NMR, which were normalized against the internal standard methylsulfonylmethane in 20-60 min intervals for 300 min of the reaction time. The experiment was repeated by using cyclohexanone. The k_{obs} was determined from a first-order plot of $-\ln[(3,5\text{-methoxyphenol})_t/(3,5\text{-methoxyphenol})_0]$ vs time.

5.4.3 X-Ray Crystallographic Determination of **98k** and **101**

For **98k**: Colorless prisms of **98k** were grown in CH_2Cl_2 at room temperature. A suitable crystal with the dimension of $0.51 \times 0.5 \times 0.45 \text{ mm}^3$ was selected and mounted on an Oxford SuperNova diffractometer equipped with dual microfocus Cu/Mo X-ray sources, X-ray mirror optics, and Atlas CCD area detector. A total of 16395 reflection data were collected by using $\text{MoK}\alpha$ ($\lambda = 0.71073$) radiation while the crystal sample was cooled at 100.00 K during the data collection. Using Olex2, the molecular structure was solved with the ShelXS structure solution program by using Direct Methods, and the data was refined with the XL refinement package using Least Squares minimization. The molecular structure of **98k** is shown in Figure 3.1.

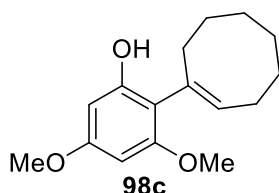
For **101**: Colorless flat needles of **101** were grown in CH₂Cl₂ at room temperature. A suitable crystal with the dimension of 0.58 × 0.24 × 0.10 mm³ was selected and mounted on an Oxford SuperNova diffractometer equipped with dual microfocus Cu/Mo X-ray sources, X-ray mirror optics, and Atlas CCD area detector. A total of 11890 reflection data were collected by using CuKα ($\lambda = 1.54184$) radiation while the crystal sample was cooled at 100.00 K during the data collection. Using Olex2, the molecular structure was solved with the ShelXS structure solution program by using Direct Methods, and the data was refined with the XL refinement package using Least Squares minimization. The molecular structure of **101** is shown in Figure 3.2.

5.4.4 Characterization Data of the Products



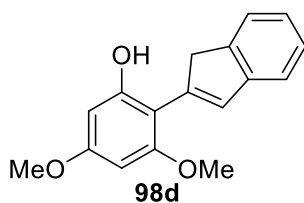
Data for **98a**: ^1H NMR (400 MHz, CDCl_3) δ 6.17 (d, $J = 2.3$ Hz, 1H), 6.05 (d, $J = 2.3$ Hz, 1H), 5.79 (s, 1H), 5.79-5.76 (m, 1H), 3.77 (s, 3H), 3.76 (s, 3H), 2.26-2.18 (m, 4H), 1.78-1.67 (m, 4H) ppm; $^{13}\text{C}\{^1\text{H}\}$

NMR (100 MHz, CDCl_3) δ 160.06, 158.13, 153.43, 133.09, 129.31, 111.50, 92.10, 91.18, 55.59, 55.28, 28.81, 25.50, 22.86, 22.02 ppm; GC-MS $m/z = 234$ (M^+).



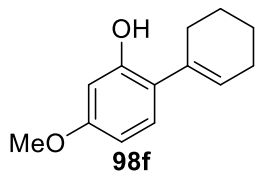
Data for **98c**: ^1H NMR (400 MHz, CDCl_3) δ 6.16 (d, $J = 2.3$ Hz, 1H), 6.06 (d, $J = 2.3$ Hz, 1H), 5.84 (s, 1H), 5.73 (t, $J = 8.1$ Hz, 1H), 3.78 (s, 3H), 3.75 (s, 3H), 2.48-2.41 (m, 2H), 2.37-2.29 (m, 2H),

1.70-1.48 (m, 8H) ppm; $^{13}\text{C}\{^1\text{H}\}$ NMR (100 MHz, CDCl_3) δ 159.95, 158.06, 153.86, 136.28, 132.17, 112.18, 92.10, 91.21, 55.44, 55.27, 30.76, 29.66, 28.86, 26.88, 26.70, 26.52 ppm; GC-MS $m/z = 262$ (M^+); HRMS Calcd for $\text{C}_{16}\text{H}_{22}\text{O}_3$ ($[\text{M}+\text{H}]^+$): 263.1642, Found: 263.1631.

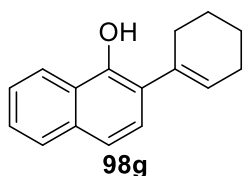


Data for **98d**: ^1H NMR (400 MHz, CDCl_3) δ 7.52 (d, $J = 7.4$ Hz, 1H), 7.46 (d, $J = 7.4$ Hz, 1H), 7.34 (t, $J = 7.4$ Hz, 1H), 7.26 (t, $J = 7.4$ Hz, 1H), 6.98 (s, 1H), 6.28 (d, $J = 2.4$ Hz, 1H), 6.17 (d, $J = 2.4$ Hz, 1H), 5.90 (s, 1H), 3.88 (s, 2H), 3.84 (s, 3H), 3.80 (s, 3H) ppm; $^{13}\text{C}\{^1\text{H}\}$ NMR

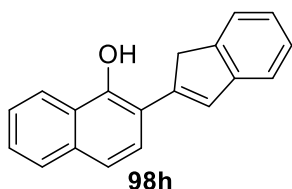
(100 MHz, CDCl_3) δ 160.79, 158.54, 154.38, 144.24, 144.10, 141.34, 130.93, 126.26, 124.80, 123.46, 120.89, 105.47, 92.62, 91.38, 55.48, 55.30, 42.20 ppm; GC-MS $m/z = 268$ (M^+); HRMS Calcd for $\text{C}_{17}\text{H}_{16}\text{O}_3$ ($[\text{M}-\text{H}]^-$): 267.1027, Found: 267.1028.



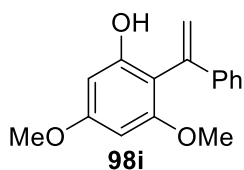
Data for **98f**: ^1H NMR (400 MHz, CDCl_3) δ 6.99 (d, $J = 8.4$ Hz, 1H), 6.51 (d, $J = 2.5$ Hz, 1H), 6.46 (dd, $J = 8.4, 2.5$ Hz, 1H), 5.85-5.81 (m, 1H), 5.79 (s, 1H), 3.78 (s, 3H), 2.28-2.17 (m, 4H), 1.82-1.65 (m, 4H) ppm; $^{13}\text{C}\{^1\text{H}\}$ NMR (100 MHz, CDCl_3) δ 159.46, 152.98, 134.64, 128.44, 127.43, 122.37, 106.17, 100.55, 55.22, 29.96, 25.40, 22.96, 21.86 ppm; GC-MS $m/z = 204$ (M^+).



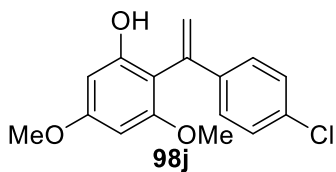
Data for **98g**: ^1H NMR (400 MHz, CDCl_3) δ 8.26-8.22 (m, 1H), 7.79-7.74 (m, 1H), 7.50-7.43 (m, 2H), 7.38 (d, $J = 8.5$ Hz, 1H), 7.21 (d, $J = 8.5$ Hz, 1H), 6.30 (s, 1H), 6.01-5.98 (m, 1H), 2.37-2.24 (m, 4H), 1.88-1.72 (m, 4H) ppm; $^{13}\text{C}\{^1\text{H}\}$ NMR (100 MHz, CDCl_3) δ 147.08, 135.33, 133.45, 128.39, 127.33, 126.03, 125.53, 125.23, 123.98, 122.90, 122.53, 119.37, 29.82, 25.49, 23.00, 21.96 ppm; GC-MS $m/z = 224$ (M^+).



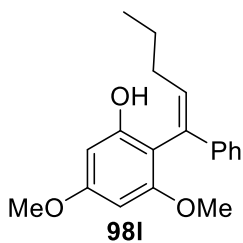
Data for **98h**: ^1H NMR (400 MHz, CDCl_3) δ 8.31-8.26 (m, 1H), 7.84-7.79 (m, 1H), 7.57-7.44 (m, 6H), 7.39-7.33 (m, 1H), 7.31-7.25 (m, 2H), 6.26 (s, 1H), 3.90 (s, 2H) ppm; $^{13}\text{C}\{^1\text{H}\}$ NMR (100 MHz, CDCl_3) δ 148.64, 144.83, 143.98, 142.86, 133.79, 129.18, 127.51, 126.79, 126.59, 125.87, 125.69, 125.08, 124.37, 123.65, 122.26, 121.16, 120.23, 116.64, 41.96 ppm; GC-MS $m/z = 258$ (M^+); HRMS Calcd for $\text{C}_{19}\text{H}_{14}\text{O}$ ($[\text{M}+\text{H}]^+$): 259.1117, Found: 259.1111.



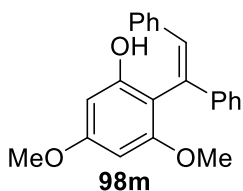
Data for **98i**: ^1H NMR (400 MHz, CDCl_3) δ 7.39-7.33 (m, 2H), 7.33-7.27 (m, 3H), 6.26 (d, $J = 2.3$ Hz, 1H), 6.12 (d, $J = 2.3$ Hz, 1H), 6.08 (d, $J = 1.4$ Hz, 1H), 5.62 (s, 1H), 5.38 (d, $J = 1.4$ Hz, 1H), 3.83 (s, 3H), 3.59 (s, 3H) ppm; $^{13}\text{C}\{^1\text{H}\}$ NMR (100 MHz, CDCl_3) δ 160.97, 158.46, 154.55, 141.38, 139.43, 128.30, 128.06, 126.00, 117.55, 109.12, 92.46, 91.59, 55.70, 55.32 ppm; GC-MS $m/z = 256$ (M^+); HRMS Calcd for $\text{C}_{16}\text{H}_{16}\text{O}_3$ ($[\text{M}-\text{H}]^-$): 255.1027, Found: 255.1029.



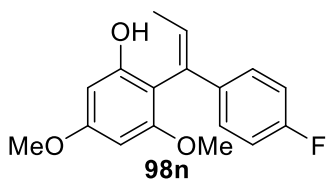
Data for **98j**: ^1H NMR (400 MHz, CDCl_3) δ 7.29-7.23 (m, 4H), 6.24 (d, $J = 2.3$ Hz, 1H), 6.09 (d, $J = 2.3$ Hz, 1H), 6.03 (d, $J = 1.3$ Hz, 1H), 5.58 (s, 1H), 5.37 (d, $J = 1.3$ Hz, 1H), 3.82 (s, 3H), 3.58 (s, 3H) ppm; $^{13}\text{C}\{^1\text{H}\}$ NMR (100 MHz, CDCl_3) δ 161.15, 158.39, 154.54, 140.51, 138.10, 133.82, 128.43, 127.35, 117.79, 108.59, 92.54, 91.61, 55.68, 55.35 ppm; GC-MS $m/z = 290$ (M^+); HRMS Calcd for $\text{C}_{16}\text{H}_{15}\text{O}_3\text{Cl}$ ($[\text{M}-\text{H}]^-$): 289.0637, Found: 289.0642.



Data for **98l**: ^1H NMR (400 MHz, CDCl_3) δ 7.34-7.20 (m, 5H), 6.51 (t, $J = 7.3$ Hz, 1H), 6.26 (d, $J = 2.3$ Hz, 1H), 6.16 (d, $J = 2.3$ Hz, 1H), 5.26 (s, 1H), 3.83 (s, 3H), 3.64 (s, 3H), 2.07-1.99 (m, 2H), 1.49 (sextet, $J = 7.4$ Hz, 2H), 0.93 (t, $J = 7.4$ Hz, 3H) ppm; $^{13}\text{C}\{^1\text{H}\}$ NMR (100 MHz, CDCl_3) δ 160.91, 158.47, 154.09, 140.19, 134.47, 131.75, 128.29, 127.13, 125.75, 106.95, 92.19, 91.52, 55.58, 55.21, 31.95, 22.35, 13.81 ppm; GC-MS $m/z = 298$ (M^+); HRMS Calcd for $\text{C}_{19}\text{H}_{22}\text{O}_3$ ($[\text{M}+\text{H}]^+$): 299.1642, Found: 299.1631.

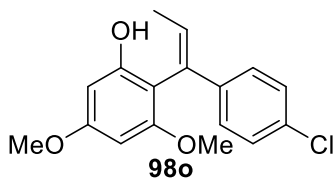


Data for **98m**: ^1H NMR (400 MHz, CDCl_3) δ 7.43-7.39 (m, 2H), 7.36-7.27 (m, 4H), 7.24-7.15 (m, 5H), 6.19 (d, $J = 2.3$ Hz, 1H), 6.17 (d, $J = 2.3$ Hz, 1H), 5.27 (s, 1H), 3.83 (s, 3H), 3.57 (s, 3H) ppm; $^{13}\text{C}\{^1\text{H}\}$ NMR (100 MHz, CDCl_3) δ 161.35, 158.86, 153.81, 141.47, 136.41, 132.76, 131.47, 128.46, 128.33, 128.26, 127.67, 127.65, 126.05, 107.46, 92.77, 92.07, 55.64, 55.17 ppm; GC-MS $m/z = 332$ (M^+); HRMS Calcd for $\text{C}_{22}\text{H}_{20}\text{O}_3$ ($[\text{M}-\text{H}]^-$): 331.1340, Found: 331.1343.

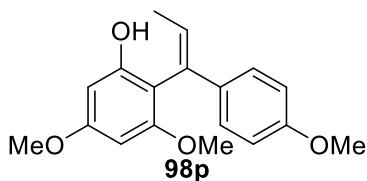


Data for **98n**: ^1H NMR (400 MHz, CDCl_3) δ 7.25-7.21 (m, 2H), 6.98-6.91 (m, 2H), 6.47 (q, $J = 6.8$ Hz, 1H), 6.23 (d, $J = 2.3$ Hz, 1H), 6.14 (d, $J = 2.3$ Hz, 1H), 5.18 (s, 1H), 3.82 (s, 3H), 3.63 (s, 3H), 1.69 (d, $J = 6.8$ Hz, 3H) ppm; $^{13}\text{C}\{^1\text{H}\}$ NMR (100 MHz, CDCl_3) δ 163.36, 161.16,

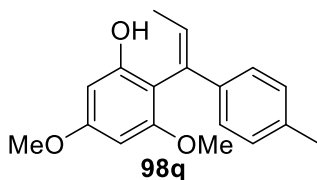
160.92, 158.47, 154.14, 136.54, 136.50, 132.13, 128.39, 128.38, 127.32, 127.24, 115.22, 115.00, 106.35, 92.35, 91.72, 55.72, 55.31, 15.49 ppm; GC-MS m/z = 288 (M^+); HRMS Calcd for $C_{17}H_{17}O_3F$ ($[M+H]^+$): 289.1234, Found: 289.1228.



Data for **98o**: 1H NMR (400 MHz, $CDCl_3$) δ 7.23-7.18 (m, 4H), 6.52 (q, J = 6.9 Hz, 1H), 6.23 (d, J = 2.3 Hz, 1H), 6.14 (d, J = 2.3 Hz, 1H), 5.18 (s, 1H), 3.82 (s, 3H), 3.62 (s, 3H), 1.70 (s, J = 6.9 Hz, 3H) ppm; $^{13}C\{^1H\}$ NMR (100 MHz, $CDCl_3$) δ 161.19, 158.46, 154.16, 138.96, 132.77, 132.13, 129.07, 128.39, 127.00, 106.03, 92.38, 91.70, 55.69, 55.29, 15.53 ppm; GC-MS m/z = 304 (M^+); HRMS Calcd for $C_{17}H_{17}O_3Cl$ ($[M+H]^+$): 305.0939, Found: 305.0937.

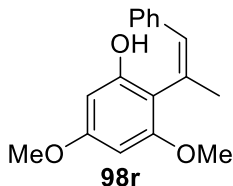


Data for **98p**: 1H NMR (400 MHz, $CDCl_3$) δ 7.24-7.20 (m, 2H), 6.82-6.78 (m, 2H), 6.45 (q, J = 6.8 Hz, 1H), 6.24 (d, J = 2.3 Hz, 1H), 6.15 (d, J = 2.3 Hz, 1H), 5.25 (s, 1H), 3.82 (s, 3H), 3.78 (s, 3H), 3.65 (s, 3H), 1.68 (d, J = 6.8 Hz, 3H) ppm; $^{13}C\{^1H\}$ NMR (100 MHz, $CDCl_3$) δ 160.94, 158.86, 158.47, 154.16, 132.82, 132.25, 126.80, 126.64, 113.67, 106.69, 92.27, 91.60, 55.72, 55.25, 55.15, 15.38 ppm; GC-MS m/z = 300 (M^+); HRMS Calcd for $C_{18}H_{20}O_4$ ($[M-H]^-$): 299.1289, Found: 299.1294.

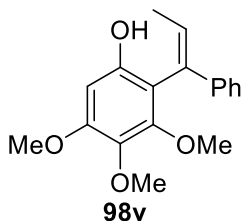


Data for **98q**: 1H NMR (400 MHz, $CDCl_3$) δ 7.21-7.17 (m, 2H), 7.10-7.06 (m, 2H), 6.53 (q, J = 6.9 Hz, 1H), 6.25 (d, J = 2.3 Hz, 1H), 6.16 (d, J = 2.3 Hz, 1H), 5.23 (s, 1H), 3.83 (s, 3H), 3.65 (s, 3H), 2.33 (s, 3H), 1.71 (d, J = 6.9 Hz, 3H) ppm; $^{13}C\{^1H\}$ NMR (100 MHz, $CDCl_3$) δ 160.93, 158.48, 154.16, 137.36, 136.87, 132.70, 129.04, 127.72, 125.54, 106.63, 92.21, 91.59,

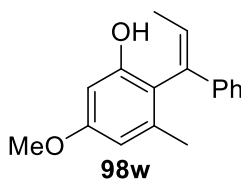
55.71, 55.25, 21.02, 15.42 ppm; GC-MS $m/z = 284$ (M^+); HRMS Calcd for $C_{18}H_{20}O_3$ ($[M+H]^+$): 285.1485, Found: 285.1478.



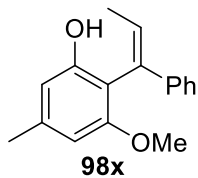
Data for **98r**: 1H NMR (400 MHz, $CDCl_3$) δ 7.18-7.10 (m, 3H), 7.10-7.05 (m, 2H), 6.76-6.74 (m, 1H), 6.17 (d, $J = 2.3$ Hz, 1H), 6.09 (d, $J = 2.3$ Hz, 1H), 5.27 (s, 1H), 3.82 (s, 3H), 3.79 (s, 3H), 2.14 (d, $J = 1.4$ Hz, 3H) ppm; $^{13}C\{^1H\}$ NMR (100 MHz, $CDCl_3$) δ 160.78, 158.28, 152.14, 136.23, 131.22, 130.74, 128.28, 127.80, 127.21, 109.06, 92.67, 91.75, 55.71, 55.28, 25.41 ppm; GC-MS $m/z = 270$ (M^+); HRMS Calcd for $C_{17}H_{18}O_3$ ($[M-H]^-$): 269.1183, Found: 269.1186.



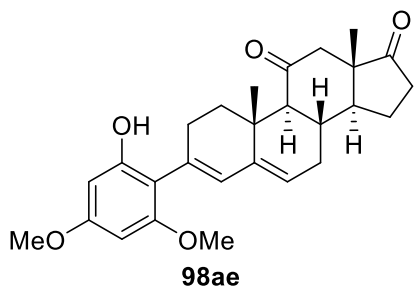
Data for **98v**: 1H NMR (400 MHz, $CDCl_3$) δ 7.29-7.20 (m, 5H), 6.50 (q, $J = 6.9$ Hz, 1H), 6.40 (s, 1H), 5.10 (s, 1H), 3.87 (s, 3H), 3.79 (s, 3H), 3.49 (s, 3H), 1.74 (d, $J = 6.9$ Hz, 3H) ppm; $^{13}C\{^1H\}$ NMR (100 MHz, $CDCl_3$) δ 153.77, 151.46, 148.90, 140.92, 136.03, 133.60, 128.47, 128.34, 127.29, 125.96, 111.27, 94.59, 60.97, 60.50, 55.80, 15.66 ppm; GC-MS $m/z = 300$ (M^+); HRMS Calcd for $C_{18}H_{20}O_4$ ($[M-H]^-$): 299.1289, Found: 299.1294.



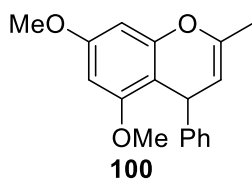
Data for **98w**: 1H NMR (400 MHz, $CDCl_3$) δ 7.30-7.20 (m, 5H), 6.60 (q, $J = 6.9$ Hz, 1H), 6.45-6.44 (m, 1H), 6.42-6.41 (m, 1H), 5.14 (s, 1H), 3.81 (s, 3H), 1.97-1.95 (m, 3H), 1.67 (d, $J = 6.9$ Hz, 3H) ppm; $^{13}C\{^1H\}$ NMR (100 MHz, $CDCl_3$) δ 159.91, 153.56, 139.81, 138.62, 135.34, 128.55, 128.43, 127.37, 125.77, 117.12, 108.28, 97.61, 55.16, 19.88, 15.32 ppm; GC-MS $m/z = 254$ (M^+); HRMS Calcd for $C_{17}H_{18}O_2$ ($[M-H]^-$): 253.1234, Found: 253.1237.



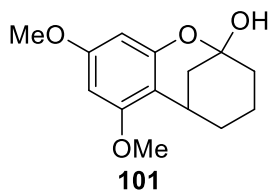
Data for **98x**: ^1H NMR (400 MHz, CDCl_3) δ 7.30-7.19 (m, 5H), 6.56 (q, $J = 6.9$ Hz, 1H), 6.52-6.50 (m, 1H), 6.38-6.36 (m, 1H), 5.08 (s, 1H), 3.65 (s, 3H), 2.38-2.37 (m, 3H), 1.70 (d, $J = 6.9$ Hz, 3H) ppm; $^{13}\text{C}\{^1\text{H}\}$ NMR (100 MHz, CDCl_3) δ 157.56, 153.30, 140.14, 139.60, 133.15, 128.51, 128.34, 127.16, 125.71, 111.05, 108.44, 104.25, 55.77, 21.88, 15.52 ppm; GC-MS $m/z = 254$ (M^+).



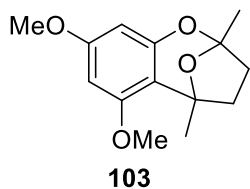
Data for **98ae**: ^1H NMR (400 MHz, CDCl_3) δ 6.15 (d, $J = 2.3$ Hz, 1H), 6.04 (d, $J = 2.3$ Hz, 1H), 5.96 (br s, 1H), 5.61 (s, 1H), 5.47-5.42 (m, 1H), 3.76 (s, 3H), 3.73 (s, 3H), 2.68-2.42 (m, 5H), 2.38-1.89 (m, 8H), 1.76-1.64 (m, 1H), 1.31-1.22 (m, 1H), 1.25 (s, 3H), 0.88 (s, 3H) ppm; $^{13}\text{C}\{^1\text{H}\}$ NMR (100 MHz, CDCl_3) δ 217.55, 208.76, 160.37, 158.49, 153.46, 141.57, 132.20, 129.45, 122.41, 110.49, 92.29, 91.34, 59.34, 55.66, 55.33, 50.50, 50.48, 50.22, 36.16, 34.96, 33.05, 32.63, 31.50, 26.47, 21.70, 18.76, 14.74 ppm; GC-MS $m/z = 436$ (M^+); HRMS Calcd for $\text{C}_{27}\text{H}_{32}\text{O}_5$ ($[\text{M}+\text{H}]^+$): 437.2323, Found: 437.2309.



Data for **100**: ^1H NMR (400 MHz, CDCl_3) δ 7.33-7.23 (m, 4H), 7.21-7.17 (m, 1H), 6.24 (d, $J = 2.4$ Hz, 1H), 6.14 (d, $J = 2.4$ Hz, 1H), 4.90 (d, $J = 4.8$ Hz, 1H), 4.63 (d, $J = 4.8$ Hz, 1H), 3.81 (s, 3H), 3.61 (s, 3H), 1.97 (s, 3H) ppm; $^{13}\text{C}\{^1\text{H}\}$ NMR (100 MHz, CDCl_3) δ 159.62, 158.26, 152.70, 147.35, 146.20, 127.99, 127.62, 125.73, 105.10, 101.79, 93.88, 92.61, 55.33, 55.22, 36.27, 19.12 ppm; GC-MS $m/z = 282$ (M^+); HRMS Calcd for $\text{C}_{18}\text{H}_{18}\text{O}_3$ ($[\text{M}+\text{H}]^+$): 283.1329, Found: 283.1349.



Data for **101**: ^1H NMR (400 MHz, CDCl_3) δ 6.02 (d, $J = 2.3$ Hz, 1H), 6.00 (d, $J = 2.3$ Hz, 1H), 3.74 (s, 3H), 3.72 (s, 3H), 3.71-3.68 (br s, 1H), 3.43-3.38 (m, 1H), 2.09-2.01 (m, 1H), 1.96 (dd, $J = 12.4$, 2.9 Hz, 1H), 1.87-1.80 (m, 1H), 1.77-1.63 (m, 2H), 1.59-1.45 (m, 2H), 1.44-1.29 (m, 1H) ppm; $^{13}\text{C}\{^1\text{H}\}$ NMR (100 MHz, CDCl_3) δ 159.43, 156.90, 156.67, 106.08, 98.64, 92.12, 90.74, 55.24, 55.10, 38.69, 36.36, 29.51, 28.10, 19.13 ppm; GC-MS $m/z = 250$ (M^+); HRMS Calcd for $\text{C}_{14}\text{H}_{18}\text{O}_4$ ($[\text{M}+\text{H}]^+$): 251.1278, Found: 251.1271.



Data for **103**: ^1H NMR (400 MHz, CDCl_3) δ 6.00 (d, $J = 2.4$ Hz, 1H), 5.96 (d, $J = 2.4$ Hz, 1H), 3.73 (s, 3H), 3.72 (s, 3H), 2.35-2.21 (m, 2H), 2.10-2.01 (m, 1H), 1.95-1.85 (m, 1H), 1.81 (s, 3H), 1.67 (s, 3H) ppm; $^{13}\text{C}\{^1\text{H}\}$ NMR (100 MHz, CDCl_3) δ 159.91, 156.62, 153.24, 110.33, 106.81, 93.10, 91.51, 83.21, 55.14, 55.05, 42.74, 38.37, 24.10, 23.10 ppm; GC-MS $m/z = 250$ (M^+); HRMS Calcd for $\text{C}_{14}\text{H}_{18}\text{O}_4$ ($[\text{M}+\text{H}]^+$): 251.1278, Found: 251.1274.

5.4.5 X-ray Crystal Data and Structure Refinements

Table 5.4 X-ray crystal data for **98k**

Empirical formula	C ₁₇ H ₁₈ O ₃
Formula weight	270.31
Temperature/K	100.00(10)
Crystal system	monoclinic
Space group	P2 ₁ /c
a/Å	9.9036(2)
b/Å	9.5634(2)
c/Å	15.2192(4)
α/°	90.00
β/°	93.961(2)
γ/°	90.00
Volume/Å ³	1438.01(6)
Z	4
ρ _{calc} /cm ³	1.249
μ/mm ⁻¹	0.085
F(000)	576.0
Crystal size/mm ³	0.51 × 0.5 × 0.45
Radiation	MoKα (λ = 0.71073)
2θ range for data collection/°	6.62 to 59.1
Index ranges	-13 ≤ h ≤ 13, -12 ≤ k ≤ 13, -20 ≤ l ≤ 20
Reflections collected	16395
Independent reflections	3669 [R _{int} = 0.0346, R _{sigma} = 0.0323]
Data/restraints/parameters	3669/0/185
Goodness-of-fit on F ²	1.034
Final R indexes [I >= 2σ (I)]	R ₁ = 0.0444, wR ₂ = 0.1001
Final R indexes [all data]	R ₁ = 0.0628, wR ₂ = 0.1117
Largest diff. peak/hole / e Å ⁻³	0.31/-0.26

Table 5.5 X-ray crystal data for **110**

Empirical formula	C ₁₄ H ₁₈ O ₄
Formula weight	250.28
Temperature/K	100.00(10)
Crystal system	monoclinic
Space group	P2 ₁
a/Å	5.53828(6)
b/Å	24.4737(4)
c/Å	8.98955(14)
α/°	90.00
β/°	91.2110(12)
γ/°	90.00
Volume/Å ³	1218.19(3)
Z	4
ρ _{calc} /cm ³	1.365
μ/mm ⁻¹	0.816
F(000)	536.0
Crystal size/mm ³	0.576 × 0.2375 × 0.1009
Radiation	CuKα (λ = 1.54184)
2θ range for data collection/°	7.22 to 147.84
Index ranges	-6 ≤ h ≤ 6, -29 ≤ k ≤ 29, -11 ≤ l ≤ 10
Reflections collected	11890
Independent reflections	4642 [R _{int} = 0.0312, R _{sigma} = 0.0317]
Data/restraints/parameters	4642/1/338
Goodness-of-fit on F ²	1.034
Final R indexes [I >= 2σ (I)]	R ₁ = 0.0372, wR ₂ = 0.0971
Final R indexes [all data]	R ₁ = 0.0399, wR ₂ = 0.1010
Largest diff. peak/hole / e Å ⁻³	0.19/-0.25
Flack parameter	0.0(5)

5.5 Experimental Procedures and Data for the Chapter 4

5.5.1 General Procedures for the Catalytic Synthesis of Indole and Quinoline Products

In a glove box, complex **79** (13 mg, 0.75 mol %) and $\text{HBF}_4 \cdot \text{OEt}_2$ (12 mg, 7 mol %) were dissolved in 1,4-dioxane (1 mL) in a 25 mL Schlenk tube equipped with a Teflon stopcock and a magnetic stirring bar. The resulting mixture was stirred for 5 to 10 min until the solution turned to a pale green color. In an alternative procedure, the complex **26** (17 mg, 3 mol %) and $\text{HBF}_4 \cdot \text{OEt}_2$ (12 mg, 7 mol %) were dissolved in 1,4-dioxane (1 mL). An arylamine (1.0 mmol), a diol (1.5 mmol), cyclopentene (204 mg, 3 equiv) and 1,4-dioxane (2 mL) were added to the reaction tube. After the tube was sealed, it was brought out of the glove box, and was stirred in an oil bath set at 110-130 °C (130-150 °C for the quinoline products) for 14 h. The reaction tube was taken out of the oil bath, and was cooled to room temperature. After the tube was open to air, the solution was filtered through a short silica gel column by eluting with CH_2Cl_2 (10 mL), and the filtrate was analyzed by GC-MS. Analytically pure product was isolated by a simple column chromatography on silica gel (280-400 mesh, hexanes/EtOAc).

5.5.2 General Procedures for the Deuterium Labeling Study and Control Experiments

Deuterium Labeling Study. In a glove box, complex **79** (13 mg, 0.75 mol %) and $\text{HBF}_4 \cdot \text{OEt}_2$ (12 mg, 7 mol %) were dissolved in 1,4-dioxane (1 mL) in a 25 mL Schlenk tube equipped with a Teflon stopcock and a magnetic stirring bar. The resulting mixture was stirred for 5 to 10 minutes until the solution turned to a pale green color. Then, aniline-

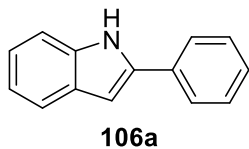
2,3,4,5,6-*d*₅ (98 mg, 0.5 mmol), 1-phenyl-1,2-ethanediol (104 mg, 0.75 mmol), and cyclopentene (102 mg, 3 equiv) in 1,4-dioxane (1 mL) were added to the reaction tube. After the tube was sealed, it was brought out of the glove box, and was stirred in an oil bath set at 110 °C for 14 h. Analytically pure product was isolated by column chromatography on silica gel (280-400 mesh, *n*-hexane/EtOAc).

Reaction of Aniline with *n*-Butanol. In a glove box, complex **79** (7 mg, 0.75 mol %) and HBF₄·OEt₂ (6 mg, 7 mol %) were dissolved in 1,4-dioxane (1 mL) in a 25 mL Schlenk tube equipped with a Teflon stopcock and a magnetic stirring bar. The resulting mixture was stirred for 5 to 10 min until the solution turned to a pale green color. Aniline (50 mg, 1.0 mmol), *n*-butanol (111 mg, 1.5 mmol) and 1,4-dioxane (2 mL) were added to the reaction tube. After the tube was sealed, it was brought out of the glove box, and was stirred in an oil bath set at 110 °C for 14 h. The reaction tube was taken out of the oil bath, and was cooled to room temperature. Analytically pure product was isolated by column chromatography on silica gel (280-400 mesh, *n*-hexane/EtOAc).

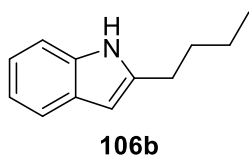
Reaction of Aniline with α -Hydroxyketone. In a glove box, complex **79** (13 mg, 0.75 mol %) and HBF₄·OEt₂ (12 mg, 7 mol %) were dissolved in 1,4-dioxane (1 mL) in a 25 mL Schlenk tube equipped with a Teflon stopcock and a magnetic stirring bar. The resulting mixture was stirred for 5 to 10 min until the solution turned to a pale green color. Then, 3-methoxyaniline (123 mg, 1.0 mmol), benzoin (318 mg, 1.5 mmol) and 1,4-dioxane (2 mL) were added to the reaction tube. After the tube was sealed, it was brought out of the glove box, and was stirred in an oil bath set at 130 °C for 14 h. The reaction tube was taken out of the oil bath, and was cooled to room temperature. Analytically pure product was isolated by column chromatography on silica gel (280-400 mesh, *n*-hexane/EtOAc).

Dehydrogenation of 1-Phenyl-1,2-ethanediol. In a glove box, complex **79** (13 mg, 0.75 mol %), 1-phenyl-1,2-ethanediol (138 mg, 1.0 mmol) and cyclopentene (204 mg, 3 equiv) were dissolved in 1,4-dioxane (3 mL) in a 25 mL Schlenk tube equipped with a Teflon stopcock and a magnetic stirring bar. The tube was brought out of the glove box, and was stirred in an oil bath set at 110 °C for 3 h. The reaction tube was taken out of the oil bath, and was cooled to room temperature. The crude mixture was analyzed by ¹H NMR.

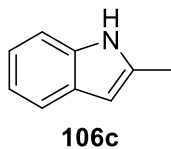
5.5.3 Characterization Data of the Products



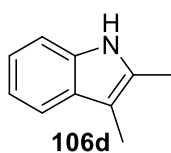
Data for **106a**: ^1H NMR (400 MHz, CDCl_3) δ 8.31 (br s, 1H), 7.69-7.65 (m, 3H), 7.49-7.44 (m, 2H), 7.43-7.40 (m, 1H), 7.38-7.33 (m, 1H), 7.26-7.21 (m, 1H), 7.19-7.14 (m, 1H), 6.87-6.85 (m, 1H) ppm; $^{13}\text{C}\{^1\text{H}\}$ NMR (100 MHz, CDCl_3) δ 137.8, 136.8, 132.3, 129.2, 129.0, 127.7, 125.1, 122.3, 120.6, 120.2, 110.9, 99.9 ppm; GC-MS $m/z = 193$ (M^+). ^1H and ^{13}C NMR spectral data are in good agreement with the literature data.^{103,104}



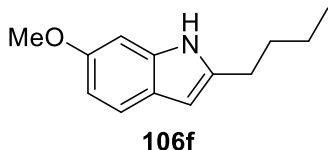
Data for **106b**: ^1H NMR (400 MHz, CDCl_3) δ 7.80 (br s, 1H), 7.58-7.55 (m, 1H), 7.32-7.29 (m, 1H), 7.18-7.09 (m, 2H), 6.29-6.26 (m, 1H), 2.80-2.73 (m, 2H), 1.77-1.69 (m, 2H), 1.45 (sextet, $J = 7.4$ Hz, 2H), 0.99 (t, $J = 7.4$ Hz, 3H) ppm; $^{13}\text{C}\{^1\text{H}\}$ NMR (100 MHz, CDCl_3) δ 140.0, 135.7, 128.8, 120.8, 119.7, 119.5, 110.2, 99.4, 31.2, 27.9, 22.4, 13.8 ppm; GC-MS $m/z = 173$ (M^+). ^1H and ^{13}C NMR spectral data are in good agreement with the literature data.¹⁰³



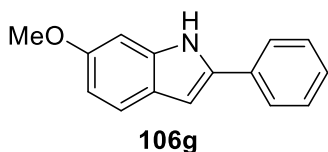
Data for **106c**: ^1H NMR (400 MHz, CDCl_3) δ 7.77 (br s, 1H), 7.57-7.53 (m, 1H), 7.30-7.27 (m, 1H), 7.17-7.08 (m, 2H), 6.26-6.24 (m, 1H), 2.44 (d, $J = 0.9$ Hz, 3H) ppm; $^{13}\text{C}\{^1\text{H}\}$ NMR (100 MHz, CDCl_3) δ 136.0, 135.0, 129.0, 120.9, 119.6(2C), 110.2, 100.3, 13.7 ppm; GC-MS $m/z = 131$ (M^+). ^1H and ^{13}C NMR spectral data are in good agreement with the literature data.^{105,106}



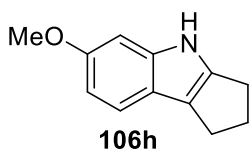
Data for **106d**: ^1H NMR (400 MHz, CDCl_3) δ 7.65 (br s, 1H), 7.50-7.47 (m, 1H), 7.27-7.24 (m, 1H), 7.15-7.07 (m, 2H), 2.37 (s, 3H), 2.24 (s, 3H) ppm; $^{13}\text{C}\{^1\text{H}\}$ NMR (100 MHz, CDCl_3) δ 135.1, 130.6, 129.4, 120.8, 119.0, 117.9, 110.0, 107.1, 11.5, 8.4 ppm; GC-MS $m/z = 145$ (M^+). ^1H and ^{13}C NMR spectral data are in good agreement with the literature data.¹⁰⁷



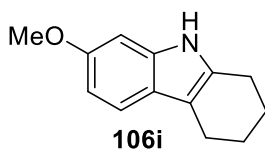
Data for **106f**: ^1H NMR (400 MHz, CDCl_3) δ 7.74 (br s, 1H), 7.41 (d, $J = 8.5$ Hz, 1H), 6.80 (d, $J = 2.3$ Hz, 1H), 6.77 (dd, $J = 8.5, 2.3$ Hz, 1H), 6.18-6.16 (m, 1H), 3.85 (s, 3H), 2.72 (t, $J = 7.5$ Hz, 2H), 1.74-1.64 (m, 2H), 1.48-1.37 (m, 2H), 0.97 (t, $J = 7.3$ Hz, 3H) ppm; $^{13}\text{C}\{^1\text{H}\}$ NMR (100 MHz, CDCl_3) δ 155.6, 138.8, 136.4, 123.0, 120.1, 108.9, 99.0, 94.5, 55.7, 31.3, 27.9, 22.4, 13.9 ppm; GC-MS $m/z = 203$ (M^+). ^1H and ^{13}C NMR spectral data are in good agreement with the literature data.¹⁰⁸



Data for **106g**: ^1H NMR (400 MHz, CDCl_3) δ 8.24 (br s, 1H), 7.64-7.60 (m, 2H), 7.51 (d, $J = 8.6$ Hz, 1H), 7.45-7.40 (m, 2H), 7.32-7.27 (m, 1H), 6.90 (d, $J = 2.3$ Hz, 1H), 6.81 (dd, $J = 8.6, 2.3$ Hz, 1H), 6.77-6.76 (m, 1H), 3.87 (s, 3H) ppm; $^{13}\text{C}\{^1\text{H}\}$ NMR (100 MHz, CDCl_3) δ 156.6, 137.6, 136.8, 132.5, 129.0, 127.2, 124.7, 123.5, 121.3, 110.2, 99.8, 94.4, 55.6 ppm; GC-MS $m/z = 223$ (M^+). ^1H and ^{13}C NMR spectral data are in good agreement with the literature data.¹⁰⁹

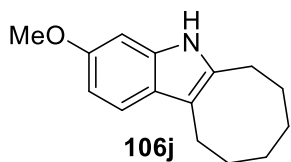


Data for **106h**: ^1H NMR (400 MHz, CDCl_3) δ 7.71 (br s, 1H), 7.33 (d, $J = 8.5$ Hz, 1H), 6.83 (d, $J = 2.3$ Hz, 1H), 6.75 (dd, $J = 8.5, 2.3$ Hz, 1H), 3.84 (s, 3H), 2.86-2.77 (m, 4H), 2.56-2.48 (m, 2H) ppm; $^{13}\text{C}\{^1\text{H}\}$ NMR (100 MHz, CDCl_3) δ 155.3, 142.2, 141.7, 119.5, 119.3, 118.9, 108.5, 95.8, 55.8, 28.6, 25.9, 24.5 ppm; GC-MS $m/z = 187$ (M^+). ^1H and ^{13}C NMR spectral data are in good agreement with the literature data.¹¹⁰

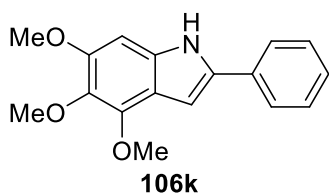


Data for **106i**: ^1H NMR (400 MHz, CDCl_3) δ 7.55 (br s, 1H), 7.33 (d, $J = 8.5$ Hz, 1H), 6.80 (d, $J = 2.3$ Hz, 1H), 6.75 (dd, $J = 8.5, 2.3$ Hz, 1H), 3.84 (s, 3H), 2.72-2.64 (m, 4H), 1.93-1.82 (m, 4H) ppm;

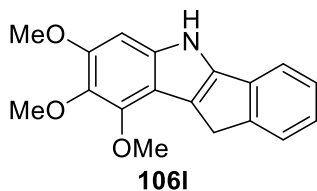
$^{13}\text{C}\{^1\text{H}\}$ NMR (100 MHz, CDCl_3) δ 155.7, 136.3, 132.8, 122.3, 118.2, 109.9, 108.2, 94.8, 55.8, 23.3, 23.2, 23.2, 20.9 ppm; GC-MS $m/z = 201$ (M^+). ^1H and ^{13}C NMR spectral data are in good agreement with the literature data.¹¹¹



Data for **106j**: ^1H NMR (400 MHz, $\text{DMSO}-d_6$) δ 10.43 (br s, 1H), 7.24 (d, $J = 8.5$ Hz, 1H), 6.79 (d, $J = 2.2$ Hz, 1H), 6.60 (dd, $J = 8.5, 2.2$ Hz, 1H), 3.74 (s, 3H), 2.81-2.72 (m, 4H), 1.71-1.59 (m, 4H), 1.43-1.31 (m, 4H) ppm; $^{13}\text{C}\{^1\text{H}\}$ NMR (100 MHz, $\text{DMSO}-d_6$) δ 154.7, 135.6, 134.5, 122.6, 117.5, 109.5, 107.6, 94.3, 55.2, 29.7, 29.3, 25.6(2C), 25.1, 21.8 ppm; GC-MS $m/z = 229$ (M^+); HRMS (IT-TOF/ESI) Calcd for $\text{C}_{15}\text{H}_{20}\text{NO}$ ($[\text{M}+\text{H}]^+$): 230.1539, Found: 230.1530.

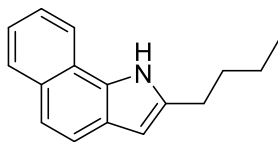


Data for **106k**: ^1H NMR (400 MHz, CDCl_3) δ 8.37 (br s, 1H), 7.63-7.60 (m, 2H), 7.44-7.39 (m, 2H), 7.31-7.27 (m, 1H), 6.86 (dd, $J = 2.3, 0.6$ Hz, 1H), 6.63 (d, $J = 0.6$ Hz, 1H), 4.14 (s, 3H), 3.90 (s, 3H), 3.86 (s, 3H) ppm; $^{13}\text{C}\{^1\text{H}\}$ NMR (100 MHz, CDCl_3) δ 151.3, 145.7, 136.0, 135.8, 133.9, 132.3, 129.0, 127.2, 124.6, 116.4, 97.5, 89.4, 61.5, 60.8, 56.2 ppm; GC-MS $m/z = 283$ (M^+); Anal. Calcd for $\text{C}_{17}\text{H}_{17}\text{NO}_3$: C, 72.07; H, 6.05; N, 4.94. Found: C, 72.27; H, 6.28; N, 4.97.

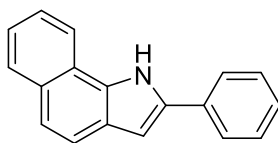


Data for **106l**: ^1H NMR (400 MHz, CDCl_3) δ 8.42 (br s, 1H), 7.53-7.50 (m, 1H), 7.40-7.37 (m, 1H), 7.31-7.27 (m, 1H), 7.20-7.15 (m, 1H), 6.67 (s, 1H), 4.12 (s, 3H), 3.93 (s, 3H), 3.87 (s, 3H), 3.80 (s, 2H) ppm; $^{13}\text{C}\{^1\text{H}\}$ NMR (100 MHz, CDCl_3) δ 150.7, 147.4, 145.5, 141.6, 137.4, 136.4, 135.0, 126.5, 125.2, 124.1, 120.2, 116.7, 113.0, 91.2, 61.6, 61.4, 56.3, 31.7

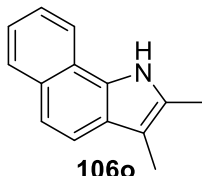
ppm; GC-MS $m/z = 295$ (M^+); HRMS (IT-TOF/ESI) Calcd for $C_{18}H_{18}NO_3$ ($[M+H]^+$): 296.1281, Found: 296.1274.

**106m**

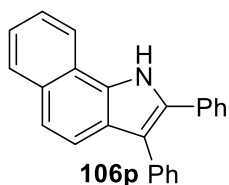
Data for **106m**: 1H NMR (400 MHz, $CDCl_3$) δ 8.58 (br s, 1H), 7.97-7.92 (m, 2H), 7.68 (d, $J = 8.6$ Hz, 1H), 7.54-7.49 (m, 1H), 7.52 (d, $J = 8.6$ Hz, 1H), 7.44-7.39 (m, 1H), 6.42-6.41 (m, 1H), 2.86 (t, $J = 7.6$ Hz, 2H), 1.79 (quintet, $J = 7.6$ Hz, 2H), 1.48 (sextet, $J = 7.5$ Hz, 2H), 1.01 (t, $J = 7.5$ Hz, 3H) ppm; $^{13}C\{^1H\}$ NMR (100 MHz, $CDCl_3$) δ 138.1, 129.8, 128.9, 125.2, 124.6, 123.2, 121.4, 120.3, 120.3, 119.0, 101.1, 31.6, 28.0, 22.4, 13.9 ppm (one carbon signal obscured or overlapping); GC-MS $m/z = 223$ (M^+). 1H and ^{13}C NMR spectral data are in good agreement with the literature data.¹⁰³

**106n**

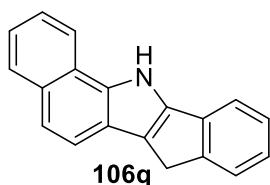
Data for **106n**: 1H NMR (400 MHz, $CDCl_3$) δ 9.01 (br s, 1H), 8.07 (d, $J = 8.2$ Hz, 1H), 7.95 (d, $J = 8.2$ Hz, 1H), 7.76-7.71 (m, 3H), 7.59-7.53 (m, 2H), 7.52-7.43 (m, 3H), 7.37-7.33 (m, 1H), 6.98 (d, $J = 2.3$ Hz, 1H) ppm; $^{13}C\{^1H\}$ NMR (100 MHz, $CDCl_3$) δ 136.2, 132.5, 131.3, 130.5, 129.1, 129.0, 127.4, 125.6, 125.3, 124.9, 123.9, 121.5, 121.2, 120.6, 119.3, 101.7 ppm; GC-MS $m/z = 243$ (M^+). 1H and ^{13}C NMR spectral data are in good agreement with the literature data.^{103,104}

**106o**

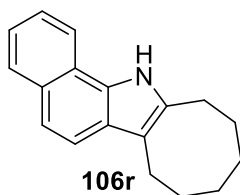
Data for **106o**: 1H NMR (400 MHz, $CDCl_3$) δ 8.40 (br s, 1H), 7.92 (d, $J = 8.3$, 2H), 7.63 (d, $J = 8.5$ Hz, 1H), 7.51 (d, $J = 8.5$ Hz, 1H), 7.52-7.47 (m, 1H), 7.41-7.36 (m, 1H), 2.46 (s, 3H), 2.32 (s, 3H) ppm; $^{13}C\{^1H\}$ NMR (100 MHz, $CDCl_3$) δ 129.9, 129.1, 128.9, 128.8, 125.1, 124.9, 123.1, 121.2, 119.7, 119.1, 118.6, 108.9, 11.6, 8.6 ppm; GC-MS $m/z = 195$ (M^+). 1H and ^{13}C NMR spectral data are in good agreement with the literature data.¹¹²



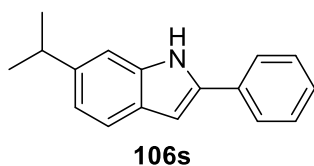
Data for **106p**: ^1H NMR (400 MHz, CDCl_3) δ 8.93 (br s, 1H), 8.07 (d, $J = 8.1$ Hz, 1H), 7.98 (d, $J = 8.0$ Hz, 1H), 7.82-7.78 (m, 1H), 7.61-7.43 (m, 9H), 7.42-7.31 (m, 4H) ppm; $^{13}\text{C}\{^1\text{H}\}$ NMR (100 MHz, CDCl_3) δ 135.0, 132.7, 132.5, 130.7, 130.5, 130.2, 128.9, 128.7, 128.5, 128.0, 127.4, 126.3, 125.6, 124.5, 124.1, 121.4, 121.2, 119.5, 119.4, 116.8 ppm; GC-MS $m/z = 319$ (M^+). ^1H and ^{13}C NMR spectral data are in good agreement with the literature data.¹¹³



Data for **106q**: ^1H NMR (400 MHz, acetone- d_6) δ 11.59 (br s, 1H), 8.34-8.31 (m, 1H), 7.95-7.92 (m, 1H), 7.75 (d, $J = 8.5$ Hz, 1H), 7.64-7.61 (m, 1H), 7.57-7.50 (m, 3H), 7.42-7.37 (m, 1H), 7.36-7.31 (m, 1H), 7.21-7.16 (m, 1H), 3.77 (s, 2H) ppm; $^{13}\text{C}\{^1\text{H}\}$ NMR (100 MHz, acetone- d_6) δ 148.4, 143.1, 136.4, 136.0, 131.2, 129.6, 127.5, 126.3, 126.3, 125.2, 124.3, 124.0, 123.5, 121.3, 121.3, 121.0, 120.2, 118.2, 30.7 ppm; GC-MS $m/z = 255$ (M^+); HRMS (IT-TOF/ESI) Calcd for $\text{C}_{19}\text{H}_{14}\text{N}$ ($[\text{M}+\text{H}]^+$): 256.1121, Found: 256.1114.

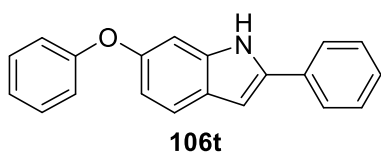


Data for **106r**: ^1H NMR (400 MHz, CDCl_3) δ 8.40 (br s, 1H), 8.00-7.93 (m, 2H), 7.70 (d, $J = 8.6$ Hz, 1H), 7.56 (d, $J = 8.6$ Hz, 1H), 7.56-7.51 (m, 1H), 7.46-7.41 (m, 1H), 3.02-2.94 (m, 4H), 1.87-1.78 (m, 4H), 1.58-1.46 (m, 4H) ppm; $^{13}\text{C}\{^1\text{H}\}$ NMR (100 MHz, CDCl_3) δ 133.8, 129.8, 128.9, 128.8, 125.1, 124.1, 123.0, 121.4, 119.6, 119.1, 118.5, 113.5, 29.9, 29.8, 26.0, 25.8, 25.8, 22.2 ppm; GC-MS $m/z = 249$ (M^+); HRMS (IT-TOF/ESI) Calcd for $\text{C}_{18}\text{H}_{20}\text{N}$ ($[\text{M}+\text{H}]^+$): 250.1590. Found 250.1582.

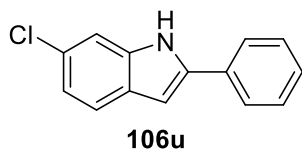


Data for **106s**: ^1H NMR (400 MHz, CDCl_3) δ 8.24 (br s, 1H), 7.69-7.65 (m, 2H), 7.61 (d, $J = 8.2$ Hz, 1H), 7.49-7.44 (m, 2H), 7.38-7.33 (m, 1H), 7.29-7.27 (m, 1H), 7.10 (dd, $J = 8.2, 1.5$ Hz,

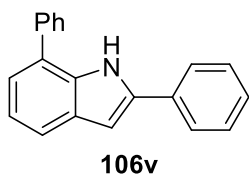
1H), 6.84 (dd, $J = 2.1, 0.8$ Hz, 1H), 3.08 (septet, $J = 7.0$ Hz, 1H), 1.38 (d, $J = 7.0$ Hz, 6H) ppm; $^{13}\text{C}\{^1\text{H}\}$ NMR (100 MHz, CDCl_3) δ 143.6, 137.4, 137.1, 132.5, 128.9, 127.4, 127.4, 124.9, 120.3, 119.7, 108.1, 99.8, 34.4, 24.4 ppm; GC-MS $m/z = 235$ (M^+). ^1H and ^{13}C NMR spectral data are in good agreement with the literature data.¹⁰⁴



Data for **106t**: ^1H NMR (400 MHz, $\text{DMSO}-d_6$) δ 11.50 (br s, 1H), 7.82-7.78 (m, 2H), 7.52 (d, $J = 8.5$ Hz, 1H), 7.46-7.40 (m, 2H), 7.38-7.32 (m, 2H), 7.30-7.26 (m, 1H), 7.10-7.05 (m, 1H), 7.01-6.96 (m, 3H), 6.90-6.88 (m, 1H), 6.75 (dd, $J = 8.5, 2.2$ Hz, 1H) ppm; $^{13}\text{C}\{^1\text{H}\}$ NMR (100 MHz, $\text{DMSO}-d_6$) δ 158.1, 152.0, 137.9, 137.6, 132.1, 129.9, 129.0, 127.3, 125.3, 124.8, 122.7, 121.2, 117.9, 112.6, 101.5, 98.7 ppm; GC-MS $m/z = 285$ (M^+); Anal. Calcd for $\text{C}_{20}\text{H}_{15}\text{NO}$: C, 84.19; H, 5.30; N, 4.91. Found: C, 84.34; H, 5.49; N, 4.96.

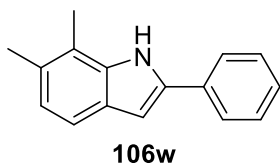


Data for **106u**: ^1H NMR (400 MHz, $\text{DMSO}-d_6$) δ 11.71 (br s, 1H), 7.87-7.83 (m, 2H), 7.54 (d, $J = 8.4$ Hz, 1H), 7.50-7.44 (m, 2H), 7.40 (d, $J = 2.0$ Hz, 1H), 7.36-7.31 (m, 1H), 7.01 (dd, $J = 8.4, 2.0$ Hz, 1H), 6.94-6.93 (m, 1H) ppm; $^{13}\text{C}\{^1\text{H}\}$ NMR (100 MHz, $\text{DMSO}-d_6$) δ 138.8, 137.5, 131.7, 129.0, 127.8, 127.4, 126.0, 125.1, 121.4, 119.8, 110.8, 98.8 ppm; GC-MS $m/z = 227$ (M^+). ^1H and ^{13}C NMR spectral data are in good agreement with the literature data.^{104,106}

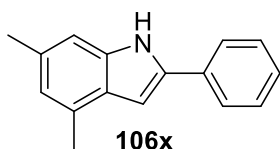


Data for **106v**: ^1H NMR (400 MHz, CDCl_3) δ 8.60 (br s, 1H), 7.80-7.76 (m, 2H), 7.74-7.67 (m, 3H), 7.66-7.60 (m, 2H), 7.54-7.46 (m, 3H), 7.40-7.36 (m, 1H), 7.33-7.29 (m, 2H), 6.98-6.97 (m, 1H) ppm; $^{13}\text{C}\{^1\text{H}\}$ NMR (100 MHz, CDCl_3) δ 139.2, 138.1, 134.6, 132.2, 129.6, 129.2, 128.9, 128.2,

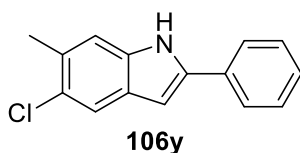
127.7, 127.4, 125.4, 125.2, 122.2, 120.7, 119.9, 100.4 ppm; GC-MS $m/z = 269$ (M^+); Anal. Calcd for $C_{20}H_{15}NO$: C, 89.19; H, 5.61; N, 5.20. Found: C, 89.00; H, 5.73; N, 5.27.



Data for **106w**: 1H NMR (400 MHz, $CDCl_3$) δ 8.14 (br s, 1H), 7.75-7.72 (m, 2H), 7.53-7.45 (m, 3H), 7.40-7.36 (m, 1H), 7.07-7.04 (m, 1H), 6.87-6.86 (m, 1H), 2.49 (s, 6H) ppm; $^{13}C\{^1H\}$ NMR (100 MHz, $CDCl_3$) δ 137.1, 137.0, 132.6, 129.8, 128.9, 127.3, 127.1, 124.9, 123.0, 117.8, 117.6, 100.4, 19.4, 13.1 ppm; GC-MS $m/z = 221$ (M^+); Anal. Calcd for $C_{16}H_{15}N$: C, 86.84; H, 6.83; N, 6.33. Found: C, 86.99; H, 6.90; N, 6.43.

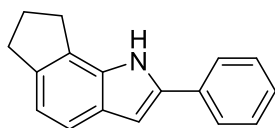


Data for **106x**: 1H NMR (400 MHz, $CDCl_3$) δ 8.13 (br s, 1H), 7.69-7.66 (m, 2H), 7.51-7.46 (m, 2H), 7.40-7.35 (m, 1H), 7.02 (s, 1H), 6.90-6.87 (m, 2H), 2.64 (s, 3H), 2.51 (s, 3H) ppm; $^{13}C\{^1H\}$ NMR (100 MHz, $CDCl_3$) δ 136.9, 136.5, 132.5, 132.3, 129.7, 128.9, 127.2, 126.9, 124.8, 122.3, 108.4, 98.3, 21.7, 18.7 ppm; GC-MS $m/z = 221$ (M^+); Anal. Calcd for $C_{16}H_{15}N$: C, 86.84; H, 6.83; N, 6.33. Found: C, 86.83; H, 6.84; N, 6.36.



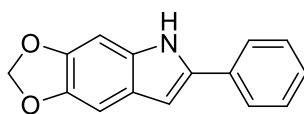
Data for **106y**: 1H NMR (400 MHz, $DMSO-d_6$) δ 11.6 (br s, 1H), 7.86-7.81 (m, 2H), 7.56 (s, 1H), 7.47-7.43 (m, 2H), 7.34 (s, 1H), 7.33-7.30 (m, 1H), 6.84-6.83 (m, 1H), 2.41 (s, 3H) ppm; $^{13}C\{^1H\}$ NMR (100 MHz, $DMSO-d_6$) δ 138.6, 136.2, 131.9, 129.0, 128.1, 128.1, 127.7, 125.0, 119.5, 113.0, 98.1, 20.4 ppm (one carbon signal obscured or overlapped); GC-MS $m/z = 241$ (M^+); HRMS (IT-TOF/ESI) Calcd for $C_{15}H_{13}NCl$ ($[M+H]^+$): 242.0731. Found: 242.0730. Data for 5-chloro-4-methyl-2-phenylindole: 1H NMR (400 MHz, $DMSO-d_6$) δ 11.7 (br s, 1H), 7.90-7.86 (m, 2H), 7.49-7.45 (m, 2H), 7.35-7.32 (m, 1H), 7.24 (d, $J = 8.5$ Hz, 1H), 7.09 (d, $J = 8.5$ Hz, 1H), 7.04-7.02 (m, 1H), 2.52 (s, 3H) ppm; $^{13}C\{^1H\}$ NMR

(100 MHz, DMSO-*d*₆) δ 138.4, 135.2, 131.9, 130.0, 129.0, 127.7, 126.0, 125.1, 123.5, 122.2, 110.4, 98.0, 16.0 ppm.

**106z**

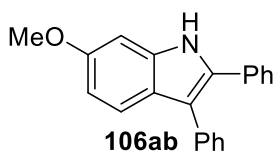
Data for **106z**: ¹H NMR (400 MHz, CDCl₃) δ 8.13 (br s, 1H), 7.73-7.69 (m, 2H), 7.52-7.45 (m, 3H), 7.37-7.33 (m, 1H), 7.12 (d, *J* = 8.0 Hz, 1H), 6.89 (d, *J* = 2.1 Hz, 1H), 3.15-3.08 (m, 4H), 2.33-2.24

(m, 2H) ppm; ¹³C{¹H} NMR (100 MHz, CDCl₃) δ 139.0, 137.0, 133.9, 132.6, 128.9, 127.8, 127.3, 125.2, 124.9, 118.6, 117.2, 100.6, 33.2, 29.9, 25.4 ppm; GC-MS *m/z* = 233 (M⁺); Anal. Calcd for C₁₇H₁₅N: C, 87.52; H, 6.48; N, 6.00. Found: C, 87.56; H, 6.58; N, 6.06.

**106aa**

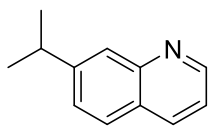
Data for **106aa**: ¹H NMR (400 MHz, CDCl₃) δ 8.23 (br s, 1H), 7.61-7.57 (m, 2H), 7.44-7.39 (m, 2H), 7.30-7.25 (m, 1H), 7.00 (s, 1H), 6.86 (s, 1H), 6.72-6.70 (m, 1H), 5.95 (s, 2H) ppm;

¹³C{¹H} NMR (100 MHz, CDCl₃) δ 145.1, 143.2, 136.6, 132.4, 131.8, 129.0, 127.1, 124.5, 123.1, 100.6, 100.2, 99.1, 91.9 ppm; GC-MS *m/z* = 237 (M⁺). ¹H and ¹³C NMR spectral data are in good agreement with the literature data.¹¹⁴

**106ab**

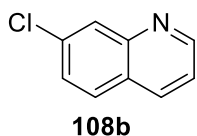
Data for **106ab**: ¹H NMR (400 MHz, DMSO-*d*₆) δ 11.39 (br s, 1H), 7.44-7.31 (m, 9H), 7.30-7.24 (m, 2H), 6.93 (d, *J* = 2.2 Hz, 1H), 6.71 (dd, *J* = 8.7, 2.2 Hz, 1H), 3.80 (s, 3H) ppm; ¹³C{¹H} NMR

(100 MHz, DMSO-*d*₆) δ 156.1, 136.9, 135.4, 132.7, 132.7, 129.7, 128.7, 128.5, 127.9, 127.2, 126.1, 122.4, 119.4, 113.3, 110.0, 94.3, 55.2 ppm; GC-MS *m/z* = 299 (M⁺). ¹H and ¹³C NMR spectral data are in good agreement with the literature data.¹¹⁵

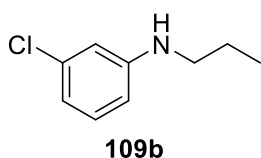
**108a**

Data for **108a**: ¹H NMR (400 MHz, CDCl₃) δ 8.87 (dd, *J* = 4.2, 1.7 Hz, 1H), 8.09 (d, *J* = 8.2 Hz, 1H), 7.93 (s, 1H), 7.74 (d, *J* = 8.4 Hz, 1H), 7.45 (dd, *J* = 8.4, 1.7 Hz, 1H), 7.32 (dd, *J* = 8.2, 4.2 Hz, 1H), 3.12 (septet, *J*

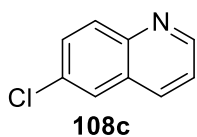
= 6.9 Hz, 1H), 1.36 (d, $J = 6.9$ Hz, 6H) ppm; $^{13}\text{C}\{^1\text{H}\}$ NMR (100 MHz, CDCl_3) δ 150.5, 150.2, 148.5, 135.6, 127.5, 126.6, 126.5, 125.5, 120.3, 34.2, 23.7 ppm; GC-MS $m/z = 171$ (M^+); HRMS (IT-TOF/ESI) Calcd for $\text{C}_{12}\text{H}_{14}\text{N}$ ($[\text{M}+\text{H}]^+$): 172.1121, Found: 172.1111.



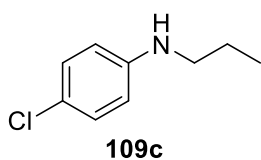
Data for **108b**: ^1H NMR (400 MHz, CDCl_3) δ 8.88 (dd, $J = 4.2, 1.7$ Hz, 1H), 8.11-8.07 (m, 2H), 7.70 (d, $J = 8.7$ Hz, 1H), 7.46 (dd, $J = 8.7, 2.2$ Hz, 1H), 7.36 (dd, $J = 8.2, 4.2$ Hz, 1H) ppm; $^{13}\text{C}\{^1\text{H}\}$ NMR (100 MHz, CDCl_3) δ 151.2, 148.4, 135.8, 135.2, 128.9, 128.3, 127.5, 126.5, 121.2 ppm; GC-MS $m/z = 163$ (M^+). ^1H and ^{13}C NMR spectral data are in good agreement with the literature data.¹¹⁶



Data for **109b**: ^1H NMR (400 MHz, CDCl_3) δ 7.08 (t, $J = 8.0$ Hz, 1H), 6.68-6.65 (m, 1H), 6.59-6.58 (m, 1H), 6.49-6.45 (m, 1H), 3.73 (br s, 1H), 3.06 (t, $J = 7.1$ Hz, 2H), 1.65 (sextet, $J = 7.2$ Hz, 2H), 1.01 (t, $J = 7.2$ Hz, 3H) ppm; $^{13}\text{C}\{^1\text{H}\}$ NMR (100 MHz, CDCl_3) δ 149.5, 134.9, 130.1, 116.7, 112.0, 111.0, 45.5, 22.5, 11.5 ppm; GC-MS $m/z = 169$ (M^+); HRMS (IT-TOF/ESI) Calcd for $\text{C}_9\text{H}_{13}\text{NCl}$ ($[\text{M}+\text{H}]^+$): 170.0731, Found: 170.0728.



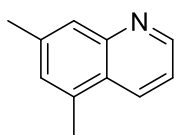
Data for **108c**: ^1H NMR (400 MHz, CDCl_3) δ 8.87 (dd, $J = 4.2, 1.7$ Hz, 1H), 8.04-8.00 (m, 1H), 8.01 (d, $J = 9.0$ Hz, 1H), 7.75 (d, $J = 2.4$ Hz, 1H), 7.61 (dd, $J = 9.0, 2.4$ Hz, 1H), 7.38 (dd, $J = 8.3, 4.2$ Hz, 1H) ppm; $^{13}\text{C}\{^1\text{H}\}$ NMR (100 MHz, CDCl_3) δ 150.5, 146.5, 135.0, 132.2, 131.0, 130.3, 128.7, 126.3, 121.8 ppm; GC-MS $m/z = 163$ (M^+). ^1H and ^{13}C NMR spectral data are in good agreement with the literature data.¹¹⁸



Data for **109c**: ^1H NMR (400 MHz, CDCl_3) δ 7.13-7.09 (m, 2H), 6.54-6.49 (m, 2H), 3.64 (br s, 1H), 3.05 (t, $J = 7.1$ Hz, 2H), 1.68-1.58 (m, 2H), 1.00 (t, $J = 7.4$ Hz, 3H) ppm; $^{13}\text{C}\{^1\text{H}\}$ NMR (100

MHz, CDCl₃) δ 147.0, 129.0, 121.5, 113.7, 45.8, 22.6, 11.6 ppm; GC-MS m/z = 169 (M⁺).

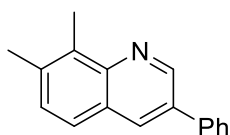
¹H and ¹³C NMR spectral data are in good agreement with the literature data.¹¹⁹



108d

Data for **108d**: ¹H NMR (400 MHz, CDCl₃) δ 8.81 (dd, J = 4.2, 1.7 Hz, 1H), 8.17-8.14 (m, 1H), 7.70 (s, 1H), 7.25 (dd, J = 8.4, 4.2 Hz, 1H), 7.13 (s, 1H), 2.56 (s, 3H), 2.46 (s, 3H) ppm; ¹³C{¹H} NMR (100 MHz, CDCl₃)

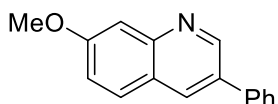
δ 149.7, 148.6, 139.1, 133.9, 132.0, 129.1, 126.4, 125.5, 119.7, 21.6, 18.2 ppm; GC-MS m/z = 157 (M⁺). ¹H and ¹³C NMR spectral data are in good agreement with the literature data.¹²⁰



108e

Data for **108e**: ¹H NMR (400 MHz, CDCl₃) δ 9.20 (d, J = 2.4 Hz, 1H), 8.23 (d, J = 2.4 Hz, 1H), 7.74-7.71 (m, 2H), 7.63 (d, J = 8.3 Hz, 1H), 7.55-7.50 (m, 2H), 7.45-7.41 (m, 1H), 7.40, (d, J = 8.3 Hz, 1H), 2.81

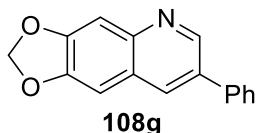
(s, 3H), 2.54 (s, 3H) ppm; ¹³C{¹H} NMR (100 MHz, CDCl₃) δ 148.5, 146.4, 138.1, 137.1, 134.1, 133.3, 132.3, 129.9, 129.1, 127.8, 127.2, 126.3, 125.0, 20.7, 13.3 ppm; GC-MS m/z = 233 (M⁺). ¹H and ¹³C NMR spectral data are in good agreement with the literature data.^{117,121,122}



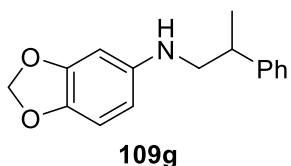
108f

Data for **108f**: ¹H NMR (400 MHz, CDCl₃) δ 9.10 (d, J = 2.3 Hz, 1H), 8.23 (d, J = 2.3 Hz, 1H), 7.76 (d, J = 8.9 Hz, 1H), 7.71-7.68

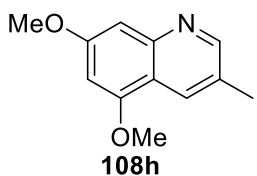
(m, 2H), 7.54-7.49 (m, 2H), 7.46 (d, J = 2.5 Hz, 1H), 7.44-7.39 (m, 1H), 7.24 (dd, J = 8.9, 2.5 Hz, 1H), 3.98 (s, 3H) ppm; ¹³C{¹H} NMR (100 MHz, CDCl₃) δ 160.7, 149.9, 149.0, 138.0, 133.0, 131.8, 129.1, 129.0, 127.8, 127.2, 123.2, 120.2, 107.1, 55.5 ppm; GC-MS m/z = 235 (M⁺). ¹H and ¹³C NMR spectral data are in good agreement with the literature data.¹¹⁷



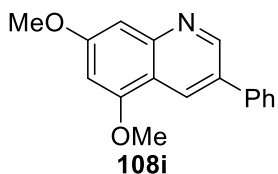
Data for **108g**: ^1H NMR (400 MHz, CDCl_3) δ 8.95 (d, $J = 2.3$ Hz, 1H), 8.08 (d, $J = 2.3$ Hz, 1H), 7.68-7.64 (m, 2H), 7.52-7.47 (m, 2H), 7.43-7.38 (m, 2H), 7.08 (s, 1H), 6.10 (s, 2H) ppm; $^{13}\text{C}\{^1\text{H}\}$ NMR (100 MHz, CDCl_3) δ 150.6, 148.1, 147.3, 145.5, 137.9, 132.3, 132.2, 129.0, 127.8, 127.2, 125.0, 105.6, 102.8, 101.7 ppm; GC-MS $m/z = 249$ (M^+). ^1H and ^{13}C NMR spectral data are in good agreement with the literature data.¹¹⁷



Data for **109g**: ^1H NMR (400 MHz, CDCl_3) δ 7.36-7.31 (m, 2H), 7.27-7.20 (m, 3H), 6.65 (d, $J = 8.3$ Hz, 1H), 6.21 (d, $J = 2.3$ Hz, 1H), 6.01 (dd, $J = 8.3, 2.3$ Hz, 1H), 5.85 (s, 2H), 3.36 (br s, 1H), 3.28 (dd, $J = 12.2, 6.0$ Hz, 1H), 3.17 (dd, $J = 12.2, 8.4$ Hz, 1H), 3.09-3.00 (m, 1H), 1.33 (d, $J = 7.0$ Hz, 3H) ppm; $^{13}\text{C}\{^1\text{H}\}$ NMR (100 MHz, CDCl_3) δ 148.3, 144.4, 143.8, 139.5, 128.7, 127.2, 126.6, 108.6, 104.6, 100.5, 96.1, 51.9, 39.1, 19.8 ppm; GC-MS $m/z = 255$ (M^+). HRMS (IT-TOF/ESI) Calcd for $\text{C}_{16}\text{H}_{18}\text{NO}_2$ ($[\text{M}+\text{H}]^+$): 256.1332, Found: 256.1330.

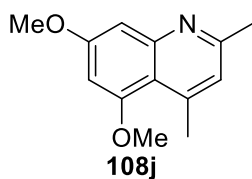


Data for **108h**: ^1H NMR (400 MHz, $\text{DMSO}-d_6$) δ 8.62 (s, 1H), 8.14 (s, 1H), 6.95 (s, 1H), 6.43 (s, 1H), 3.89 (s, 3H), 3.88 (s, 3H), 2.41 (s, 3H) ppm; $^{13}\text{C}\{^1\text{H}\}$ NMR (100 MHz, CDCl_3) δ 160.2, 155.3, 152.4, 148.3, 129.5, 127.2, 116.3, 99.3, 97.9, 55.5, 55.3, 18.4 ppm; GC-MS $m/z = 203$ (M^+); HRMS (IT-TOF/ESI) Calcd for $\text{C}_{12}\text{H}_{14}\text{NO}_2$ ($[\text{M}+\text{H}]^+$): 204.1019, Found: 204.1015.

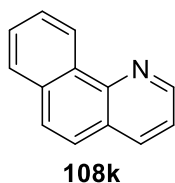


Data for **108i**: ^1H NMR (400 MHz, CDCl_3) δ 9.09 (d, $J = 2.4$ Hz, 1H), 8.61 (d, $J = 2.4$ Hz, 1H), 7.73-7.69 (m, 2H), 7.52-7.47 (m, 2H), 7.42-7.37 (m, 1H), 7.05 (d, $J = 2.2$ Hz, 1H), 6.54 (d, $J = 2.2$ Hz, 1H), 3.98 (s, 3H), 3.96 (s, 3H) ppm; $^{13}\text{C}\{^1\text{H}\}$ NMR (100 MHz, CDCl_3) δ 161.2, 156.1, 150.1, 149.4, 138.3, 130.9, 129.0, 128.1, 127.6, 127.1, 116.5, 99.4, 98.4, 55.8, 55.6 ppm;

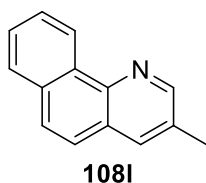
GC-MS $m/z = 265$ (M^+); HRMS (IT-TOF/ESI) Calcd for $C_{17}H_{16}NO_2$ ($[M+H]^+$): 266.1176, Found: 266.1170.



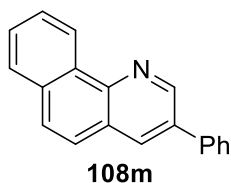
Data for **108j**: 1H NMR (400 MHz, $CDCl_3$) δ 6.95 (d, $J = 2.4$ Hz, 1H), 6.83-6.82 (m, 1H), 6.41 (d, $J = 2.4$ Hz, 1H), 3.89 (s, 3H), 3.86 (s, 3H), 2.74 (s, 3H), 2.58 (s, 3H) ppm; $^{13}C\{^1H\}$ NMR (100 MHz, $CDCl_3$) δ 160.3, 158.7, 158.5, 151.3, 145.5, 121.9, 114.7, 100.1, 97.6, 55.4, 55.3, 24.6, 24.0 ppm; GC-MS $m/z = 217$ (M^+); HRMS (IT-TOF/ESI) Calcd for $C_{13}H_{16}NO_2$ ($[M+H]^+$): 218.1176, Found: 218.1171.



Data for **108k**: 1H NMR (400 MHz, $CDCl_3$) δ 9.34-9.30 (m, 1H), 9.03-9.00 (m, 1H), 8.17-8.14 (m, 1H), 7.91 (d, $J = 7.7$ Hz, 1H), 7.81 (d, $J = 8.8$ Hz, 1H), 7.79-7.65 (m, 3H), 7.53-7.49 (m, 1H) ppm; $^{13}C\{^1H\}$ NMR (100 MHz, $CDCl_3$) δ 148.8, 146.5, 135.8, 133.5, 131.4, 128.1, 127.8, 127.7, 127.0, 126.3, 125.3, 124.3, 121.7 ppm; GC-MS $m/z = 179$ (M^+). 1H and ^{13}C NMR spectral data are in good agreement with the literature data.¹²³

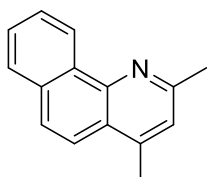


Data for **108l**: 1H NMR (400 MHz, $CDCl_3$) δ 9.30-9.27 (m, 1H), 8.84 (d, $J = 2.2$ Hz, 1H), 7.90-7.86 (m, 2H), 7.78-7.72 (m, 2H), 7.70-7.65 (m, 1H), 7.58 (d, $J = 8.8$ Hz, 1H), 2.52 (s, 3H) ppm; $^{13}C\{^1H\}$ NMR (100 MHz, $CDCl_3$) δ 150.2, 144.4, 135.0, 133.1, 131.4, 131.2, 127.7, 127.6, 127.6, 126.9, 126.0, 125.0, 124.0, 18.5 ppm; GC-MS $m/z = 193$ (M^+). 1H and ^{13}C NMR spectral data are in good agreement with the literature data.¹²⁴



Data for **108m**: 1H NMR (400 MHz, $CDCl_3$) δ 9.34-9.31 (m, 1H), 9.28 (d, $J = 2.3$ Hz, 1H), 8.31 (d, $J = 2.3$ Hz, 1H), 7.94-7.90 (m, 1H), 7.83 (d, $J = 8.8$ Hz, 1H), 7.80-7.69 (m, 4H), 7.73 (d, $J = 8.8$ Hz, 1H), 7.57-

7.52 (m, 2H), 7.48-7.43 (m, 1H) ppm; $^{13}\text{C}\{^1\text{H}\}$ NMR (100 MHz, CDCl_3) δ 147.8, 145.5, 137.9, 134.5, 133.5, 133.3, 131.3, 129.1, 128.1, 128.1, 128.0, 127.8, 127.3, 127.2, 126.1, 125.4, 124.3 ppm; GC-MS $m/z = 255$ (M^+). ^1H and ^{13}C NMR spectral data are in good agreement with the literature data.¹²²



Data for **108n**: ^1H NMR (400 MHz, CDCl_3) δ 9.38-9.33 (m, 1H), 7.91-7.88 (m, 1H), 7.87 (d, $J = 9.0$ Hz, 1H), 7.77 (d, $J = 9.0$ Hz, 1H), 7.73-7.64 (m, 2H), 7.25 (s, 1H), 2.79 (s, 3H), 2.71 (s, 3H) ppm; $^{13}\text{C}\{^1\text{H}\}$ NMR (100 MHz, CDCl_3) δ 157.2, 145.6, 143.9, 133.4, 131.6, 127.7, 127.5, 126.7, 126.2, 124.7, 123.7, 123.3, 121.2, 25.3, 19.0 ppm; GC-MS $m/z = 207$ (M^+). ^1H and ^{13}C NMR spectral data are in good agreement with the literature data.¹²⁵

BIBLIOGRAPHY

1. (a) Heck, R. F. *J. Am. Chem. Soc.* **1968**, *90*, 5518-5526. (b) Heck, R. F. *J. Am. Chem. Soc.* **1968**, *90*, 5526-5531. (c) Heck, R. F. *J. Am. Chem. Soc.* **1968**, *90*, 5531-5534. (d) Heck, R. F. *J. Am. Chem. Soc.* **1968**, *90*, 5538-5542. (e) Heck, R. F. *J. Am. Chem. Soc.* **1968**, *90*, 5542-5546. (f) R. F. Heck, *J. Am. Chem. Soc.* **1969**, *91*, 6707-6714. (g) Heck, R. F.; Nolley, J. P. *J. Org. Chem.* **1972**, *37*, 2320-2322.
2. (a) Tamao, K.; Sumitani, K.; Kumada, M. *J. Am. Chem. Soc.* **1972**, *94*, 4374-4376. (b) Miyaura, N.; Yamada, K.; Suzuki, A. *Tetrahedron Lett.* **1979**, 3437-3440. (c) Miyaura, N.; Suzuki, A. *J. Chem. Soc., Chem. Commun.* **1979**, 866-867. (d) King, A. O.; Okukado, N.; Negishi, E. *J. Chem. Soc., Chem. Commun.* **1977**, 19, 683-684. (e) Negishi, E. *Acc. Chem. Res.* **1982**, *15*, 340-348. (f) Milstein, D.; Stille, J. K. *J. Am. Chem. Soc.* **1978**, *100*, 3636-3638. (g) Hatanaka, Y.; Hiyama, T. *J. Org. Chem.* **1988**, *53*, 918-920.
3. Selected reviews for the transition metal-catalyzed cross-coupling reactions: (a) Corbet, J.-P.; Mignani, G. *Chem. Rev.* **2006**, *106*, 2651-2710. (b) Alberico, D.; Scott, M. E.; Lautens, M. *Chem. Rev.* **2007**, *107*, 174-238. (c) Kambe, N.; Iwasaki, T.; Terao, J. *Chem. Soc. Rev.* **2011**, *40*, 4937-4947. (d) Han, F.-S. *Chem. Soc. Rev.* **2013**, *42*, 5270-5298.
4. Selected reviews for the C-H functionalizations: (a) Labinger, J. A.; Bercaw, J. E. *Nature* **2002**, *417*, 507-514. (b) Hartwig, J. F. *Nature* **2008**, *455*, 314-322. (c) Ackermann, L.; Vicente, R.; Althammer, A. *Org. Lett.* **2008**, *10*, 2299-2302. (d) Giri, R.; Shi, B.-F.; Engle, K. M.; Maugel, N.; Yu, J.-Q. *Chem. Soc. Rev.* **2009**, *38*, 3242-3272. (e) Mkhaliid, I. A. I.; Barnard, J. H.; Marder, T. B.; Murphy, J. M.; Hartwig, J. F. *Chem. Rev.* **2010**, *110*, 890-931. (f) Hashiguchi, B. G.; Bischof, S. M.; Konnick, M. M.; Periana, R. A. *Acc. Chem. Res.* **2012**, *45*, 885-898. (g) Gensch, T.; Hopkinson, M. N.; Glorius, F.; Wencel-Delord, J. *Chem. Soc. Rev.* **2016**, *45*, 2900-2936.
5. (a) Li, C.-J. *Acc. Chem. Res.* **2009**, *42*, 335-344. (b) Chem, X.; Engle, K. M.; Wang, D.-H.; Yu, J.-Q. *Angew. Chem. Int. Ed.* **2009**, *48*, 5094-5115. (c) Scheuermann, C. J. *Chem. Asian J.* **2010**, *5*, 436-451. (d) Yeung, C. S.; Dong, V. M. *Chem. Rev.* **2011**, *111*, 1215-1292. (e) Liu, C.; Zhang, H.; Shi, W.; Lei, A. *Chem. Rev.* **2011**, *111*, 1780-1824. (f) Ackermann, L. *Acc. Chem. Res.* **2014**, *47*, 281-295. (g) Wu, Y.; Wang, J.; Mao, F.; Kwong, F. Y. *Chem. Asian. J.* **2014**, *9*, 26-47. (h) Li, S.-S.; Qin, L.; Dong, L. *Org. Biomol. Chem.* **2016**, *14*, 4554-4570.
6. (a) Lyons, T. W.; Sanford, M. S. *Chem. Rev.* **2010**, *110*, 1147-1169. (b) Ackermann, L. *Chem. Rev.* **2011**, *111*, 1315-1345. (c) Engle, K. M.; Mei, T.-S.; Wasa, M.; Yu, J.-Q. *Acc. Chem. Res.* **2012**, *45*, 788-802. (d) Brückl, T.; Baxter, R. D.; Ishihara, Y.; Baran, P. S. *Acc. Chem. Res.* **2012**, *45*, 826-839. (e) Rouquet, G.; Chatani, N. *Angew. Chem. Int. Ed.* **2013**, *52*, 11726-11743.

7. (a) Ritleng, V.; Sirlin, C.; Pfeffer, M. *Chem. Rev.* **2002**, *102*, 1731-1770. (b) Beccalli, E. M.; Broggini, G.; Martinelli, M.; Sottocornola, S. *Chem. Rev.* **2007**, *107*, 5318-5365.
8. (a) Zhang, Y.; Li, C.-J. *Eur. J. Org. Chem.* **2007**, *2007*, 4654-4657. (b) Deng, G.; Ueda, K.; Yanagisawa, S.; Itami, K.; Li, C.-J. *Chem. Eur. J.* **2009**, *15*, 333-337. (c) Antonchick, A. P.; Burgmann, L. *Angew. Chem., Int. Ed.* **2013**, *52*, 3267-3271.
9. (a) Fujiwara, Y.; Moritani, I.; Danno, S.; Asano, R.; Teranishi, S. *J. Am. Chem. Soc.* **1969**, *91*, 7166-7169. (b) Moritani, I.; Fujiwara, Y. *Synthesis* **1973**, 524-533.
10. Piera, J.; Bäckvall, J.-E. *Angew. Chem., Int. Ed.* **2008**, *47*, 3506-3523.
11. Boele, M. D. K.; van Strijdonck, G. P. F.; de Vries, A. H. M.; Kamer, P. C. J.; de Vries, J. G.; van Leeuwen, P. W. N. M. *J. Am. Chem. Soc.* **2002**, *124*, 1586-1587.
12. Weissman, H.; Song, X.; Milstein, D. *J. Am. Chem. Soc.* **2001**, *123*, 337-338.
13. (a) Chatani, N.; Asaumi, T.; Yorimitsu, S.; Ikeda, T.; Kakiuchi, F.; Murai, S. *J. Am. Chem. Soc.* **2001**, *123*, 10935-10941. (b) DeBoef, B.; Pastine, S. J.; Sames, D. *J. Am. Chem. Soc.* **2004**, *126*, 6556-6557. (c) Sezen, B.; Sames, D. *J. Am. Chem. Soc.* **2005**, *127*, 5284-5285.
14. Yi, C. S.; Yun, S. Y.; Guzei, I. A. *Organometallics* **2004**, *23*, 5392-5395.
15. Kwon, K.-H.; Lee, D. W.; Yi, C. S. *Organometallics* **2010**, *29*, 5748-5750.
16. (a) Yi, C. S.; Zeczycki, T. N.; Guzei, I. A. *Organometallics* **2006**, *25*, 1047-1051. (b) Yi, C. S.; Zeczycki, T. N.; Lindeman, S. V. *Organometallics* **2008**, *27*, 2030-2035.
17. (a) Ullmann, F.; Bielecki, J. *Ber. Dtsch. Chem. Ges.* **1901**, *34*, 2174-2185. (b) Goldberg, I. *Ber. Dtsch. Chem. Ges.* **1906**, *39*, 1691-1692.
18. Selected reviews for the oxidative direct arylations: (a) McGlacken, G. P.; Batemann, L. M. *Chem. Soc. Rev.* **2009**, *38*, 2447-2464. (b) Ashenurst, J. A. *Chem. Soc. Rev.* **2010**, *39*, 540-548. (c) You, S.-L.; Xia, J.-B. *Top. Curr. Chem.* **2010**, *292*, 165-194.
19. Li, R.; Jiang, L.; Lu, W. *Organometallics* **2006**, *25*, 5973-5975.
20. Lu, W.; Yamaoka, Y.; Taniguchi, Y.; Kitamura, T.; Takaki, K.; Fujiwara, Y. *J. Organomet. Chem.* **1999**, *580*, 290-294.
21. Stuart, D. R.; Fagnou, K. *Science* **2007**, *316*, 1172-1175.
22. Stuart, D. R.; Villemure, E.; Fagnou, K. *J. Am. Chem. Soc.* **2007**, *129*, 12072-12073.
23. Zhao, X.; Yeung, C. S.; Dong, V. M. *J. Am. Chem. Soc.* **2010**, *132*, 5837-5844.

24. (a) Jia, C.; Piao, D.; Oyamada, J.; Lu, W.; Kitamura, T.; Fujiwara, Y. *Science* **2000**, 287, 1992-1995. (b) Jia, C.; Lu, W.; Oyamada, J.; Kitamura, T.; Matsuda, K.; Irie, M.; Fujiwara, Y. *J. Am. Chem. Soc.* **2000**, 122, 7252-7263.
25. Dupont, J.; Consorti, C. S.; Spencer, J. *Chem. Rev.* **2005**, 105, 2527-2572.
26. Ackermann, L.; Jeyachandran, R.; Potukuchi, H. K.; Novák, P.; Büttner, L. *Org. Lett.* **2010**, 12, 2056-2059.
27. Cheng, C.; Chen, W.-W.; Xu, B.; Xu, M.-H. *J. Org. Chem.* **2016**, 81, 11501-11507.
28. Chatani, N.; Fukuyama, T.; Kakiuchi, F.; Murai, S. *J. Am. Chem. Soc.* **1996**, 118, 493-494.
29. Tlili, A.; Schranck, J.; Pospesch, J.; Neumann, H.; Beller, M. *Angew. Chem., Int. Ed.* **2013**, 52, 6293-6297.
30. Selected reviews for the aldehydic C-H bond activations: (a) Park, Y. J.; Park, J.-W.; Jun, C.-H. *Acc. Chem. Res.* **2008**, 41, 222-234. (b) Garralda, M. A. *Dalton Trans.* **2009**, 3635-3645. (c) Willis, M. C. *Chem. Rev.* **2010**, 110, 725-748.
31. Jia, X.; Zhang, S.; Wang, W.; Luo, F.; Cheng, J. *Org. Lett.* **2009**, 11, 3120-3123.
32. Chan, C.-W.; Zhou, Z.; Chan, A. S. C.; Yu, W.-Y. *Org. Lett.* **2010**, 12, 3926-3929.
33. Tang, B.-X.; Song, R.-J.; Wu, C.-Y.; Liu, Y.; Zhou, M.-B.; Wei, W.-T.; Deng, G.-B.; Yin, D.-L.; Li, J.-H. *J. Am. Chem. Soc.* **2010**, 132, 8900-8902.
34. Review for the dehydrative cross-couplings: Kumar, R.; Van der Eyckn, E. V. *Chem. Soc. Rev.* **2013**, 42, 1121-1146.
35. (a) Tsuji, J.; Takahashi, H.; Morikawa, M. *Tetrahedron Lett.* **1965**, 6, 4387-4388. (b) Trost, B. M.; Fullerton, T. J. *J. Am. Chem. Soc.* **1973**, 95, 292-294. (c) Trost, B. M.; Crawley, M. L. *Chem. Rev.* **2003**, 103, 2921-2944.
36. (a) Sundararaju, B.; Achard, M.; Brunau, C. *Chem. Soc. Rev.* **2012**, 41, 4467-4483. (b) Butt, N. A.; Zhang, W. *Chem. Soc. Rev.* **2015**, 44, 7929-7967. (c) Gumrukcu, Y.; de Bruin, B.; Reek, J. N. H. *Catalysts* **2015**, 5, 349-365.
37. Ozawa, F.; Okamoto, H.; Kawagishi, S.; Yamamoto, S.; Minami, T. Yoshifuji, M. *J. Am. Chem. Soc.* **2002**, 124, 10968-10969.
38. Li, Y.-X.; Xuan, Q.-Q.; Liu, L.; Wang, D.; Chen, Y.-J.; Li, C.-J. *J. Am. Chem. Soc.* **2013**, 135, 12536-12539.
39. Gumrukcu, Y.; de Bruin, B.; Reek, J. N. H. *Chem. Eur. J.* **2014**, 20, 10905-10909.
40. Bunno, Y.; Murakami, N.; Suzuki, Y.; Kanai, M.; Yoshino, T.; Matsunaga, S. *Org. Lett.* **2016**, 18, 2216-2219.

41. Kumar, G. S.; Kapur, M. *Org. Lett.* **2016**, *18*, 1112-1115.
42. Smith, M. B.; March, J. *March's Advanced Organic Chemistry*; Wiley: New York, **2001**.
43. Lee, D.-H.; Kwon, K.-H.; Yi, C. S. *Science* **2011**, *333*, 1613-1616.
44. Lee, D.-H.; Kwon, K.-H.; Yi, C. S. *J. Am. Chem. Soc.* **2012**, *134*, 7325-7328.
45. Ackermann, L.; Mulzer, M. *Org. Lett.* **2008**, *10*, 5043-5045.
46. Ackermann, L.; Pospech, J.; Potukuchi, H. K. *Org. Lett.* **2012**, *14*, 2146-2149.
47. (a) Ackermann, L.; Vicente, R.; Althammer, A. *Org. Lett.* **2008**, *10*, 2299-2302. (b) Ackermann, L.; Lygin, A. V.; Hofmann, N. *Angew. Chem. Int. Ed.* **2011**, *50*, 6379-6382. (c) Ackermann, L.; Pospech, J.; Graczyk, K.; Rauch, K. *Org. Lett.* **2012**, *14*, 930-933.
48. (a) Gore, P. H. *Chem. Rev.* **1955**, *55*, 229-281. (b) Olah, G. A. *Friedel-Crafts Chemistry*; Wiley: New York, **1973**. (c) Sartori, G.; Maggi, R. *Advances in Friedel-Crafts Acylation Reactions*; CRC Press: FL, **2010**.
49. (a) Yato, M.; Ohwada, T.; Shudo, K. *J. Am. Chem. Soc.* **1991**, *113*, 691-692. (b) Sato, Y.; Yato, M.; Ohwada, T.; Saito, S.; Shudo, K. *J. Am. Chem. Soc.* **1995**, *117*, 3037-3043.
50. (a) Barnard, C. F. J. *Organometallics* **2008**, *27*, 5402-5422. (b) Wu, J.; Lan, J.; Guo, S.; You, J. *Org. Lett.* **2014**, *16*, 5862-5865. (c) Froese, J.; Hudlicky, J. R.; Hudlicky, T. *Org. Biomol. Chem.* **2014**, *12*, 7810-7819. (d) Gadge, S. T.; Bhanage, B. M. *RSC Adv.* **2014**, *4*, 10367-10389.
51. Halima, T. B.; Zhang, W.; Yalaoui, I.; Hong, X.; Yang, Y.-F.; Houk, K. N.; Newman, S. G. *J. Am. Chem. Soc.* **2017**, *139*, 1311-1318.
52. Hu, J.; Adogla, E. A.; Ju, Y.; Fan, D.; Wang, Q. *Chem. Commun.* **2012**, *48*, 11256-11258.
53. Yi, C. S.; Lee, D. W. *Organometallics* **2010**, *29*, 1883-1885.
54. Kwon, K.-H.; Lee, D. W.; Yi, C. S. *Organometallics* **2012**, *31*, 495-504.
55. Kalutharage, N.; Yi, C. S. *J. Am. Chem. Soc.* **2015**, *137*, 11105-11114.
56. (a) Hoshimoto, Y.; Ohashi, M.; Ogoshi, S. *J. Am. Chem. Soc.* **2011**, *133*, 4668-4671. (b) Curran, S. P.; Connon, S. J. *Org. Lett.* **2012**, *14*, 1074-1077.
57. (a) Middleton, E. Jr.; Kandaswami, C.; Theoharides, T. C. *Pharm. Rev.* **2000**, *52*, 673-751. (b) Boots, A. W.; Haenen, G. R.; Bast, A. *Eur. J. Pharmacol.* **2008**, *585*, 325-337.

58. Selected recent examples: (a) Fristrup, P.; Kreis, M.; Palmelund, A.; Norrby, P.-O.; Madsen, R. *J. Am. Chem. Soc.* **2008**, *130*, 5206-5215. (b) Koren-Selfridge, L.; Londino, H. N.; Vellucci, J. K.; Simmons, B. J.; Casey, C. P.; Clark, T. B. *Organometallics* **2009**, *28*, 2085-2090. (c) Sigman, M. S.; Werner, E. W. *Acc. Chem. Res.* **2012**, *45*, 874-884.
59. Wang, X.; Guram, A.; Caille, S.; Hu, J.; Preston, J. P.; Ronk, M.; Walker, S. *Org. Lett.* **2011**, *13*, 1881-1883.
60. Yang, D.; Zhu, Y.; Yang, N.; Jiang, Q.; Liu, R. *Adv. Synth. Catal.* **2016**, *358*, 1731-1735.
61. Zhang, Y.; Sigman, M. S. *Org. Lett.* **2006**, *8*, 5557-5560.
62. Murphy, S. K.; Bruch, A.; Dong, V. M. *Angew. Chem., Int. Ed.* **2014**, *53*, 2455-2459.
63. Sasano, K.; Takaya, J.; Iwasawa, N. *J. Am. Chem. Soc.* **2013**, *135*, 10954-10957.
64. Chen, J.; Shao, Y.; Zheng, H.; Cheng, J.; Wan, X. *J. Org. Chem.* **2015**, *80*, 10734-10741.
65. Yu, S.-Y.; Zhang, H.; Gao, Y.; Mo, L.; Wang, S.; Yao, Z.-J. *J. Am. Chem. Soc.* **2013**, *135*, 11402-11407.
66. Yoshida, M.; Ohno, S.; Namba, K. *Angew. Chem., Int. Ed.* **2013**, *52*, 13597-13600.
67. Seoane, A.; Casanova, N.; Quiñones, N.; Mascareñas, J. L.; Gulías, M. *J. Am. Chem. Soc.* **2014**, *136*, 834-837.
68. Kujawa, S.; Best, D.; Burns, D. J.; Lam, H. W. *Chem. Eur. J.* **2014**, *20*, 8599-8602.
69. Han, Y.-P.; Song, X.-R.; Qiu, Y.-F.; Li, X.-S.; Zhang, H.-R.; Zhu, X.-Y.; Liu, X.-Y.; Liang, Y.-M. *Org. Lett.* **2016**, *18*, 3866-3869.
70. Kuppusamy, R.; Muralirajan, K.; Cheng, C.-H. *ACS Catal.* **2016**, *6*, 3909-3913.
71. (a) Maryanoff, B. E.; Reitz, A. B. *Chem. Rev.* **1989**, *89*, 863-927. (b) Murphy, P. J.; Lee, S. E. *J. Chem. Soc., Perkin Trans. I* **1999**, 3049-3066. (c) Byrne, P. A.; Gilheany, D. G. *Chem. Soc. Rev.* **2013**, *42*, 6670-6696.
72. (a) Wang, Z.; Zhang, G.; Guzei, I.; Verkade, J. G. *J. Org. Chem.* **2001**, *66*, 3521-3524. (b) El-Batta, A.; Jiang, C.; Zhao, W.; Anness, R.; Cooksy, A. L.; Bergdahl, M. *J. Org. Chem.* **2007**, *72*, 5244-5259. (c) Dong, D.-J.; Li, H.-H.; Tian, S.-K. *J. Am. Chem. Soc.* **2010**, *132*, 5018-5020.
73. (a) Peterson, D. J. *J. Org. Chem.* **1968**, *33*, 780-784. (b) van Staden, L. F.; Gravestock, D.; Ager, D. J. *Chem. Soc. Rev.* **2002**, *31*, 195-200.

74. (a) Tebbe, F. N.; Parshall, G. W.; Reddy, G. S. *J. Am. Chem. Soc.* **1978**, *100*, 3611-3613. (b) Hartley, R. C.; Li, J.; Main, C. A.; McKiernan, G. J. *Tetrahedron* **2007**, *63*, 4825-4864.
75. Hu, F.; Xia, Y.; Ye, F.; Liu, Z.; Ma, C.; Zhang, Y.; Wang, J. *Angew. Chem., Int. Ed.* **2014**, *53*, 1364-1367.
76. Prakash, S.; Muralirajan, K.; Cheng, C.-H. *Chem. Commun.* **2015**, *51*, 13362-13364.
77. Yi, C. S.; Lee, D. W. *Organometallics* **2009**, *28*, 4266-4268.
78. Xue, W.-J.; Li, Q.; Gao, F.; Zhu, Y.; Wang, J.; Zhang, W.; Wu, A.-X. *ACS Comb. Sci.* **2002**, *14*, 478-483.
79. (a) Ficht, S.; Roglin, L.; Ziehe, M.; Breyer, D. *Synlett* **2004**, 2525-2528. (b) Boshta, N. M.; Bomkamp, M.; Waldvogel, S. R. *Tetrahedron* **2009**, *65*, 3773-3779. (c) Pingali, S. R. K.; Jursic, B. S. *Tetrahedron Lett.* **2011**, *52*, 4371-4374.
80. Wu, Y.-C.; Liu, L.; Liu, Y.-L.; Wang, D.; Chen, Y.-J. *J. Org. Chem.* **2007**, *72*, 9383-9386.
81. For indoles: (a) Kochanowska-Karamyan, A. J.; Hamann, M. T. *Chem. Rev.* **2010**, *110*, 4489-4497. (b) Bronner, S. M.; Im, G.-Y. J.; Garg, N. K. *Heterocycles in Natural Product Synthesis*; Wiley-VCH Verlag GmbH & Co. KGaA **2011**, 221-265. (c) Kaushik, N. K.; Kaushik, N.; Attri, P.; Kumar, N.; Kim, C. H.; Verma, A. K.; Choi, E. H. *Molecules* **2013**, *18*, 6620-6662. (d) Xu, W.; Gavia, D. J.; Tang, Y. *Nat. Prod. Rep.* **2014**, *31*, 1474-1487. (e) Mielczarek, M.; Devakaram, R. V.; Ma, C.; Yang, X.; Kandemir, H.; Purwono, B.; Black, D. StC.; Griffith, R.; Lewis, P. J.; Kumar, N. *Org. Biomol. Chem.* **2014**, *12*, 2882-2894. (f) Hwang, D.-J.; Wang, J.; Li, W.; Miller, D. D. *ACS Med. Chem. Lett.* **2015**, *6*, 993-997.
82. For quinolines: (a) Kaur, K.; Jain, M.; Reddy, R. P.; Jain, R. *Eur. J. Med. Chem.* **2010**, *45*, 3245. (b) Montalban, A. G. *Heterocycles in Natural Product Synthesis*; Wiley-VCH Verlag GmbH & Co. KGaA **2011**, 399-339.
83. (a) Fischer, E.; Jourdan, F. *Ber. Dtsch. Chem. Ges.* **1883**, *16*, 2241-2245. (b) Fischer, E.; Hess, O. *Ber. Dtsch. Chem. Ges.* **1884**, *17*, 559-568. (c) Lim, B.-Y.; Jung, B.-E.; Cho, C.-G. *Org. Lett.* **2014**, *16*, 4492-4495. (d) Porcheddu, A.; Mura, M. G.; De Luca, L.; Pizzetti, M.; Taddei, M. *Org. Lett.* **2012**, *14*, 6112-6115. (e) Wagaw, S.; Yang, B. H.; Buchwald, S. L. *J. Am. Chem. Soc.* **1999**, *121*, 10251-10263.
84. (a) Larock, R. C.; Yum, E. K. *J. Am. Chem. Soc.* **1991**, *113*, 6689-6690. (b) Larock, R. C.; Yum, E. K.; Refvik, M. D. *J. Org. Chem.* **1998**, *63*, 7652-7662. (c) Varela-Fernández, A.; Varela, J. A.; Saá, C. *Synthesis* **2012**, *44*, 3285-3295. (d) Liu, B.; Song, C.; Sun, C.; Zhou, S.; Zhu, J. *J. Am. Chem. Soc.* **2013**, *135*, 16625-16631. (e) Zhou, B.; Yang, Y.; Tang, H.; Du, J.; Feng, H.; Li, Y. *Org. Lett.* **2014**, *16*, 3900-3903.

85. Selected reviews for the indole synthesis: (a) Gribble, G. W. *J. Chem. Soc., Perkin Trans. 1* **2000**, 1045-1075. (b) Cacchi, S.; Fabrizi, G. *Chem. Rev.* **2005**, *106*, 2873-2920. (c) Humphrey, G. R.; Kuethe, J. T. *Chem. Rev.* **2006**, *106*, 2875-2911. (d) Krüger, K.; Tillack, A.; Beller, M. *Adv. Synth. Catal.* **2008**, *350*, 2153-2167. (e) Taber, D. F.; Tirunahari, P. K. *Tetrahedron* **2011**, *67*, 7195-7210. (f) Vicente, R. *Org. Biomol. Chem.* **2011**, *9*, 6469-6480. (g) Djakovitch, L.; Batail, N.; Genelot, M. *Molecules* **2011**, *16*, 5241-5267. (h) Platon, M.; Amardeil, R.; Djakovitch, L.; Hierso, J.-C. *Chem. Soc. Rev.* **2012**, *41*, 3929-3968. (i) Inman, M.; Moody, C. J. *Chem. Sci.* **2013**, *4*, 29-41.
86. Selected reviews for the quinoline synthesis: (a) Barluenga, J.; Rodríguez, F.; Fañanás, F. J. *Chem. Asian. J.* **2009**, *4*, 1036-1048. (b) Prajapati, S. M.; Patel, K. D.; Vekariya, R. H.; Panchal, S. N.; Patel, H. D. *RSC Adv.* **2014**, *4*, 24463-24476.
87. (a) Lerchen, A.; Vásquez-Céspedes, S.; Glorius, F. *Angew. Chem., Int. Ed.* **2016**, *55*, 3208-3211. (b) Liang, Y.; Jiao, N. *Angew. Chem., Int. Ed.* **2016**, *55*, 4035-4039. (c) Kong, L.; Yu, S.; Zhou, X.; Li, X. *Org. Lett.* **2016**, *18*, 588-591. (d) Wang, H.; Moselage, M.; González, M. J.; Ackermann, L. *ACS Catal.* **2016**, *6*, 2705-2709. (e) Zhang, Z.-Z.; Liu, B.; Xu, J.-W.; Yan, S.-Y.; Shi, B.-F. *Org. Lett.* **2016**, *18*, 1776-1779.
88. (a) Würtz, S.; Rakshit, S.; Neumann, J. J.; Dröge, T.; Glorius, F. *Angew. Chem., Int. Ed.* **2008**, *47*, 7230-7233. (b) Huang, F.; Wu, P.; Wang, L.; Chen, J.; Sun, C.; Yu, Z. *J. Org. Chem.* **2014**, *79*, 10553-10560.
89. Wei, Y.; Deb, I.; Yoshikai, N. *J. Am. Chem. Soc.* **2012**, *134*, 9098-9101.
90. (a) Tsuji, Y.; Huh, K.-T.; Watanabe, Y. *Tetrahedron Lett.* **1986**, *277*, 377-380. (b) Tsuji, Y.; Huh, K.-T.; Watanabe, Y. *J. Org. Chem.* **1987**, *52*, 1673-1680.
91. (a) Cho, C. S.; Lim, H. K.; Shim, S. C.; Kim, T. J.; Choi, H.-j. *Chem. Commun.* **1998**, 995-996. (b) Cho, C. S.; Lee, M. J.; Shim, S. C.; Kim, M. C. *Bull. Korean Chem. Soc.* **1999**, *20*, 119-121. (c) Cho, C. S.; Oh, B. H.; Shim, S. C. *J. Heterocyclic Chem.* **1999**, *36*, 1175-1178. (d) Cho, C. S.; Oh, B. H.; Kim, J. S.; Kim, T.-J.; Shim, S. C. *Chem. Commun.* **2000**, 1885-1886. (e) Cho, C. S.; Kim, J. S.; Oh, B. H.; Kim, T.-J.; Shim, S. C.; Yoon, N. S. *Tetrahedron* **2000**, *56*, 7747-7750.
92. Aramoto, H.; Obora, Y.; Ishii, Y. *J. Org. Chem.* **2009**, *74*, 628-633.
93. (a) Tursky, M.; Lorentz-Petersen, L. R.; Olsen, L. B.; Madsen, R. *Org. Biomol. Chem.* **2010**, *8*, 5576-5582. (b) Monrad, R. N.; Madsen, R. *Org. Biomol. Chem.* **2011**, *9*, 610-615.
94. Kim, J.; Lee, D.-H.; Kalutharage, N.; Yi, C. S. *ACS Catal.* **2014**, *4*, 3881-3885.
95. Kalutharage, N.; Yi, C. S. *Org. Lett.* **2015**, *17*, 1778-1781.
96. (a) Kakiuchi, F.; Murai, S. *Acc. Chem. Res.* **2002**, *35*, 826-834. (b) Albrecht, M. *Chem. Rev.* **2010**, *110*, 576-623.

97. Yi, C. S.; Yun, S. Y. *Org. Lett.* **2005**, *7*, 2181-2183.
98. (a) Schilling, J. B.; Goddard, W. A.; Beauchamp, J. L. *J. Am. Chem. Soc.* **1986**, *108*, 582-584. (b) Rybtchinski, B.; Milstein, D. *Angew. Chem., Int. Ed.* **1999**, *38*, 870-883. (c) Jun, C.-H. *Chem. Soc. Rev.* **2004**, *33*, 610-618. (d) Xia, Y.; Lu, G.; Liu, P.; Dong, G. *Nature* **2016**, *539*, 546-550.
99. Yi, C. S.; Yun, S. Y. *J. Am. Chem. Soc.* **2005**, *127*, 17000-17006.
100. (a) Chung, K.; Banik, S. M.; De Crisci, A. G.; Pearson, D. M.; Blake, T. R.; Olsson, J. V.; Ingram, A. J.; Zare, R. N.; Waymouth, R. M. *J. Am. Chem. Soc.* **2013**, *135*, 7593-7602. (b) Manzini, S.; Urbina-Blanco, C. A.; Nolan, S. P. *Organometallics* **2013**, *32*, 660-664. (c) Tseng, K.-N. T.; Kampf, J. W.; Szymczak, N. K. *Organometallics* **2013**, *32*, 2046-2049. (d) hakraborty, S.; Lagaditis, P. O.; Förster, M.; Bielinski, E. A.; Hazari, N.; Holthausen, M. C.; Jones, W. D.; Schneider, S. *ACS Catal.* **2014**, *4*, 3994-4003.
101. Pouget, C.; Fagnere, C.; Basly, J.-P.; Leveque, H.; Chulia, A.-J. *Tetrahedron* **2000**, *56*, 6047-6052.
102. Nay, B.; Peyrat, J.-F.; Vercauteren, J. *Eur. J. Org. Chem.* **1999**, *1999*, 2231-2234.
103. Peña-López, M.; Neumann, H.; Beller, M. *Chem. Eur. J.* **2014**, *20*, 1818-1824.
104. Zhang, J.; Meng, L.-G.; Li, P.; Wang, L. *RSC Adv.* **2013**, *3*, 6807-6812.
105. Liu, Y.; Yao, B.; Deng, C.-L.; Tang, R.-Y.; Zhang, X.-G.; Li, J.-H. *Org. Lett.* **2011**, *13*, 1126-1129.
106. Ambrogio, I.; Cacchi, S.; Fabrizi, G.; Prastaro, A. *Tetrahedron* **2009**, *65*, 8916-8929.
107. Liu, K. G.; Robichaud, A. J.; Lo, J. R.; Mattes, J. F.; Cai, Y. *Org. Lett.* **2006**, *8*, 5769-5771.
108. Rutherford, J. L.; Rainka, M. P.; Buchwald, S. L. *J. Am. Chem. Soc.* **2002**, *124*, 15168-15169.
109. Shen, M.; Leslie, B. E.; Driver, T. G. *Angew. Chem. Int. Ed.* **2008**, *47*, 5056-5059.
110. Miyata, O.; Takeda, N.; Kimura, Y.; Takemoto, Y.; Tohnai, N.; Miyata, M.; Naito, T. *Tetrahedron* **2006**, *62*, 3629-3647.
111. Banwell, M. G.; Kelly, B. D.; Kokas, O. J.; Lupton, D. W. *Org. Lett.* **2003**, *5*, 2497-2500.
112. Tursky, M.; Lorentz-Petersen, L. L. R.; Olsen, L. B.; Madsen, R. *Org. Biomol. Chem.* **2010**, *8*, 5576-5582.

113. Zhang, X.; Si, W.; Bao, M.; Asao, N.; Yamamoto, Y.; Jin, T. *Org. Lett.* **2014**, *16*, 4830-4833.
114. Du, P.; Brosmer, J. L.; Peters, D. G. *Org. Lett.* **2011**, *13*, 4072-4075.
115. Zhou, F.; Han, X.; Lu, X. *Tetrahedron Lett.* **2011**, *52*, 4681-4685.
116. Hirner, J. J.; Zacuto, M. J. *Tetrahedron Lett.* **2009**, *50*, 4989-4993.
117. Bharate, J. B.; Bharate, S. B.; Vishwakarma, R. A. *ACS Comb. Sci.* **2014**, *16*, 624-630.
118. Pan, J.; Wang, X.; Zhang, Y.; Buchwald, S. L. *Org. Lett.* **2011**, *13*, 4974-4976.
119. Larrosa, M.; Guerrero, C.; Rodríguez, R.; Cruces, J. *Synlett* **2010**, *14*, 2101-2105.
120. Yi, X.; Xi, C. *Org. Lett.* **2015**, *17*, 5836-5839.
121. Yan, R.; Liu, X.; Pan, C.; Zhou, X.; Li, X.; Kang, X.; Huang, G. *Org. Lett.* **2013**, *15*, 4876-4879.
122. Zhang, Y.; Wang, M.; Li, P.; Wang, L. *Org. Lett.* **2012**, *14*, 2206-2209.
123. Iosub, A. V.; Stahl, S. S. *Org. Lett.* **2015**, *17*, 4404-4407.
124. Monrad, R. N.; Madsen, R. *Org. Biomol. Chem.* **2011**, *9*, 610-615.
125. Piechowska, J.; Gryko, D. T. *J. Org. Chem.* **2011**, *76*, 10220-10228.